SCIENCE&ENGINEERING SYMPOSIUM PROCEEDINGS 16-19 OCTOBER

THEME: "Advanced Technologies – Key to Capabilities at Affordable Costs"

DISTRIBUTION STATEMENT A
Approved for Public Release
Distribution Unlimited

VOL. VI. ARMAMENT

CO-SPONSORED BY
NAVAL MATERIAL COMMAND
AIR FORCE SYSTEMS COMMAND

- Avionics
- Propulsion
- Flight Dynamics
- Basic Research
- Material
- Armament
- Human Resources

PROCEEDINGS

OF THE

1978 SCIENCE AND ENGINEERING SYMPOSIUM

16 - 19 OCTOBER 1978

NAVAL AMPHIBIOUS BASE
CORONADO, CALIFORNIA

VOLUME VI

APPROVED FOR PUBLIC RELEASE;
DISTRIBUTION UNLIMITED

SYMPOSIUM OFFICIALS

CO-SPONSORS

NAVAL MATERIAL COMMAND

AIR FORCE SYSTEMS COMMAND

HOSTS

NAVAL OCEAN SYSTEMS CENTER
WEST COAST COORDINATOR

NAVAL AMPHIBIOUS BASE
FACILITIES

CO-CHAIRMEN

WILLIAM KOVEN
Associate Technical Director
Naval Air Research and Technology
Naval Air Systems Command

DR. BERNARD KULP
Chief Scientist
Director of Science and Technology
Air Force Systems Command

DEPUTY CO-CHAIRMEN

JAMES MULQUIN
Advanced Systems Technology Planning
Naval Air Research and Technology
Naval Air Systems Command

MAJOR LARRY FEHRENBACHER
Assistant to Chief Scientist
Director of Science and Technology
Air Force Systems Command

PREFACE

The initial co-sponsored Air Force Systems Command/Naval Material Command Science and Engineering Symposium was held at the Naval Amphibious Base, Coronado on 16 - 19 October 1978. The theme of the 1978 Symposium was "Advanced Technologies - Key to Capabilities at Affordable Cost."

The objectives of this first joint Navy/Air Force Science and Engineering Symposium were to:

- Provide a forum for military and civilian laboratory scientific and technical researchers to demonstrate the spectrum and nature of 1978 achievements by their services in the areas of
  - Armament
  - Avionics
  - Basic Research
  - Flight Dynamics
  - Human Resources
  - Materials
  - Propulsion
- Recognize outstanding technical achievement in each of these areas and select the outstanding technical paper within the Navy and the Air Force for 1978
- Assist in placing the future Air Research and Development of both services in correct perspective and to promote the exchange of ideas between the Navy and Air Force Laboratories
- Stress the need for imagination, vision and overall excellence within the technology community, assuring that the air systems of the future will not only be effective but affordable.

Based upon the success of the initial joint symposium (which was heretofore an Air Force event), future symposia are planned with joint Navy/Air Force participation.

TABLE OF CONTENTS

VOLUME I

AVIONICS

R. S. VAUGHN, NADC — COL R. LOPINA, AFAL
CO-CHAIRMEN

VOLUME II

PROPULSION

AERO-PROPULSION

A. A. MARTINO, NAPC — COL G. STRAND, AFAPL
CO-CHAIRMEN

ROCKET PROPULSION

B. W. HAYES, NWC — COL W. F. MORRIS, AFRPL

CO-CHAIRMEN

VOLUME III

FLIGHT DYNAMICS

C. A. DeCRESCENTE, NADC COL G. CUDAHY, USAF, AFFDL
CO-CHAIRMEN

VOLUME IV

BASIC RESEARCH

DR. E. H. WEINBERG, NAL DR. L. KRAVITZ, AFOSR
CO-CHAIRMEN

VOLUME V

MATERIALS

F. S. WILLIAMS, NADC — COL P. O. BOUCHARD, USAF, AFML
CO-CHAIRMEN

VOLUME VI

ARMAMENT

DR. J. MAYERSAK, AFATL R. M. HILLYER, NWC
CO-CHAIRMEN

VOLUME VII

HUMAN RESOURCES

H. J. CLARK, AFHRL DR. J. HARVEY, NTEC
CO-CHAIRMEN

VOLUME VIII

AVIONICS, PROPULSION, AND FLIGHT DYNAMICS (CLASSIFIED)

VOLUME IX

MATERIALS, ARMAMENT, AND HUMAN RESOURCES (CLASSIFIED)

ARMAMENT TECHNOLOGY - FUNCTIONAL OVERVIEW

BY

JOSEPH R. MAYERSAK, PhD

AIR FORCE ARMAMENT LABORATORY
EGLIN AFB FLORDIA, 32542

The majority of studies pertaining to possible conflicts between the Warsaw Pact forces and NATO forces characterize such a conflict with a significant numerical superiority in aircraft and land combat vehicles on the part of the Warsaw Pact forces. Alternate studies treating the NATO force threat response suggest that to kill rate requirements, and in turn the sortie generation requirements, exceed those levels capable by NATO forces. Investigations suggest the increased air capability required is not longer achievable in aircraft heredity, nor for that manner, affordable through increase in aircraft population. It is well recognized that improved conventional munitions offered to provide the increased capability to allow the postulated threat to be managed. The large focus of attention in systems to provide leverage on the ability to attrit enemy aircraft and land combat vehicles is in the area of precision guided munitions employing passive, active, and semiactive terminal guidance with a midcourse guidance correction (Figure 1).

In the review of conventional weapon elements encompassing munitions, guided weapons, guns and rockets, aircraft integration, and explosives the community has elected to focus considerable attention on precision guided and precision fuzed guided weapons (Figure 2). Armament acquisition activities by the Navy--the Naval Weapons Center and the Naval Surface Weapons Center--the Army--the Missile Research and Development Command and the Armament Research and Development Command--and the Air Force--Armament Development and Test Center and the Aeronautical Systems Division--have all focused increasing amounts of attention on improved conventional munitions (Figure 3).

The approach currently in favor involves an evolutionary process. The current technological base is being used in the evolutionary sense of improving conventional weapon concepts through product improvement programs. The process is one of making the systems better. It is generally agreed that significant response leverage against the Warsaw Pact threat requires revolutionary concepts rather than evolutionary concepts (Figure 4). The scientific community has had difficulty in obtaining support for its revolutionary development efforts. The approach of making it different when compared to making it better is to perceive to be one of high risk. Often the spokesman for the high payoff associated with high risk development efforts remain silent. In addition, the design philosophy, even when the technology is recognized to have merit, becomes difficult to detail (Figure 5). The evolutionary process evolved as one which places focused attention on systems of increasing complexity digital systems and digital interfaces in the weapons community are providing weapon capabilities not associated with such systems in the past. The utilization of lock on after launch guided weapons incorporating federated modular digital guidance control systems offers to provide more capable, survivable and versatile ordnances. It also offers to provide complex, less understandable,

more costly ordnances (Figure 6). Consider the ever increasing role of data processing in the power offered by digital computers. It is well agreed in the community that the ability to handle large amounts of data at extremely high rates is an advantageous capability. It is also well agreed that the cost of the microprocessors and minicomputers, as well as the size of these elements, are coming down to be one entirely of space affordable. It is recognized that the cost of the software associated with such systems will increase. The fact that evolutionary processes are being applied can be found in the tendency of the desire currently to emulate analog system performance in the analog market. The true power of computer aided processing lies not in the ability to do calculations more rapidly or at a higher rate, even though this is desirous, but in the means of addressing new solutions to current problems and to effect solutions to problems heretofore not solvable. The concern relative to the computers role in a defensive process can be equated to a poll taking. Man on the street interviews at this time would find few subjects completely familiar with digital computers. The higher order language and machine codes associated with such devices, and the software packages which could be generated would be limited. Man on the street interviews ten year from now will find subjects exponentially more familiar with all of these skills suggesting that the expertise in the scientific community will have experienced even a more phenomenal growth rate. The management of the software community when everyone in the community is capable of generating software would be a major task of containment and in focusing of efforts (Figure 7).

The evolutionary concerns of the technical base are not only associated with computer systems. The trends toward making the systems more complex to the point that the fighting man in the field can no longer understand the processes involved is a concern. Precision guided munitions and precision fuzed munitions represent such complex systems and these development processes are in the genesis of their long term growth. The environmental effects as represented by concerns expressed by the environmental community relative to the use of depleted uranium projectiles and as typified by the difficulty in implementing the Pave Paws radar systems due to concerns about RF radiation levels will continue to grow. The weapons development process will become more complicated with technological, social, economic, and political issues being a concern. The affordability of conventional weapons must be associated with timely solution. Discussions with the fighting man on the front line leaves the interviewer with the belief that his concerns are focused on what can be supplied immediately to upgrade its capability not what will be offered years from now. The adage that better is often the enemy of good enough certainly can be found in consideration of the Patriot weapons system development. Patriot required nineteen years to place it in the field and during this time the Russians fielded no less than six surface to air missile systems. The duplication concerns by the various monitoring agencies in the Government are real

relative to the cost when weapons enter into production. These concerns should be less arduous when addressing a coordinated innovative R&D phase between the various weapons developers. It will be necessary for the R&D efforts to be coordinated to minimize duplication but a strong case can be made for duplication in the innovative R&D process. The coordination efforts to insure commonality in the production base between Air Force, Navy and Army systems represent the area where the most significant cost savings can be effected (Figure 8). The armament community has had difficulty in committing its product line not only to the user of those development efforts, but to the community at large. The clear articulation of the technical position often is distorted in the interpretative processes of the mass media effort, however, the mass media concerns R&D couched and some level of realism (Figure 9).

At all times it should be remembered that the dependence on technology to provide the balance of conventional force carries with it the requirement to maintain close hold on that technology. It also carries with it the requirement to maintain the differential between the national base and the base of potential adversaries. If the leverage of technological advantage is lost due to the compromise of technology the numerical superiority of enemy forces becomes a clear deciding factor. It should be remembered that Lenin himself, the founder of the competing system, coined the phraseology that there is a certain quality in quantity itself (Figure 10).

ARMAMENT TECHNOLOGY

FUNCTIONAL OVERVIEW

DR JOSEPH MAYERSAK
CHIEF SCIENTIST
AIR FORCE ARMAMENT LABORATORY

Figure 1.

CONVENTIONAL WEAPONS ELEMENTS

- MUNITIONS

  BOMBS – WARHEADS – FUZES – MINES – DISPENSERS AND DISPENSER MUNITIONS

- GUIDED WEAPONS – AIR-TO-AIR AND AIR-TO-SURFACE

  TERMINAL SEEKERS – MIDCOURSE GUIDANCE – CONTROL TECHNIQUES – INTEGRATION TECHNIQUES

- GUNS AND ROCKETS

  GUN MECHANISMS – AMMUNITION – FEED SYSTEMS – LAUNCHERS

- AIRCRAFT INTEGRATION

  CARRIAGE – SEPARATION – STORES MANAGEMENT – RACKS AND EJECTOR MECHANISMS

- EXPLOSIVES

Figure 2.

ARMAMENT ACQUISITION ACTIVITIES

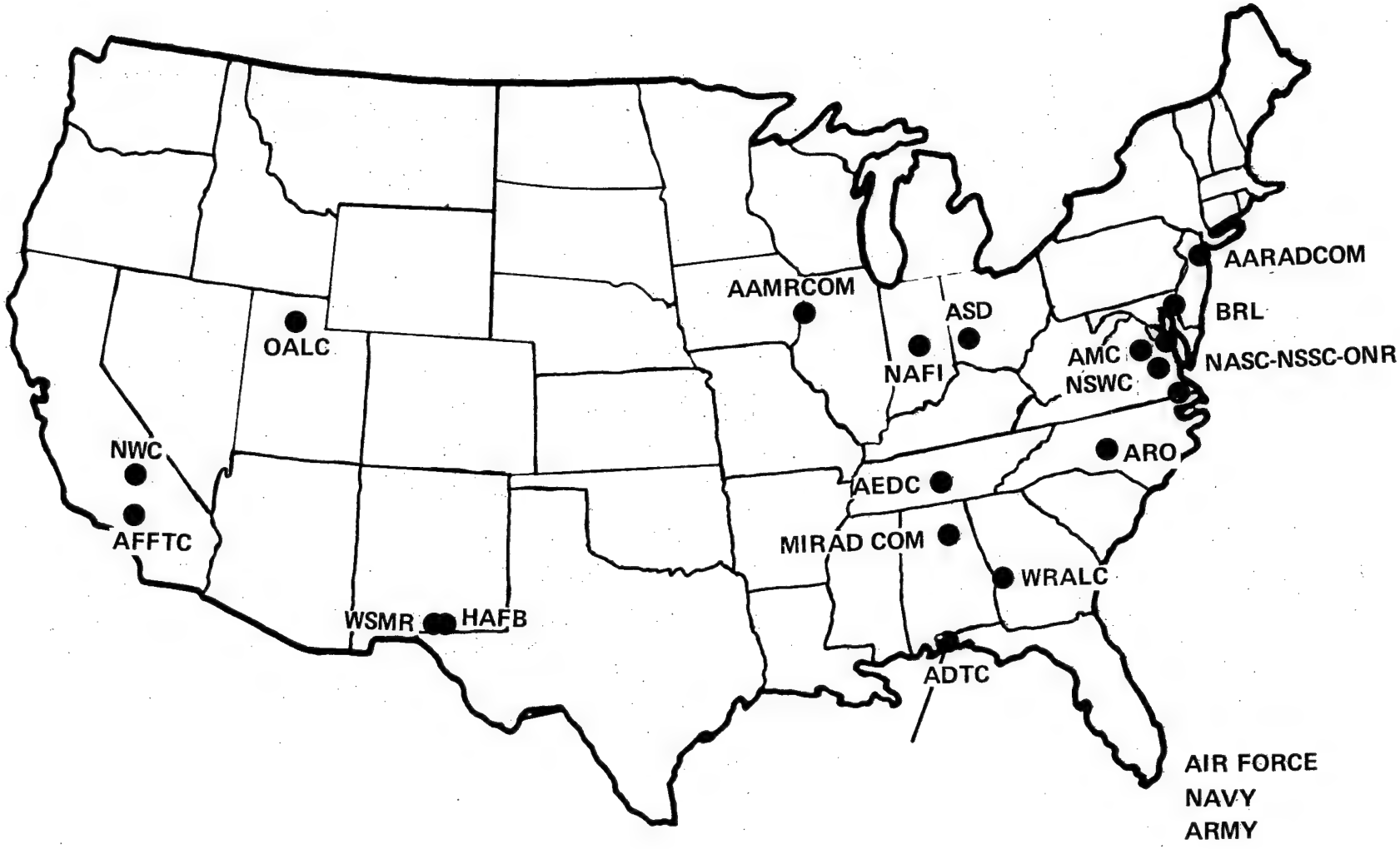

Figure 3.

EVOLUTION PROCESS

- GREATER EMPHASIS ON GUIDED WEAPONS
- DIGITAL SYSTEMS AND INTERFACES AT ALL LEVELS
- AUTOMATED FUNCTIONS
- MORE CAPABLE, SURVIVABLE AND VERSATILE
  - LOWER CROSS SECTION
  - STANDOFF
  - MODULAR COMPONENTS
  - LOCK-ON AFTER LAUNCH

Figure 4.

EVOLUTION PROCESS (CONT'D)

- AIRCRAFT INTEGRATION
  - CONFORMAL – MINIMUM IMPACT ON AIRCRAFT CAPABILITY
  - DIGITAL AIRCRAFT – WEAPON COMMUNICATION LINK
- EXPLOSIVES
  - LESS SENSITIVE
  - HEAT RESISTANT

Figure 5.

EVOLUTION PRODUCTS

- MUNITIONS
  - GREATER USE OF COMPUTER AIDED MODELING
    - HYDRO CODES
  - MORE SENSOR DIRECTED WEAPONS
- GUIDED WEAPONS
  - DIGITAL INTEGRATION
  - MORE CAPABLE SENSORS
  - IMBEDDED MICROPROCESSORS
  - INCREASED RELIABILITY
- GUNS
  - NEW LIGHTER WEIGHT MECHANISMS
  - MORE CAPABLE AMMUNITION

Figure 6.

EVOLUTION CONCERNS

- COMPUTER ROLE
  - CURRENT IMAGE
    - INCREASED DATA HANDLING GOOD
    - DIGITAL INTERFACES ARE GOOD
  - ACTUAL SITUATION
    - ANALOG TECHNIQUES BEING IMPLEMENTED DIGITALLY
    - INTERFACE STANDARDS AND CONTROL NEEDED
      - POTENTIAL MANAGEMENT NIGHTMARES
  - FUTURE
    - UNIVERSAL ACCEPTANCE
      - EVERYONE A PROGRAMMER
    - SOFTWARE MANAGEMENT
    - DIGITAL THEORY
    - MANAGEMENT CONTAINMENT EFFORTS
      - HOL
  - COMMERCIAL EXPLOSION

Figure 7.

EVOLUTION CONCERNS

- SYSTEM COMPLEXITY
  - INCREASING WITH IMBEDDED MICROPROCESSORS
- PRECISION GUIDED MUNITIONS AND SENSOR AIMED WEAPONS
  - JUST SCRATCHING SURFACE
- ENVIRONMENTAL EFFECTS
  - PAVE PAWS SYNDROME
  - DEPLETED URANIUM
- AFFORDABILITY

Figure 8.

OLIPHANT

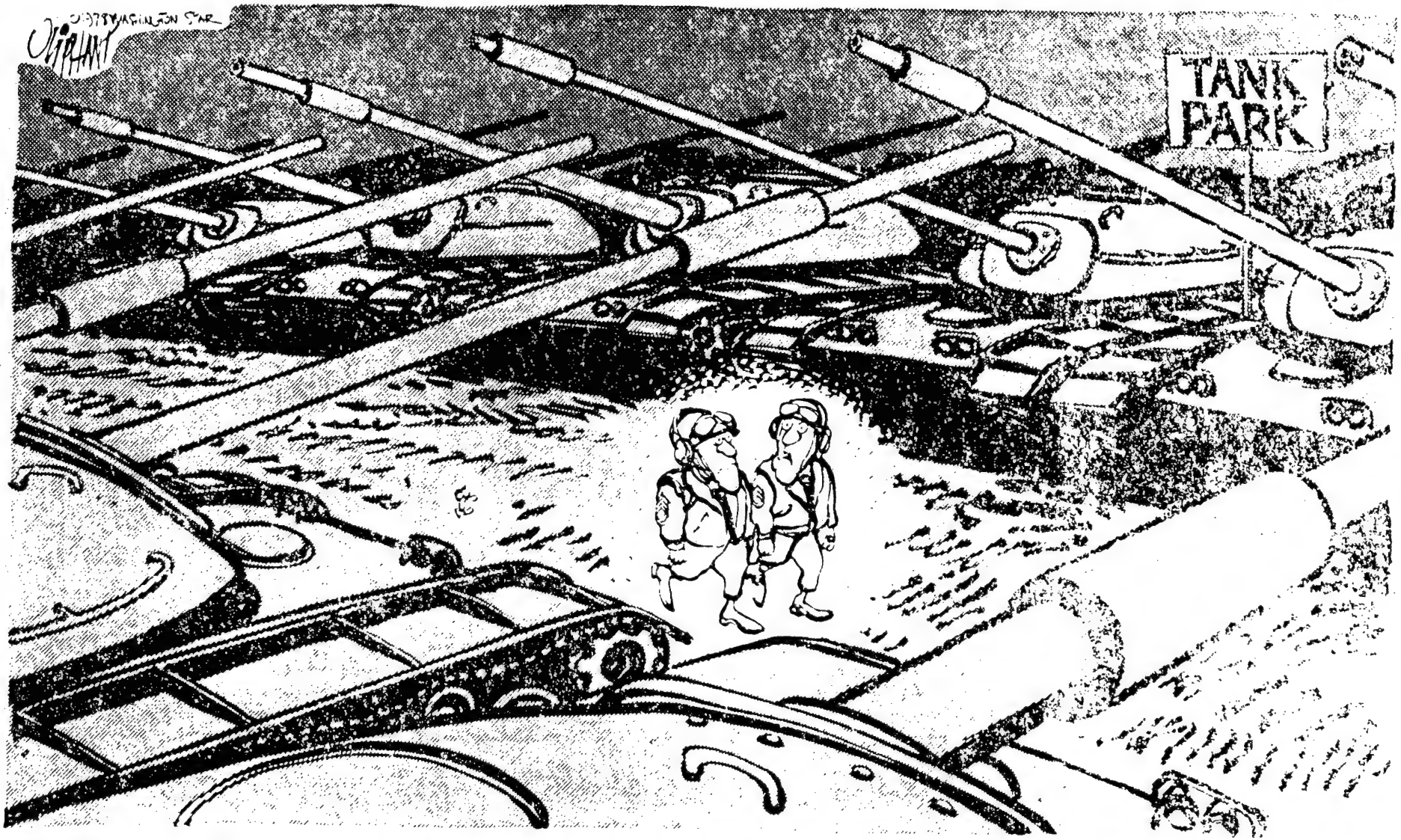

"I keep telling myself the Pentagon would never expose us to dangerous radiation levels – but how is it they've given us uranium bullets and we're starting to glow in the dark?"

CONCLUSION

- WEAPONS DEVELOPMENT WILL BE MORE COMPLICATED

- ISSUES
  - TECHNICAL
  - SOCIAL
  - POLITICAL
  - ECONOMIC

Figure 10.

BIOGRAPHICAL SKETCH

Dr Joseph R. Mayersak currently is the Chief Scientist of the Air Force Armament Laboratory. He has held positions as Senior Program Manager with Honeywell, Inc and Manager-Advanced Systems, LTV Aerospace Corporation in the areas of precision guided and sensor fuzed munitions. He has extensive design and test experience relating to IR and Millimeter Wave Seeker Systems. He has held academic positions at Michigan Technological University and Rice University, and he has been associated with Applied Physics Laboratory, John Hopkins University and has been a consultant to the US Army Research Office, US Army Tank Research and Development Command, US Air Force Armament Laboratory and HEW. He has a BSME and MSME degree from Michigan Technological University and holds his Doctorate in Mechanical and Aerospace Engineering from Rice University.

Dr Mayersak is a Registered Professional Engineer in Michigan, listed in Who's Who in the Midwest, Who's Who in American Men and Women of Science, Dictionary of International Bibliography and is an honorary member of Pi Tau Sigma and the Society of the Sigma Xi.

THE DIGITAL INTEGRATING SUBSYSTEM - MODULARITY, FLEXIBILITY & STANDARDIZATION OF HARDWARE AND SOFTWARE

BY

Mr. Davis L. Gardner

Guided Weapons Division
Air Force Armament Laboratory
Eglin AFB, Florida

The Digital Integrating Subsystem (DIS)
Modularity, Flexibility, & Standardization
Of Hardware And Software

Abstract

With the development of the microcomputer and other digital LSI components, many functions within tactical guided weapons that were once performed using analog techniques and components can now be accomplished digitally. Many complex algorithms once considered too bulky and time consuming are being considered again in the light of the increased computational capability offered by microcomputers. There is currently an influx of new digital computers available for use in everything from microwave ovens to sophisticated weapon guidance systems. With these computers has come a host of different digital interfaces, languages, and software support packages.

In the "analog" days standardization was difficult if not impossible to accomplish. Almost every system improvement meant a new point design. The same situation can occur now in the "digital" world if standards are not developed and adhered to in the design of digital hardware and software.

The Digital Integrating Subsystem (DIS) is a new technology program which will demonstrate the effectiveness of establishing standards for software and hardware in digital subsystems for tactical guided weapons. The computing load required by these subsystems can be performed either by one large, very fast, expensive central computer or it can be distributed among two or more less capable and less expensive computers. In distributing the computing requirement among a federated family of computers, a communication conduit and signal protocol must be established between the computers. The conduit and protocol requirements can be accomplished by extending the internal computer bus or by providing a serial time division multiplex bus between the computers.

The DIS includes a federated family of microcomputers internal to a guided weapon. Each of these computers is functionally dedicated to perform the computational tasks

of a particular subsystem (i.e., guidance, autopilot, etc.). The computers communicate with each other on a standardized, time division serial multiplex data bus in accordance with a rigid protocol of signal structure while communicating with their respective subsystems over standardized peripheral interfaces. The DIS is designed to accommodate multiple weapon configurations and is capable of handling the processing load of the "core avionics" functions of these tactical guided weapons. Standard software languages and retargetable compilers will further yield flexibility, and aid in reducing life cycle costs through standardized software support equipment.

All of the above-mentioned technical capabilities must come with reduced cost. The DIS concept will result in lower costs through standardized software, signal protocol, interfaces, support equipment and a truly flexible and modular system design approach.

1.0 Introduction

The cost to procure and support a variety of tactical weapons is directly proportional to the degree by which the guidance subsystem design was influenced or controlled by requirements for modularity, standard communication protocol, standard hardware interfaces, standard software languages and the use of non-proprietary computer architectures. The above listed requirements would not have been applicable to the older analog subsystems used 3 to 5 years ago. It is very difficult to modularize a weapon which uses analog implementation in the various subsystems because the various subsystems are designed for a particular mission profile. The cost to perform a retrofit on this style weapon is usually prohibitive. Usually a change to an "analog" style weapon ripples throughout the weapon and causes a massive and expensive wiring harness change. A totally "analog" weapon offers little modularity and flexibility for future improvements, not to mention the cost associated with field support. In many instances the field support philosophy employed has been one of the large contributors to the life cycle cost.

Cost alone should drive the designers of guidance subsystems to the use of digital components and techniques. An added benefit with digital design is modularity and flexibility: systems can be built that are capable of performing more than one task, and can be easily reprogrammed to accomplish these different tasks.

With the advent of the microprocessor and other digital chip developments such as A/D converters, D/A converters, S/D converters, etc., many functions can now be accomplished more efficiently and with greater accuracy than with analog components. The use of the digital devices alone does not solve all the problems associated with digital type systems. In fact the proliferation of interfaces in the new digital explosion is as wide spread as in the analog world. Along with these new digital "super circuits" there must be standardized interfaces, signal structure protocol, and software languages and compilers. These standardized techniques and hardware must be created to insure optimum efficiency, modularity, and flexibility throughout the system. This is the intent of the DIS development effort.

The DIS is being structured such that a basic weapon can be missionized through software changes and the replacement or addition of different subsystems through standard

hardware interfaces. The DIS described herein has been configured to illustrate that tactical weapon systems can be configured to offer modularity of function, hardware, and software.

2.0 Digital Integrating Subsystem (DIS)

2.1 Objective

One of the key words used in expressing the objective of the DIS is "standard". It should be pointed out that to standardize just for the sake of standardizing will not work on all systems and is not the intent of the DIS program. The objective here is to standardize at a level which does not inhibit technology growth.

The objective of the DIS program is to develop a tactical weapon guidance system that offers modular functional capability, modular hardware design, and modular software capabilities through the use of standard High Order Language (HOL) software, standard subsystem interfaces, standard computer architecture, standard serial digital multiplex data bus and standard signal protocol. The design of the DIS has been influenced by each element of the above stated objective.

This objective has been selected to help deter the development of "independent" guidance systems and subsystems. An "independent" guidance system is defined as a guidance system that is developed for a specific weapon or form of weapon and is unique from tailpipe to nose cone. It is a guidance system which does not share modules or subsystems used in other "independent" weapon guidance systems, and usually purchased from a sole source contractor.

Legitimate questions might include, "why not develop 'independent' weapon systems?"; and, "why should various weapon systems share common modules?" The answer is cost. By developing modular subsystems for use in a variety of weapon systems the development (nonrecurring) and production (recurring) costs can be reduced. For example, if company "X" develops a weapon guidance system that is of the "independent" type, this company has spent large amounts of money developing a unique guidance processor, weapon communication bus, inertial guidance system, and sensor/seeker. The uniqueness of this contractor's approach places him in a sole source position. This development cost is not warranted

since the use of modular subsystems developed under the DIS concept would eliminate this high cost sole source position.

2.2 Rationale

The long term "game plan" is to develop weapon guidance subsystems that can be produced in large quantities in a competitive climate. If an "independent" guidance system is accepted for the Air Force inventory, the developer of this system has a sole source position and his bid price for production units will so indicate this enviable position. However, by using the standard interfaces, hardware, signal protocol, architecture, and software developed in the DIS, each guidance system can be procured competitively, thus reducing the total weapon system cost. Also, these subsystems will be purchased in larger quantities (several weapons using the same modules) reducing the total system cost.

There is another advantage to the DIS concept and that is the reduced life cycle costs of weapon systems through reduced logistics costs. The non-proliferation of modules, software, and subsystem configurations makes modular weapons more maintainable thus reducing logistics costs. The reduction in the proliferation of different support software would alone make a significant reduction in the logistics costs.

Currently there is not a digital "standard" encompassing computer architecture, digital multiplex data bus, digital interfaces, signal structure protocol and software for use within the tactical weapon. All of these techniques are being addressed and controlled for the first time through the DIS.

The very nature of a totally digital weapon guidance system is that it easily lends itself to the incorporation of future advances in technology. This is further enhanced by the continued advancement in LSI digital processing components.

The DIS as described herein allows the guidance system to be reconfigured to fit different weapon/target scenarios. The DIS even allows the choice of the number and power of digital computers used in various guidance system configurations. The digital approach is also in step with the digital

techniques currently being used in aircraft avionics, flight control, and communication. Digital avionics in both weapon and aircraft allows for easy interface between the two for weapon initialization and targeting.

2.3 History of DIS Concept

2.3.1 Digital Guided Weapon Technology (DGWT)

The development of the DIS concept and the organization of the program office at AFATL is illustrated in Figure 1. The first investigative and development work was performed under the Digital Guided Weapon Technology program. The objective of that program was to investigate the utilization of microprocessors in the digital autopilot role of tactical weapons. The work performed in this effort was centered around a single very high speed central processor that would perform the autopilot functions and have some growth capability to work some other functions associated with other subsystems within the weapon (i.e., LORAN receivers, etc.). A digital emulation of an existing analog autopilot was developed and transitioned to the GBU-15 SPO. This unit, known as the Weapon Control Unit (WCU), performed the digital autopilot function as well as several other weapon subsystem functions associated with the control of discrete functions within the GBU-15. The WCU was designed as a high speed central processor with special function I/O interfaces which allowed it to fit into what was previously an all analog type weapon.

2.3.2 DPAP - The Digital Processing and Partitioning (DPAP) contract was initiated in late 1976. The purpose of this contract was to provide the AFATL with development specifications for a digital processing subsystem for a family of tactical air-to-surface weapons. This digital processing subsystem included digital computers and a multiplex data bus, and was later called the DIS.

This study and specification development was performed by Charles Stark Draper Laboratory Inc. (CSDL). The output from the Digital Guided Weapon Technology program, along with various postulated weapon configurations performing in certain scenarios were used as the basis for performing a partitioning analysis, determining computer processing load requirements, and establishing weapon multiplex bus requirements. The requirements for DIS were formulated from these perceived weapon system requirements, from aircraft avionics

development programs, and from the National Committee for MIL-STD-1553A Update. It was important that the DIS specification development have inputs from both the weapon systems developers and aircraft avionic systems developers because of weapon-aircraft interface requirements prior to weapon launch.

2.3.3 In-House Efforts

Prior to the issuance of the RFP for the DIS and after completion of the study performed by CSDL a limited amount of in-house hardware and software work is being performed. A breadboard hookup of 5 terminals communicating on a time division multiplex bus has been designed and partially fabricated. The purpose of this in-house effort is to get some "hands on" experience with techniques recommended by the CSDL study and called out in the DIS specification.

At this point in time the breadboard hookup has not been completed. However, the in-house configuration will consist of 3 ea LSI-11/Ms and 2 ea LSI-11s functioning as the DIS computers for 5 subsystems communicating on the serial multiplex bus. Software written in FORTRAN will be developed on a PDP-11/03 development station. Various bus interface unit designs and multiplex bus techniques will be tested using this in-house equipment. At a later date JOVIAL J73/I capability will be added.

The DIS configuration and the rationale for this configuration is developed in the following pages.

2.3.4 Future Application

After the current DIS effort is completed, the verified specifications will be available for application to some future weapon guidance system or will be the basis of a retrofit to an existing system.

2.4 DIS Technical Description

2.4.1 Functional Requirements

Figure 2 illustrates some typical functions that must be performed by digital subsystems located within a tactical air-to-surface weapon. The question that immediately arises is just how all of these functions are to be accomplished in

the most efficient manner. As a result of the partitioning work performed by CSDL the functional requirements were determined to be most effectively distributed as shown in Figure 3.

In the process of determining which form the functional requirements would take, it was necessary to consider the various forms of computer system architecture. These are Central, Distributed, and Federated. Figure 4 illustrates the generic form of a Central System architecture. Here one very fast (and expensive) digital computer communicates with the various subsystems that make up a typical air-to-surface weapon guidance system. The communication network is required to handle the total data and information flow between all subsystems and the centrally located computer. This requires that the traffic density be very high on the communication network. The traffic density is so high that it would require a parallel bus with a multi-level priority interrupt capability. This is the technique employed in the DGWT effort previously mentioned. The processor used there required a throughput capability of 3 million equivalent adds per second. In order to optimize this architecture and reduce dead time due to the movement of data on the communication network, fiber optic techniques were proposed.

Figure 5 illustrates the Distributed Systems architecture. In this form there are a number of computing elements and some number of subsystems. Again, the communication network is located between the computing elements and the subsystems. This system architecture form also requires rather high speed communication paths be established between the subsystems and the computing elements. Depending upon detailed requirements, the number of computing elements may be less than, equal to, or greater than the number of subsystems. Usually a communication path is established between each computing element and each subsystem. In some utilizations of this architecture the computational tasks required by a particular subsystem may be executed by any one of the computing elements. This concept requires that the operational software be duplicated in all of the computers used to service the same subsystem.

The system architecture selected as the optimum for the DIS is the Federated System architecture. This form is illustrated in Figure 6. The communication network in this architecture provides data paths between the computing elements only. Industry standard interfaces are used

between a computing element and its associated subsystem. The traffic density on the communication network is very low and can be handled using a serial time division multiplex bus. Usually no raw data is passed across the communication network. All raw data is passed between the computing element and its associated subsystem.

There are several advantages to the Federated System architecture:

- lower bus traffic density

- standard interfaces to the bus from the computing elements

- simple serial time division multiplex communication network (bus)

- standard processing elements

- standard interfaces between the subsystems and processing elements

- very flexible and modular system

- lower logistics costs

- optimized software per computing element

- easily converted to embedded computing elements using same software and communication network

As technology advances in the production of more compact computing elements, the Federated System architecture can be easily converted to an Embedded System. This architecture is shown in Figure 7.

The functional requirements typical of an air-to-surface tactical weapon were illustrated in Figure 2. These same functional requirements are partitioned for accomplishment under a Federated System Architecture. This is the system architecture chosen for DIS.

Actually the Embedded System architecture has some advantages over the Federated approach since the interfaces between the computing element and subsystem are not required.

This form of system architecture was not chosen at this time since many of the subsystems have not been developed and it is not necessary to use the Embedded architecture to demonstrate the attributes of the DIS concept. As the microprocessor technology advances it will be easy to convert the Federated System into an Embedded System. This easy conversion would be almost impossible to accomplish without a complete system redesign if the Central or Distributed System architecture had been selected.

Another advantage of the Federated System architecture is that it can operate as part Federated and part Embedded during the transition period.

2.4.2 DIS Hardware Configuration

The components of the DIS are discussed below. The major hardware components are the computing element (microcomputer), the communication network (bus), and the Bus Interface Units (BIU).

2.4.2.1 DIS Microcomputers

The number of microcomputers required in a typical DIS configuration depends on the complexity of the guidance system being implemented. Figure 8 illustrates a generic system block diagram. This system configuration contains 5 DIS computers. Each computer communicates with the bus via a Bus Interface Unit (BIU). The general requirement placed upon the DIS computer is that it be compact, lightweight, reliable under extreme environmental conditions, and have a moderate to high processing throughput. Under the first contracted effort, it is required that the DIS computer not be a newly developed item requiring a new CPU chip be masked and produced. This approach was chosen to illustrate that current chip technology can be used to obtain the required computer architecture.

Several factors were considered in establishing the specification of the DIS computer. Among these were size, environment, architecture, peripheral interfaces, available computer families, programming language, software support, and hardware techniques. Each of the above had to be considered relative to the scenario the DIS would be employed in and the impact on logistics associated with supporting the DIS in the field. Other factors which will affect the final computer architecture include chip technology instruction set, addressing modes, memory organization, register

organization, address space, interrupt structure, word length, and throughput.

As a result of the above considerations the selected DIS computer architecture requires two separate computers. These are referred to as Class I and Class II computers. Actually, the architectures are very similar with the main differences being in throughput and hardware floating point capabilities.

Several instruction mixes were considered. In order to agree on the most applicable mix and to have something firm to base performance measurements against, the instruction mix for DIS has the following constituents:

Load and Store	36%
Add/Subtract	14%
Multiply	6%
Divide	1%
Shift	4%
Logical	8%
Test and Branch	30%
I/O Control	1%

Using the above instruction mix the Class I computer is to have a throughput of 150 Kops and the Class II computer is to have a throughput of 500 Kops. The mixture of Class I and Class II computers in a particular system will depend upon the complexity of the subsystems making up the weapon guidance system. The other salient characteristics of the DIS computers are given in Table I.

Without going into the complete specification of the DIS computer some of the other requirements are discussed below.

The DIS computers shall be upward compatible--that is, software written and executed on the Class I computer shall execute on the Class II computers. The same set of support software will thus support both computers. The hardware

TABLE 1

DIS Computer Requirements

	CLASS I	CLASS II
Throughput (instruction mix)	150 KOPS Minimum	500 KOPS Minimum
Instruction Times (Max.)		
ADD	3.0 usec	0.75 usec
SUBTRACT	3.0 usec	1.0 usec
MULTIPLY	16.0 usec	8.0 usec
DIVIDE	24.0 usec	12.0 usec
LOAD	3.0 usec	0.75 usec
BRANCH	4.0 usec	1.5 usec
LOGICAL AND	3.0 usec	1.5 usec
DATA IN/OUT	3.0 usec	1.0 usec
Floating Pt. Option MULT	90.0 usec	45.0 usec
Floating Pt. Option DIV	90.0 usec	45.0 usec
Computational Precision:		
Fixed Point Arithmetic	16-bit	16-bit
Double Precision	YES	YES
Floating Point Arithmetic	24-bit mantissa*	24-bit mantissa*
	6-bit exponent	6-bit exponent*
Addressing Modes		
1) DIRECT	YES	YES
2) INDEXED	YES	YES
General Registers	8 Minimum	8 Minimum

TABLE 1 (Continued)

Interval Timers:		
Type A (100 usec to 1 sec)	YES	YES
Type B (10 usec to .1 sec)	Not Required	YES
Interrupt Capability	8-LEVEL	8-LEVEL
Memory Space:		
RAM Minimum	4096 words	4096 words
Expandable to	32768 words	32768 words
ROM (PROM, EAROM) Minimum	4096 words	8192 words
Expandable to	32768 words	32768 words
Input/Output		
SERIAL	500,000 bits/sec	500,000 bits/sec
PARALLEL	100,000 words/sec	250,000 words/sec
DMA	500,000 words/sec	500,000 words/sec

Note: All rates and capacities are expressed for a 16-bit word length except for the floating point option.
*Plus one sign bit

floating point capability shall be a removable option for both DIS computers to allow increased flexibility. For real time applications, two timers shall be available--one having a resolution of 100 microseconds and one have a resolution of 10 microseconds. Both computers shall operate from RAM and ROM for optimization of firmware interchangeability. Each DIS computer is limited to a total volume of 150 cubic inches, to weigh not more than 6 pounds and to consume no more than 40 watts power.

In order to interface with a variety of guidance system subsystems three types of I/O interfaces are provided for each computer, these interfaces will function with each computer. The I/O cards are (1) bit-serial, (2) bit-parallel (direct memory access), and (3) bit-parallel (programmed I/O). A fourth I/O card is designed to provide an interface between the DIS computer and the MIL-STD-1553 serial multiplex bus that is a part of the aircraft avionics. The DIS computer designated the "Bus Controller" contains this I/O capability. (Refer to Figure 8).

2.4.2.2 Serial Time Division Multiplex Bus

As discussed earlier the Federated system architecture requires that the communication network be provided between the computing elements. Figure 8 illustrates this "bus". The term "bus" as applied here includes the physical transmission medium, the bus interface units (BIU), and the bus supervisor. One of the BIUs is usually assigned the bus supervisor role.

2.4.2.2.1 Concept

The bus is designed to operate under a "round robin passing protocol" concept. Using this technique each subsystem will be given control of the bus in turn; however, only one BIU shall transmit at a time. For a given weapon configuration, the order in which BIUs transmit is fixed. Each BIU determines its time for transmitting by recognizing the end of transmission (EOT) of the BIU that is designated to precede it. Without any data to transmit the BIU will transmit its ID and EOT so that bus control can be automatically transferred to the next BIU in sequence. Figure 9 illustrates this concept. Under this structure bus operation is asynchronous and control of the bus is dynamic.

2.4.2.2.2 Characteristics

Signals are transferred over the bus in serial digital form using Manchester bi-phase level modulation. A logic "1" is transmitted as a bipolar coded signal (i.e., a positive level followed by a negative level). A logic "0" is also a bipolar coded signal (i.e., a negative level followed by a positive level).

The bit rate is 1 million bits per second. A total of 20 bits form a word. A word consists of 16 information bits, 3 syc bits, and a parity bit. Figure 10 illustrates the three word formats used in the DIS. The most significant bit is transmitted first with the less significant bits following.

The three types of words transmitted are the beginning of message (BOM), the end of transmission (EOT), and the data words. The BOM and EOT are the only control words required. The three bit time periods for the sync waveform is unique in that during this time period (3 u sec.) an invalid Manchester waveform is transmitted. The waveform is positive for the first half of the time period and negative for the last half of the time period.

Information is transmitted by one or more continuous messages terminated by an EOT. Each message can be of a different length (number of data words), however, no single message may exceed 34 words including control and data words. Figure 11 illustrates a transmission including several messages.

There is a break between the time when one BIU completes a transmission and the time before another BIU starts to transmit. This intertransmission interval is set at a maximum of 4 microseconds. This "dead time" allows the bus to settle between the end of one transmission and the beginning of the next. Figure 12 illustrates this interval.

The physical transmission medium consists of a two conductor twisted, shielded, jacketed cable. The line to line distributed capacitance is held to less than 30 picofarads per foot with a nominal characteristic impedance of 75 ohms at a measurement frequency of 1 MHz. The shield on this cable is to provide a minimum of 75% coverage. The attenuation is limited to 1.5 dB per 100 ft. and it is

required to meet the EMC requirements of MIL-E-6051. Due to the overall length of the bus, (approximately 20 feet maximum) the use of unterminated stubs are allowed. The load of a "listening" BIU presents a load on the line of not less than 1,000 ohms (line-to-line).

At the present time wire cable is planned, however, work will be undertaken in the next few years to investigate the use of fiber optic transmissions. This form of data transmission should have a higher level of EMP immunity.

The BIU provides the interface between the subsystem and the transmission medium. In most instances, the BIU will be embedded in each subsystem. The BIU has sufficient "smarts" to handle the decision processes associated with maintaining the round-robin communication sequence and performing error detection on the received messages. The output of the BIU to the various subsystems will be transferred over an interface structured to meet the I/O requirements of that particular subsystem.

The largest function performed by the BIU is bus supervision. The bus supervisor has the responsibility for assuring continuous and proper operation of the round robin passing protocol. It knows the correct round robin sequence and will keep track of the last identifiable transmission. After a dead period of 8 microseconds, the bus supervisor BIU will restart the round robin sequence by transmitting the EOT word pertinent to the last identifiable transmission. If this does not result in the round robin sequence being restarted, the supervisor BIU will transmit the EOT word for the BIU next in sequence in an attempt to get the sequence working again. The bus supervisor continues to step through the EOT words of all BIU in sequence until transmission is reestablished. The bus supervisor reinitiates operation of the bus upon power application and after power interruptions. The microcomputer functioning as the bus supervisor is the interface point between the weapon bus and MIL-STD-1553 bus that is located within the aircraft. Figure 13 illustrates the hierarchy of bus structures. The interface point with all the illustrated buses is through the bus controller for that particular bus.

Each BIU contains the self test circuitry necessary to stop a transmission if the transmission time exceeds the maximum time allowed for 34 words.

2.4.3 DIS Software

In order to provide the total system modularity required of the DIS, it is necessary that the application software and support software not be a restrictive factor. Software is constantly becoming the cost determining factor associated with digital system implementation in the Air Force. Figure 14 illustrates this trend.

There are several approaches that can be taken to control this cost driver. These include (1) the use of High Order Language (HOL), (2) limit the number of HOLs that can be used, (3) control the DIS microcomputer architecture through standards and specifications, (4) prevent the use of proprietary computer designs, and (5) reduce the cost and quantity of compilers through the use of retargetable compilers.

2.4.3.1 High Order Language

It is almost impossible to obtain enough assembly language documentation to insure the transportability of an assembly language program from one computer to another. Usually an assembly language programmer will perform tricks in the assembly program to make the program more efficient for a particular computer. These tricks and the machine dependent attributes of the program make the program very difficult to document and make it impossible to transport to another computer without a program rewrite.

Programs for use in the DIS will be written in an HOL in accordance with AFR 800-14 and AFR 300-10. These programs may require more memory space than the equivalent assembly language programs, but they will be well documented and transportable to other computers that operate with the same HOL. The HOLs approved are FORTRAN IV, JOVIAL J3, JOVIAL J73, COBOL, and PL/I.

There has been much speculation about the inefficiency of HOLs as compared to assembly languages. The AFATL is currently planning an experiment where already existing assembly language program modules will be rewritten in JOVIAL J73 and be executed on the same original computer. The results from this experiment will provide evidence as to the measure of efficiency of the HOL. The modules to be rewritten are typical of software used in tactical weapons.

The larger memory space required for HOL implementation is not a hard cost driver since advancing technology in solid state memory is reducing costs in this area.

The whole picture related to use of a HOL may be improved with the development of HOLs that are more applicable to guided weapon functions. JOVIAL J73/I is more applicable in this respect than FORTRAN IV. Other more powerful language and compilers are now on the horizon such as DOD-I.

2.4.3.2 Computer Architecture Control/Proliferation

The use of the DIS specification to procure computers prevents the contractor from selling to the Government their proprietary computer. This means that there will always be a competitive environment in which to procure computers because the architecture called for in the DIS specification is a non-proprietary, Air Force owned architecture.

2.4.3.3 Retargetable Compilers

Most compilers generated to date have not been retargetable. This means that a new compiler had to be generated for each new computer required to accept a particular HOL. The cost of generating a new compiler was prohibitive for some programs. This meant that the program was forced to another computer or was forced to live with the restriction of the assembly language. There has been a change in the structure of compilers. Some compilers generated today are modular; that is, the compiler is broken up into sections. Figure 15 illustrates the difference between a conventional compiler and a modular compiler.

The conventional compiler does not have the proper structure for retargeting. The modular compiler, as the name implies, is composed of a scanner module, a parser module, and a code generator module. The retargeting process is primarily concerned with the code generation portion of the compiler. The compiler that is resident in computer A can be retargeted to computer B by writing only a code generator for computer B and combining it with the original parser and scanner. This removes the necessity of creating a whole new compiler for computer B. (See reference 2) The JOVIAL J73/I is a retargetable compiler. This compiler is now resident in the AFAL DEC-10 computer. It can be retargeted to other computers (microprocessors) as illustrated in

Figure 16. The cost of retargeting the J73 compiler to these 3 computers is much less than creating 3 totally new compilers. The DIS computers are candidates for this retargeting process.

The other benefit of using retargetable compilers is that HOL programs can be generated on large fast computers such as the DEC-10. The output of the DEC-10 is then a machine code source program for the smaller microprocessors.

By using HOL, top down structuring of the application programs, DIS computers, and retargetable compilers, a very high level of flexibility modularity, and standardization is available at competitive costs.

2.4.4 Typical Application of DIS

Figure 17 illustrates a typical application of the concepts that have been discussed in this paper. Five DIS computers are used in this configuration. This particular guidance concept uses a Low Cost Inertial Guidance Subsystem (LCIGS) updated with velocity and position data from a Tactical Global Positioning System (TGPS) Class M receiver. Initialization of the weapon guidance system is accomplished via the MIL-STD-1553 interface of the DIS supervisor computer with the aircraft prior to weapon launch. Should the weapon application not require the use of the TGPS Class M receiver, it and its associated DIS computer (Navigation Aiding Management) would simply be removed from the weapon without changing the configuration of the remainder of the system.

Some other form of velocity/position updates could be substituted for the TGPS Class M receiver. In this case software modules (firmware) would be swapped out in the NAM computer, and the reconfiguration of the system would be essentially complete.

2.5 Payoff

By using the DIS concept to attain total digital weapon guidance systems, "before-the-fact" standardization is achieved. Payoff to the Air Force includes:

(1) Decreased costs

(2) Enhanced modularity

(3) Easy missionization

(4) Increased effectiveness

(5) Simplified maintenance

(6) Increased flexibility

(7) Transferability of algorithms

(8) Nonproliferation of design concepts.

REFERENCES

1. Nathan, McCoy, Kalomiris, Kubic, Rye, Digital Processing Analyses/Partitioning, Charles Stark Draper Laboratory Final Report R-1122.

2. Bladen, Capt James B., Modular Compiler Retargeting for Microprocessors. NAECON 1978 Volume 3.

3. Draft MIL-STD-XYZ, Weapon Internal Time Division Multiplex Data Bus. AFATL/DLMM, Eglin AFB, FL.

4. Modular Digital Missile Report. ONR Report CR-233-052-3, 4 May 1977.

5. The Analytical Sciences Corp. Report No. 2189, Hardware Probe for Software System Testing, April 1975.

6. Professional Development Seminar, Military Software, Wright-Patterson AFB, OH, July 1972.

7. Digital Integrating Subsystem Program Documentation (SOW, RFP, etc.) AFATL/DLMM, Eglin AFB, FL.

8. Gardner, Davis L., The Case for Modularity of Tactical Weapon Guidance Systems. 10 Nov 1976. AFATL/DLMM, Eglin AFB, FL. (Unpublished Paper)

Page 1471 Blank

DIGITAL WEAPON INTEGRATION

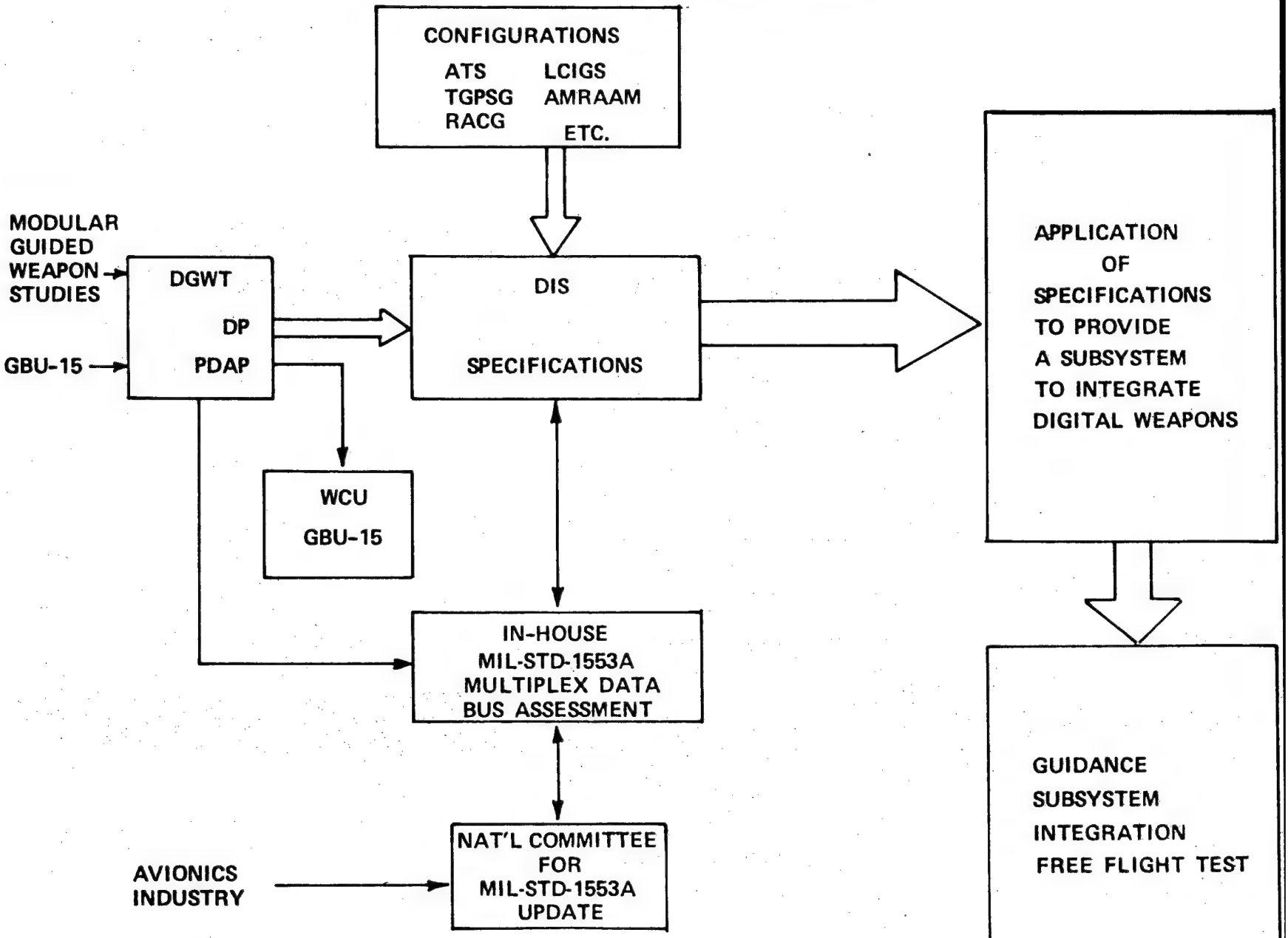

FIGURE 1
UNCLASSIFIED

TYPICAL GUIDED WEAPON DIGITAL COMPUTING REQUIREMENTS

FUNCTIONAL PARTITIONING

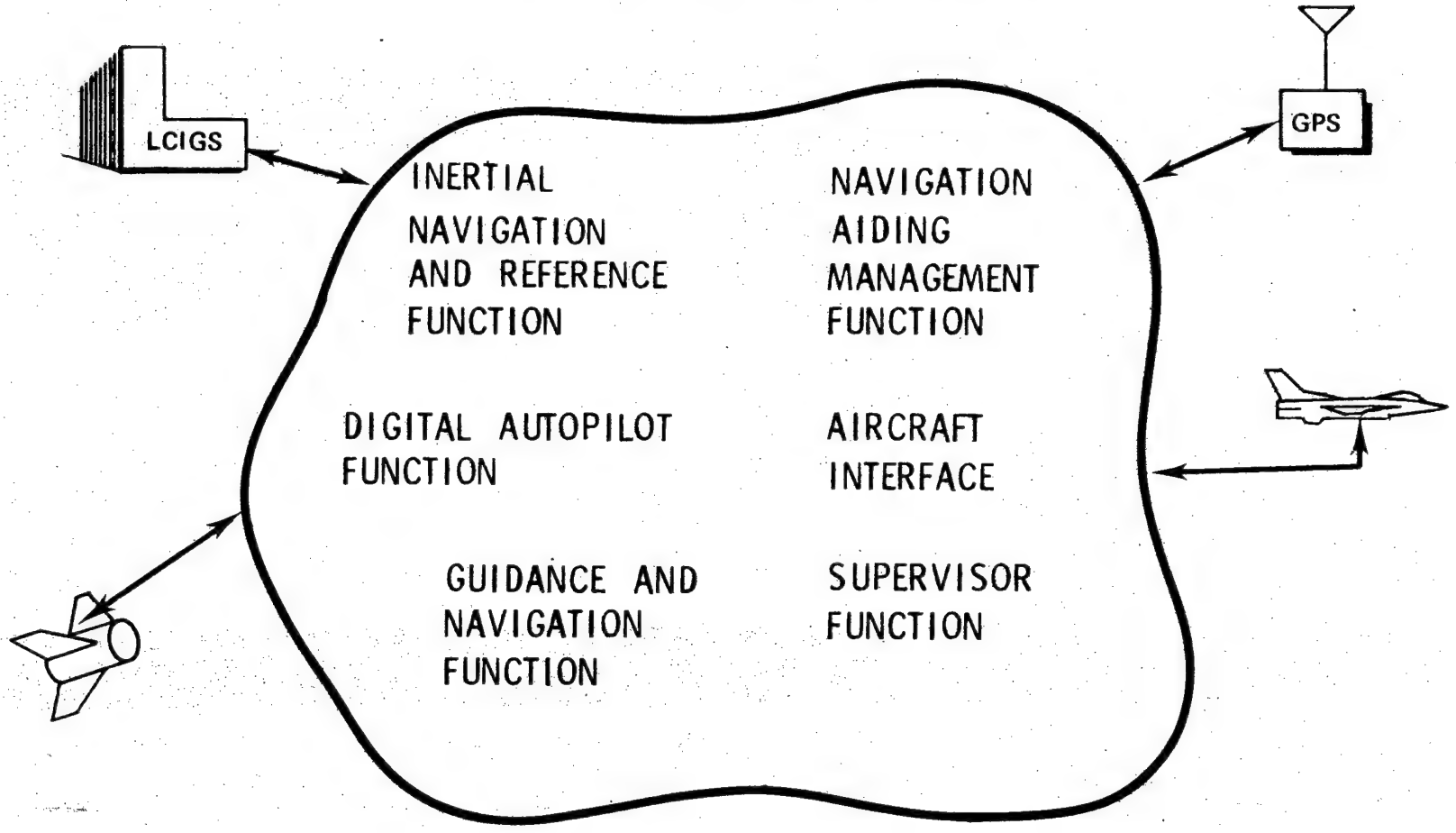

1473

FIGURE 2
UNCLASSIFIED

TYPICAL GUIDED WEAPON DIGITAL COMPUTING REQUIREMENTS

FUNCTIONAL PARTITIONING

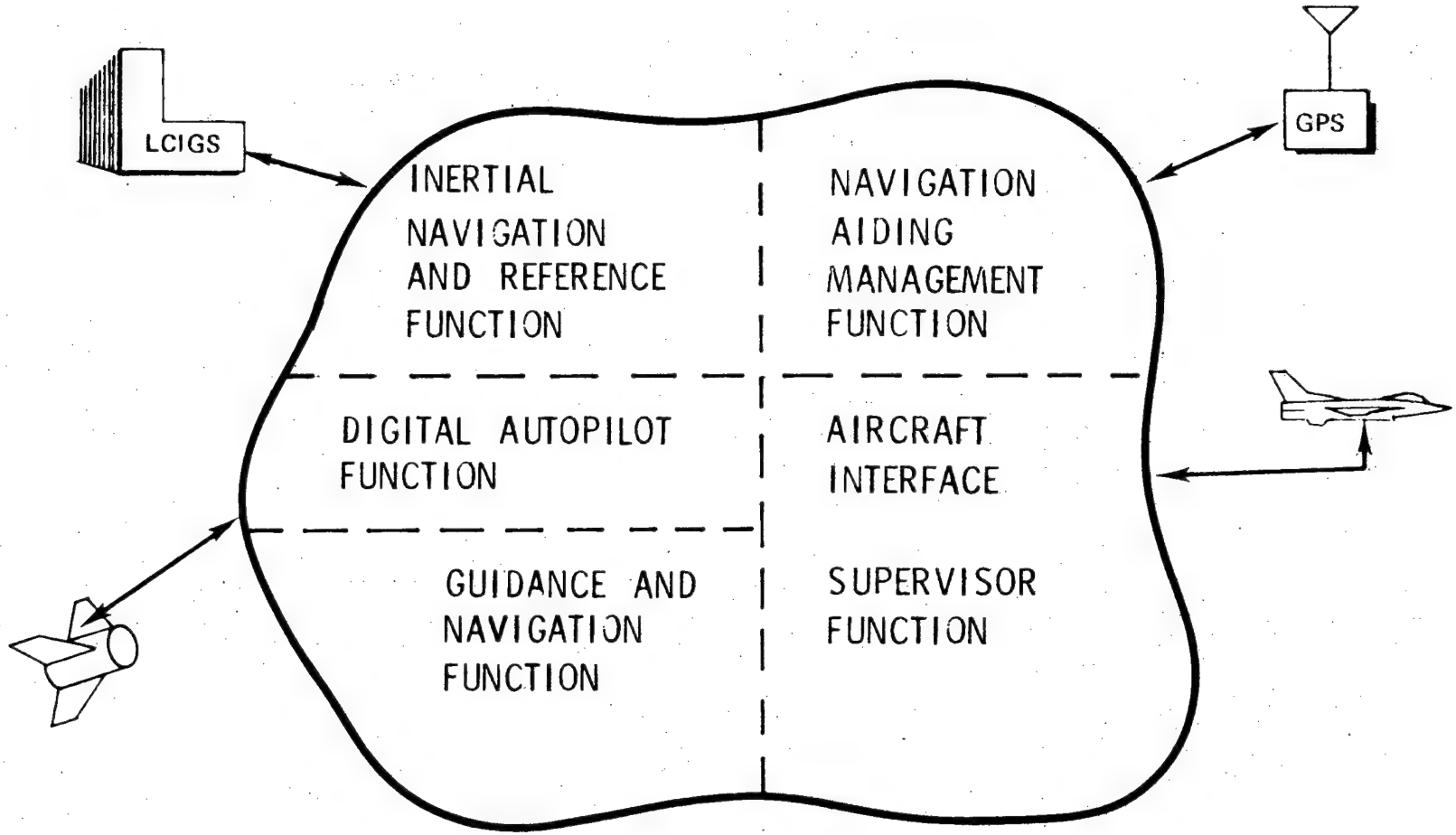

FIGURE 3
UNCLASSIFIED

CE - COMPUTING ELEMENT
SS - SUBSYSTEM

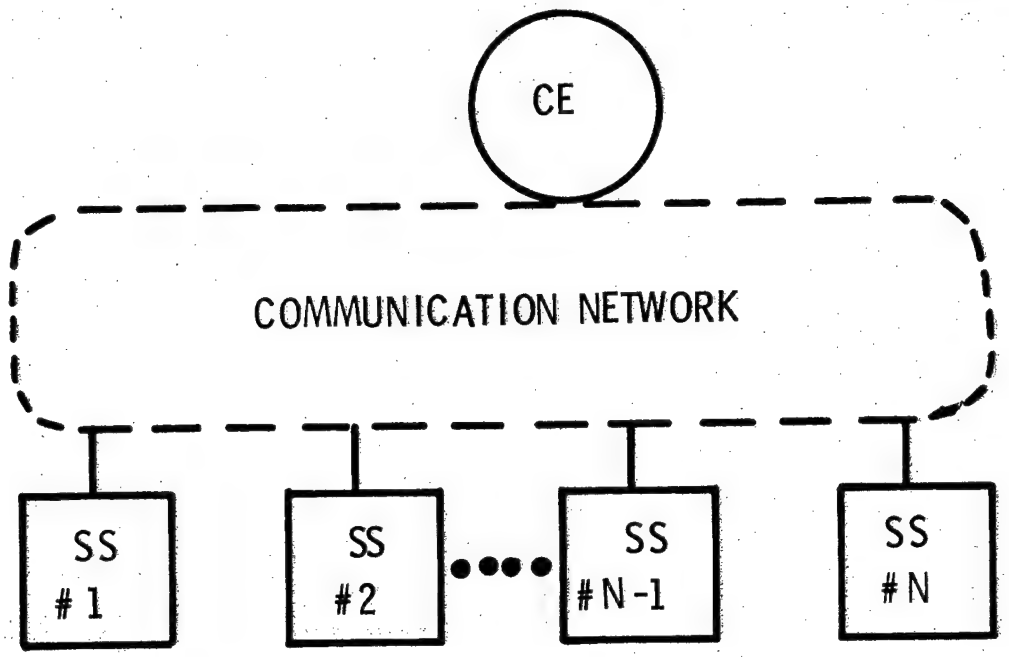

CENTRAL COMPUTER SYSTEM ARCHITECTURE

1475

FIGURE 4
UNCLASSIFIED

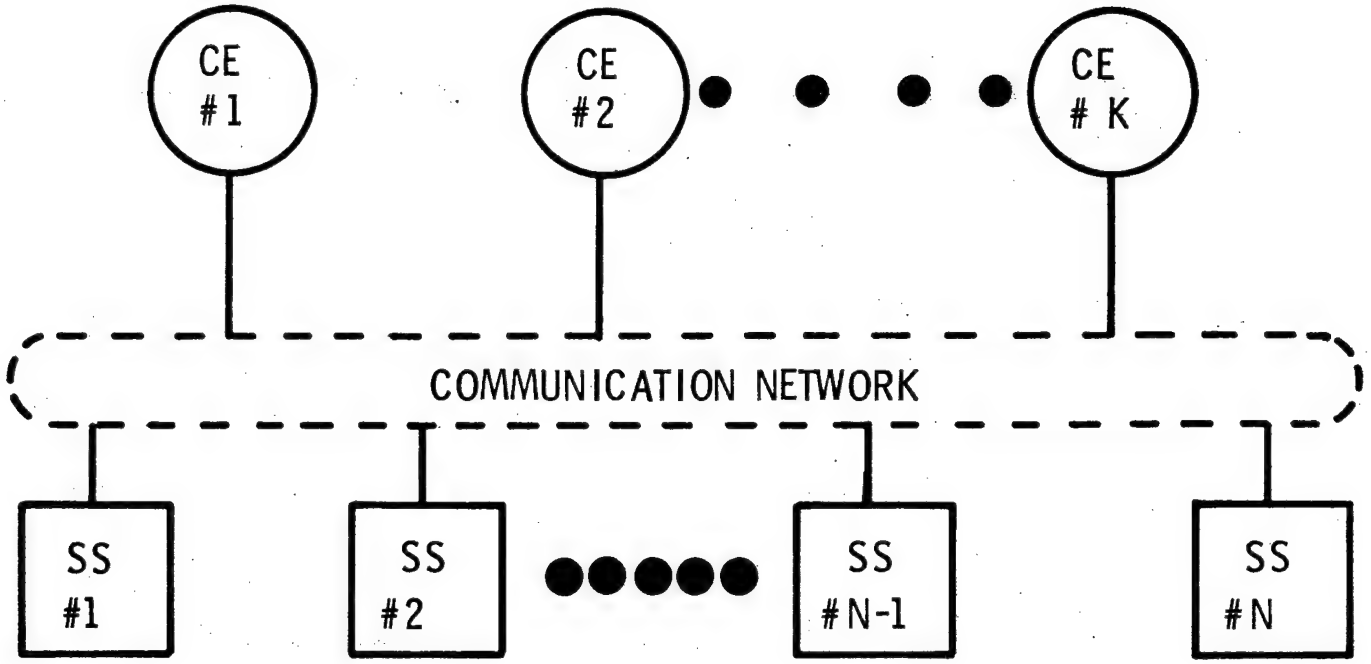

DISTRIBUTED COMPUTER SYSTEM ARCHITECTURE

1476

FIGURE 5
UNCLASSIFIED

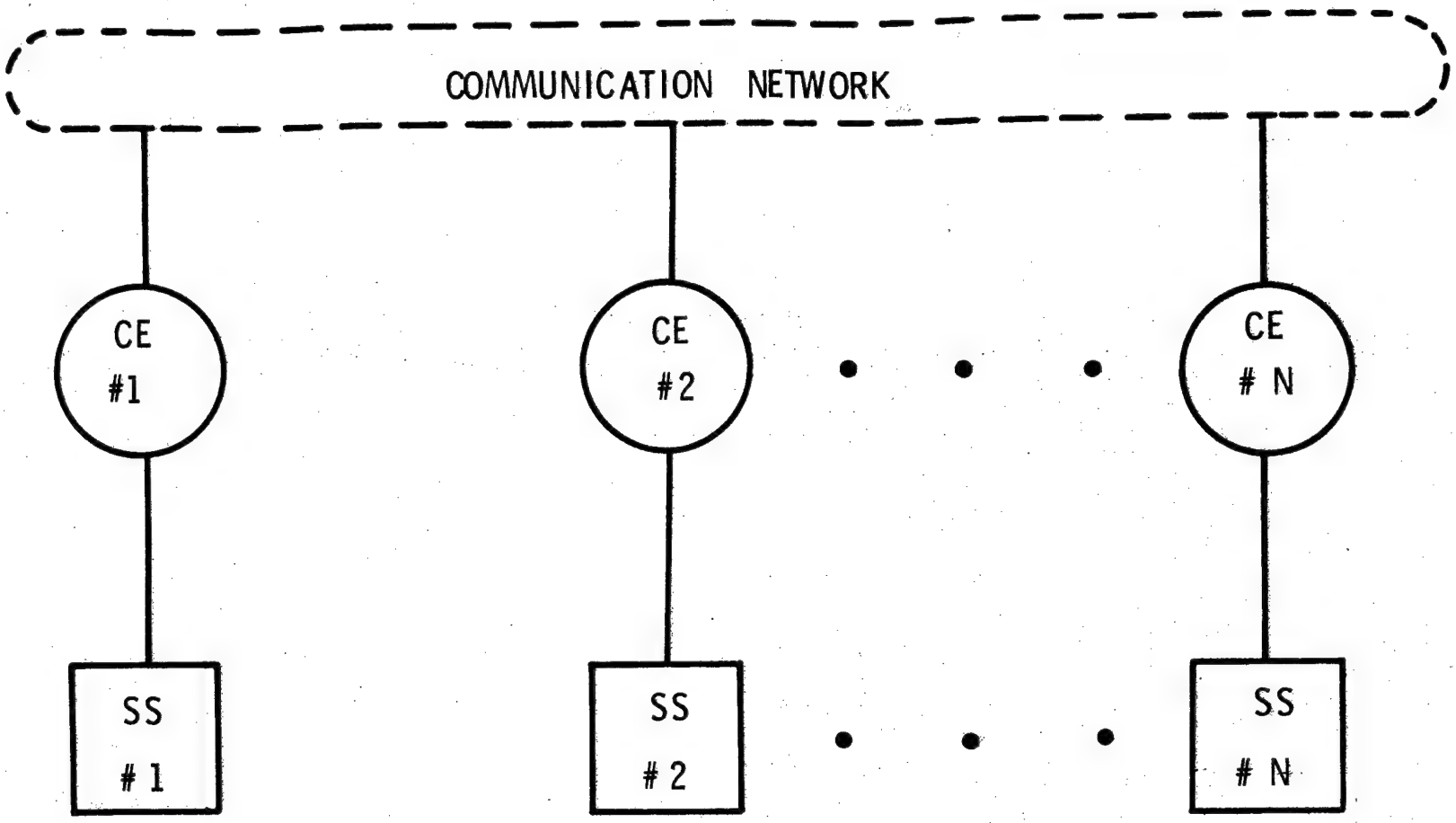

FEDERATED COMPUTER SYSTEM ARCHITECTURE

FIGURE 6
UNCLASSIFIED

1477

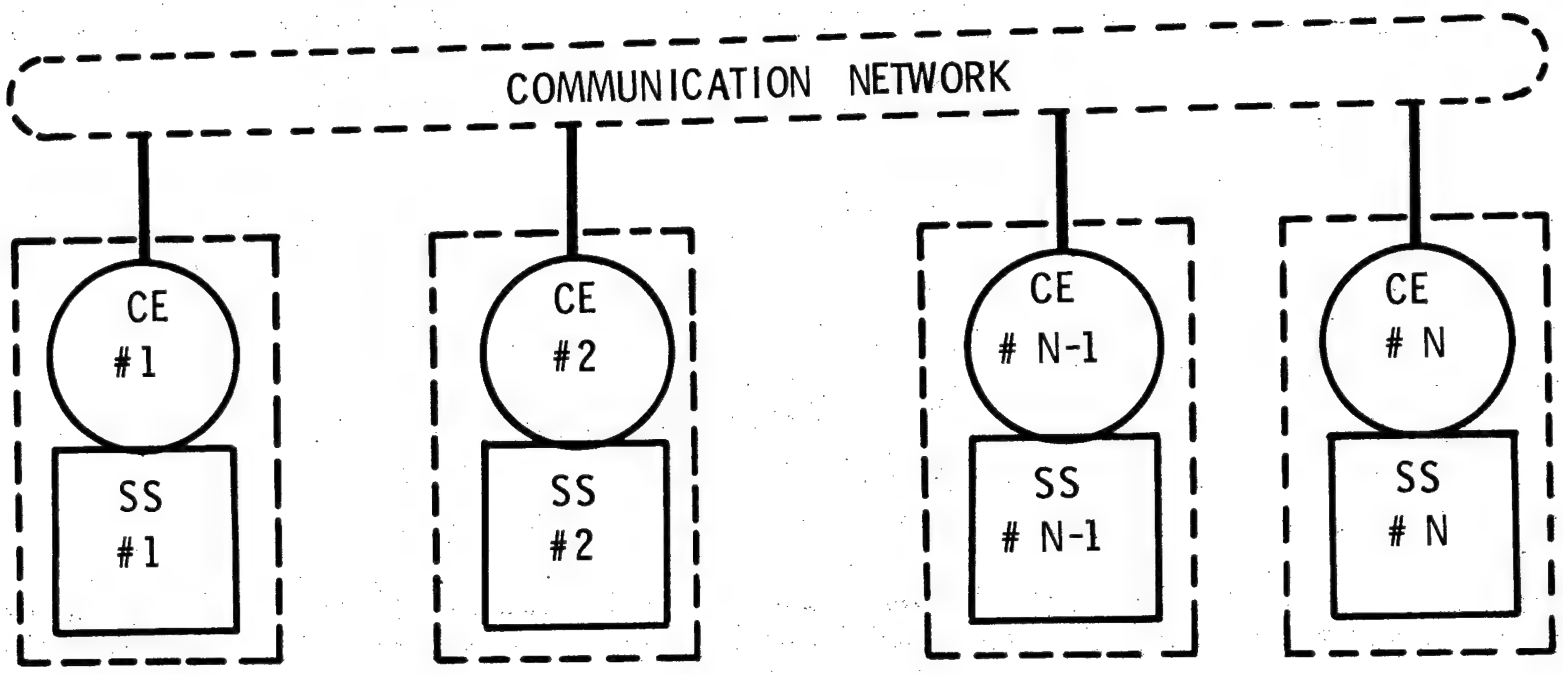

EMBEDDED COMPUTER SYSTEM ARCHITECTURE

1478

FIGURE 7
UNCLASSIFIED

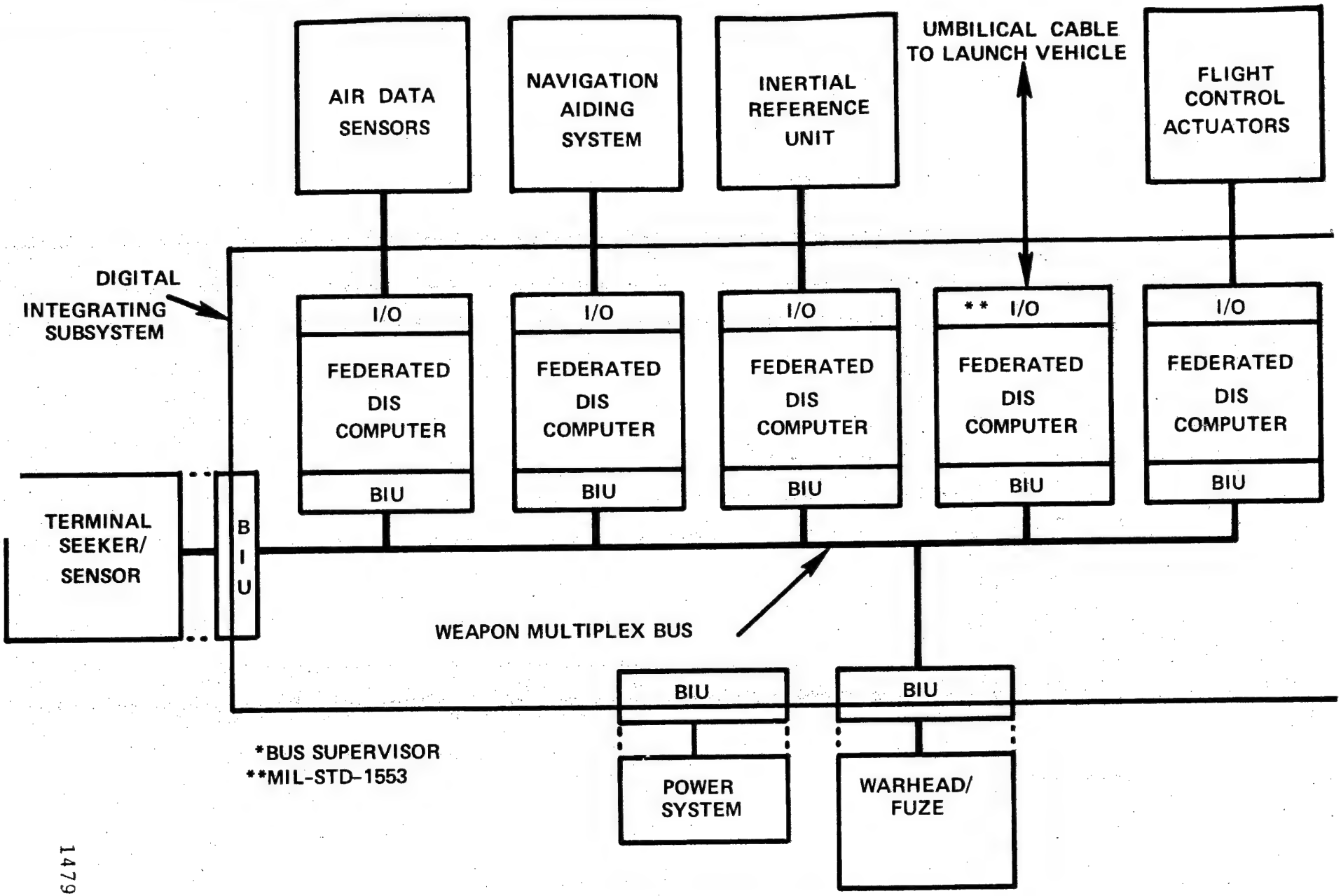

1479

FIGURE 8 TYPICAL SYSTEM BLOCK DIAGRAM

UNCLASSIFIED

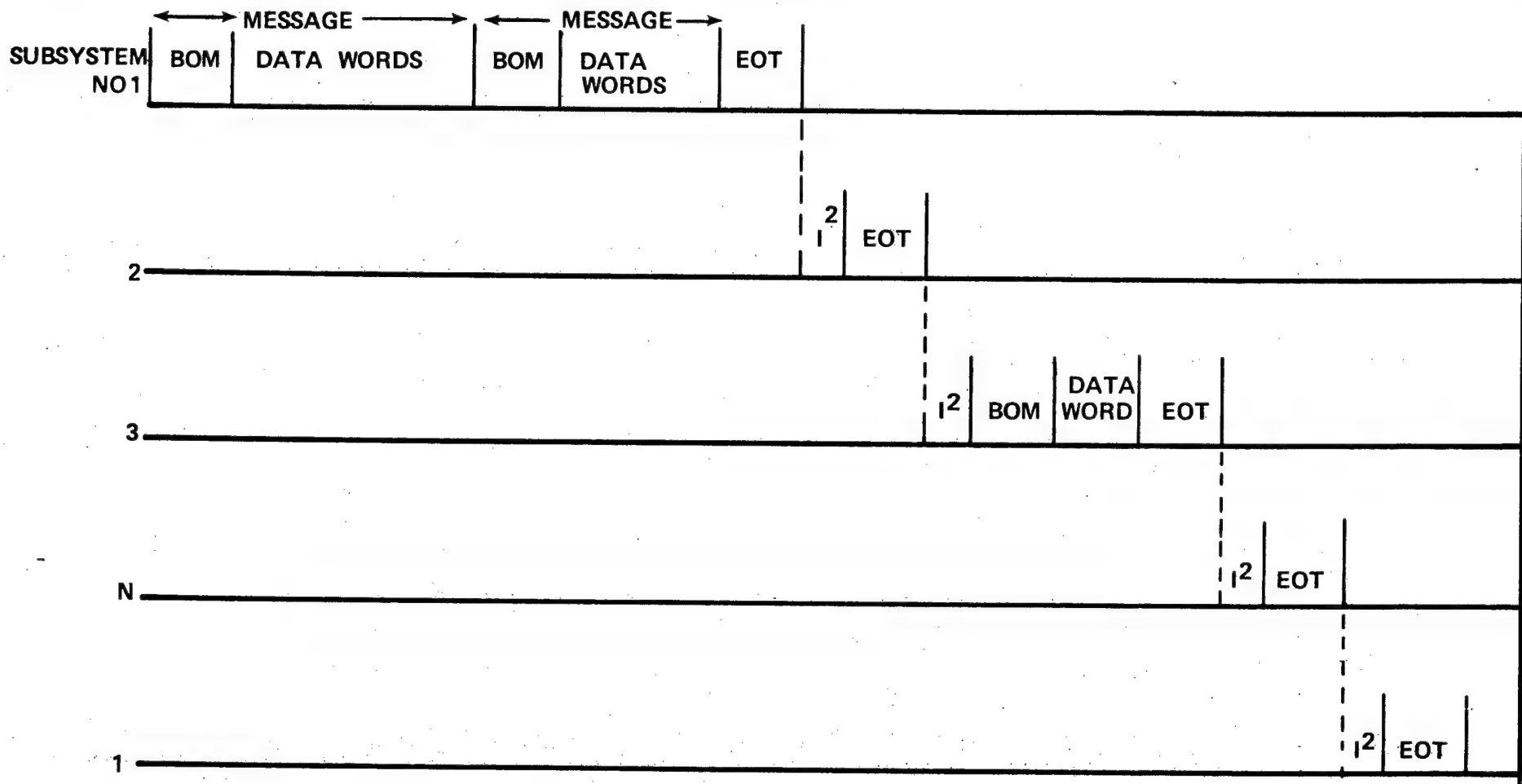

BOM = BEGINNING OF MESSAGE WORD
FOT = END OF TRANSMISSION WORD
I^2 = INTERMESSAGE INTERVAL

1480

FIGURE 9 TYPICAL COMMUNICATION EXCHANGE

UNCLASSIFIED

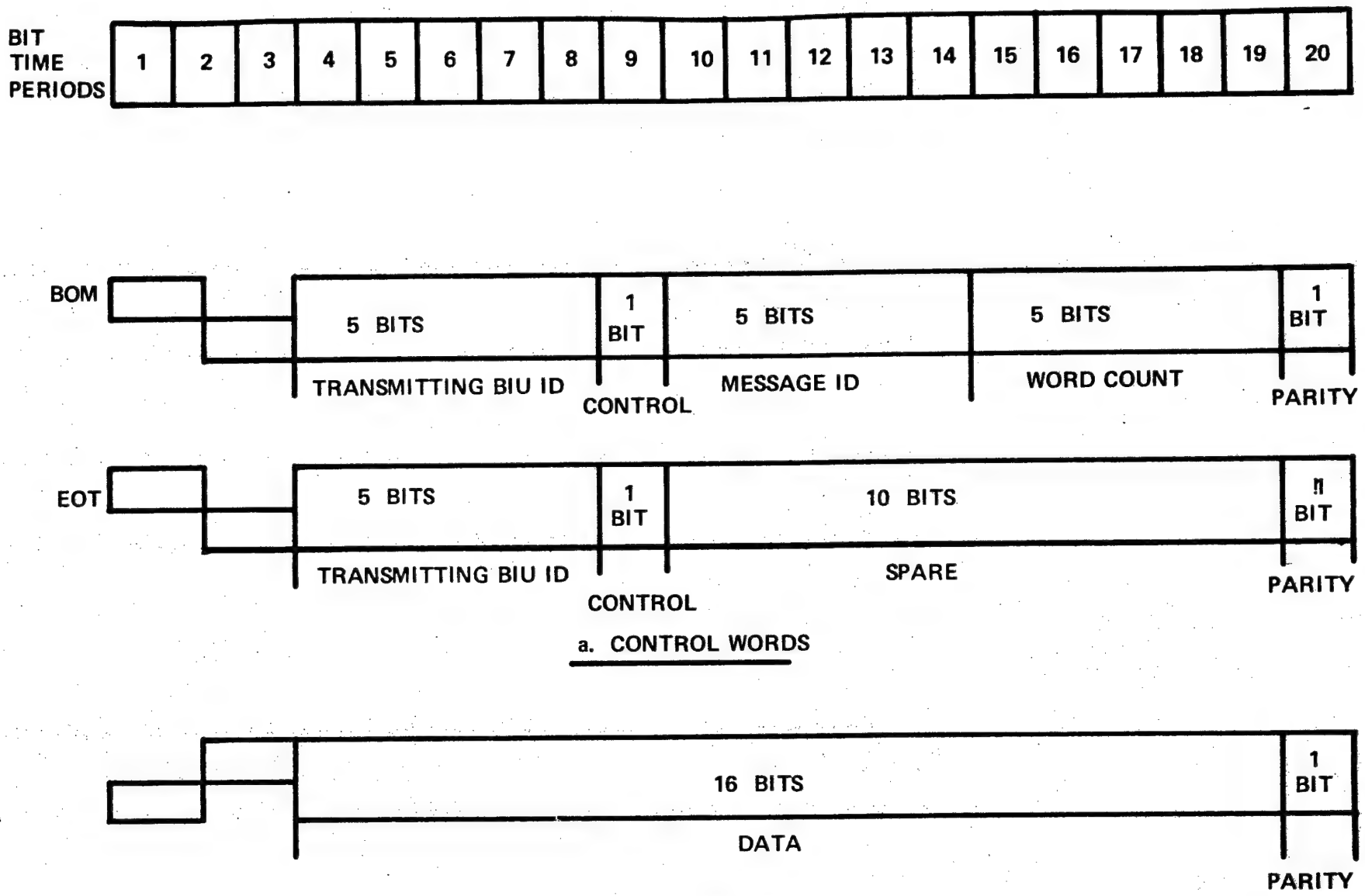

FIGURE 10 WORD FORMATS
UNCLASSIFIED

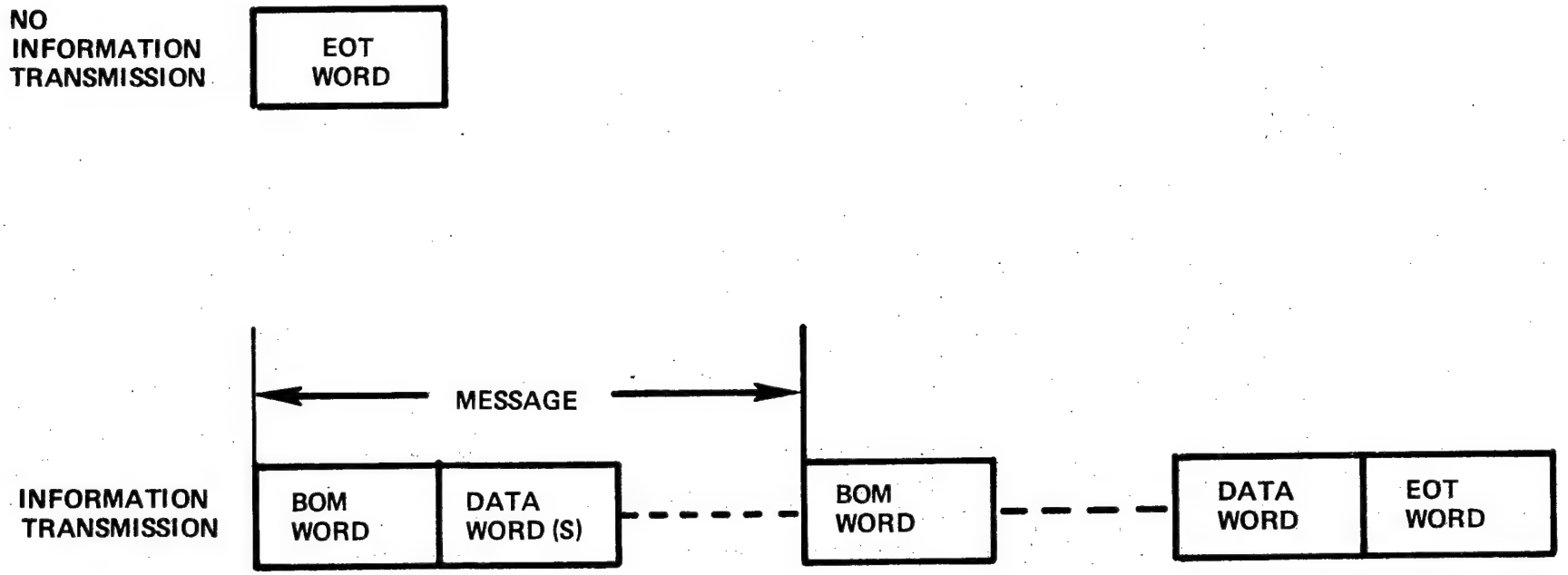

FIGURE 11 TRANSMISSION FORMATS
UNCLASSIFIED

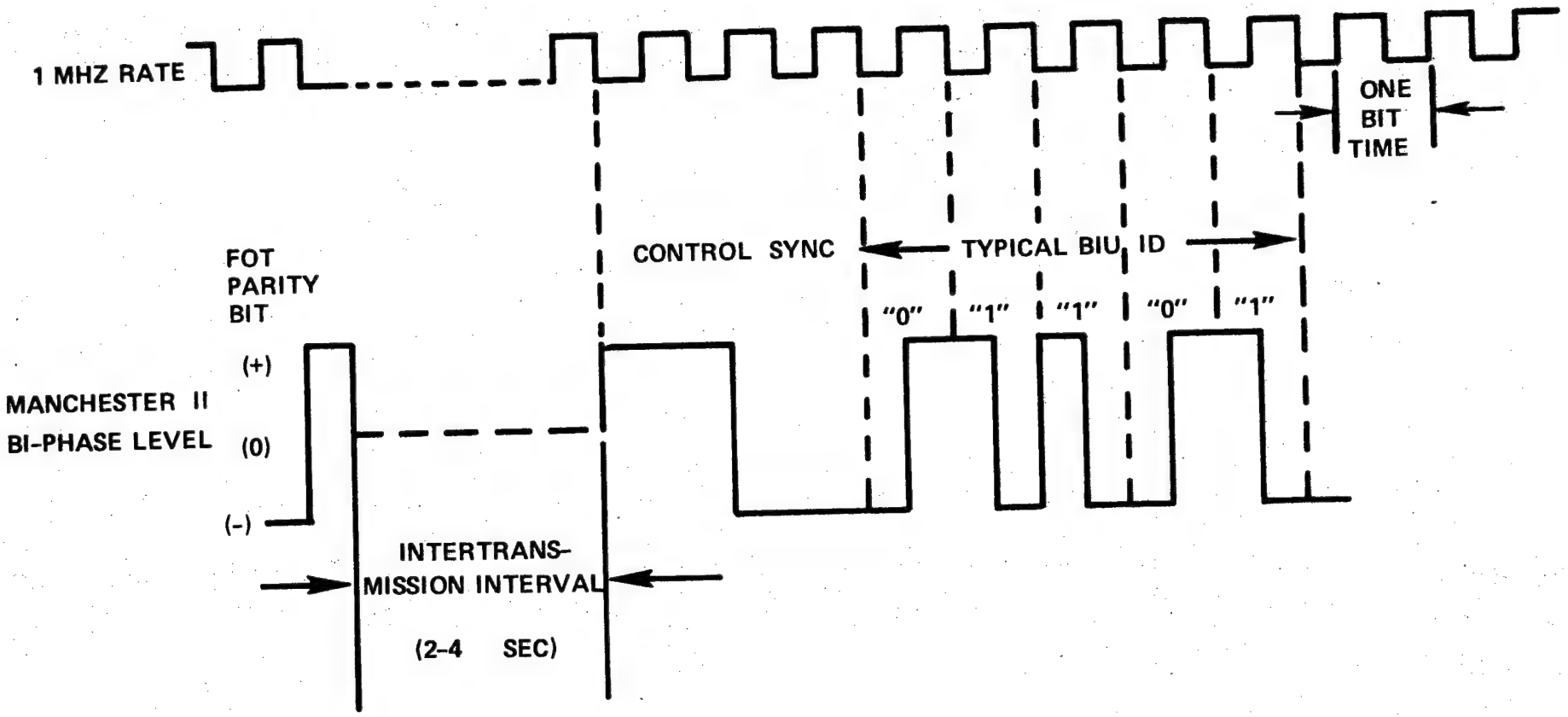

1483

FIGURE 12 INTERTRANSMISSION INTERVAL

UNCLASSIFIED

HIERARCHICAL MULTIPLEX DATA BUSES

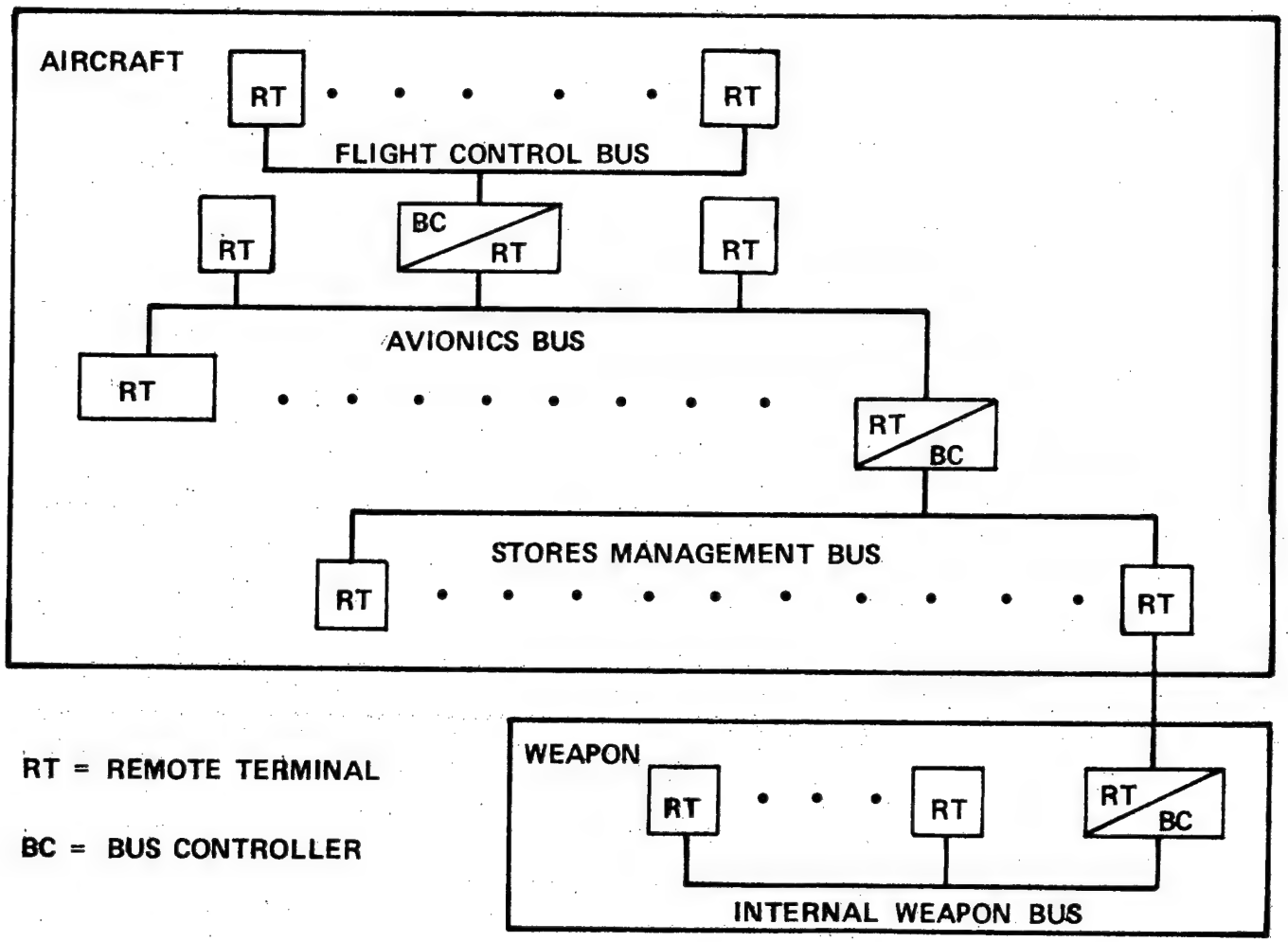

FIGURE 13
UNCLASSIFIED

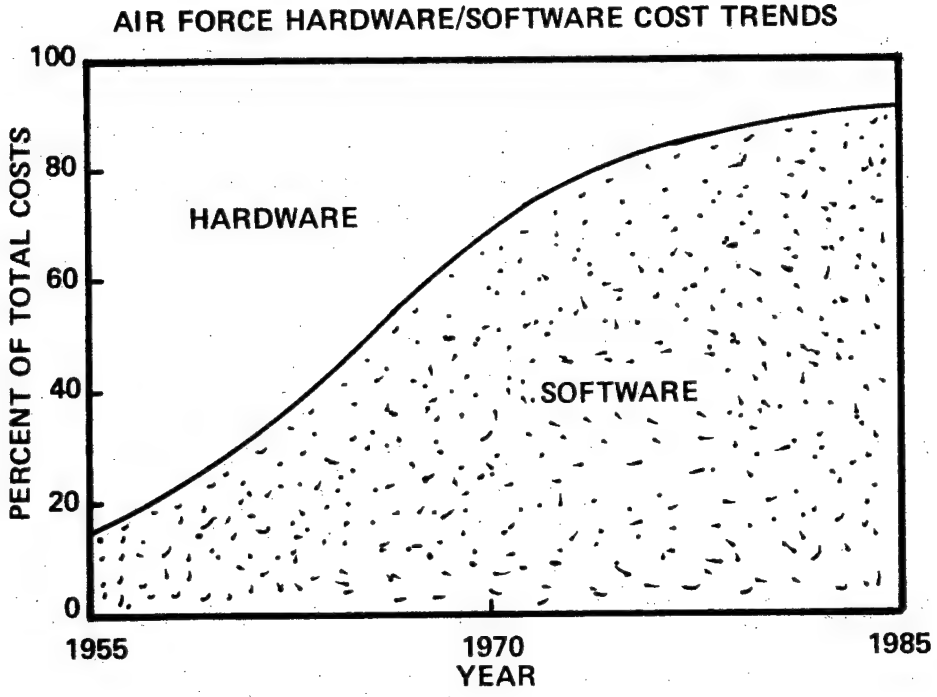

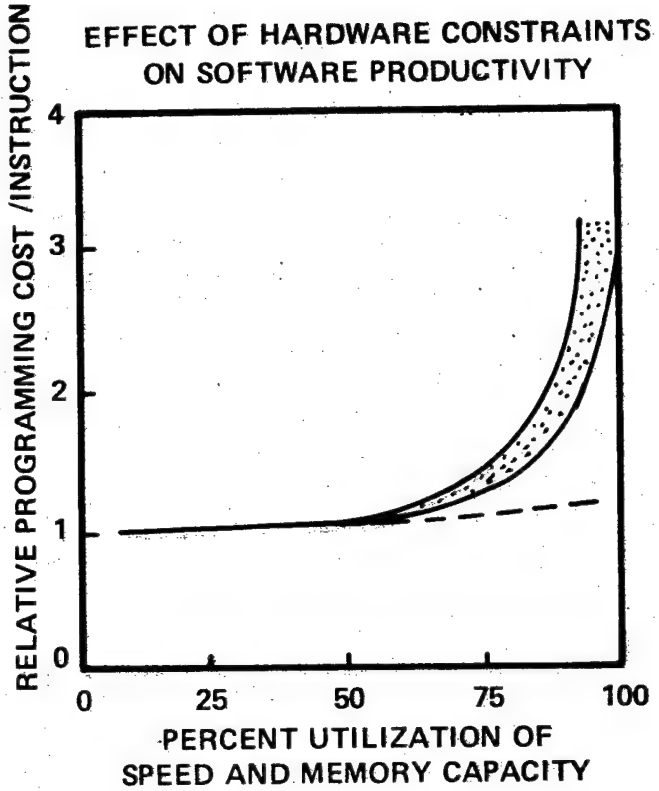

- SOFTWARE COST BREAKDOWN
  - ANALYSIS AND DESIGN: 36%
  - CODING AND AUDITING: 19%
  - CHECKOUT AND TEST: 45%

1485

FIGURE 14
UNCLASSIFIED

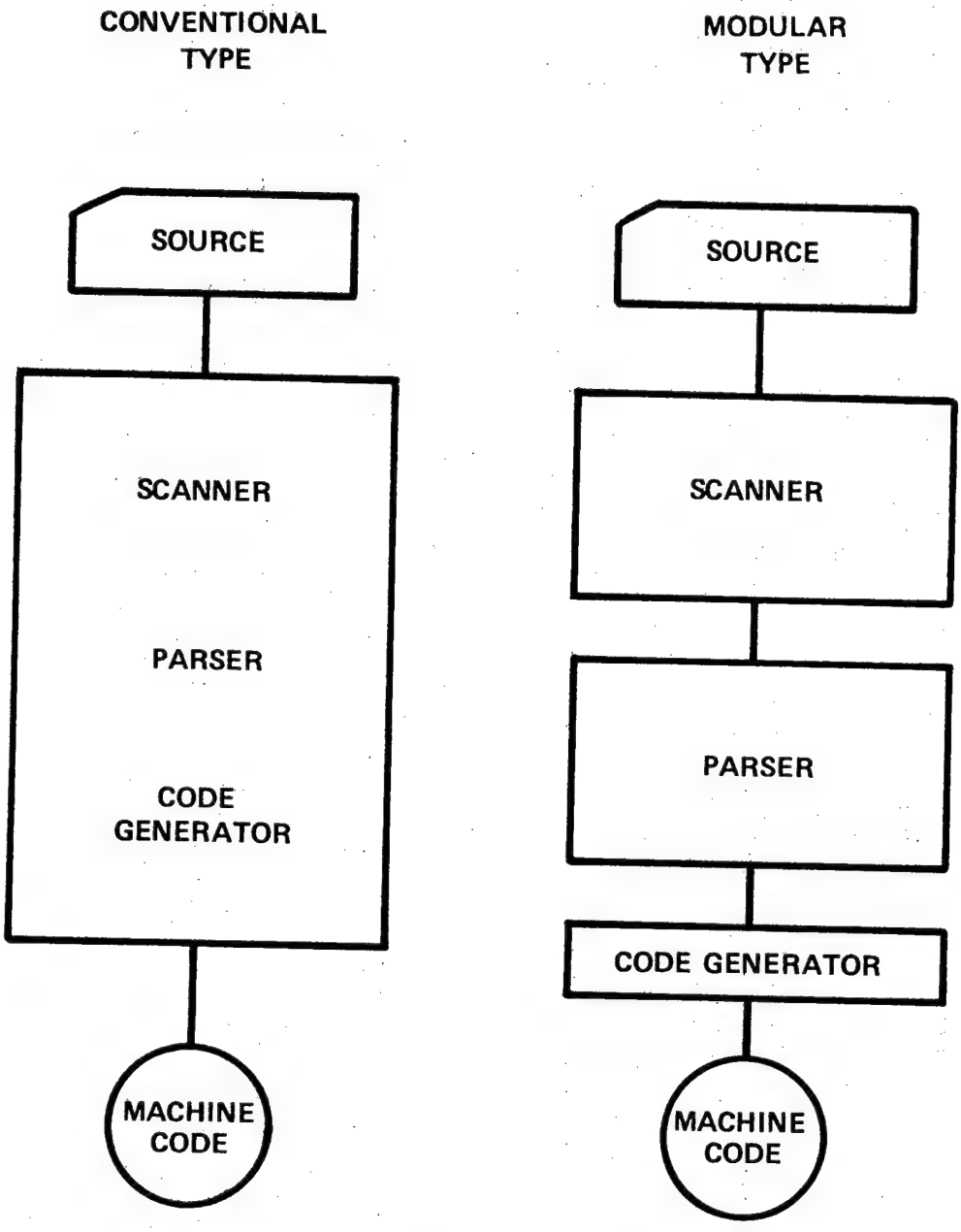

FIGURE 15 CONVENTIONAL VS MODULAR COMPILERS
UNCLASSIFIED

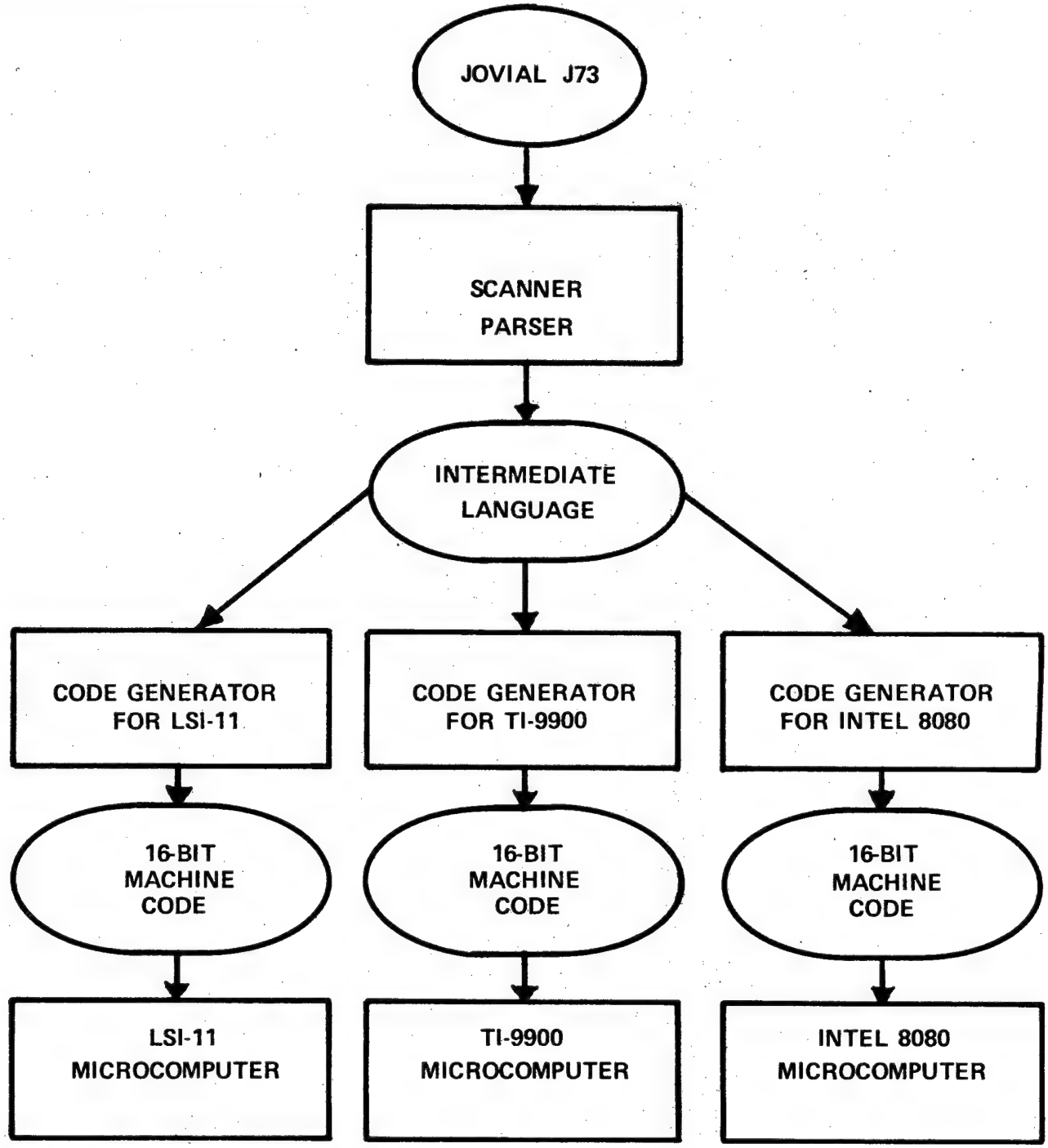

FIGURE 16 STANDARDIZATION USING A MODULAR COMPILER
UNCLASSIFIED

TYPICAL DIS APPLICATION

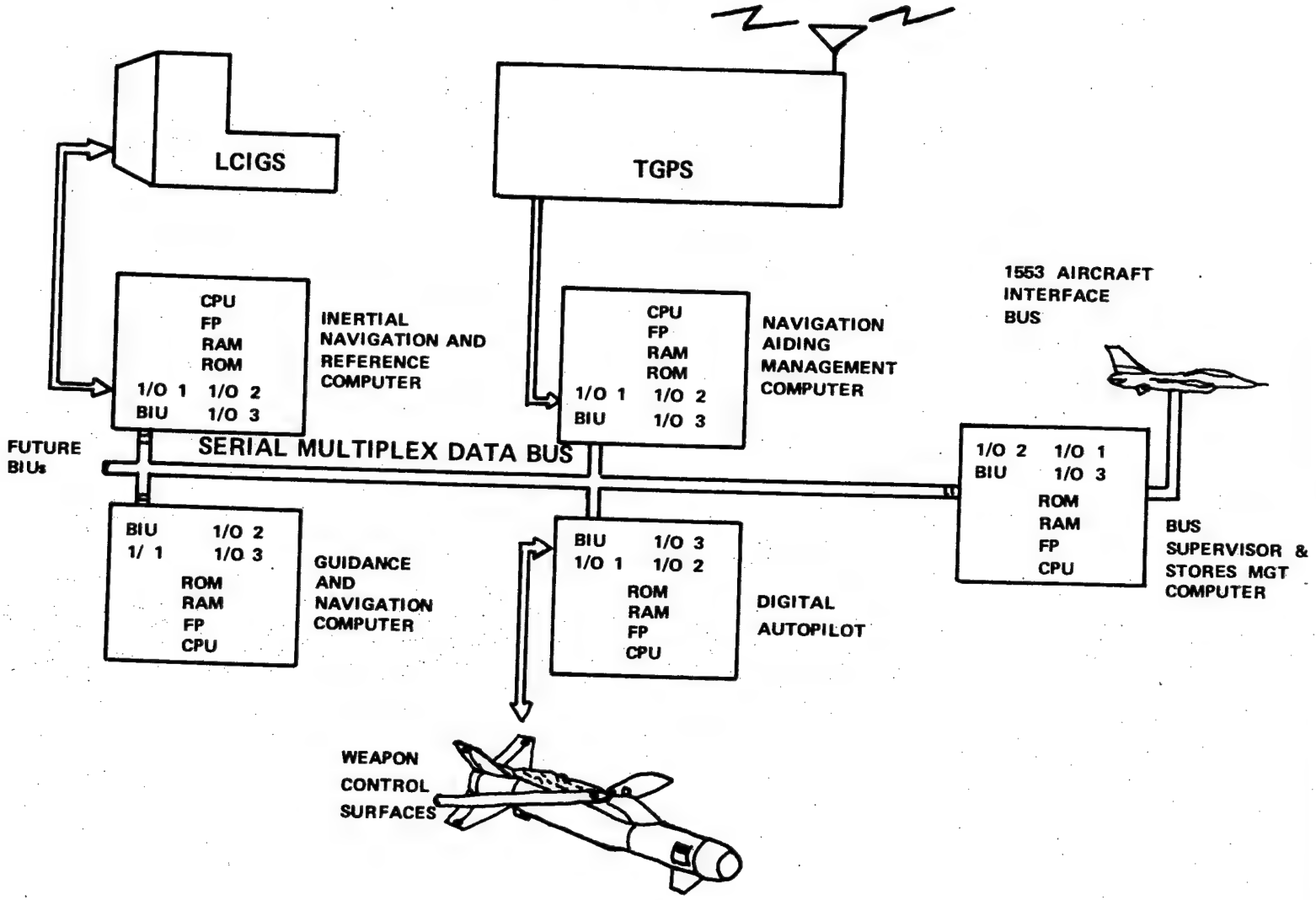

FIGURE 17
UNCLASSIFIED

Biographical Sketch

Mr. Davis L. Gardner was born in Chipley, Florida on July 5, 1931. He graduated from Auburn University with Honor receiving a Bachelor of Electrical Engineering Degree in August 1956. From 1956 until 1964 Mr. Gardner was heavily involved in circuit design. Experience during this time period covered the design of high altitude rocket instrumentation system, high voltage power supplies, low noise amplifiers, TM antennas, Radar Data Systems, IRIG Timing equipment, Ground Telemetry Stations, and UHF Power Amplifiers.

From 1964 until 1975 Mr. Gardner was Director of Systems Engineering for a private firm. His experience during this time period included the design of computer controlled data acquisition systems, data transmission systems, radar signature analysis equipment, shipboard computer interface systems, radar data systems, and industrial computer and microcomputer systems.

In 1975 he returned to government employment as Chief Engineer on the Tactical Global Positioning System Guidance Program. In January 1977 Mr. Gardner assumed the duties of Technical Advisor for the Midcourse Guidance Branch of the Guided Weapons Division of the Air Force Armament Laboratory at Eglin AFB, Florida.

Mr. Gardner is a member of Eta Kappa Nu and Phi Kappa Phi honorary societies.

BANK-TO-TURN (BTT) TECHNOLOGY

BY

Robert M. McGehee

Air Force Armament Laboratory
Eglin AFB, Florida

Bank-To-Turn (BTT) Technology

Abstract

Future United States Air Force requirements dictate the need for dramatic increases in Short Range Air-to-Air Missile (SRAAM) manueverability and accuracy. Many current missile designs, which are characterized by cruciform airframes and skid-to-turn (STT) steering, cannot be extended to meet these requirements due to low aerodynamic efficiency. BTT steering provides the capability to design missile airframes which optimize aerodynamic performance and thus, obtain the SRAAM manueverability and accuracy requirements. In addition, other advantages can be obtained which improve overall missile controllability, such as:

small trim angle of attack ($\alpha \leq 14°$)

high normal acceleration (100g)

small side slip angles ($\beta \leq 3°$)

minimum induced roll moments

small control surface deflections

The Air Force Armament Laboratory initiated a technology effort in FY76 to investigate BTT steering for a SRAAM application. Based on excellent results, this effort was continued. The FY78 BTT effort demonstrated hardware in the loop feasibility.

Introduction

The concept of BTT is not new. Airplane designs have relied on BTT to maximize range, payload, and maneuverability. Successful application of the BTT concept to missiles has been demonstrated by systems which do not employ terminal homing guidance. Some examples are the BOMARC missile, SAGMI, HAST, and the UPSTAGE Experiment. Preliminary design of an air-to-air missile using BTT was done under a US Navy funded contract as part of the AGILE program. Results of this effort, although intended for a specific missile, indicated that BTT was a viable concept for terminally guided missiles. (Ref 1.)

BTT steering provides the capability to design assymetric missile airframes which can optimize aerodynamic performance in one plane and improve missile controllability. Unlike symmetric designs characteristic of STT vehicles, results have shown that BTT control allows airframe designs which can achieve well over 100 g maneuvers with angle of attack ≤ 14 degrees. Furthermore, BTT steering minimizes induced rolling moments since the vehicle maintains small sideslip angles ($\beta \leq 3$ degs). Fin deflection angles are in general reduced since yaw control deflections are needed for stabilization purposes only and roll control deflections are not needed to counter large roll moments.

The overall objective of this technology program was to provide a means for improving overall missile performance through the development and application of BTT steering. The approach taken was different than the normal one of maximizing the performance based on a set of definitive mission requirements. The only mission baseline was a generalized short range air-to-air missile. The objective was to demonstrate maximum performance achievable with BTT. Terminal accuracy was a key issue; therefore this effort required design of a control system which maximized not only midcourse but also endgame performance of a baseline airframe. The contractor was furnished a baseline aerodynamic configuration (figure 1) with comparable aerodynamic data. While this control concept can be applied to all classes of missiles, both air-to-air and air-to-ground, a short range air-to-air concept was selected as the baseline to emphasize potential performance advantages.

The 80 to 1 dynamic pressure ratio requires that the autopilot gains be dynamically varied during free flight, resulting in an adaptive autopilot design. The autopilot is adapted with a dither frequency injected in the yaw channel. The highly maneuverable airframe is capable of pulling 100 g's normal to its yaw plane and achieving roll rates in excess of 500°/sec. These factors give rise to the following questions:

1. Is there state of the art subsystem hardware technology (actuators, gyros, accelerometers), that can satisfy the BTT performance requirements?

2. Is there state of the art seeker hardware that has acceptable performance characteristics when subjected to the required roll rates?

3. How do the high gain filters in the autopilot affect the system noise susceptability?

4. Does the baseline airframe require modifications?

5. Will a high (100 g) "g" environment result in unacceptable subsystem degradation?

Risk areas 1-4 have been or will be resolved by the conclusion of the FY78 effort. The fifth area will be studied analytically but demonstration is beyond the current scope. The resulting control system which evolved from the design and analysis process employs an adaptive autopilot that responds to BTT steering commands generated with a proportional guidance navigation law (using closing velocity).

Background

The FY76/7T study was to define a Bank-To-Turn Steering mechanization, along with other complimentary control system elements (guidance law and stability loop mechanization), such that a high-g planar wing vehicle (or modification thereof) has a significantly improved system

capability for the SRAAM mission. The control system features a high gain (dither) adaptive autopilot that schedules loop gains over the wide dynamic pressure variation of the vehicle flight envelope. The bank-to-turn steering algorithms provide information to the adaptive autopilot for executing proprotional navigation based upon the rectilinear seeker line-of-sight rate outputs. It was found that a small amount of skid-to-turn guidance resulted in improved missile system performance with, bank-to-turn primarily utilized when high "g" maneuvers are required.

A follow-on FY77 effort paid specific attention to analyzing the effects of related control system non-linearities and noise, including those due to autopilot sensors, actuators and guidance sensors. A detailed assessment was made of terminal accuracy in the presence of noise effects. Detailed component specifications were generated and evaluated with respect to the current state-of-the-art. The FY78 effort will demonstrate the BTT control concept via autopilot, actuator and seeker hardware-in-the-loop testing. Analytical versus hardware evaluation is presently being conducted using a hybrid simulation and associated physical effect simulators.

Control System Configuration

The block diagram of the BTT flight control system (FCS) is shown in Figure 3 with the values of the parameters listed in Table 1. The control system is basically like most missile autopilots with the exception of the roll command channel and the self-adaptive network.

BTT steering is accomplished in the roll command channel (Figure 4) by rolling the missile so that the line-of-sight vector is located in the missile pitch plane. Seeker biases and cross-coupling are likely due to the large axial (30-40g's) and pitch (100 g's) accelerations of the missile airframe. Some skid-to-turn (STT) capability is added to steer the missile when the yaw guidance signal is in the roll deadband which significantly improves system performance. Figure 5 shows the effect of adding small amounts of STT capability in the presence of seeker noise. Note that an addition of approximately 2 g capability in the lateral plane virtually eliminates accuracy error due to seeker cross-coupling. A small deadband is employed in the roll steering channel to eliminate potential stability

problems for small line-of-sight errors. The commanded roll rate is proportional to the yaw line-of-sight (LOS) rate. This effectively rolls the missile to an attitude in which the total LOS rate is in the missile pitch plane. The roll guidance gain is controlled by two nonlinear functions of the pitch LOS rate. A switching function is employed which causes the missile to roll in such a direction that the initial roll angle will be no more than 90 degrees. If it were not employed, an initial roll maneuver of up to 180 degrees would be possible. The second nonlinear function attempts to maintain a constant roll guidance loop gain by dividing the gain by the magnitude of the pitch LOS rate. Figure 6 compares the results of a fixed gain versus a constant guidance loop gain for identical flight conditions. Note the divergent yaw LOS rate during the endgame for a fixed gain system. The lower limit of 1 deg/sec prevents division by zero. The roll rate command limit of ≈500 deg/sec precludes roll commands from exceeding roll rate gyro limits and actuator rate limits.

The self-adaptive control network will adjust its own characteristics in order to provide a desired control system performance in a changing dynamic environment. The FCS's stability and dynamics is controlled by output gain (Kr) of the self-adaptive network (figure 3) which schedules other loop gains and limiters. The yaw rate channel was selected as the driver for the adaptive loop, since large steering signals (which are present in the pitch and roll channels) would contaminate the dither signal used for the adaptive process. The yaw rate channel is excited by an externally generated sinusoidal dither signal whose amplitude is "sensed" by bandpass filters. The filtered signals are rectified then differenced to generate an error signal. The error signal is then passed through a noise filter which also suppresses dither frequency harmonics. The signal is then integrated at a rate (K_I) which is a function of Kr (in order to maintain a more constant adaptive loop transient response over the 80 to 1 dynamic pressure variation) to generate Kr. In this way a constant yaw rate loop cross-over frequency is maintained which is identical to the dither frequency. The adaptive gain is then used to:

1) schedule the pitch and yaw acceleration gains
2) schedule the pitch, yaw and roll rate gains
3) schedule the command "g" limiters

The pitch and yaw rate loops are used for airframe short period damping and, along with the roll loop, use lead/lag, forward loop shaping. This permits easier gain scheduling of the pitch and yaw acceleration loops and gives the roll loop the ability to attain commanded roll rate values. The double lead shaping network in the pitch and yaw loops add phase margin at the loop cross-over frequency without significantly decreasing gain margin. All three rate loops also employ a 20 degree fin command limit.

The pitch and yaw acceleration loops are utilized for steering and to provide a method to implement a missile acceleration control limiter. The adaptive gain Kr is used to schedule the acceleration loop gains and also the command "g" limiters in order to mechanize an alpha/beta limit. Double lag networks in both acceleration loops were employed to provide gain margin in the presence of the flight path aero zeros.

Requirements were established for the various subsystem (gyros, accelerometers, actuators and seekers) components upon the completion of the autopilot and airframe design studies. These requirements were used in a search of off-the-shelf components. An example of the detailed requirements is shown in table 2. Available components were located for all subsystems. Closed loop seeker testing using BTT requirements has been demonstrated (Ref 2). No airframe changes (from the baseline design) are necessary for satisfactory performance. The system noise has been evaluated theoretically and hardware evaluation is planned in 1978.

Performance Results

The simulation utilized for the guided performance evaluation was a 6 degree-of-freedom digital model of the system. Single and double table look-up routines were programmed to calculate the detailed non-linear aerodynamic coefficients. The modeled actuators, rate gyros, and accelerometers include biases, cross-coupling, in-axis coupling, deadbands and dynamic characteristics (figure 7). Simulation runs were terminated at the point of closest approach between the missile and target center of gravity.

Eleven engagements were selected using the various launch speeds, target maneuvers and aspect angles listed in Table 3. A pictorial scenario of these encounters,

which describes the sign convention of the target aspect angle (A_T) and maneuvers (N_{YT} and N_{ZT}), is shown in Figure 8. All engagements were boresight launches directed against a constant speed, 9g laterally accelerating target. In addition, conditions 5 through 11 performed a double maneuver by instantly converting the lateral acceleration into a vertical (out-of-plane) 9g acceleration at 0.25 seconds time-to-go. This maneuver places the target approximately 9 feet below the missile maneuvering plane at the time of missile impact. If the BTT FCS were not responsive to this maneuver, the 9 feet would be additive to the nominal miss distance incurred by the single maneuver tactic.

The results of the performance evaluation show significant improvement over existing air-to-air missiles in miss distance, flight time (which includes a 0.4 second guidance lock-out), maximum angle of attack and vertical load factors for each launch range at the 11 engagement conditions.
ore detailed information must be obtained from Ref 3 & 4. The BTT FCS was found to be sufficiently responsive to out-maneuver any last effort, out-of-plane evasive actions. Performance evaluation has been conducted at other flight conditions (different altitudes) in the BTT envelope with similar results.

Conclusions and Recommendations

A bank-to-turn steering mechanization has been developed and evaluated for a tactical missile concept, resulting in exceptional short range performance, by employing the maximum maneuvering capability of an unsymmetrical airframe. The control system employs BTT steering, an adaptive autopilot and proportional navigation (with closing velocity). The bank-to-turn steering mechanization allows the large "g" capability of the airframe pitch axis to be applied in a direction to reduce the total line-of-sight rate. The adaptive autopilot assures adequate performance throughout a large flight envelope, without exceeding critical values of angle-of-attack and side-slip. A small amount of skid-to-turn maneuvering in conjunction with proportional navigation with closing velocity provides high accuracy against maneuvering targets from all aspects.

Available components were identified which would provide satisfactory performance. Minimal modifications are

necessary for application to this high performance system. The feasibility of the BTT concept has been shown analytically. To further demonstrate the concept, closed-loop hardware testing of the guidance and control subsystems must be accomplished. This is being done in FY78 and will include the following hardware: autopilot, actuator, and seeker. This effort is presently underway. Results of this effort will be presented at the symposium.

Based on favorable results of the FY78 program future efforts should address g harding of subsystems (gyros, accelerometers, seekers, actuator) to withstand a 100-150 g environment.

References

1. Investigation of Bank-To-Turn Steering for Highly Maneuverable Tactical Air-To-Air Missiles, J. D. Froning, Jr., M. M. Briggs, J. W. Burrow, and W. C. Freestad, Naval Weapon Center, Dec 1970, NAVY-NWC-5026, AD 513-439L.

2. High Angular Rate AAM Sensor Demonstration, K. Kiser, MacDonnell Douglas Astronautics Co - West, AFATL-TR-77-102.

3. Bank-To-Turn Steering for Tactical Missiles, R. I. Emmert, R. D. Ehrich, G. P. Joseph, A. M. Thunguldstad, K. O. Smith, Rockwell International Corporation, AFATL-TR-76-150.

4. Detailed Stability and Control Investigations of a Bank-To-Turn (BTT) Configuration, R. I. Emmert, R. D. Ehrich, D. E. Fought, K. O. Smith, Rockwell International Corporation, AFATL-TR-78-10.

Body
Parabolic Forebody
2:1 Elliptical Cross Section
Blunt Base

Wings
Planar Wings
Clipped Double Delta Planform

Tails
Cruciform
Clipped Double Delta Planform
All Movable

Launch Weight = 165 Lbs
Burnout Weight = 115 Lbs
Thrust = 4712 Lbs
Total Impulse = 12,250 Lb-Sec

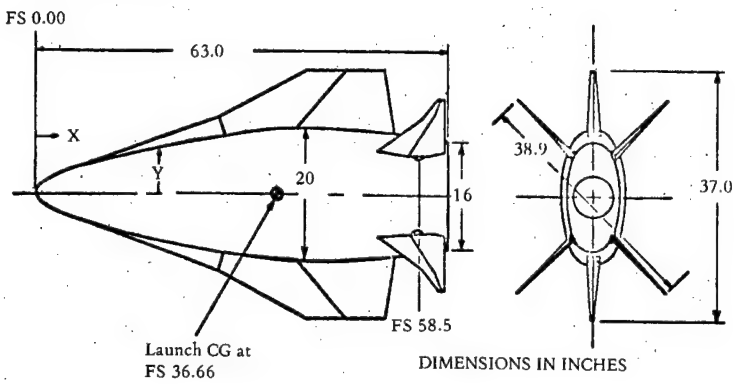

Figure 1. BTT Vehicle Characteristics

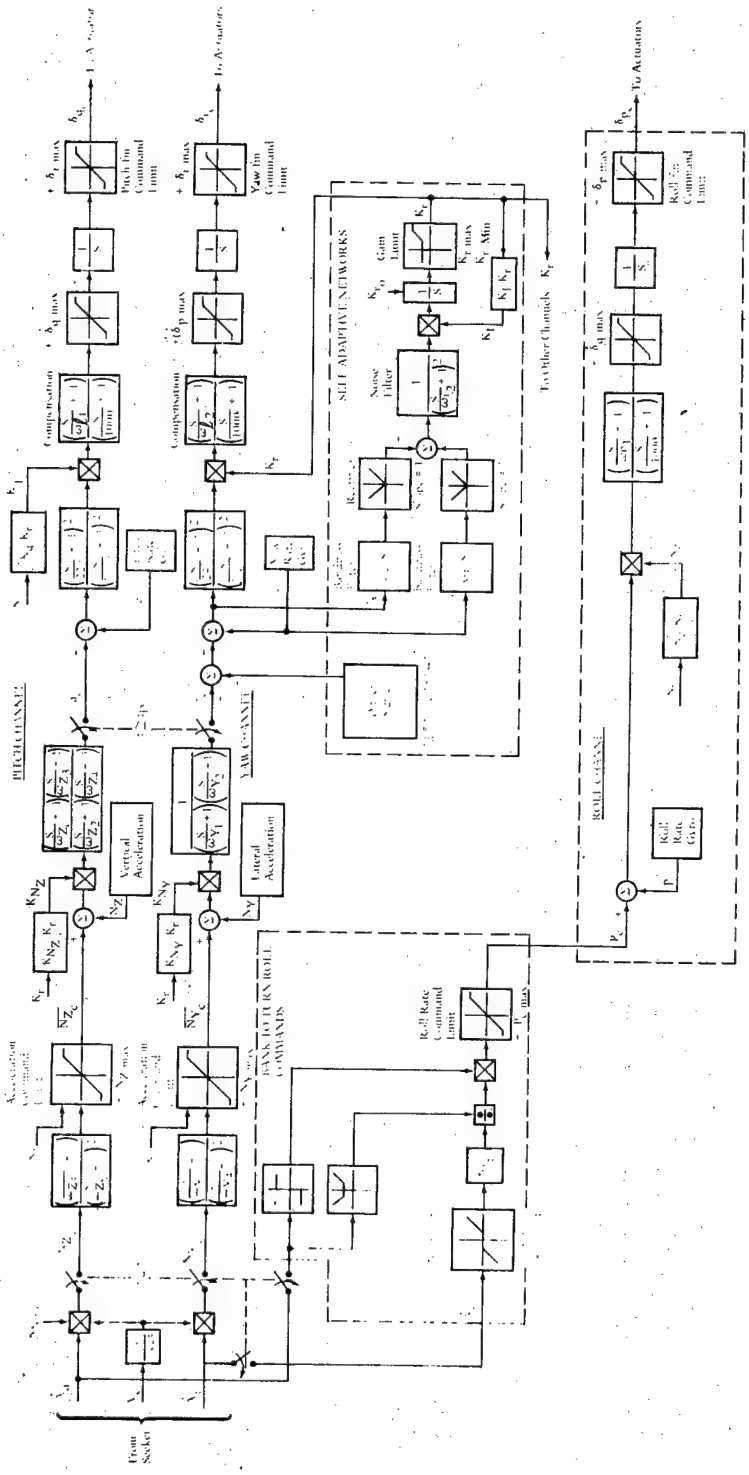

Figure 3. Flight Control System Functional Block Diagram

TABLE 1. VALUES OF BLOCK DIAGRAN PARAMETERS

Variable Name		Value of Derivation
K_{NAV}	$\frac{g}{deg/sec}$	4
ω_{y_1}	$\frac{rad}{sec}$	15
ω_{y_2}	$\frac{rad}{sec}$	80
ω_{y_3}	$\frac{rad}{sec}$	20
ω_{y_4}	$\frac{rad}{sec}$	100
K_{NY}	$\frac{deg/sec}{g}$	$26.65\ K_r - 10.145 \quad 0 \leq K_r \leq 1.3$ $24.5 \quad 1.3 < K_r \leq 5.5$ $5.512\ K_r - 5.816 \quad K_r > 5.5$
$N_{y_{MAX}}$	g	$0.05\ N_{Z_{MAX}}$
$N_{z_{MAX}}$	g	$70/Kr - 2.0\ Kr + 2$ LIMIT: $9.3 \leq NZmax \leq 100$
ω_{ℓ_1}	$\frac{rad}{sec}$	70
ω_{ℓ_2}	$\frac{rad}{sec}$	60
$\dot{\delta}_{c_{MAX}}$	$\frac{deg}{sec}$	300
ω_{z_1}	$\frac{rad}{sec}$	5
ω_{z_2}	$\frac{rad}{sec}$	1
ω_{z_3}	$\frac{rad}{sec}$	150
ω_{z_4}	$\frac{rad}{sec}$	12
ω_{z_5}	$\frac{rad}{sec}$	20
ω_{z_6}	$\frac{rad}{sec}$	100
t_D	sec	0.4
K_q	ND	$0.7656\ K_r + 0.3961$
$(P_C)_{max}$	$\frac{deg}{sec}$	500
$K_{\ddot{X}_p}$	ND	900

TABLE 1. VALUES OF BLOCK DIAGRAM PARAMETERS (CONCLUDED)

Variable Name		Value of Derivation
K_p	ND	$0.03579\ K_r + 0.01347 \quad 0 \leq K_r \leq 4.77$ $0.06052\ K_r - 0.1046 \quad K_r > 4.77$
K_{NZ}	$\frac{deg/sec}{g}$	$16.22\ K_r - 4.468 \quad 0 \leq K_r \leq 1.2$ $15.00 \quad 1.2 < K_r \leq 4.5$ $10\ K_r - 30 \quad K_r > 4.5$
ω_{P_1}	$\frac{rad}{sec}$	20
$(\delta_{P,q,r})_{max}$	deg	20
ω	$\frac{rad}{sec}$	85
r_{MAX}	$\frac{deg}{sec}$	4
ω_{r_2}	$\frac{rad}{sec}$	85
K_I*	$\frac{1}{deg}$	$0.0412\ K_r - 0.00584$
K_{r_o}	ND	0.6327
$K_{r_{MAX}}$	ND	14.65
$K_{r_{MIN}}$	ND	0.4332
G_F (S)	ND	S [illegible]
$P_{DEADBAND}$	$\frac{deg}{sec}$	0.1

ND = Nondimensional
*K_I is reduced by a factor of five after t_n

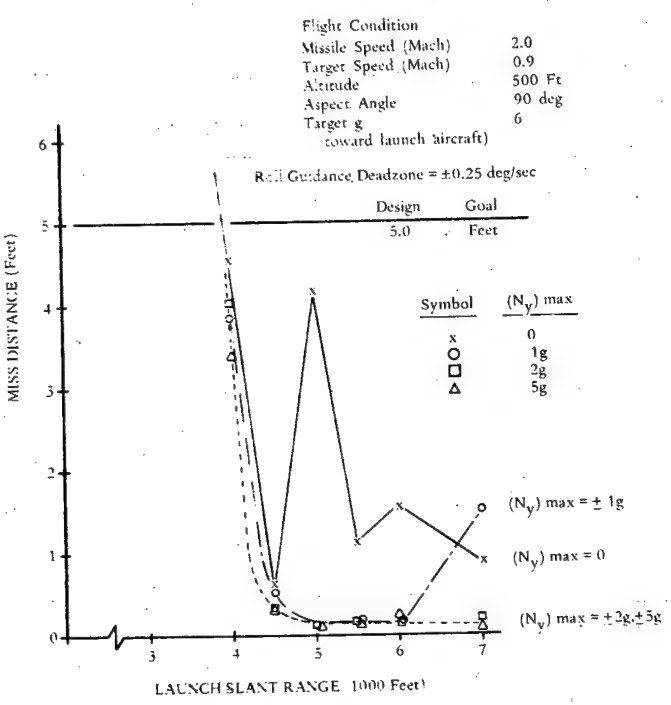

Figure 3. System Sensitivity to Skid-to-Turn Capability (± (Ny) max) With 0.25 deg/sec Seeker Bias

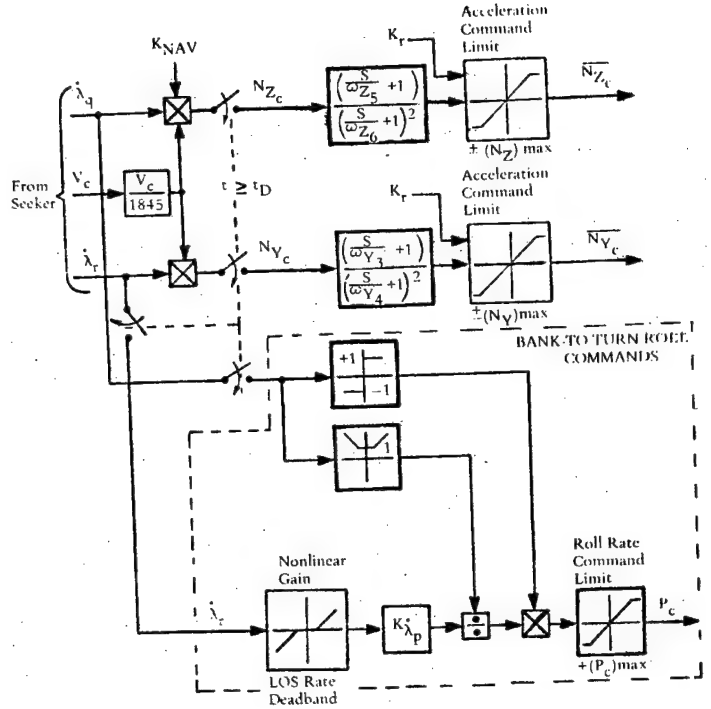

Figure 4. Bank-to-Turn Mechanization

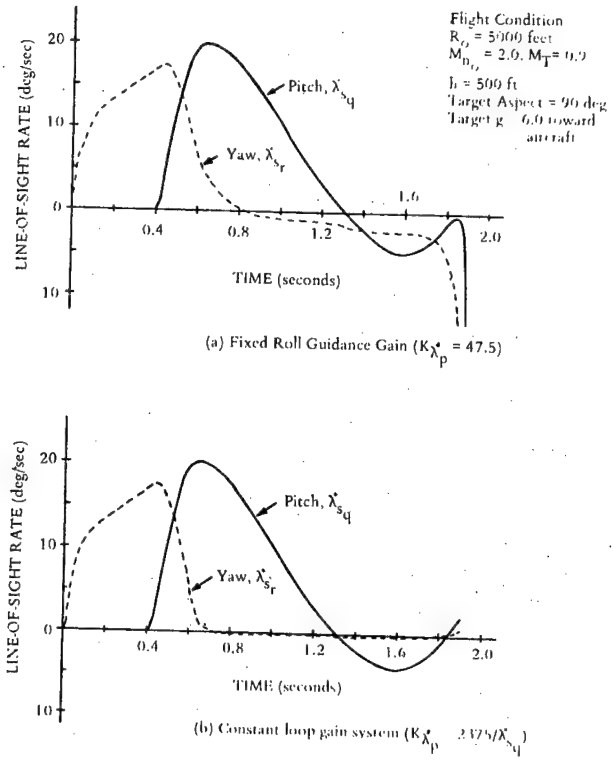

Figure 6. Simulation-Generated LOS Rate Time Histories for Two Roll Guidance Mechanizations

Parameter	Roll		Pitch		Yaw	
	Reqmt.	Capab.	Reqmt.	Capab.	Reqmt.	Capab.
range (deg/sec)	± 500	± 500	± 150	± 100**	± 75	** ± 50
frequency response (phase lag at 85 rad/sec less 10 deg)	10 deg	14 deg*	10 deg	28 deg*	10 deg	28 deg*
(e. g. ζ = 0.5, w_o = 487) (a) ω_o	487	628	487	314	487	314
(b) ζ	0.5	0.5–0.9	0.5	0.5–0.9	0.5	0.5–0.9
threshold (deg/sec)	± 0.10	± 0.05	± 0.02	± 0.01	± 0.02	± 0.01
hysteresis (deg/sec)	± 0.5	± 0.25	± 0.20	± 0.10	± 0.10	± 0.05
offset (deg/sec)	6.0	3.0	2.0	1.0	1.0	0.5
linear acceleration sensitivity (deg/sec/g)	0.2	0.10	0.06	0.03	0.04	0.02
g^2 sensitivity (deg/sec/g^2)	$6x10^{-4}$	$3x10^{-4}$	$6x10^{-4}$	$3x10^{-4}$	$6x10^{-4}$	$3x10^{-4}$
angular acceleration sensitivity (deg/sec/deg/sec^2)	10^{-3}	$7x10^{-4}$	10^{-3}	$7x10^{-4}$	10^{-3}	$7x10^{-4}$
noise (deg/sec rms)		2.0		1.0		0.5
size (diam x length) inch		$1x3^{1/2}$		$1x3^{1/2}$		$1x3^{1/2}$
cost (dollars in 1000 units)		300		300		300

*Electronic compensation will allow requirement to be met
**Component selection to be revised to meet updated requirements

TABLE 2. RATE GYRO SPECIFICATIONS

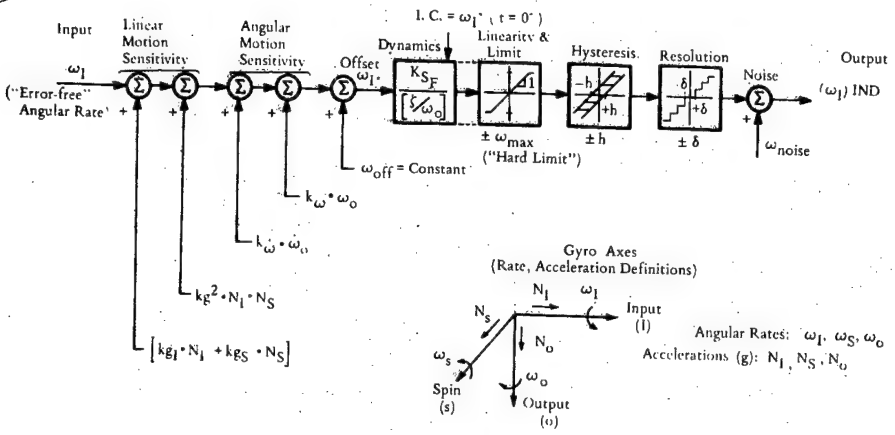

Figure 7. Rate Gyro Simulation Model

Condition	V_M - F/S	V_T - F/S	A_T (Deg)	N_{YT} (g)	N_{ZT} or T_{TG} 0.25 Sec (g)	Altitude (Ft)
1	932.4	932.4	45	9	0	20,000
2	932.4	932.4	90	9	0	20,000
3	932.4	932.4	135	9	0	20,000
4	932.4	932.4	180	9	0	20,000
5	932.4	932.4	45	9	-9	20,000
6	932.4	932.4	90	9	-9	20,000
7	932.4	932.4	135	9	-9	20,000
8	932.4	932.4	180	9	-9	20,000
9	828.8	1,243.	45	9	-9	20,000
10	828.8	1,243.	90	9	-9	20,000
11	828.8	1,243.	135	9	-9	20,000

TABLE 3. PERFORMANCE EVALUATION ENGAGEMENT CONDITIONS

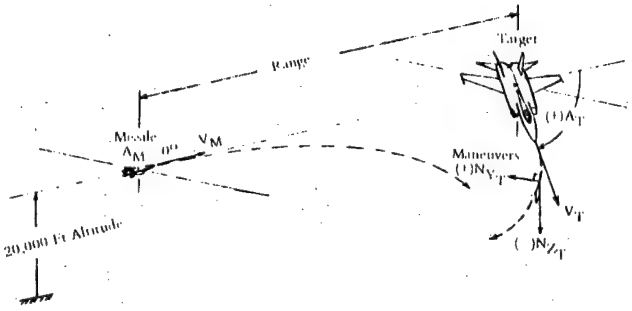

Figure 8. Performance Evaluation Engagement Conditions

Biographical Sketch

Mr. Robert M. McGehee was employed by the Air Force Armament Laboratory in Jan 1971. He has served in the Systems Analysis & Simulation Branch of the Guided Weapons Division from 1971 until the present. His responsibilities include guidance and control, aerodynamics, hybrid simulation, hardware-in-the-loop analysis and flight evaluation of guided weapons.

Mr. McGehee received the Bachelor of Science Degree in Aerospace Engineering from Auburn University in 1970. He has taken graduate courses in electrical engineering and economic management from the University of Florida. Mr. McGehee was also employed by Lockheed Aircraft Corp., Marietta, Georgia, as a co-op trainee from 1965-1969. This training included reliability, weights, plant engineering, flight testing, wind tunnel testing and research. Mr. McGehee is a member of Tau Beta Pi, Sigma Gamma Tau and Delta Chi. He is also a member of SAE Aerospace Control and Guidance Systems Committee.

Mr. McGehee is presently serving as program manager for the Bank-to-Turn control guidance development effort at the Air Force Armament Laboratory.

ADVANCES IN MICROWAVE STRIPLINES WITH AMPLIFICATIONS

BY

Joseph A. Mosko

Electronic Warfare Department

Naval Weapons Center
China Lake, California

Advances in Microwave Striplines with Applications

Abstract

This decade has seen the ever increasing utilization of the radio frequency spectrum by the Soviets. This in turn has required our various ARM and ECM receiving systems to operate over increased bandwidths with particular emphasis on providing performance up into J- and K-Bands.

The Naval Weapons Center has been conducting research and development activities in the area of microwave strip-transmission lines including component and antenna feed circuit developments. Goals have been to (1) improve component performance (bandwidth and upper frequency extension), (2) improve component intracompatibility for integration into networks, and (3) utilize computer aided design, evaluation, and manufacturing techniques to improve producibility and reduce cost.

The paper will discuss the results of this investigative work to date and describe several potential operational applications.

Introduction

Microwave striplines are transmission lines that may be coupled or uncoupled, and usually etched on dielectric sheets to transport or process microwave energy. The designs can be relatively complex, highly tailored to the application and still at greatly lower costs than other forms of transmission lines. Practically speaking, striplines were "born" in 1955. The earliest form was microstrip (Figure 1a); that is, transmission lines were above a suitable ground plane etched on relatively low dielectric constant ($2 < \epsilon_r < 4$) plastic sheets. After certain shortcomings were realized, such as excessive radiation losses from striplines, the balanced stripline (Figure 1b) became popular. This form has transmission line conductor patterns surrounded by a suitable dielectric material and spaced between two zero potential groundplanes. Most workers in this field attribute the immense popularity of balance stripline--or stripline for short--compared to microstrip line to: (a) Cohn's classic paper (Reference 1) which allowed everyone to accurately design strip transmission lines very easily since 1955; (b) high quality transmission lines (i.e., almost free from any unwanted mode of wave propagation) can easily be achieved even over decades of bandwidth.

The newly founded technology matured very quickly. In the next decade almost all we know today in this specialized area was developed chiefly due to DoD sponsored research and development activities at Stanford Research Institute (SRI) and Radiation Systems, Inc. (RSi). Others who made notable contributions and thus impacted on today's technology were Texas Instruments (TI), Hughes Aircraft Company (HAC), Bendix Research Laboratory, and the Naval Weapons Center (NWC). Although naming individuals may lead to arguments, it is very safe to single out three extraordinary contributors: Seymour B. Cohn, J. Paul Shelton, and Leo Young.

During the last ten years, relatively minor contributions from basic research on striplines are found. Major focus shifted to high dielectric microstrip with a number of significant contributions recorded. The recent works in stripline seemed to focus mostly on computer aided design (CAD) and computer aided manufacture (CAM). From a DoD user standpoint, this application of these modern techniques is very important in that cost effective weapon systems can be synthesized, designed, and deployed. At this time, we would like to describe some ongoing efforts that are expected to provide a technology which allows us to better meet new threat challenges at affordable cost.

Multi-Section Microwave Couplers

Coupling of microwave energy from one transmission line to another was recognized and exploited almost from the start. Figure 2a shows such an early coupler while Figure 2b is the cross-section view of the coupled lines involved. Maximum coupling occurred at the frequency when the coupled lines were one quarter wavelength long. The frequency response is indicated in Figure 2c. Coplanar coupled lines on relatively low dielectric constant materials are weakly, or loosely, coupled even when their separation is quite small (Reference 2). For example: For a 50 Ω coupler in a teflon dielectric, the coupling is -13 dB when the separation of the strips is 10% of the groundplane spacing.

To make this type of coupler useful for a variety of signal processing needs, where -3dB coupling is required, the broadside coupled version was soon thereafter introduced (Reference 3, 4). It's cross-section view is shown in Figure 2d suggesting overlapped strips separated by a fixed distance. Thus, in the late 50's, a variety of microwave circuits were being made with couplers therein having almost unheard of bandwidths of operation; that is, instead of having the usual 10% or lower frequency range, suddenly some systems (especially the passive ones) had almost 2:1 bandwidth capabilities.

With the advent of frequency independent and also log-periodic antennas, it soon became desirable to have still more frequency coverage for various EW systems to cover threat activities more effectively. This need was soon fulfilled by the theoretical and also practical applications labor of the almost legendary Dr. S. B. Cohn (Reference 5). His pioneering work truly and vividly showed the virtues of symmetric three-section couplers. (We might add that R. Levy in England at that time also made multi-section and wideband couplers but they were asymmetric (Reference 6). This type of coupler has, for many applications an undesirable phase variation between coupler outputs with frequency and thus never became very popular for signal processing applications.) Although Cohn built high quality -3 dB couplers covering 5:1 bandwidths, it seemed that only coaxial transmission line systems could provide the necessary coupling parameters. That of course, represented costly manufacture as far as reasonably complex microwave systems involving such components are concerned.

The problem associated with the realization of that first broadband stripline coupler (and to some extent even today) can be quickly grasped by considering Figures 3 and 4. First, if the single section coupler of Figure 2a had

two looser or weeker coupled sections attached to it on each end as suggested in Figure 3a, the overall coupling response of the three-section coupler would be flatter and also of lesser mean magnitude than that of the original single section coupler. The typical response is shown in Figure 3b while the relative spacings of the coupled striplines for center and end sections are shown in Figures 3c and 3d. It is noteworthy that the coupler is completely planar - which is highly desirable from a manufacturing standpoint - with the required coupling variation of the striplines being achieved by line separations. To raise the nominal coupling amplitude from weak to tighter coupling (Figure 4b), the broadside strip configuration once again needs to be utilized as suggested in Figures 4a, 4c, and 4d. However there is a problem. The required change in coupling achieved by greater/lesser stripline separations, destroys the planar nature of the three layer sandwich type device. Thus, common and cost attractive photo-etch type manufacture is not directly applicable as before with the coplanar couplers.

Paul Shelton was also working on various multisection coupled lines at that time. He had, what turned out to be an elegant solution to the previously described problem which is depicted in Figure 5 and was first published in the 14th USAF Antenna Symposium Record (Reference 7). He thus provided us the capability to have a tightly coupled section as in Figure 5b, and anything less as in Figure 5d; better still, we could have a planar conductor pattern for photo-etching. His classical open literature paper (Reference 8) indeed was the key to not only practical, inexpensive, and high quality couplers and phase shifters at that time, but later also the key to power dividers, filters, etc! The 14th USAF Antenna Symposium Record is still more remarkable (Reference 7). The work by Shelton, et al, resulted in the first systematic synthesis and design of wide-band multi-quarter-wavelength directional couplers. Soon thereafter, other contributions on coupler synthesis appeared - some more elegant and others more refined (References 9-12).

Althogether, it was generally believed that the wide-band microwave coupler problem has truly been solved. Time proved this observation to be optimistic. It turned out that the junction problems owing to the step discontinuities between the cascaded quarter wavelength sections were so severe that almost any 3 dB-type coupler had poor directivity in the microwave frequency region. Also, the measured coupling versus frequency response was quite erratic. Figure 5a shows a scaled drawing of seven quarter-wavelength-section coupler illustrating the offset junction discontinuities. Figure 6 shows a typical measured performance for a

5:1 bandwidth, 3 dB hybrid of this type. Thus, we see as Levy did (Reference 6) with another type of stepped coupler, that the theory may be sound, but there nevertheless are practical limitations at higher microwave frequencies. In order that such a coupler perform well, the important point is that the offset distance between the adjacent, cascaded, coupled strips be small compared to the line widths at the junctions. Making the width-to-length ratio of each $\lambda/4$ section small helps, though the relative offset remains unaltered. Unfortunately, even this is seldom practical because the length is inversely proportional to the center frequency of operation--and presumably fixed--while narrowing the width requires one to reduce the groundplane spacing of the stripline assembly. The latter action will greatly raise the I^2R losses for the coupler--an old problem traded for a new one. It is also interesting to note that several ridiculous patents have been issued on "improved" stepped couplers which may have mislead many inexperienced members of the microwave community (References 13 and 14).

Thus, we experienced a dilemma. The newly developed coupler synthesis called for stepped, coupled transmission lines; the step discontinuities caused poor, or degraded, coupler directivities at the higher microwave frequencies. Once again, new theoretical and practical works resulted in significant breakthroughs which were very much needed.

Tapered Microwave Couplers

During the early 60's, Dr. DuHamel researched wideband Magic-T's (couplers with $0^o/180^o$ phase characteristics) with the first successful design published in the 15th USAF Antenna Symposium Record. This type of coupler is shown in Figure 7. It immediately attracted great attention because: (a) it was wideband (multioctave); (b) it had good directivity at higher microwave frequencies; and (c) it was a stripline design which was relatively easy to manufacture utilizing common photo-etching techniques. It might be noted, that DuHamel's tapered Magic-T and R. Levy's (Reference 6) asymmetrical coupler are quite similar except the former is tapered with one severe discontinuity, while the latter is a stepped multi-section design with several sizable discontinuities. Moreover, the former has good directivity while the latter is poorer in comparable frequency bands of operation. Therefore, the earlier suspicions about large step discontinuities causing degraded directivities in couplers seemed to be confirmed.

Soon after these difficulties were fully recognized, another significant contribution was made by Tresselt

(Reference 15), namely the tapered quadrature coupler. See Figure 8 for a direct comparison between the classical stepped $\lambda/4$ and the tapered line type quadrature coupler. Although his theory only modified an optimum equal-ripple stepped design with a suitable weighting function to make it a tapered line design, it nevertheless was important. His non-equal ripple, approximate design method did motivate others later to improve on it, especially after the benefit of improved directivity along with good coupling were demonstrated (Reference 16). Now the hybrid was to solve all the problems. This coupler is smooth --no steps at all. Therefore, when designed properly, excellent directivities are almost guaranteed, given certain materials, bandwidth, center frequency, etc. As seen from measurements on one of our best couplers in Figure 9, it's certainly true that these couplers have much better directivities than the old stepped kind--but as some designers may know, there are nevertheless at least a few problems with the tapered devices.

Tapered couplers are relatively complex for several reasons. First, it is almost inconceivable that anyone would attempt to develop such a device without the aid of carefully prepared computer synthesis and coupled line design programs. Second, the accurate realization of the tapered lines along the full length of the coupler is extremely difficult by hand. In the development of wideband hybrids, a precision artwork generation system (Gerber) seems to be essential. Third, during construction the alignment is critical, and difficult to assure.

Although most of the above assertions seem to be self-evident, some supporting evidence will nevertheless be offered for them. Figure 10a shows the mean values of measured responses of two supposedly "identical" families of hybrids. All manual steps, from preparing artwork (on a Coradograph type precision drafting table with ± 0.001 inch plotting accuracy) to the final assembly and tests, were duplicated in this experiment. The final negatives from which the two different families of couplers were etched were "good" in the sense that any evaluation of them, other than actually measuring the frequency response of couplers derived from them, would make each negative equally desirable! Furthermore, the worst case measured coupling variations between the various members of one family are given in Figure 10b and reveal very good repeatibility for all components manufactured using the same negative. This indicates that an accurate photo-etching negative is mandatory (though difficult to achieve) and that with accurate

assembly techniques, one may make devices with very similar response characteristics. Also, note that the measured isolation was good for all couplers involved in this experiment.

It is generally assumed, and quite appropriately, that two "identical" couplers drawn on a precision Gerber photo-plotter would give experimental tapered couplers which would test out alike.

Whereas most designers did have access to the Corado-graph (manual) type precision plotter for drawing coupler art masters for later photo-etching, and whereas relatively few had access to Gerber photo-plotters, a new general class of microwave couplers--called ministep couplers--was invented and reported on at the 22nd USAF Antenna Symposium (Reference 17). This theory unified the quadrature couplers (stepped and tapered) as well as Magic-T's and other more general couplers which at any specific frequency may have any desired amplitude and phase difference between coupler output signals that the designer may like. That is, instead of merely being able to design quadrature coupler (90^{o} phasing), and Magic-T's ($0^{o}/180^{o}$ phasing), one may design for coupler output phases of 60^{o} and 120^{o}, or say 45^{o} and 135^{o} depending upon which coupler port is excited. A quadrature coupler ministep implementation is depicted in Figure 11 for several of the infinite possibities. With Figure 12, one can quickly see how to control in-band as well as out-of-band coupling responses of various couplers as well as coupled output amplitude (Reference 17). Whereas the original goal was to accurately draw and construct wideband stripline couplers with only a Carodograph (not Gerber), Figure 13 shows that that goal was successfully reached. The point there was that the repeatability of two ministep couplers (Figure 13) was much better than the more common continuously tapered couplers of comparable bandwidth as in Figure 10. Furthermore, with the design flexibility of large or small step sizes, it might be noted that repeatably one may design high quality stripline couplers operating into J-Band (say 12 GHz) as seen in Figure 14. Unfortunately, this kind of performance has not been achieved as yet throughout J-Band, and above.

Constraints Placed On Couplers By Network Considerations

In the interest of cost, performance, reliability, size, weight, etc, it is beneficial to integrate all microwave components (such as quadrature couplers, Magic-T's, phase shifters, filters...) of a microwave network (say a monopulse comparator) into one unit, all internally inter-

connected, and photo-etched all at one time; in other words, as a single unit. Moreover, the more technically complex a network becomes, the more likely transmission line crossings become necessary. These crossings usually* take place in the various necessary network couplers. When the network consists of an assembly of identical couplers, or devices, there is no problem. However, if different types of couplers and/or Magic-T's (or whatever) need be integrated, then there is a problem if all planar dielectric sheets are to be etched and sandwiched together. The problem is analogous to the multistep, broadside coupler discussed earlier. Obviously, the simple Shelton coupled line pair (Reference 8) does not have enough degrees of freedom for the above mentioned, "real world" problem that the designer often faces (Reference 18). Let's now discuss some of the approaches that are presently being researched to solve this problem as well as potentially improve J-Band coupler performance.

Current Research Efforts On New Striplines and Techniques

If the directivity of a J-Band coupler were good but the coupling response not acceptable, the so-called J-Band coupler problem would be trivial--no matter what the bandwidth of operation is. That's because enough analytical techniques/methods exist (Reference 11, 17) which can take the last measured coupling response and improve it significantly. Unfortunately, the directivity is usually poor and improvements there are more difficult. Indeed, if coupling and directivity is poor, even the computer algorithms (Reference 17) for coupling improvements tend to be unreliable. The reason for this, we believe, is that this otherwise very robust algorithm is fundamentally based on TEM mode propagation on striplines; at the present state of evolution of microwave couplers, most (certainly all the obvious ones like step-discontinuities in couplers) scattering mechanisms in couplers have been avoided. Nevertheless, a non-uniform transmission line--although tapered--is not strictly speaking a TEM mode system as we would like to have. The following approach will address the potentially non-TEM scattering problem as well as the intra-network component compatibility problem which was previously discussed.

The Shelton line pair, Figures 5b-5d, does not seem to have enough freedom for coupling control when other con-

*That is, not necessarily in conventional couplers. For example, one may design a crossing of two lines that is uncoupled to any desired value--say -30 dB, or less, of coupling.

straints are placed on it. That is, the overlapped (broadside) strip configuration of Figure 5b has greater/lesser coupling for closer/farther strip separations, given a fixed impedance level and homogeneous dielectric constant of the material. By introducing additional zero potential conductors to the existing groundplanes as suggested in Figure 15, we gain the coupling control shown in Figures 16 and 17. The important point to note first is that the whole conductor structure is still planar in nature. Therefore, conventional precision photo-etch manufacturing is retained.

Wherever possible, the well known nomenclature of Shelton (Reference 8) will be used throughout. That is, w is the normalized stripwidth, w_c is the coupled line overlapped, s is the separation of the planes containing coupled strips, etc.....

Let's first consider Figure 16, the special case of Figure 15c, which has two coupled strips in the center and four symmetrically spaced zero potential strips a normalized distance g from any nearest edge of a coupled strip. Then, depending on the gap g, coupling varies between -3.38 dB to -5.65 dB. Of course, for the given material parameters: ϵ_r = 2.53 (Rexolite 1422 dielectric), outer ground plane separation b = 1., center spacer thickness s = 0.106, the coupled strip widths w had to vary from 0.407 to 0.292 in order that the coupler impedance remains 50 Ω. As intuition would tell us, the narrower the gap dimension g, the lower the coupling between the two striplines; also the narrower the typical strip width w. Although Figure 16 only shows normalized gap dimensions g equal to 50%, 25%, and 10% of the outside groundplane spacing, numerous other values of coupling have just been synthesized suitable for various coupler developments. From Figure 16 we thus see that it is possible to have compatibility between various couplers in a network and also be able to cross lines therein.

Figure 17 shows theoretical examples of control of coupling with other physical constraints. First are shown three Shelton line designs (top row) to be compared to three identical coupled lines with the four additional groundplanes in place (bottom row). The first pair of designs shows that two strips can be completely overlapped and when the gap g (stripline edge to nearest groundplane edge) varies from infinity (conventional Shelton line design) to 0.50, the coupling does not vary to the first three places (i.e., k = 0.677 or -3.38 dB); the normalized strip width must vary from 0.423 to 0.407 in order that the coupler impedance level remains at 50 Ω. Next we notice that two moderately coupled Shelton lines in center of Figure 17 can

either be slightly overlapped (w_c = 0.123 with w = 0.504) to highly overlapped (w_c = 0.233 with w = 0.286) providing that g = 0.1. For many coupler designs, g = 0.1 (i.e., 10% of the outer ground-plane separation) is achievable without great difficulty. It would appear this particular example holds significant promise that the stripline layout of couplers can be controlled; for example the center portion of the tapered quadrature coupler of Figure 8b, although smooth and graceful, nevertheless is more non-uniform or changing than most of the coupler layout. Presently, only heuristic arguments on coupler smoothness are given; recently more specific and quantitative data was presented on problems (not solutions) with "smooth" but non-uniform couplers which made this whole qualitative discussion precise (Reference 19).

Whereas tapered couplers, Figure 18a, are synthesized as numerous sections of parallel coupled sections Figure 18b, with currents flowing parallel to the center line of the coupler, and whereas the coupled lines seem to become significantly "non-parallel" such as in the center of Figure 18a, then problems due to non-parallel current flow are manifested. As indicated in Figure 19, a very peculiar coupler was synthesized (Reference 19). It consisted of a particular constant angle, β, crossing of two transmission lines (of varying strip width--in order that impedance requirements were met). From the synthesis, it was a straightforward problem to calculate the coupler unbalance (CU), i.e., the difference between coupled and direct coupler outputs. Also, the coupler unbalance was measured for various couplers of β angle variation. For couplers where β was small, the difference between TEM mode theory involving assumed parallel current flow in the coupler, and experiment was very small indeed. For large values of β, the discrepancy was very significant as seen in Figure 20.

The last example of Figure 17 shows that loosely coupled lines can now be synthesized in a variety of ways. The classical Shelton pair design has w_c = -0.093 (coupled strips have a separation of 9.3% of the groundplane spacing). On the other hand, w_c equals zero together with g = 0.1 and the nearest groundplane on the other side of the center spacer is precisely colinear as shown in the lower right hand corner of Figure 17. One point that should be made is that the fringing capacitance terms from a strip to a near ground-plane such as in the lower two examples of Figure 17, become highly non-linear with spacing dimensions. This, first, makes the synthesis procedure slightly more difficult to keep stable and, second, it also indicates the benefits and/or critical nature of the new, more complicated design.

At the time of this writing, time permitted only one experiment involving the new stripline geometry. A - 6 dB three-quarter-wavelength stepped quadrature coupler was designed to operate from 0.7 to 2.8 GHz. The center $\lambda/4$ section resembled the lower left cross-section of Figure 17; the outermost $\lambda/8$ sections resembled the upper right of Figure 17 except that the additional four groundplanes are g = 0.5 distance away. The other half of the outer $\lambda/4$ section was designed to have a cross-section very similar to the lower right hand design of Figure 17. It was hoped that by such an experiment, the severe junction problems of a conventional three-section coupler would be improved enough to notice that improvement over the conventional approach. Unfortunately, the first experimental attempt resulted in no measurable improvements. It seems that the step discontinuities in the striplines, although smaller, together with step discontinuities in groundplanes resulted in similar performance as the standard approach. Though this was somewhat disappointing, we recognize that the technique should have been applied to a tapered device which is more complicated to synthesize because of the number of points involved in accurately simulating a tapered line. Having learned something from this earlier believed to be expedient test, a more ambitious design shall follow.

Conclusion

Advances in striplines were traced from early innovations to the latest synthesis results. Over the years one can see where first there existed a need or deficiency in the theoretical realm involving striplines, which was soon removed, and then there was a mechanical/practical limitation recognized. That in turn was "solved" by some new contribution and the process seemed to repeat once again. Fortunately, the quality and overall capabilities of various couplers, phase shifters, filters, or whatever, which represent applications of striplines, have been improved markedly during this period.

Presently, a new design of coupled striplines has been postulated and synthesized. By being more complex than existing state-of-the-art striplines, the new transmission line has more degrees of freedom that "appear" to be exploitable. With this newly earned freedom, the designer hopefully will achieve better performing couplers, and other devices, in the new threat bands of interest, or concern. The recently started experimental effort should prove to what degree some of these eagerly anticipated improvements are now achievable.

Acknowledgement

It is with pleasure that I acknowledge the help of several persons who were involved at various stages of the work summarized in this paper. First, there were Dr. S. B. Cohn and Paul Shelton who greatly influenced me in my early stages of career. Then, there were Professors K. K. Mei and J. R. Whinnery of the University of California, Berkeley, who stimulated the theory part of some of the work reported here. Robert G. Corzine of the Naval Weapons Center (NWC), China Lake, California, has been a valuable person to sound out on various practical and also conceptual aspects of this work for many years; also for carefully reviewing and suggesting improvements in the text of the paper. Finally, if it had not been for the expert services that Deanna Johnson and John Lopez provided during the preparation of the paper, it simply could not have been done.

REFERENCES

1. S. B. Cohn, "Problems in Strip Transmission Lines," IRE Trans., PGMTT-3, 2, pp. 119-126 (March 1955).

2. S. B. Cohn, "Shielded Coupled-Strip Transmission Lines," IRE Trans., PGMTT-3, pp. 29-38 (October 1955).

3. S. B. Cohn, "Characteristic Impedances of Broadside-Coupled Strip Transmission Lines," IRE Trans., PGMTT-8, 6, pp. 633-637 (November 1960).

4. E. M. Jones and J. T. Bolljahn, "Coupled-Strip-Transmission-Line Filters and Directional Coupler", IRE Trans., PGMTT-4, 2, pp. 75-81 (April 1956).

5. C. B. Cohn, "The Re-Entrant Cross Section and Wide-Band 3-dB Hybrid Couplers," IEEE Trans. on Microwave Theory and Techniques, Vol. MTT-11, No.4, pp. 254-258 (July 1963)

6. R. Levy, "General Synthesis of Asymmetric Multi-Element Coupled-Transmission-Line Directional Couplers," IEEE Trans. on Microwave Theory and Techniques, Vol. MTT-11, No. 4, pp. 226-237 (July 1963).

7. J. P. Shelton, R. VanWagoner, and J. J. Wolfe, "Tandem Couplers and Phase Shifters; A New Class of Unlimited Bandwidth Components," presented at the 1964 14th Annual Symposium, USAF Antenna R&D Program, AF Avionics Lab., in cooperation with the University of Illinois, Monticello, Ill., or see Microwaves, pp. 14-19 (April 1965).

8. J. P. Shelton, Jr., "Impedances of Offset Parallel-Coupled Strip Transmission Lines," IEE Trans. on Microwave Theory and Techniques, Vol. MTT-14, No. 1, pp. 7-15, (January 1966).

9. E. G. Cristal and L. Young, "Theory and Tables of Optimum Symmetrical TEM-Mode Coupled-Transmission-Line Directional Couplers," IEEE Trans. on Microwave Theory and Techniques, Vol. MTT-13, pp. 544-558 (September 1965).

10. P. P. Tuolious and A. C. Todd, "Synthesis of Symmetrical TEM-Mode Directional Couplers," IEEE Trans. on Microwave Theory and Techniques, Vol. MTT-13, pp. 536-544 (September 1965).

11. J. P. Shelton and J. A. Mosko, "Synthesis and Design of Wide-Band Equal-Ripple TEM Directional Couplers and Fixed Phase Shifters," IEEE Trans. on Microwave Theory and Techniques, Vol. MTT-14, pp. 462-473 (October 1966).

12. J. A. Mosko and J. P. Shelton, "Design Tables for Wide-Band Equal-Ripple TEM Directional Couplers and Fixed Phase Shifters," ADI Auxiliary Publications Project, Photoduplication Service, Library of Congress, Washington, D. C. to obtain a copy: Document 9017; advance payment $3.75 photoprints, $2.00 35mm microfilm payable to Chief, Photoduplication Service, Library of Congress.

13. E. E. Beech, "Stepped-Impedance Directional Coupler," U.S. Patent 3,617,952, Filed August 27, 1969, Issued November 7, 1971.

14. R. P. Barbatoe, "Quadrature Hybrid Coupler Network Comprising Three Identical Tandem Fifteen Cascaded Section Couplers," U.S. Patent 3,626,332, Filed April 23, 1970, Issued December 7, 1971.

15. C. P. Tresselt, "The Design and Construction of Broadband, High-Directivity, 90-Degree Couplers Using Nonuniform Line Techniques, IEEE Trans. on Microwave Theory and Techniques, Vol. MTT-14, No. 12, pp. 647-656 (December 1966).

    Also see: C. P. Tresselt, "Tapered Line Directional Couplers," U.S. Patent 3,528,038, Filed July 11, 1969 Issued September 8, 1970.

16. D. W. Kammler, "The Design of Descrete N-Section and Continuously Tapered Symmetrical Microwave TEM Directional Couplers," IEEE Trans. on Microwave Theory and Techniques, Vol. MTT-17, No. 8, pp. 577-590 (August 1969).

17. J. A. Mosko, "The Ministep Coupler; A New General Theory of Quadrature Couplers," Prepared for Presentation at the Twenty-Second Annual Symposium on USAF Antenna Research and Development, Monticello, Ill. (October 1972).

18. G. L. Millican, and R. C. Wales, "Practical Strip-Line Microwave Circuit Design," IEEE Trans. on Microwave Theory and Techniques, Vol. MTT-17, No. 9, pp. 696 (September 1969).

19. J. A. Mosko, "Practical Problems With Multi-Octave Stripline Couplers," Paper delivered at the 1975 ERASE Conference, San Diego, California (November 1975).

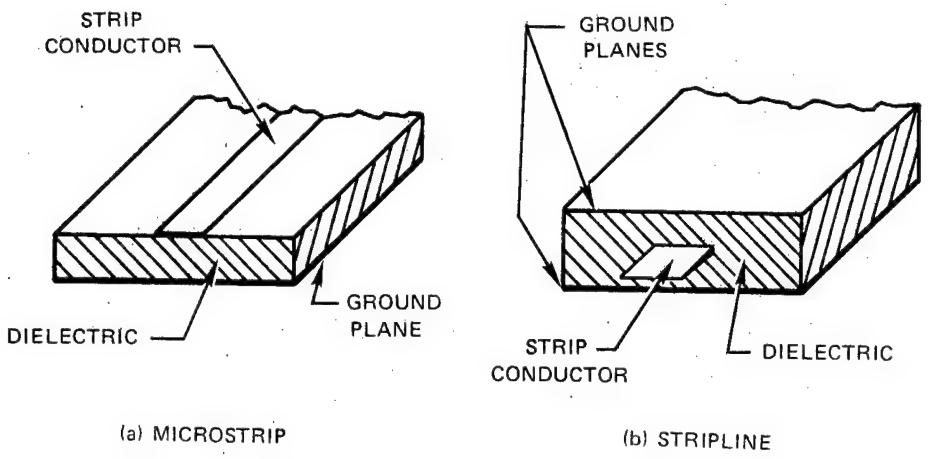

FIGURE 1. Microwave Strip Transmission Lines.

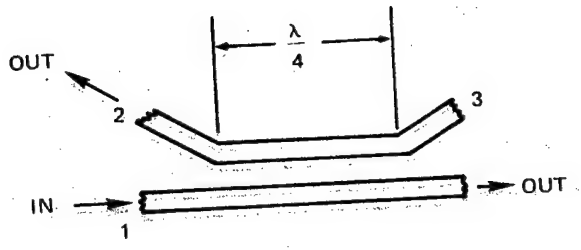

TYPICAL CONDUCTOR CONFIGURATION
(COPLANAR)

(a)

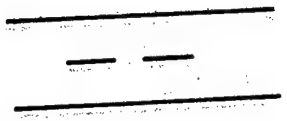

COPLANAR COUPLED

(b)

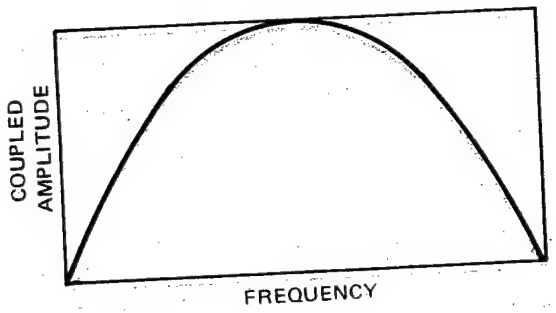

FREQUENCY RESPONSE

(c)

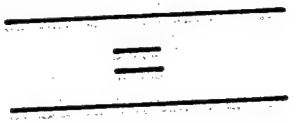

BROADSIDE
COUPLED

(d)

FIGURE 2. Earliest Broadband Coupler.

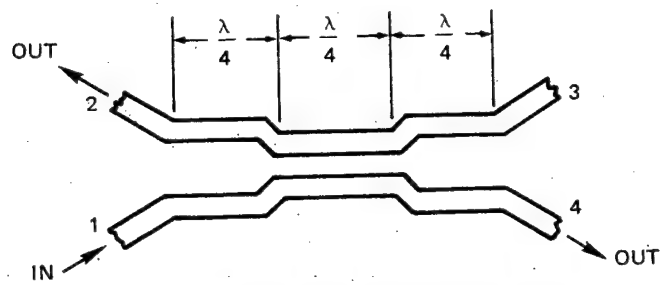

TYPICAL CONDUCTOR CONFIGURATION
FOR WEAK COUPLING (COPLANAR)

(a)

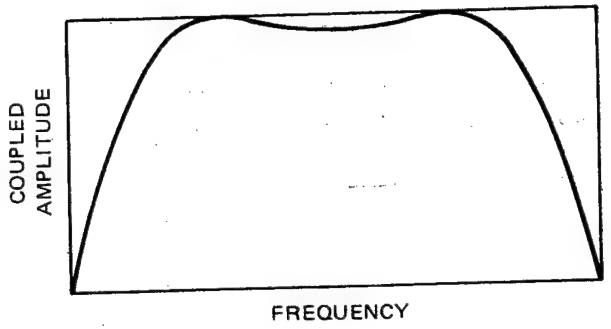

COUPLING RESPONSE

(b)

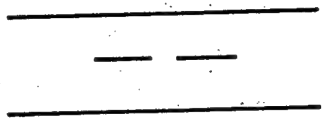

CENTER SECTION

(c)

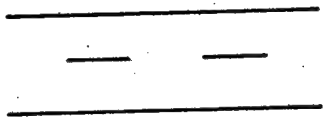

END SECTIONS

(d)

FIGURE 3. Three-Quarter-Section Coplanar Stripline Coupler.

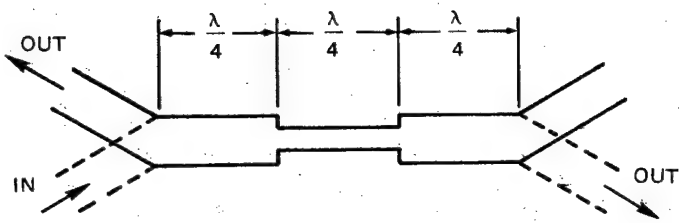

TYPICAL CONDUCTOR CONFIGURATION FOR TIGHT COUPLING (BROADSIDE)

(a)

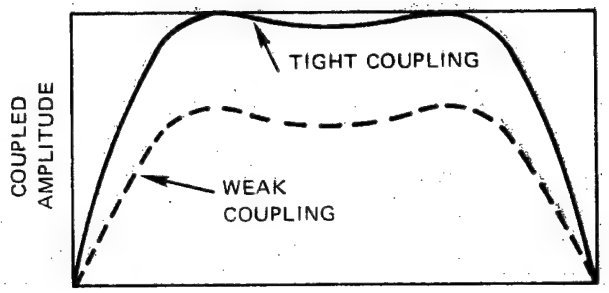

COUPLING RESPONSES

(b)

CENTER SECTION

(c)

END SECTIONS

(d)

FIGURE 4. Three-Quarter-Wavelength Broadside Stripline Coupler.

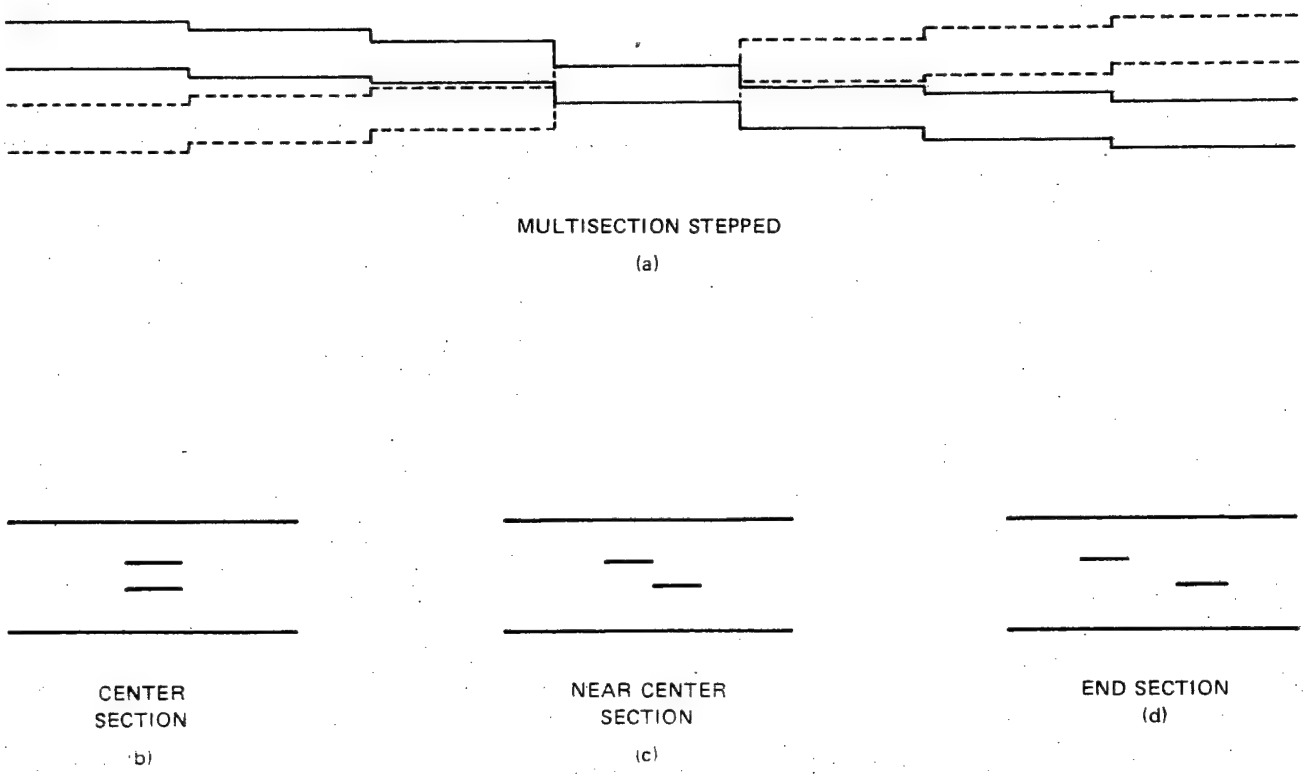

FIGURE 5. Classical Wideband Multisection Coupler and Cross-Section Views.

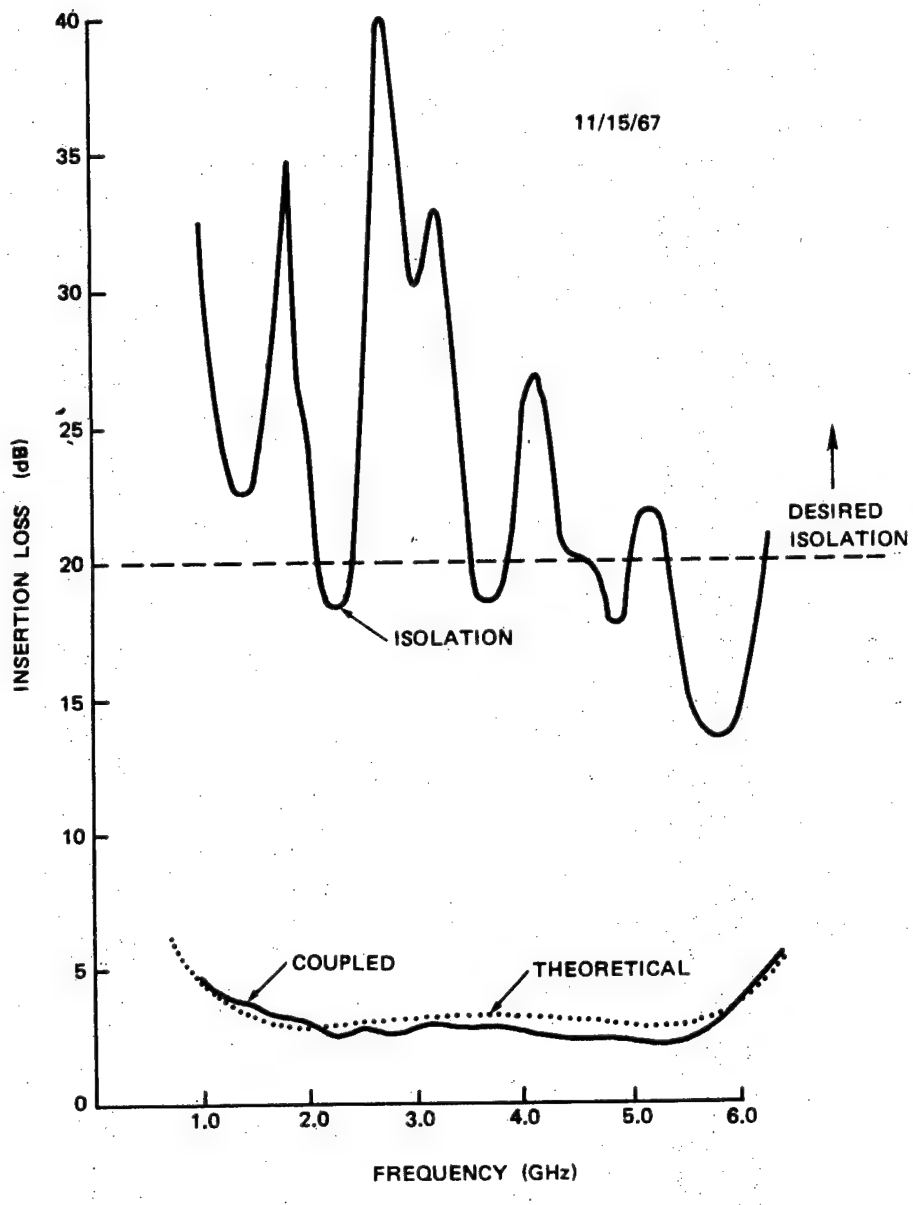

FIGURE 6. Response Plot for -3.01 dB 3 λ/4 Stepped Quadrature Couplers.

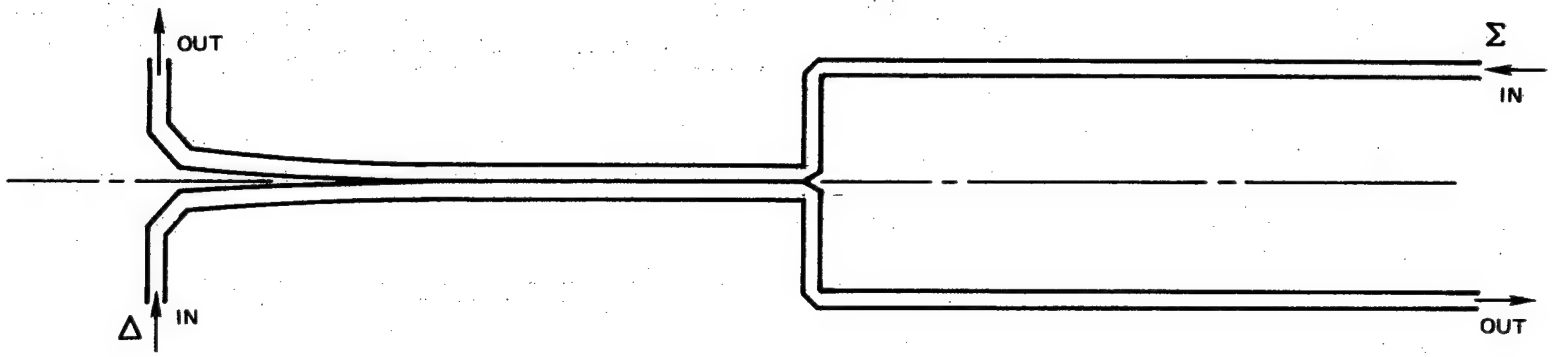

FIGURE 7. Tapered-Line Magic-T.

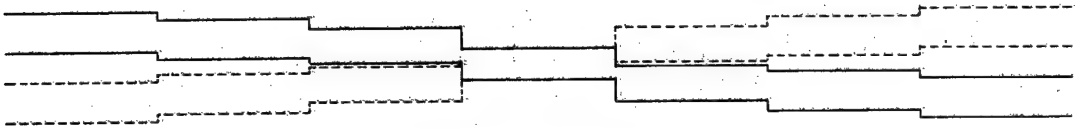

(a) STEPPED COUPLER

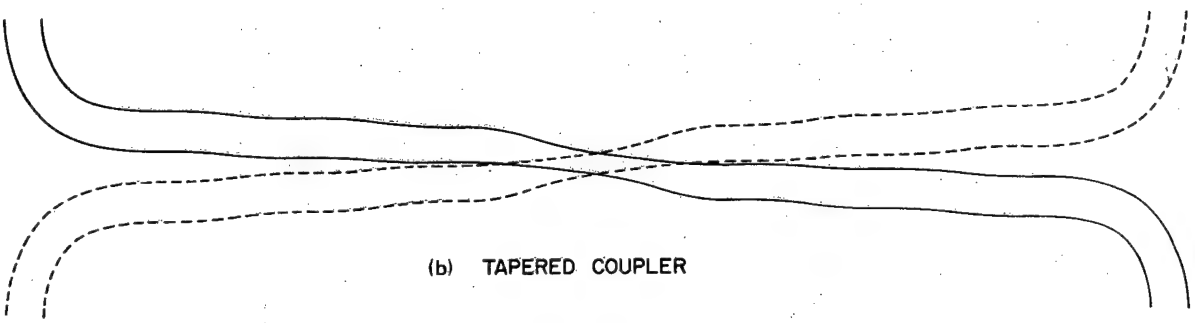

(b) TAPERED COUPLER

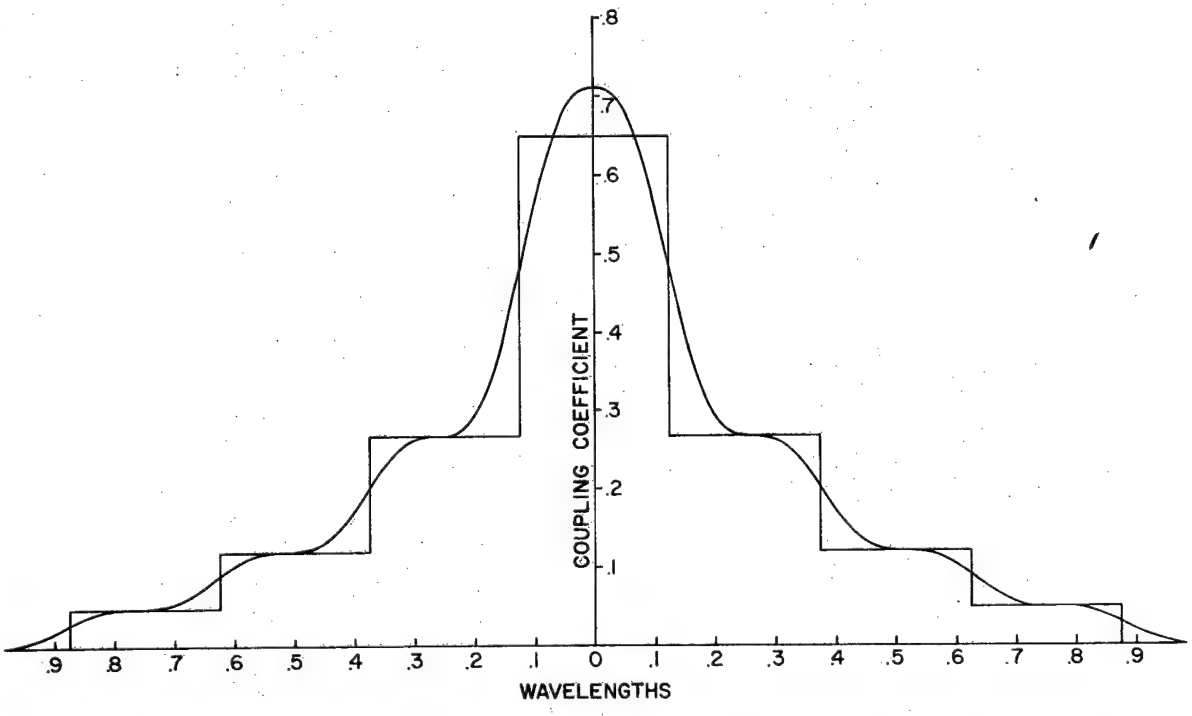

(c) COUPLING VERSUS DISTANCE FUNCTION FOR STEPPED & TAPERED COUPLER DESIGNS

FIGURE 8. Quadrature Couplers.

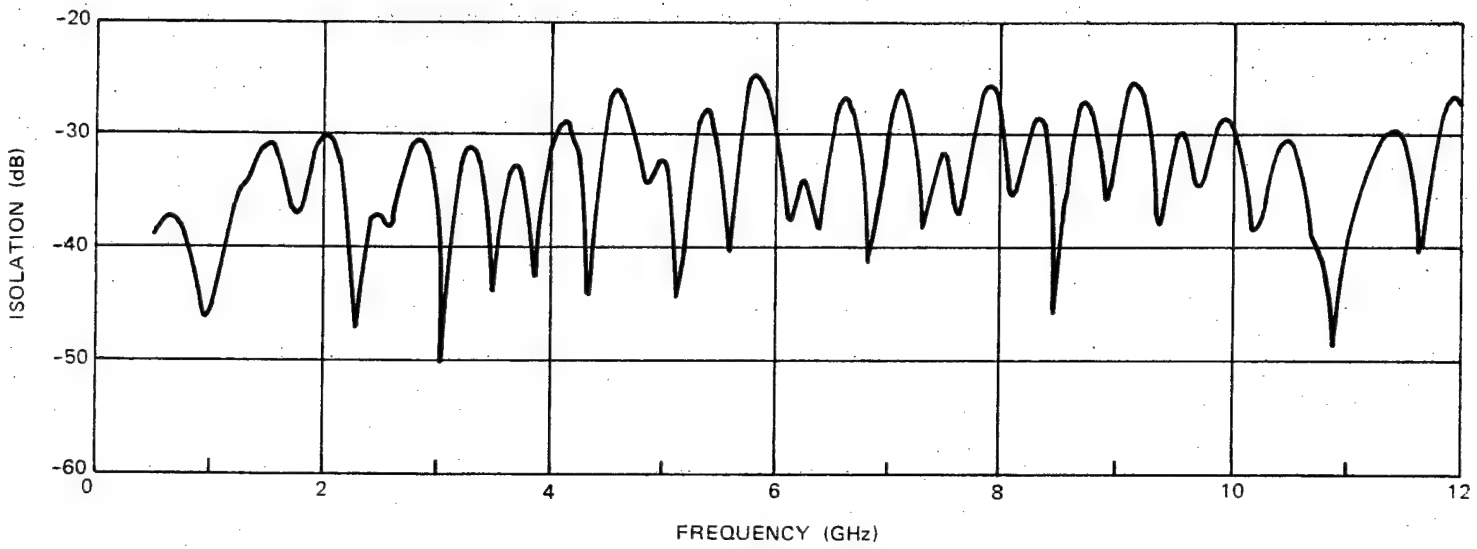

FIGURE 9. Measured Isolation on a 16.5:1 Bandwidth (0.7 - 11.6 GHz) -3 dB Stripline Quadrature Hybrid.

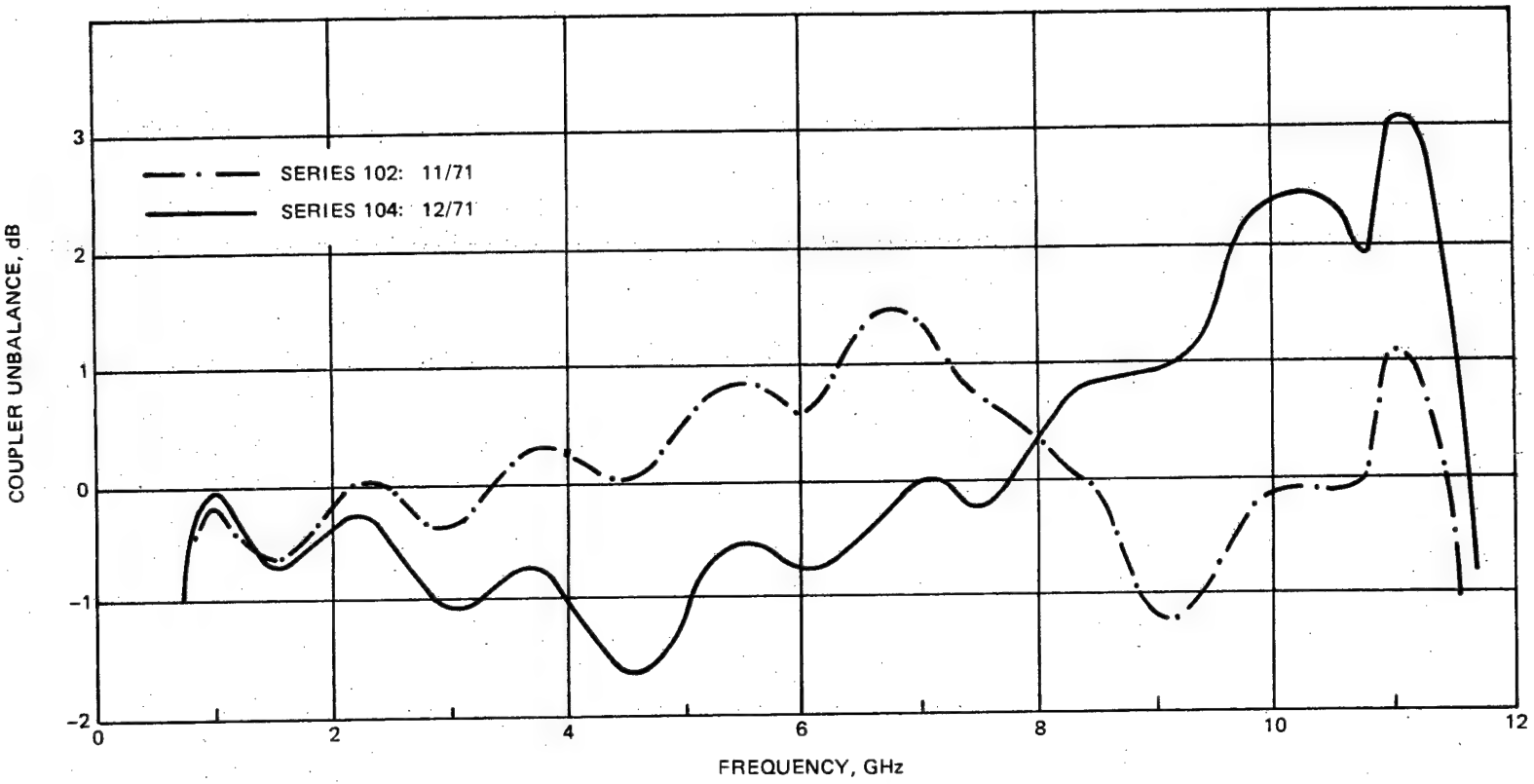

(a) AVERAGE UNBALANCE BETWEEN OUTPUTS OF WIDEBAND 3 dB COUPLERS VERSUS FREQUENCY

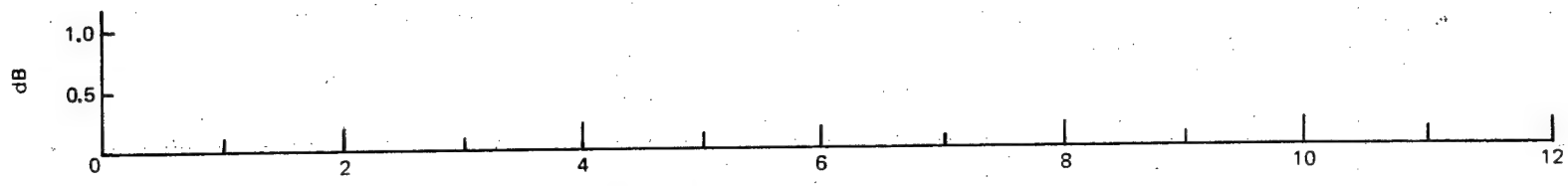

(b) TYPICAL DEVIATIONS BETWEEN MEASUREMENTS OF COUPLERS WITHIN SERIES 102 OR 104 ABOVE VERSUS FREQUENCY

FIGURE 10. Experimental Study of Repeatability for Tapered Couplers.

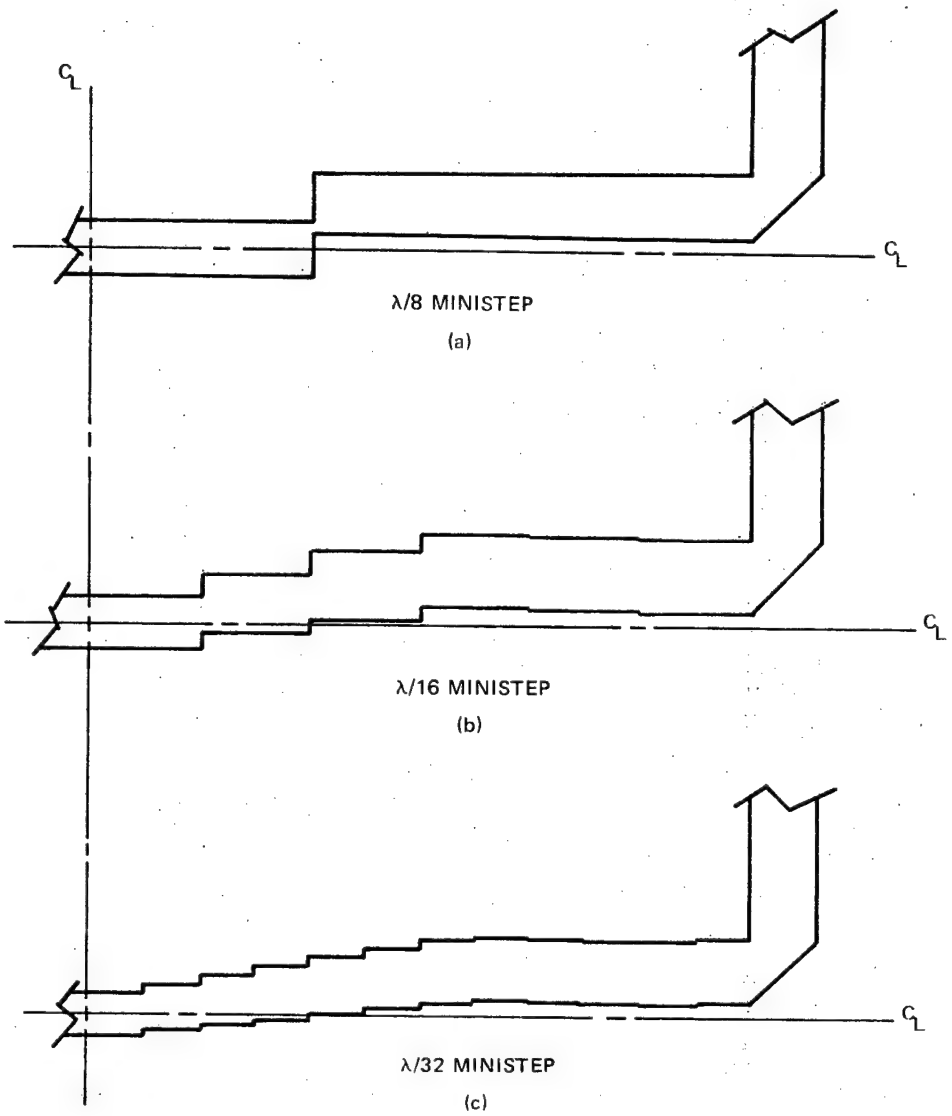

FIGURE 11. Typical Sections of 4:1 Bandwidth, 8.34 dB Stripline Quadrature Couplers (b = 1/16; ε_r = 2.54; Passband: 1-4 GHz; 8.34 ± 0.31 dB).

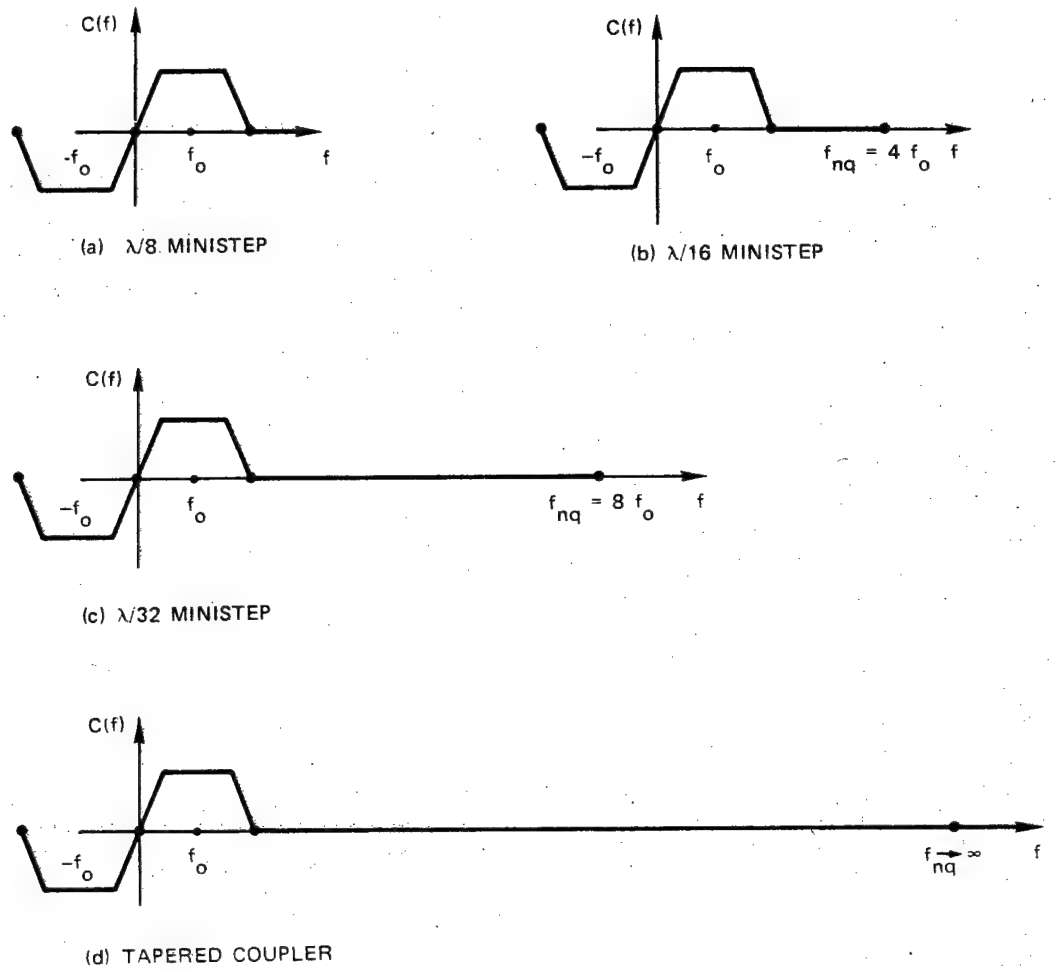

FIGURE 12. Frequency Response of Various Couplers.

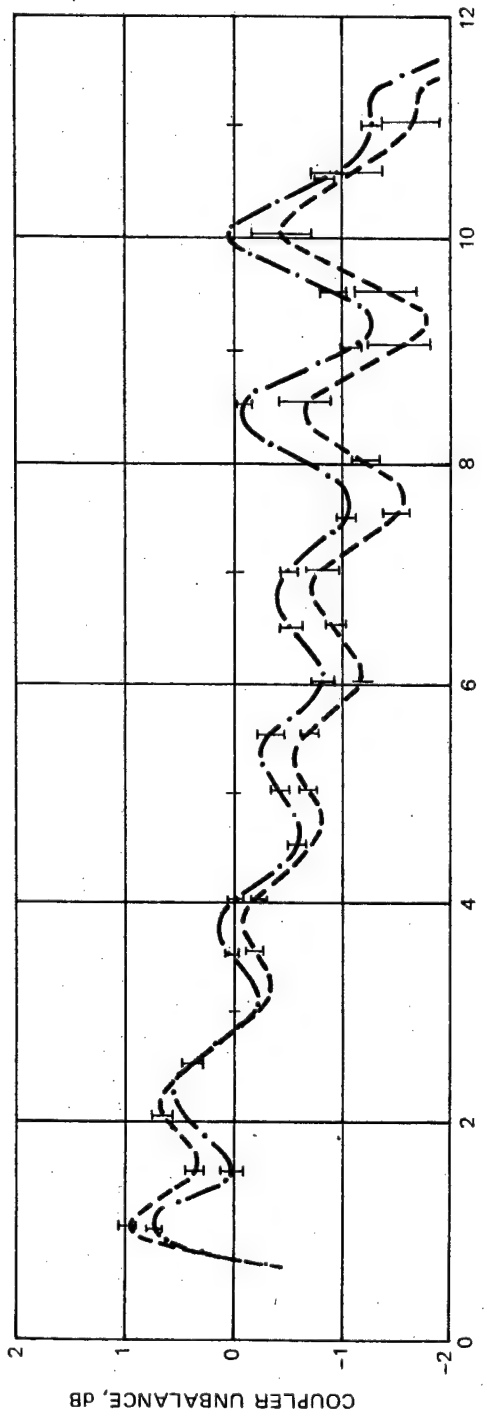

FIGURE 13. Test of Repeatability for Ministep Couplers.

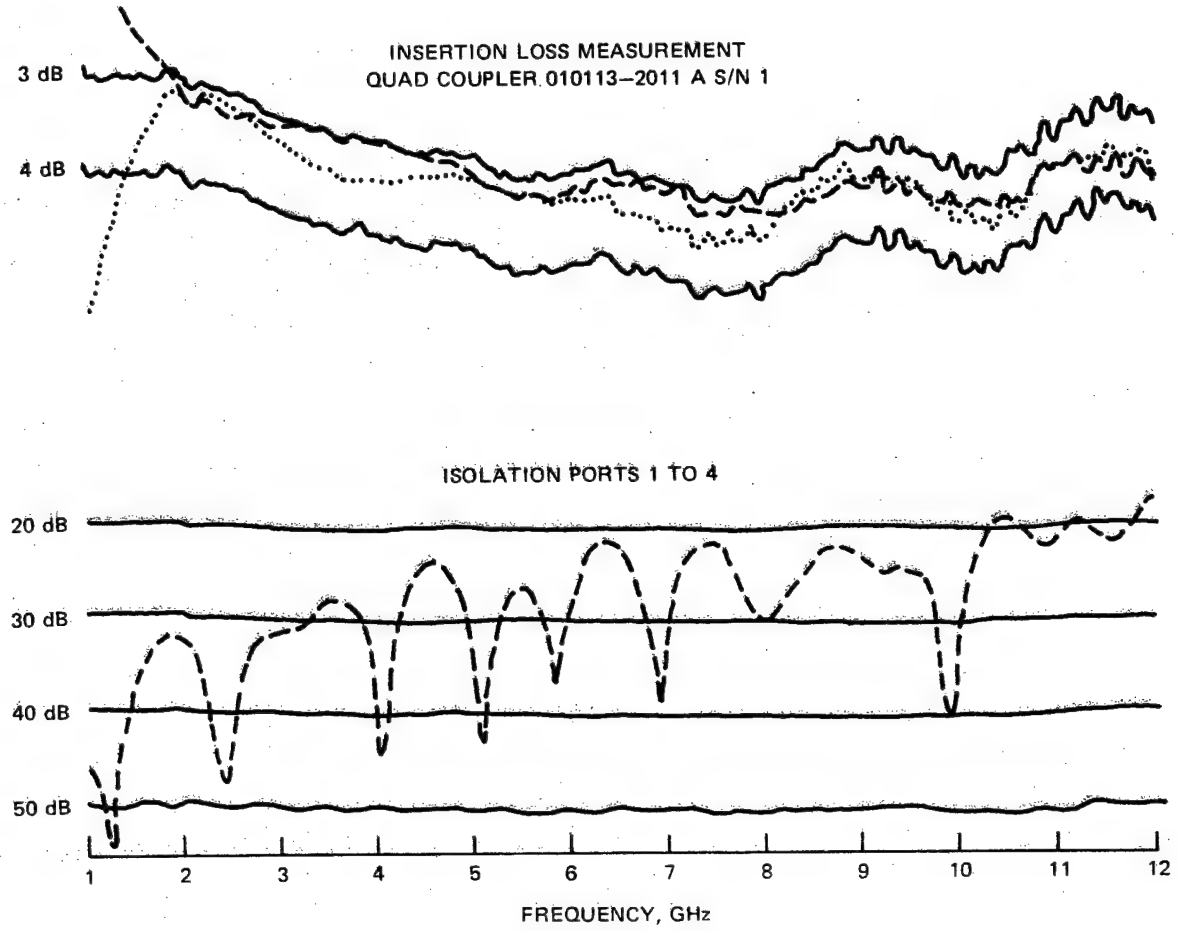

FIGURE 14. Measured Frequency Response on λ/80 Ministep.

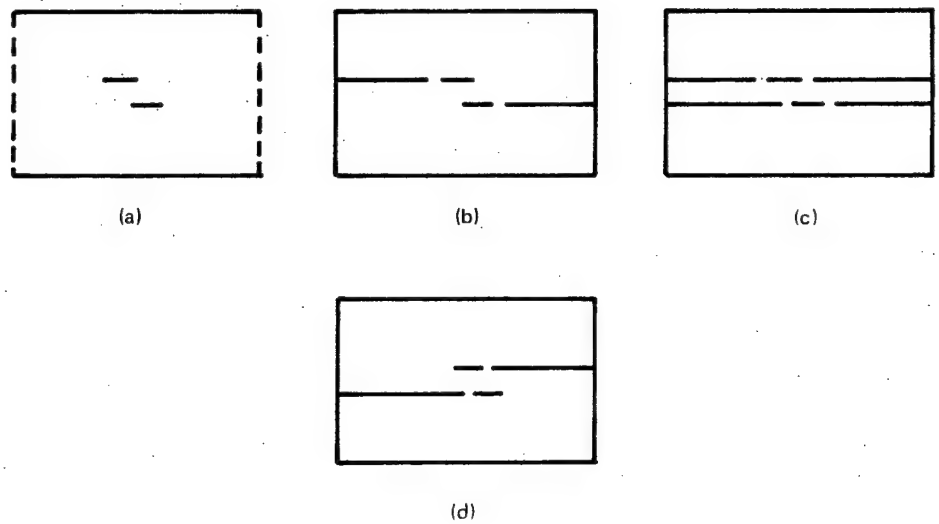

FIGURE 15. Broadside Coupled Stripline Configurations.

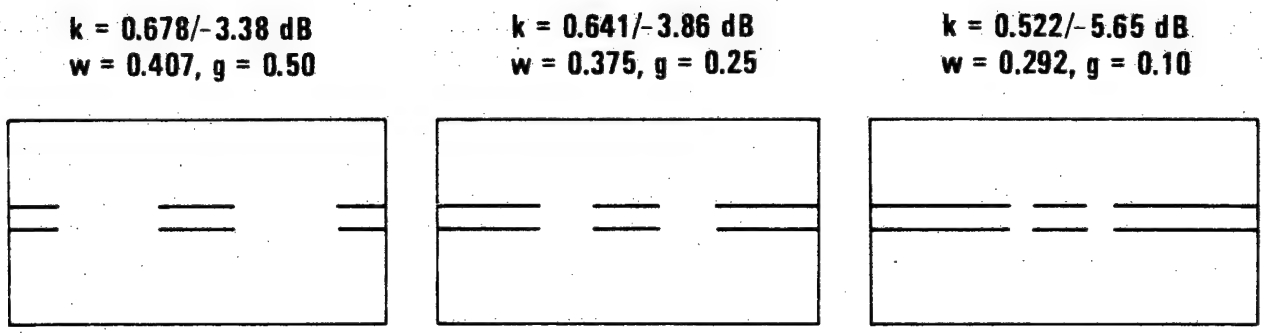

$Z_0 = 50\ \Omega$

$\epsilon_r = 2.53$

S = 0.106

b = 1.0

FIGURE 16. Six Strip Components Intercompatibility.

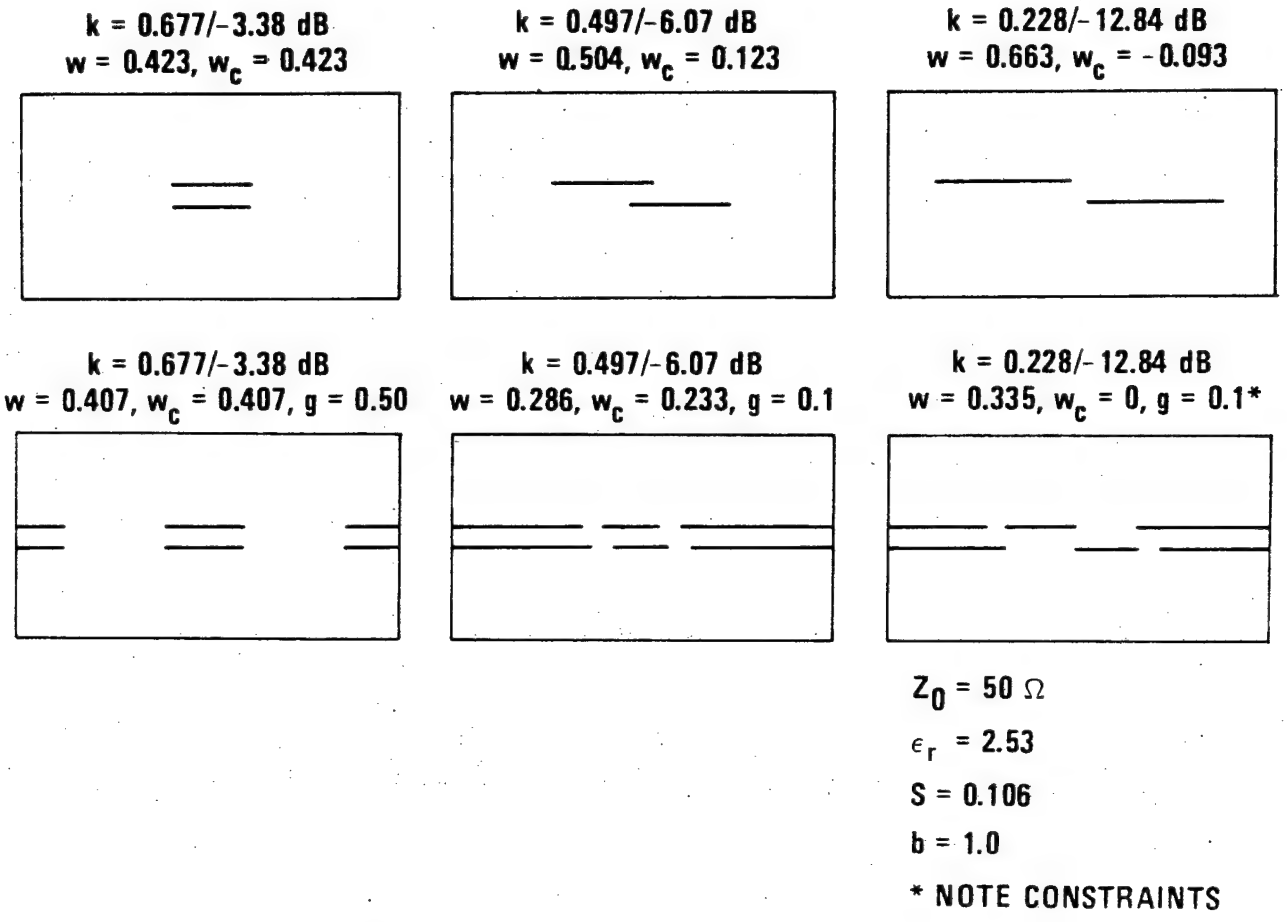

FIGURE 17. Two-Conductor Versus Six-Conductor Stripline.

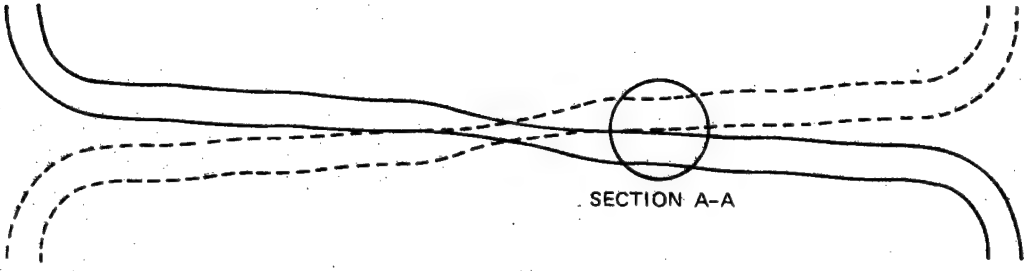

(a) TAPERED COUPLER

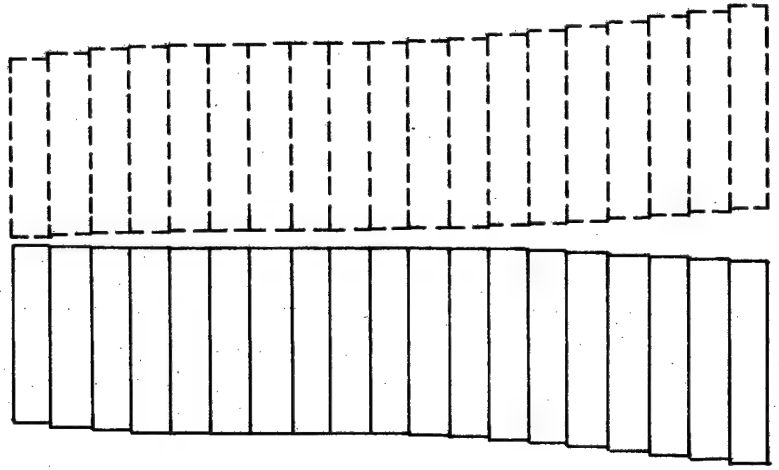

(b) SECTION A-A

FIGURE 18. Quadrature Hybrid.

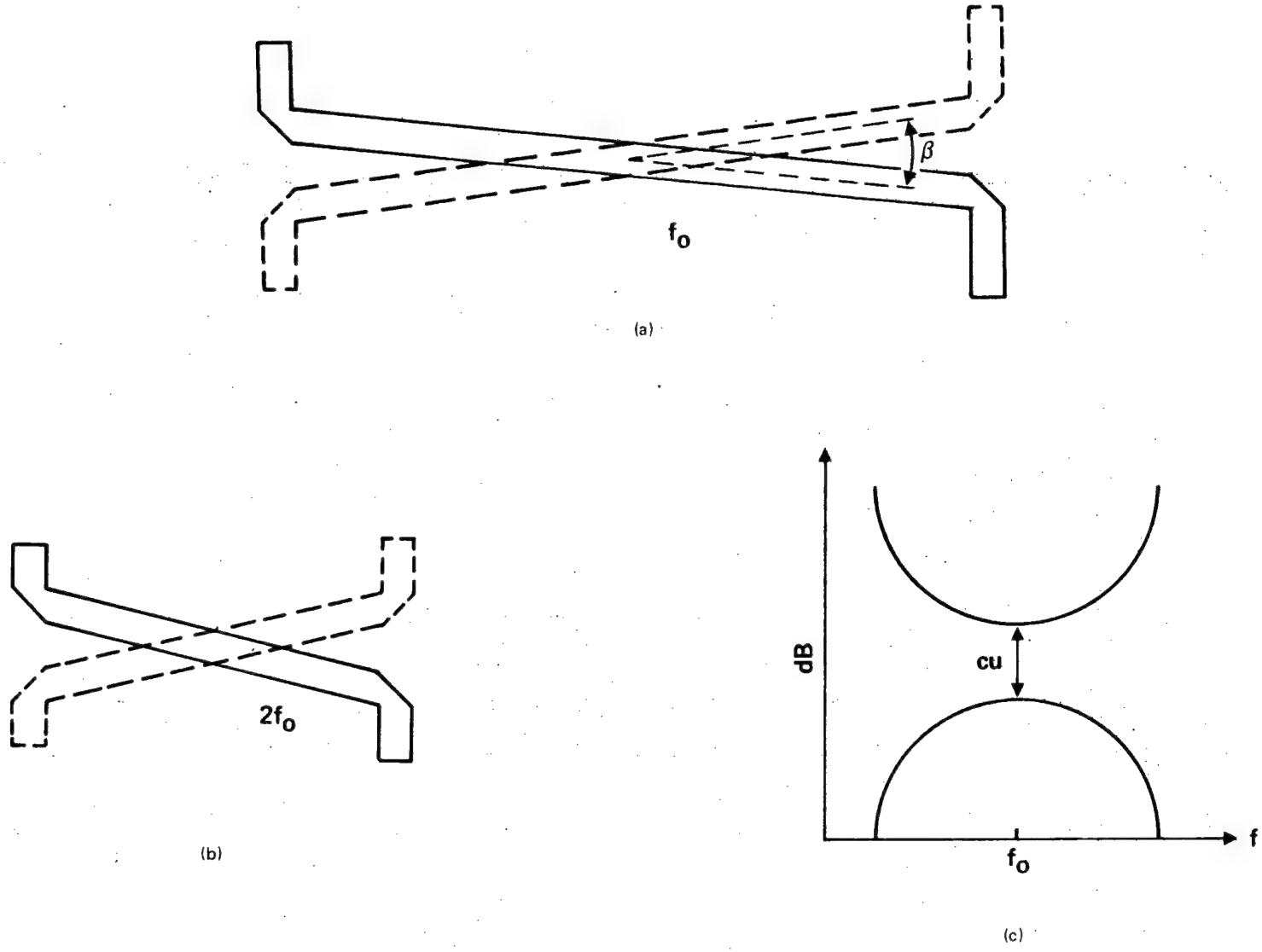

FIGURE 19. Crossover Angle in Couplers.

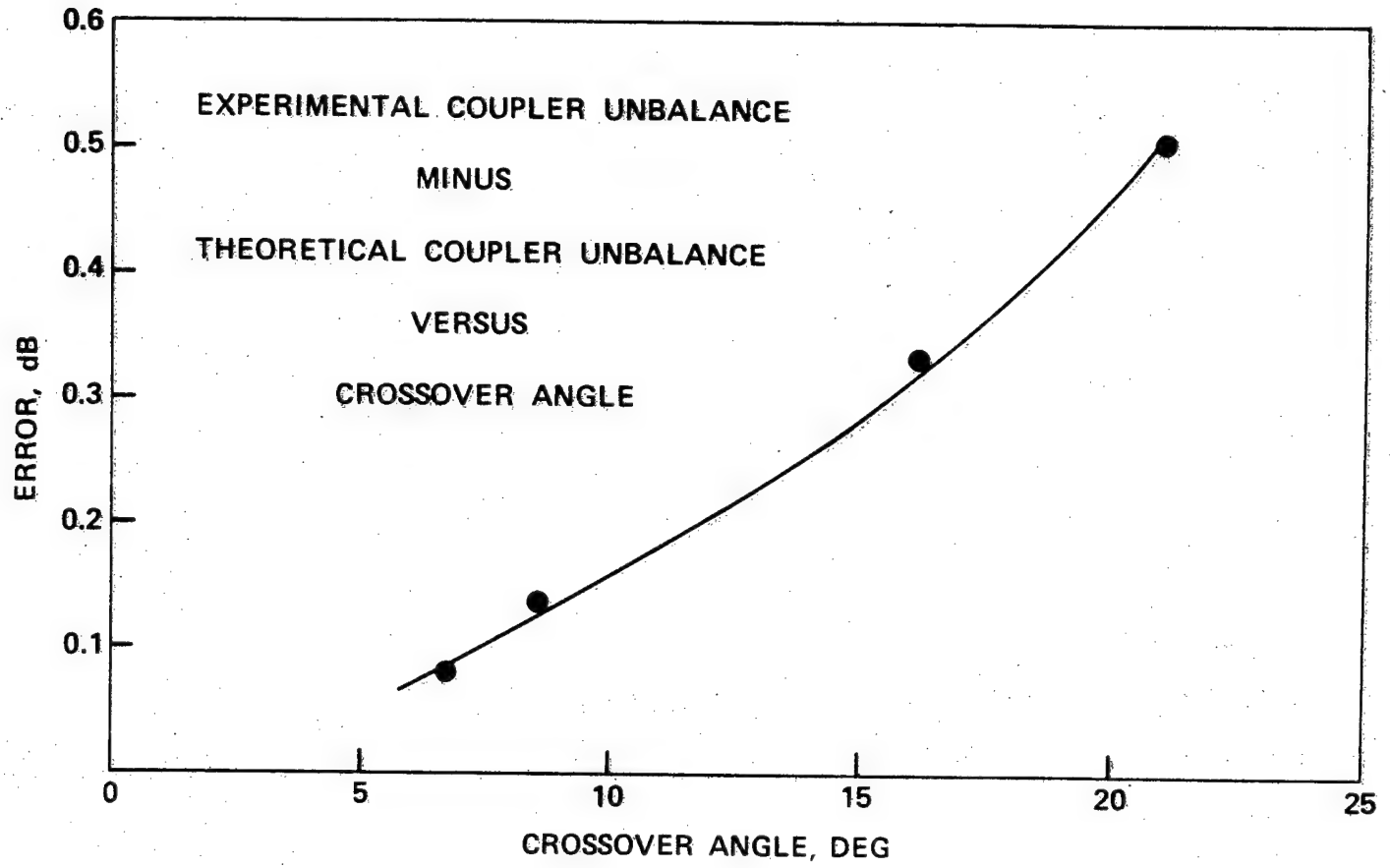

FIGURE 20. Coupler Crossover Angle Experiment.

BIOGRAPHICAL SKETCH

Joseph A. Mosko was born in Czechoslovakia on June 16, 1936. He received the B.S. degree in electrical engineering from San Jose State University, San Jose, California in 1959, and the M.S. degree in engineering from the University of California, Los Angeles, in 1964. From 1963 to 1972 he was enrolled at the University of California, Berkeley where he has completed all course requirements and examinations for the PhD degree in electrical engineering.

Since 1959 he has been employed by the Naval Weapons Center, China Lake, California. Except for the periods that he attended UCLA and Cal/Berkeley for advanced training on first a WEPCOSE Scholarship and later on a NWC Fellowship, he has worked on various frequency independent antennas, wideband stripline components, and various direction finding or fuzing problems.

His numerous publications and patents are all in his area of specialization. Since 1971, he has held the position of Consultant in Electromagnetics and Microwave Components. Although he worked on numerous projects, his major contributions are limited to the Shrike, HARM, and ERASE programs. Some of his more noteworthy awards/honors besides his Fellowships: Past IEEE reviewer of papers on microwave couplers and hybrids; "Engineer of the Year" at NWC (1965), William B. McLean Award (1973); and College Federal Council's Outstanding Accomplishment in Self Development (1978).

CONSIDERATIONS FOR THE DESIGN OF MICROWAVE SOLID-STATE TRANSMITTERS

BY

Marko Afendykiw

Jon Bumgardner

Darry Kinman

Weapons Department

Naval Weapons Center
China Lake, California

1543

Nomenclature

η	- combining efficiency
Po	- peak output power
fa	- carrier frequency
$G_L{}^1$	- load conductance
Go	- stabilizing load conductance
Yo	- device coupled line admittance
β_1	- device coupling coefficient
β_2	- load coupling coefficient
BW_L	- locking bandwidth
$(N/C)_T$	- output interline F.M. single sideband noise
Qa	- unloaded Q of the combining cavity
A	- locking gain
Pi	- peak input locking power
N	- number of combined devices
Pd	- peak power from each device
B	- sampling bandwidth used to measure $(N/C)_T$ and $(N/C)_R$
M	- device noise measure
To	- 290° Kelvin
$(N/C)_R$	- input interline F.M. single sideband noise
β_{max}	- maximum coupling that can be practically obtained without degrading the combiner
$\overline{Y}$	- admittance that the device must be transformed to for oscillation
Y_d	- device admittance
$(2a)_{oma}$	- cavity diameter
χ_{om}	- mth root of the zeroth order Bessel function of the first kind
fo	- resonance frequency of unperturbed cylindrical cavity
$\Delta\tau$	- volume of cavity perturbation
τ	- volume of unperturbed cavity
Q_{ext}	- cavity external Q
$\overline{G}$	- admittance at cavity midplane measured along coaxial module

Considerations for the Design of Microwave Solid-State Transmitters

Abstract

The Solid-State Transmitter is the key element of modern active radar seekers. Major components of a Solid-State Transmitter include: (a) microwave power generating diodes (IMPATTs), (b) microwave diode power combining structrues, and (c) microwave diode bias modulators. The transmitter size, weight, d-c power requirements, cooling system capacity requirements, and cost are primarely determined by the transmitter output RF power requirement and the total d-c to r-f conversion efficiency.

The state-of-the-art of Solid-State Transmitter component technology is reviewed.

Design considerations and implementation of efficient power combining structures is presented. Development at NWC of a TM_{010} mode resonant cylindrical cavity power combining structure is discussed. Combining ten Silicon Double-Drift IMPATTs the combiner has achieved 170 watts peak power with 97% combining efficiency at low Ku-band.

Design of a high-efficiency (93.5%) IMPATT diode combiner modulator is given.

Preliminary measurements of the combiner performance in injection-lock and free-running mode and the degration of the combiner performance caused by the individual diode failures is presented.

Introduction

Solid-State Transmitter is the key element of modern active radar seekers. Practical realization of a Solid-State Transmitter suitable for active seeker applications has become possible due to impressive technological progress in the area of microwave power generating diodes (Ref. 1). In this paper no attempt will be made to make a detailed tradeoff study, justifying the use of solid-state devices over vacuum tubes or hybrid transmitters. The inherent advantages of semiconductors over vacuum tubes are well known, as well as the fact that solid-state microwave power device performance is improving at a faster rate than that of the tubes. This is not to say that a Solid-State Transmitter will satisfy all radar requirements. Tubes certainly have the advantage in long range applications, mainly due to the large amount of power that is required. However, for short and medium range systems solid-state transmitters are becoming a strong contender.

The key elements of a Solid-State Transmitter, Fig. 1, include the following:

1. Microwave Power Generating Diodes (Devices)
2. Microwave Power Combining Structures (Combiners)
3. Microwave Diode Bias Modulators (Modulators)
4. Primary d-c Power Source
5. Transmitter Cooling System

The transmitter size, weight, primary d-c power requirement, cooling system capacity, and cost are primarily determined by the transmitter output RF power requirement and the total d-c to r-f transmitter efficiency. This conversion efficiency is mainly determined by the product of the individual efficiencies of the devices (1), the combiners (2), and the modulators (3). Attention in the design must also be given to the transmission loss between the transmitter final power stage and the antenna. This loss may be significant in certain commonly used transmitter configurations and ultimately determines the power available at the seeker antenna.

The main effort at the Naval Weapons Center, China Lake has been directed at exploring ways to make optimum use of state of the art solid-state devices in active radar seeker transmitters. To accomplish this goal new and unique design techniques are needed, since at present no single device is available that will meet the desired power level requirements.

In the following sections of this paper the state of the art in commercially available microwave power generating diodes will be presented. Design considerations to accumulate or combine power of many individual diodes will be discussed with consideration given to total output power, combining efficiency, output power interline noise, transmitter locking gain and bandwidth, and stability.

The results of a resonant cavity TM_{010} mode power combining structure and high efficiency bias modulator designed and fabricated at the Naval Weapons Center will be presented and the preliminary results discussed.

I. Devices

At the present time the IMPATT diodes (IMPact Avalanche and Transit Time diodes) are the most powerful solid-state pulse power generating devices at microwave frequencies suitable for application in missile seeker transmitters. There is no other solid-state device that has the peak power capability, the efficiency, and the average power capability as an IMPATT diode.

The operating frequency of IMPATTs now covers the frequency range up to 250 GHz (Ref. 2). Commercially available IMPATTs in X- and Ku-bands, both Silicon (Si) and Gallium Arsenide (GaAs), are tabulated in Fig. 2 & 3. Pulse power Si IMPATTs are offered commercially by Hewlett-Packard and Nippon Electric. These are flat profile double-drift devices with d-c to r-f conversion efficiency of approximately 10%.

GaAs pulsed IMPATTs are offered commercially by Varian. These are single drift p+ grown junction devices with modified-read doping profiles. The conversion efficiency of these GaAs IMPATTs is about 20% at X-band and 16 to 17% at Ku-band. Commercial Silicon IMPATT offered by Nippon can deliver 32 watts of peak power at 1.0 μsec pulse width and 10% duty cycle. Hewlett-Packard markets a double-drift Ku-band IMPATT that can provide a minimum of 17.5 watts peak power in the 12 to 15 GHz frequency range at 125 nsec pulse width and 10% duty cycle. Varian Ku-band GaAs IMPATT diodes, developed under Navy and Air Force sponsorships, can deliver as high as 16 watts peak power.

Raytheon Semiconductor Research Division reported developing GaAs modified-read double-drift pulsed IMPATTs. Although, at present, these are laboratory devices they can generate 30-35 watts peak power, with 26-27% efficiency at 30% duty cycle at X-band, and 20-25 watts peak power with 26-27% efficiency at 30% duty cycle at Ku-band, and indicate the potential of the GaAs modified-read double-drifts. As the materials technology of the p-doped epitaxial growth of GaAs double-drifts improves, it is expected to achieve pulse power levels in 40 watt range at X-band and 30 watts in Ku-band with over 30% conversion efficiency.

Chip-level combining in which individual chips are connected electrically in series and thermally in parallel (using Diamond IIa pads) shows great promise in achieving high power levels and high efficiency from individual devices. Work at Georgia Tech. resulted in very encouraging power outputs that are free of spurious and parametric oscillations. Combining four GaAs IMPATT chips 60 watts peak power was achieved with over 90% combining efficiency and approximately 25% dc-to-rf conversion efficiency at X-band.

II. Transmitter System Considerations

Radar specifications that a solid state transmitter would be required to satisfy are:

1. Peak power
2. Duty factor
3. Pulse width
4. Pulse rise and fall times
5. Bandwidth
6. Carrier frequency
7. F. M. noise
8. A. M. noise

Fig. 4 shows a block diagram of the basic components of a radar transmitter. Spectral purity (F.M. noise) is determined mainly by the microwave frequency reference and to some degree by the I.F. reference. Waveform coding to improve signal to clutter and signal to noise can be implemented at either the microwave or I.F. level. If waveform coding or frequency agility is used, which greatly spreads the spectrum beyond that of the pulse, it would be best to implement it at the microwave level, in order for decoding to take place at the first mixer. This approach allows the first I.F. bandwidth to be kept at a minimum, giving better interference and noise rejection. Coding and frequency agility can also be implemented more efficiently at the I.F. level, if it causes negligable spectral expansion. Next an upconverter is needed to give an I.F. offset, which is determined by receiver considerations.

The part of the solid state transmitter that has made the greatest advancement in recent years is the final power stage. This is due to improvement in both devices and circuit combining techniques. Presently this component is the key item in active solid state radar missile seekers and is the area of development which is given the major emphasis at China Lake.

III. Microwave Solid-State Power Combining

In the past few years great progress has been made in the output power and efficiency of microwave solid-state avalanche devices, in particular, pulsed IMPATT diodes. Impressive results have been achieved by maximizing output power from individual IMPATT diodes by means of:

1. More efficient heat removal
2. Use of Double-Drift Structures
3. Practical realization of Modified-Read doping profiles
4. Parallel connection of the diode chips by means of multi-mesa construction
5. Series connection of several chips in a package (chip level combining).

However, at the present time to achieve useful power levels for practical utilization of the IMPATTs in the active missile seeker applications, combining output powers from several diodes by means of some type of microwave circuit is required.

The most effective method so far developed to combine multiple diodes was invented by Rucker (Ref. 3) and put into a theoretical context by Kurokawa (Ref. 4). Basically the idea is to couple each diode to a common resonant cavity, which allows combining of the individual diode powers only at the cavity frequency of resonance. Outside the resonance frequency of the cavity the diode is terminated in a fixed resistance, which suppresses unwanted oscillations. Using this approach eliminates other modes of oscillation and minimizes spurious oscillations due to parametric effects.

A. Cylindrical Cavity TM_{010} Power Combiner

Physical implementation of the Rucker's idea, Fig. 5, incorporates a resonant cylindrical cavity operating in a TM_{omo} mode (m=1,2,3,..) as the basic power combining resonator. Coupled to the cavity via the magnetic field are individual coaxial modules that are spaced around the periphery of the cavity. Individual diodes are mounted at one end of each coaxial module and the other end of the module is terminated in a stabilizing load. Bias current for each diode is also, usually, introduced at this end; however, other bias configurations are possible. Power from the combiner cavity is coupled to the external load by means of an electric probe located at the center of the cavity, i.e., at the point of maximum electric field. Fine resonant frequency tuning of the cavity is accomplished by either a metallic or dielectric plunger usually located at the cavity wall that is opposite the output coupling probe.

The main advantage of the resonant cylindrical cavity combiner operating in a TM_{omo} mode over other resonators is that the magnetic field is uniform around the cavity periphery and consequently the individual coaxial modules can be "packed" very close to each other around the cavity periphery. Thus, physically compact microwave structures that occupy minimum volume per output power capacity can be realized.

The number of diodes that can be combined at a desired operating frequency is primarely determined by the diameter of the cylindrical cavity and the package size of the diode.

The general expression of an air-filled cylindrical cavity diameter operating in TM_{omo} mode is given by

$$(2a)_{omo} = \left(\frac{c\,\chi_{om}}{\pi}\right)\frac{1}{f_o} \qquad (1)$$

For a given mode of operation, i.e., m = 1,2,3,., the cavity diameter is inversely proportional to frequency. Thus, for a given diode size fewer number of diodes can be combined at higher frequencies. Since the cavity diameter is increased with the order of the root of the Bessel function, higher order mode cavities are used to increase the number of diodes to be combined. Successful operation of higher than fundamental mode cavities requires mode suppression techniques to suppress undesired modes which can be easily excited in such cavities. The power that is extracted by these modes is not available at the combiner output.

In designing the combiner cavity to operate at a specified resonant frequency and the desired TM_{omo} mode, perturbations of the cavity volume caused by the coaxial IMPATT modules, the tuning plunger, and the output coupling probe must be taken into account.

The individual coaxial modules, located at the point of almost maximum magnetic field, cause outward volume perturbation. The output coupling probe and the frequency tuning plunger are located at the point of maximum electric field and cause inward volume perturbation. The resonant frequency of the "perturbed" cavity is given by the expression

$$fa = fo\left[1 + C \cdot \frac{\Delta\tau}{\tau}\right] \qquad (2)$$

where C is a parameter that depends on cavity geometry and position of pertrubation.

The numerical value of parameter C is approximately -0.5 for outward volume perturbations at the point of maximum magnetic field, and approximately -1.85 for inward volume perturbations at the point of maximum electric field. Both of these perturbations lower the resonance frequency of unperturbed cavity.

By using Eq. 2, in conjunction with Eq. 1, cavity diameter 2a can be determined such that perturbed cavity resonates at the desired operating frequency.

B. Power Combiner Design Guidelines

An equivalent circuit for the combiner oscillator is shown in Fig. 6.

To design a combiner oscillator, the following information is required:

1. Frequency of oscillation
2. Output power
3. Combining efficiency
4. Locking bandwidth
5. Output Interline noise

Power output to an external load from an N- diode resonant cavity combiner at resonance is given by the expression (Ref. 4):

$$P_o = P_d \cdot N \left(1 - \frac{Q_{ext}}{Q_{ext} + Q_a}\right)\left(1 - \frac{\overline{G}}{G_o}\right) \tag{3}$$

The factor in brackets in Eq. 3 may be interpeted as the combining efficiency,

$$\eta = \left(1 - \frac{Q_{ext}}{Q_{ext} + Q_a}\right)\left(1 - \frac{\overline{G}}{G_o}\right) \tag{4}$$

In terms of the circuit coupling factors Eq. 4 can be written as:

$$\eta = \left(1 - \frac{1}{1 + \beta_2}\right)\left(1 - \frac{\overline{G}}{G_o}\right) \tag{5}$$

The necessary condition required for negative resistance oscillation to take place at resonance can also be written in terms of the coupling factors as:

$$\frac{\overline{G}}{G_o} = \frac{1 + \beta 2}{1 + \beta_2 + \left[\frac{2NG_o}{Y_o}\right]\beta_1} \tag{6}$$

Combining Eq. (5) and (6) gives efficiency as a function of the circuit parameters at resonance:

$$\eta = \frac{\left[\frac{2NG_o}{Y_o}\beta_1\right]\beta_2}{\left[1+\beta_2\right]\left[1+\beta_2+\left(\frac{2NG_o}{Y_o}\right)\beta_1\right]} \tag{7}$$

where β_1 is the device line coupling and β_2 is the load coupling factors. This relationship has been plotted in Fig. 7 for several values of combining efficiency.

From a practical standpoint the load coupling (β_2) and the device line coupling (β_1) are limited due to degration of resonant frequency (fa) and combining cavity unloaded Q (Qa) with increased coupling. It is therefore necessary to keep β_1 and particulary β_2 within an upper maximum values. For a practical design β_2 should fall within the following limits for a given efficiency:

$$\frac{\eta}{1-\eta} < \beta_2 < \frac{2\eta}{1-\eta} \tag{8}$$

The range of β_1 and stabilizing load to coupling line impedance (G_o/Y_o) can then be determined from Fig. 7. Locking gain (A) is determined by the locking bandwidth for most practical cases, however, it also determines the transmitter F.M. noise $(N/C)_T$. Except for extremely low noise systems, the gain requirement for low F.M. noise is easily satisfied by the locking bandwidth gain. Due to clutter, there is a limit to how much the radar sensitivity can be improved by decreasing F.M. noise.

Outlined in Fig. 10 is a flow chart which can be used as a guideline for the design of symmetrical power combiners. The chart contains fundamental design equations which allow the realization of a combiner design from the basic system requirements, using combining efficiency as the most important parameter. Use of the flow graph requires a good knowledge of the particular type of combiner cavity to be used, along with the coupling limitations.

IV. High Efficiency Modulator

The basic requirements of pulse modulators that are used to excite the IMPATT diodes are:

a). High efficiency
b). Small size
c). Good reliability
d). Suppression of bias oscillations

Overall efficiency of the transmitter is determined mainly by the IMPATT diodes, due to their relatively low efficiencies (10% to 20%) compared to the combiner and modulator efficiencies (over 90%). In the future, as diode efficiencies improve, the modulator will become an increasingly important factor in overall efficiency. This is an important consideration, since for some high efficiency diodes it may be necessary to trade off modulator efficiency for bias circuit stability.

The effects of bias circuit oscillations range from creating unwanted signals to IMPATT diode burnout. In addition to the above requirements, the modulator has a large effect on the pulsed RF waveform (risetime, falltime, peak power amplitude and phase modulation over the pulse, pulse width). The net result of these requirements is that a modulator must be carefully designed to mate a given diode to the waveform specifications. The basic nature of IMPATT diodes is that output power is highly sensitive to changes in bias current. Therefore, it is necessary to use a constant current circuit as the final modulator drive stage.

The NWC bias modulator design, Fig. 15, uses a directly coupled, modified Darlington circuit as a broadband constant-current source. Due to the low dynamic resistance of the IMPATT diodes, it is possible to use a low emmitter resistance and low saturation resistance r-f transistors, while maintaining a constant current. Adjustable shunt feedback is used to optimize the phase transient response. The predrive stages use a complementary-symmetry emmitter follower driven by an emmitter coupled difference amplifier. A d-c pedestal voltage is supplied to the IMPATT to keep the voltage drop across the drive transistors within their breakdown limits.

Circuit protection is provided for drive transistor overvoltage and minimum average current to the diodes.

Photographs of the NWC 10 diode modulator power stages, packaged within a 4.65 inch diameter, is shown in Fig. 16. The bias modulator control and monitor assembly is shown in Fig. 16a.

The modulator achieved a maximum efficiency of 93.5% at a pulse width of 125 nanoseconds and 10% duty cycle.

U. S. Patent protection of certain of the innovative design details is being applied for at this time.

V. Resonant Cavity TM_{010} Mode 10-Diode Power Combiner

Cross-sectional view of the 10-diode power combiner designed and fabricated at the Naval Weapons Center, China Lake is shown in Fig. 11.

The combiner incorporates TM_{010} mode cylindrical cavity as a basic resonator with the cavity diameter equal to 16.5mm and its height equal to 3.0mm. Single-diode coaxial modules are located around the circular periphery of the cavity and are magnetically coupled to the fields inside the cavity. The inside diameter of each coaxial module is 4.0mm and its characteristic impedance equals 50 ohms. Individual IMPATTs are soldered into special slugs and then threaded into the water cooled heat sink. This diode assembly is then attached to the combiner body by means of screws, with each diode making an electrical contact with the center conductor of each individual coaxial module.

Bias to each IMPATT is provided via coaxial module center conductor. To reduce package parasitics each IMPATT is recessed into its slug holder to the depth of approximately 0.5mm. Each coaxial module is terminated in a stabilizing load to prevent spurious and parametric oscillations and is fabricated from ECCOSORB MF-116 material. Diode bias pins are spring-loaded to maintain good electrical contact with each diode. Power from the combiner cavity is coupled to the external load by means of an adjustable (to change load coupling factor β_2) electric probe located at the center of the cavity. The cavity resonance frequency is adjusted by means of a metallic plunger.

The combiner individual parts are fabricated from tellurium copper. To maintain good electrical contact between individual combiner parts, 0.001 inch shoulder is machined into each mating surface.

The combiner is loaded with H-P 5082-0772 and HIMP-7003 IMPATT diodes. These are Silicon Double-Drift IMPATTs with the following characteristics when operated at 14.0 GHz with 125 nanosec. pulse width and 10% duty cycle:

Output Power = 17.5 watts peak
Efficiency = 9.0%
Peak Operating Current = 1.6 amps
Peak Operating Voltage = 121 volts
Breakdown Voltage @0.5mA = 93 volts
Junction Capacitance = 1.9pF
Thermal Impedance = 7.0°C/watt
Junction Temp. Rise = 120°C

The diode chips are packaged in a N-46 ceramic package that measures 3.12mm (max.) across the top cap.

The large-signal impedance of these diodes is approximately Zd = -4.0+j6.0 ohms at 14.0 GHz and with the diode recessed into the mounting slug to reduce external inductance arising from the magnetic energy stored in the cylindrical region around the package.

Impedance matching of each diode to satisfy necessary conditions for oscillations to take place are accomplished by means of a double quarter-wavelength transformer and a low impedance (8.0 ohms) line transformer connected in cascade between the IMPATT terminal plane and the cavity midplane as shown in Fig. 12. The transformer impedance ratio, $(Z_3/Z_2)^2$, can be selected to be in the range, $1 < (Z_3/Z_2)^2 < 39$ and thus can match the midplane cavity impedance that falls into the range of $21 < Zm < 820$ ohms. The terminal plane of each IMPATT can be individually adjusted with respect to the cavity midplane impedance. This design feature allows each diode to be individually matched to the combiner midplane impedance. Minimal preselection of diodes is thus required and consequently the diodes exhibiting somewhat different electrical characteristics can be individually matched.

A photograph of an assembled 10-diode power combiner, with the bias modulator attached at the top, is shown in Fig. 13. The modulator mounts directly to the combiner body that serves as a heat-sink for the modulator output power transistors.

The output coupling line, terminated in an OSM-201 connector, can be locked in place after desired output load coupling has been achieved. During operation water is circulated through the combiner heat sink to prevent excessive heat build-up.

A photograph of the power combiner parts is shown in Fig. 14.

VI. Combiner Performance

This section summerizes preliminary results of the 10-diode power combiner performance evaluation.

1. The maximum power achieved in a free-running mode (i.e., no injection lock signal applied) was 170 watts peak at 12.410 GHz with the diodes operating under rated bias current at 125 nanosec. pulse width and 10% duty cycle. Since each diode in the combiner was capable of approximately 17.5 watts peak this result implies power combining efficiency of approximately 97%. No spurious or parametric conditions were observed indicating well stabilized combiner circuit.

2. The output power spectrum of free-running power combiner is shown in Fig. 17. and the corresponding detected RF output pulse is shown in Fig. 18. The spectrum shape is indicative of distinct FM effect within the RF output pulse. The frequency profile measurements of the RF output pulse are shown in Fig. 19 and indicate approximately 11 MHz total frequency variation or "chirp" within the pulse. Frequency chirping is also observed in single-diode oscillator tests and must be due to IMPATT diode parameter variations with temperature during pulse turn-on.

The results, however, are not very accurate since a microwave pulse counter with 50 nanosecond gate was used in frequency profile measurements (min. gate capability of EIP 451 counter used in these frequency measurements). At these frequencies the gate width of at least 10 nanoseconds is needed to obtain more accurate frequency measurements. Higher frequency excursions within the pulse are likely.

3. Fig. 20 shows output power spectrum with the combiner delivering 100 watts peak power and operating in injection lock mode with 20 db gain. The FM effect is less pronounced for this mode of operation.

Frequency profile measurements, shown in Fig. 21, indicate total frequency excursion within the pulse of approximately 5 MHz. Most of the frequency variation for both, free-running and injection-lock with high gain, occurs within 60-70 nanoseconds into the pulse.

It is expected that at lower injection-lock gains the FM effect within the pulse will be further reduced.

Pulse shaping of IMPATT diode bias current can also be used to reduce FM effects. However, this technique will lower modulator efficiency.

4. Time delay of RF output pulse with respect to applied bias current pulse in the combiner operating in free-running mode is shown in Fig. 22. For this mode of operation the delay is approximately 18 nanosec.

For the combiner operating in injection-lock mode the delay is reduced to approximately 8 nanoseconds for 20.0 db locking gain, as shown in Fig. 23.

This time delay, which is due to oscillations build-up time, causes the RF output pulse to be shorter than the bias current pulse width. In a solid-state transmitter design this factor must be taken into account when designing the bias modulator waveform in order to realize the desired RF output waveform.

5. Interline noise improvement under injection lock is shown in Fig. 24. The carrier-to-interline noise is better than 50 db for 20 db locking gain.

With 54.2 db locking gain the carrier-to-interline noise is better than 20 db, as shown in Fig. 25, which corresponds to only 380 microwatt reference signal injection locking the combiner that delivers 100 watts of pulsed power.

For comparsion, the power spectrum of free-running combiner is shown in Fig. 26.

The power spectrum of the CW reference signal used in these experiments is shown in Fig. 27.

6. Tests were conducted to determine the combiner output power degradation when one of the combiner diodes failed. These tests were conducted with the combiner output power reduced to 30 watts peak to reduce the possibility of damaging the remaining diodes. It was assumed that similar results would be observed at full combiner power.
Two tests were performed:

a). Diode failing in short circuit:
With one out of ten diodes failing and presenting a short circuit at the diode terminal plane the combiner power dropped by approximately 1.0 db.

b). Diode failing in open-circuit:
The combiner output power dropped 5 db when one out of ten diodes failed and presented an open circuit at its terminal plane.

These preliminary tests indicate that an open-circuited diode presents a considerable impedance mismatch to the remaining diodes. In a combiner operating under full power this condition may cause damage to the remaining diodes.

VII. Summary

The main benefits of the work presented in this paper are twofold:

a). Design considerations and implementation of high peak power, high efficiency transmitter components suitable for solid-state radar seeker applications have been developed.

b). Areas of future development efforts have been identified.

Since higher power systems are demanded it is essential to develop higher power and more efficient solid-state devices. Other areas that need improvement are more compact modulators and broadband power combining circuits.

Acknowledgment

The authors wish to acknowledge the outstanding work of William Nurnberger, John Piri, and Charles Smith of the NWC power combiner team who contributed to the design, fabrication, testing, and optimization of the combiner hardware and without whose help the work could not have been accomplished.

References

1. M. Afendykiw, " Solid-State Microwave Power Generating Devices Survey", NWC Technical Memorandum 3132, May 1977.

2. R. L. Bernick, et.al., "Millimeter Wave Sources", Wright-Patterson Air Force Report, AFAL-TR-77-163, 1978

3. C. T. Rucker, "A Multiple-Diode High Average Power Avalanche Diode Oscillator", IEEE Trans. Microwave Theory and Techniques, Vol. MTT-17, Dec. 1969, pp 1156-1158.

4. K. Kurokawa, "The Single-Cavity Multiple-Device Oscillator", IEEE Trans. Microwave Theory and Techniques, Vol. MTT-19, Oct. 1971, pp 793-801

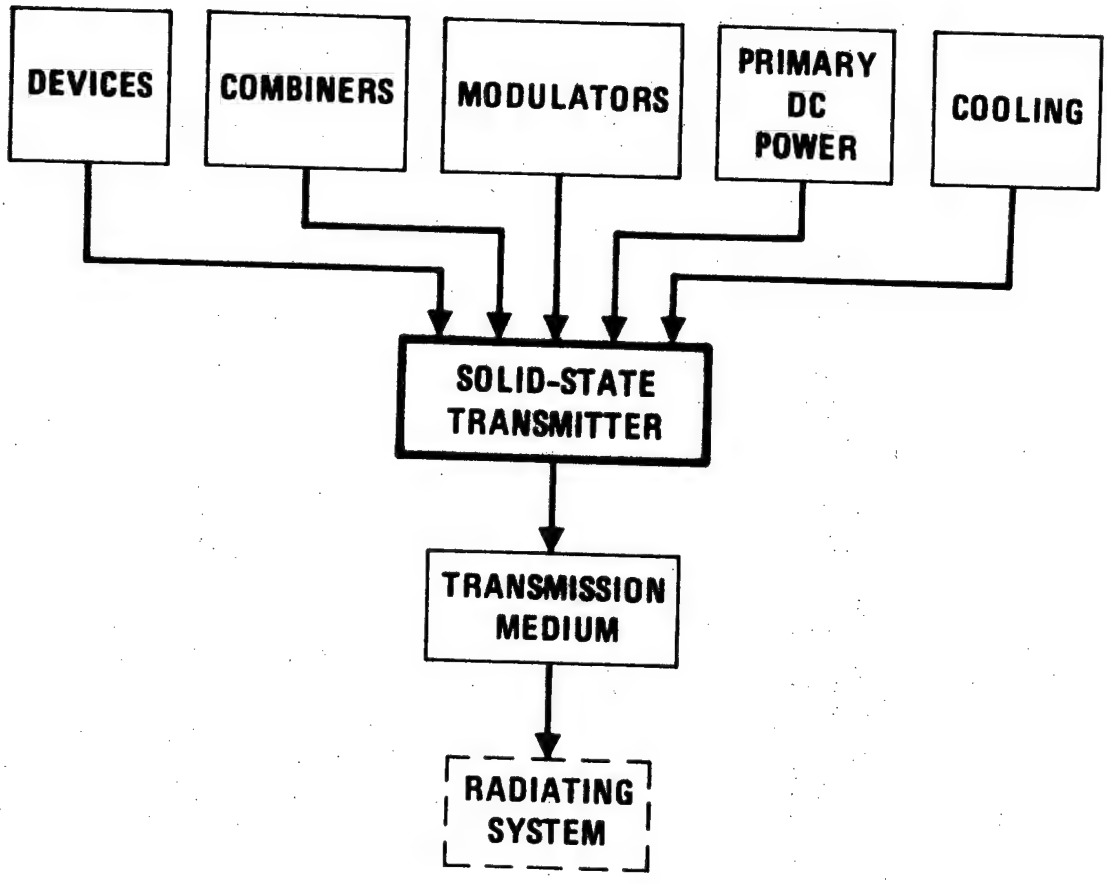

FIGURE 1. Key Elements of a Solid-State Transmitter.

FREQ, GHz	POWER, PEAK	EFF.	DUTY	PULSE WIDTH	DIODE TYPE	SOURCE
8.0–12.4	14.0 W	12.0%	25%	800 ns	Si DOUBLE-DRIFT	H-P
9.0–10.0	~20.0 W	~20%	25%	1.0 μs	GaAs MODIFIED-READ	VARIAN
10.0	32 W	10%	10%	1.0 μs	Si DOUBLE-DRIFT	NIPPON

FIGURE 2. Commercially Available Pulsed Power Impatt Diodes at X-Band.

FREQ. GHz	POWER, PEAK	EFF.	DUTY, %	PULSE WIDTH	DIODE TYPE	SOURCE
12.4–18.0	11.0 W @ 16.5 GHz	11.5%	25	800 ns	Si DOUBLE-DRIFT	H-P
13.0–15.0	17.5 W MIN	8.5% MIN	10	125 ns	Si DOUBLE-DRIFT	H-P
14.0	13.0–16.0 W	16.0–20.0%	10	125 ns	GaAs MODIFIED-READ	VARIAN[a]
15.0	13.0 W	9%	10%	1.0 μs	Si DOUBLE-DRIFT	NIPPON

[a] DEVELOPED FOR NWC/TRI-FAST PROGRAM

FIGURE 3. Commercially Available Pulsed Power Impatt Diodes at Ku-Band.

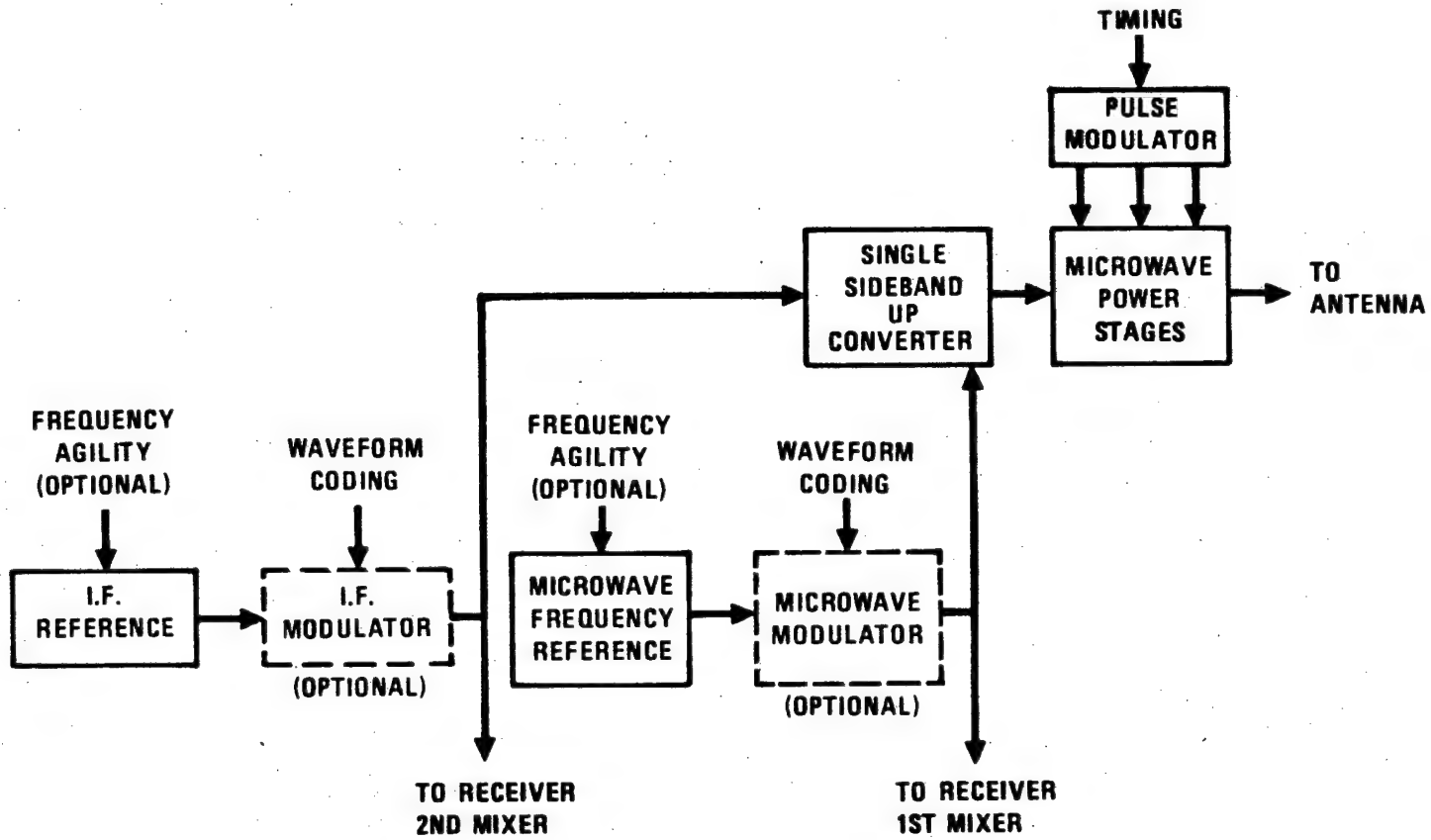

FIGURE 4. Radar Transmitter Block Diagram.

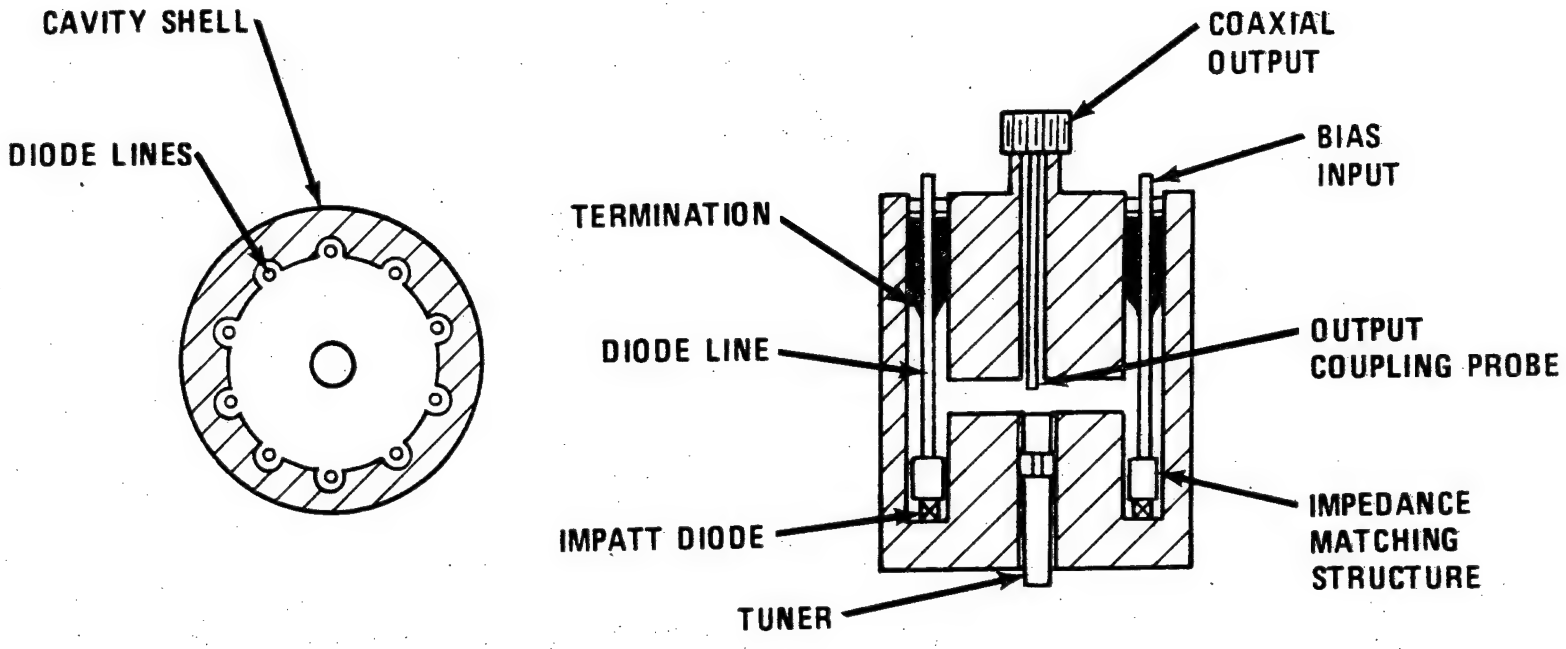

FIGURE 5. Schematic Drawing of 10-Diode Cylindrical Cavity TM 010 Mode Power Combiner.

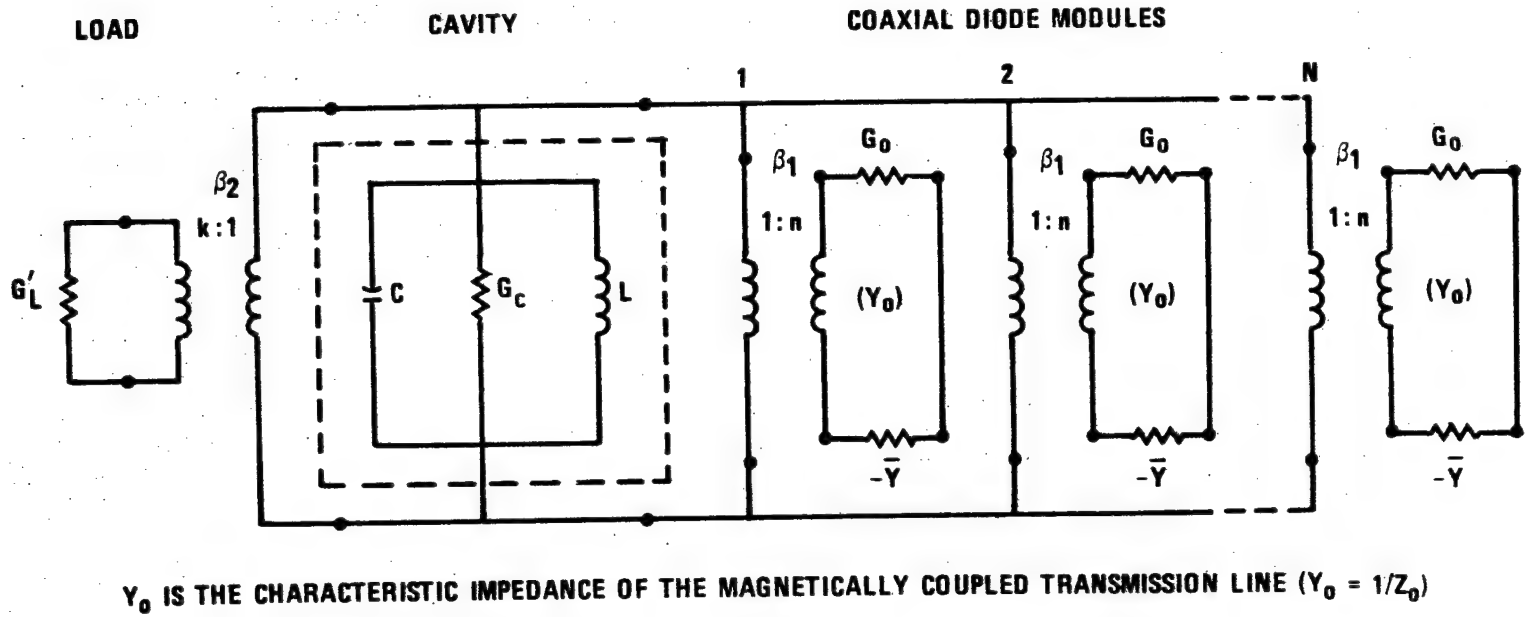

FIGURE 6. An Equivalent Circuit for 10-Diode Power Combiner Circuit.

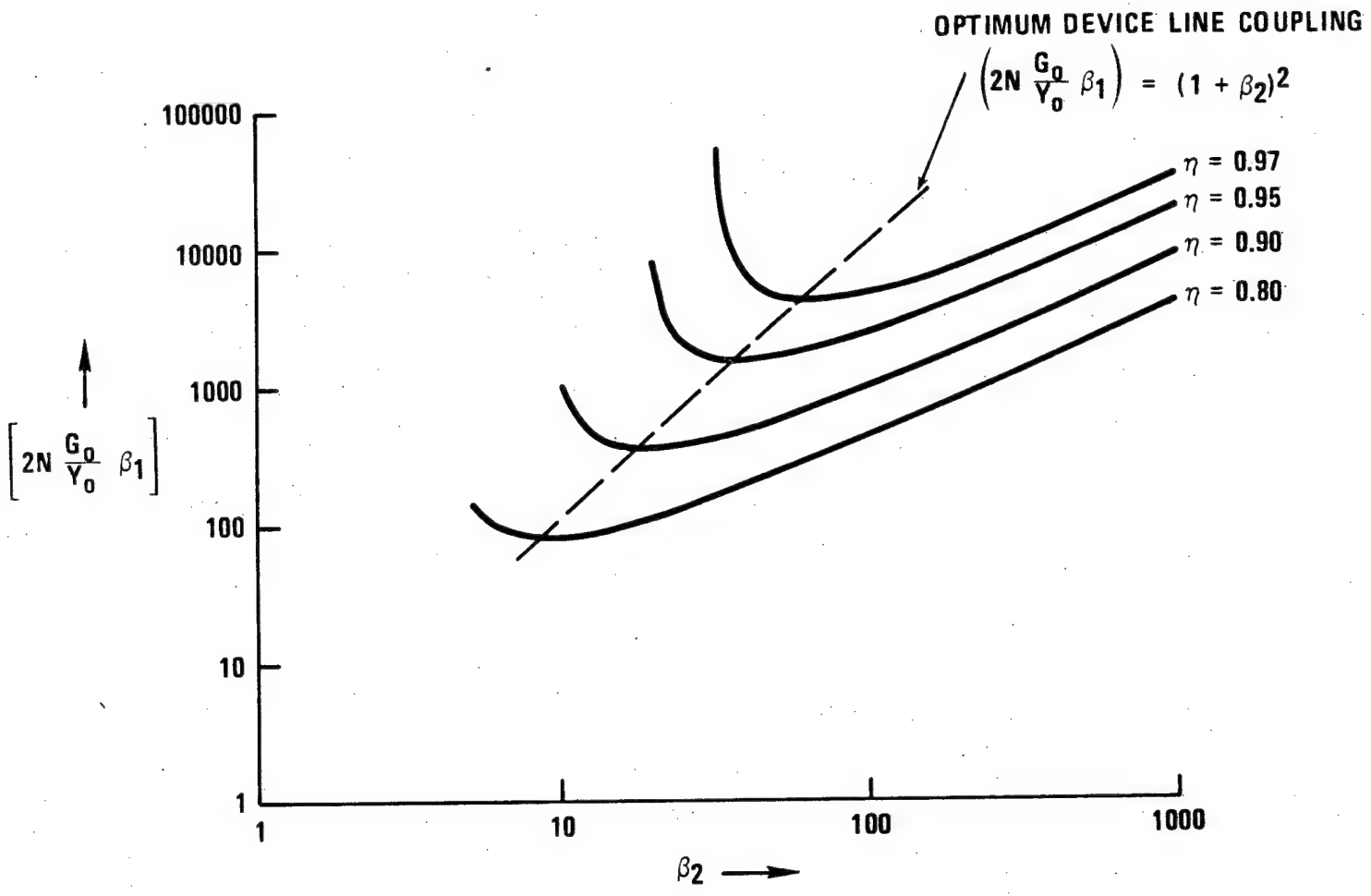

FIGURE 7. Multiple Device Line Coupling vs. Load Coupling.

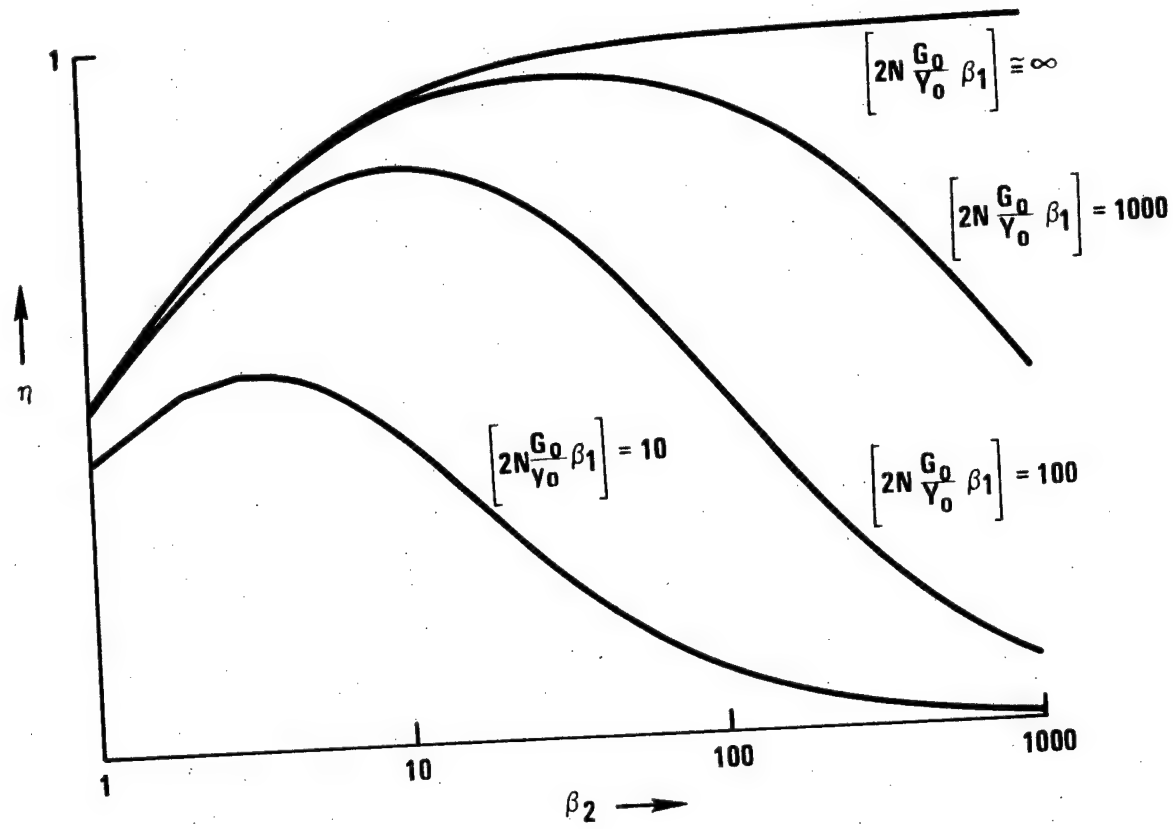

FIGURE 8. Combining Efficiency vs. Load Coupling.

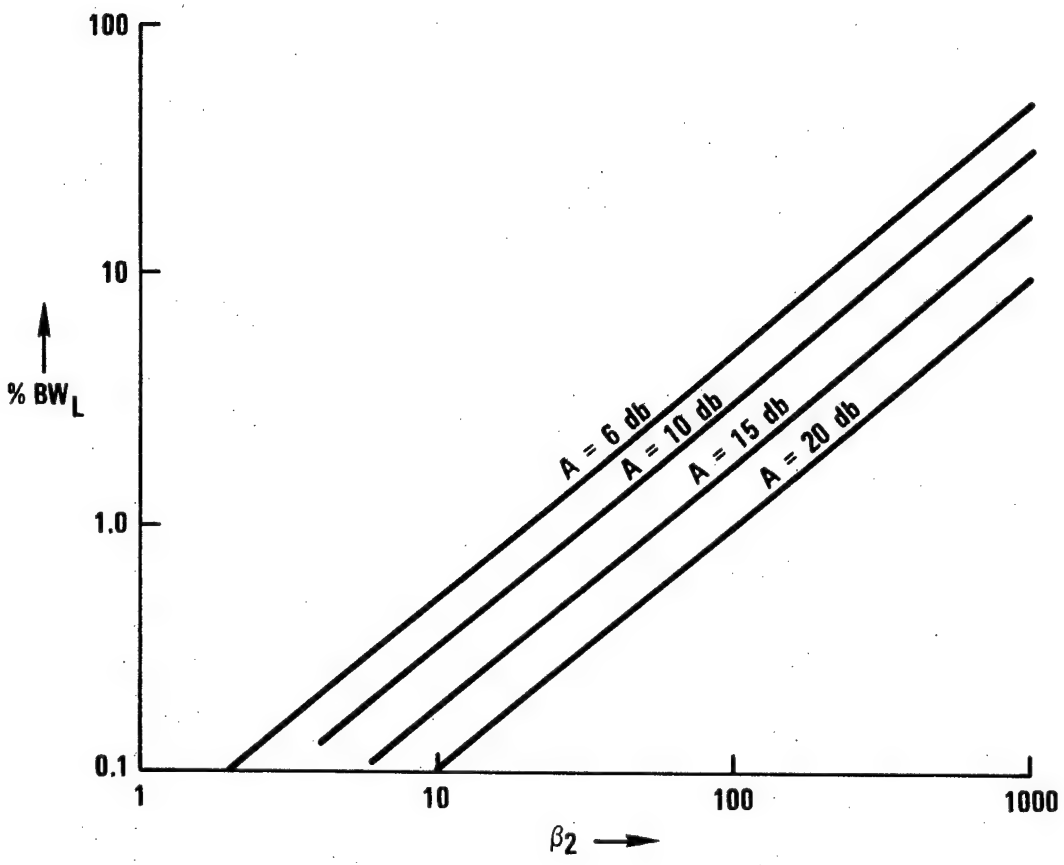

FIGURE 9. Percent Locking Bandwidth vs. Load Coupling.

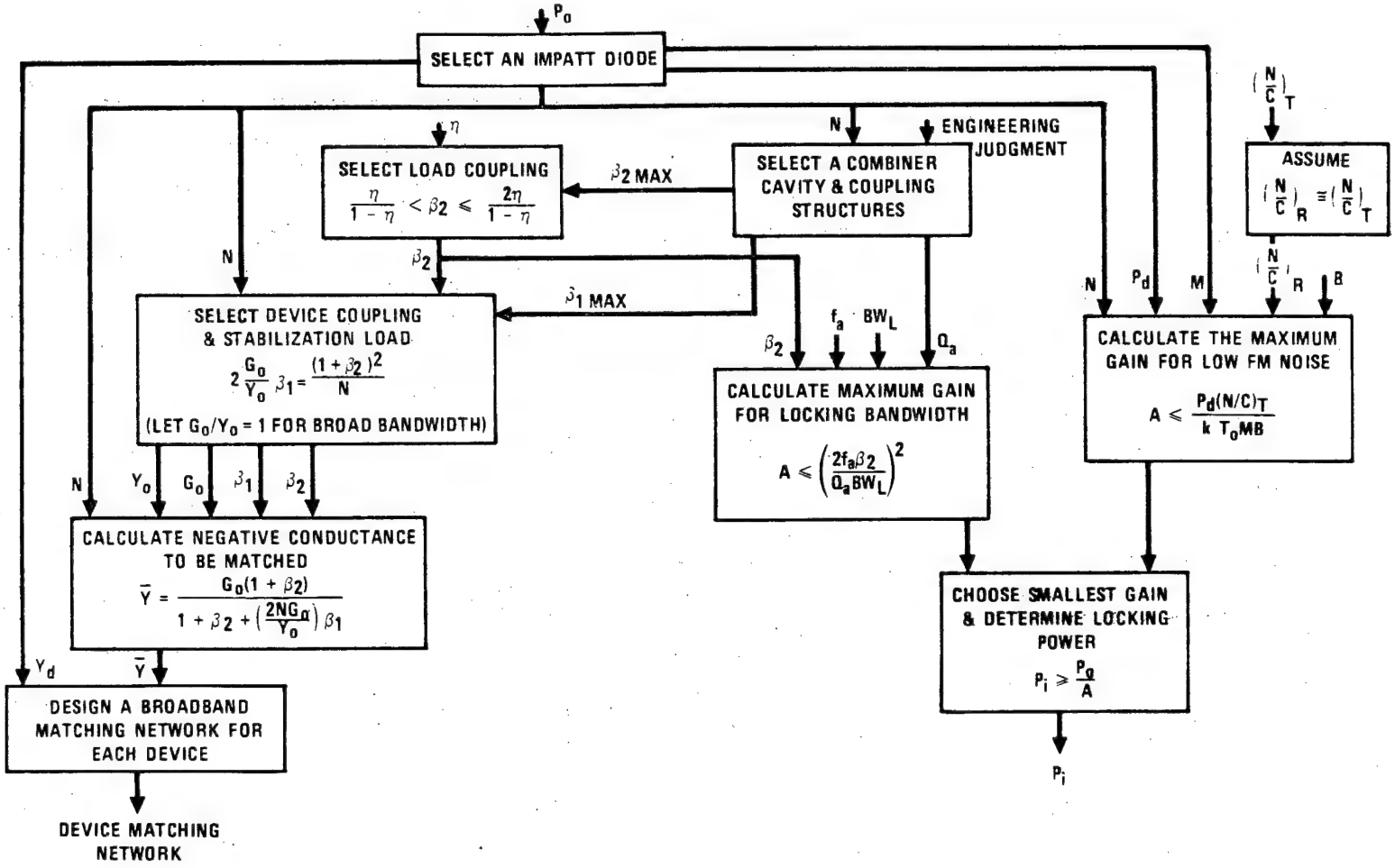

FIGURE 10. Power Combiner Design Flowchart.

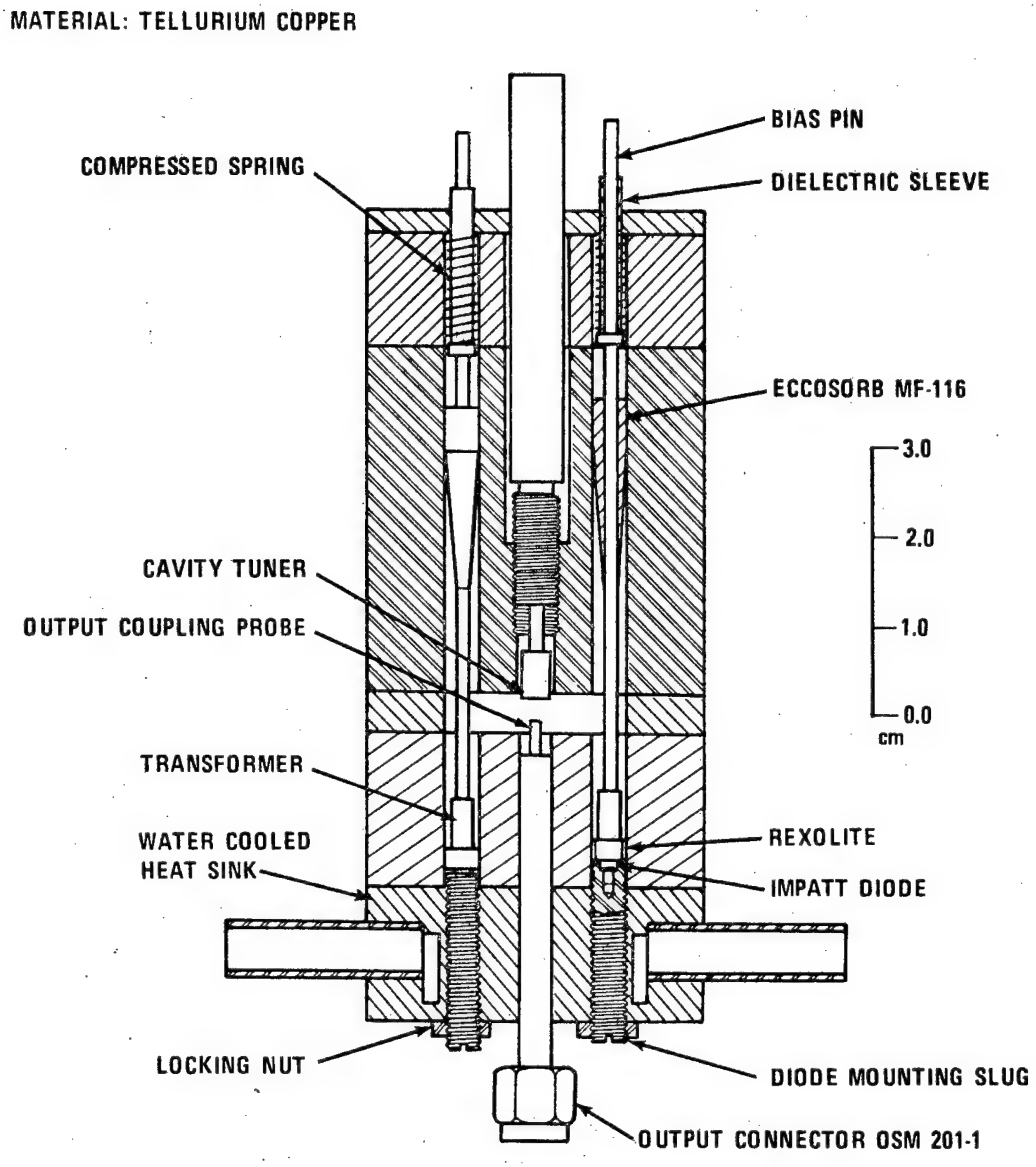

FIGURE 11. Resonant Cylindrical Cavity TM 010 Mode 10-Diode Power Combiner.

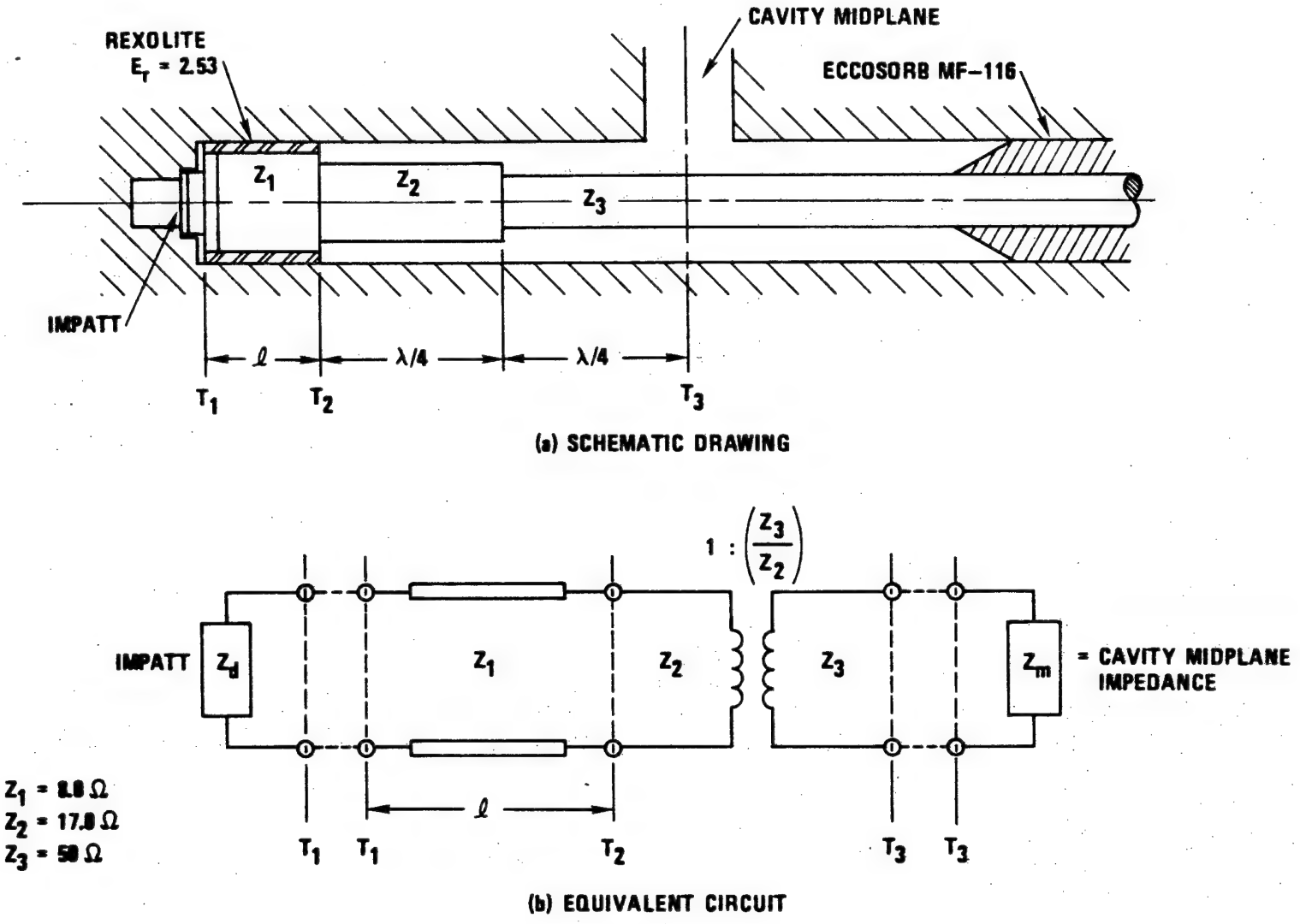

FIGURE 12. Impatt Diode Matching Structure.

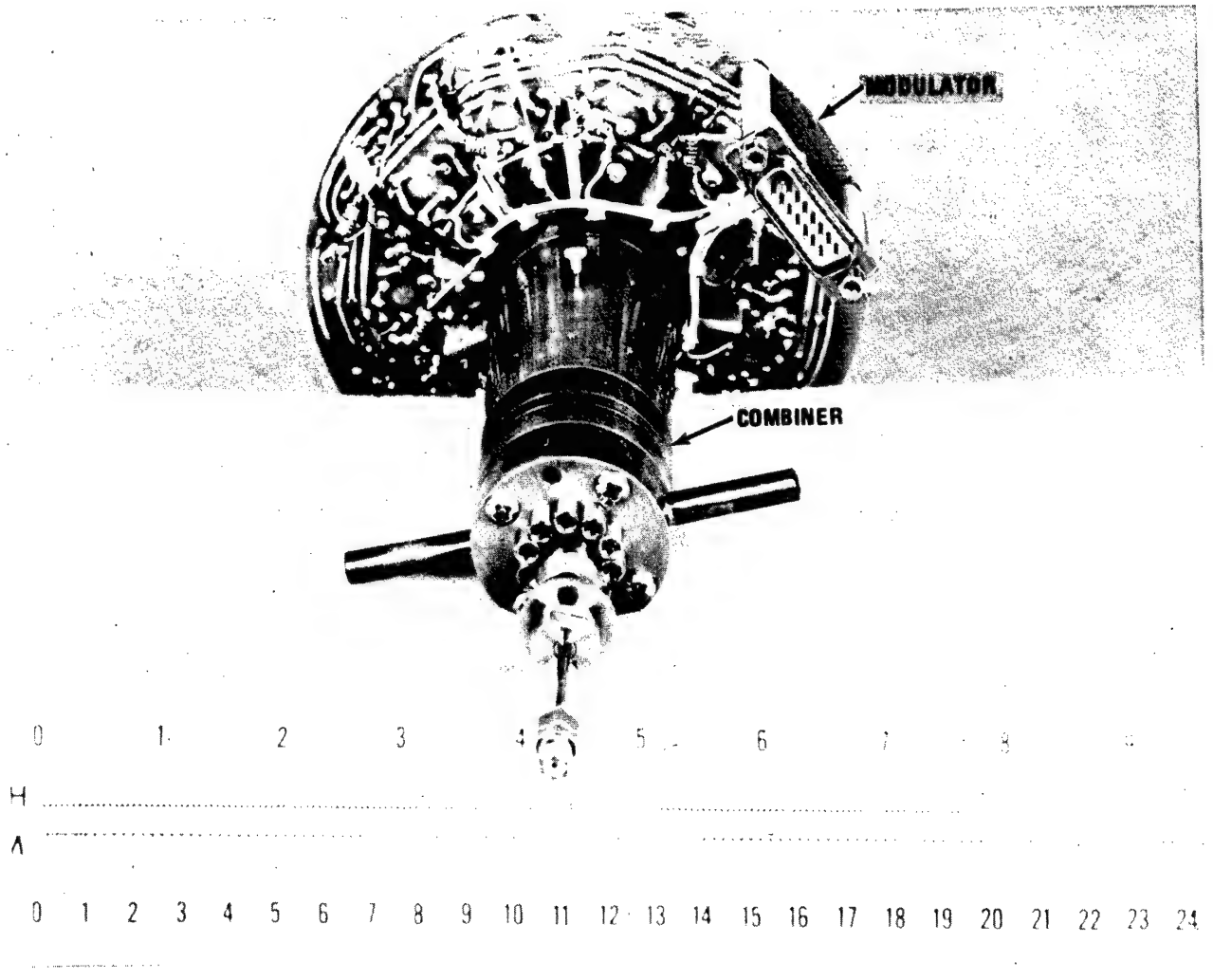

FIGURE 13. TM $_{010}$ Cavity 10-Diode Power Combiner and Modulator

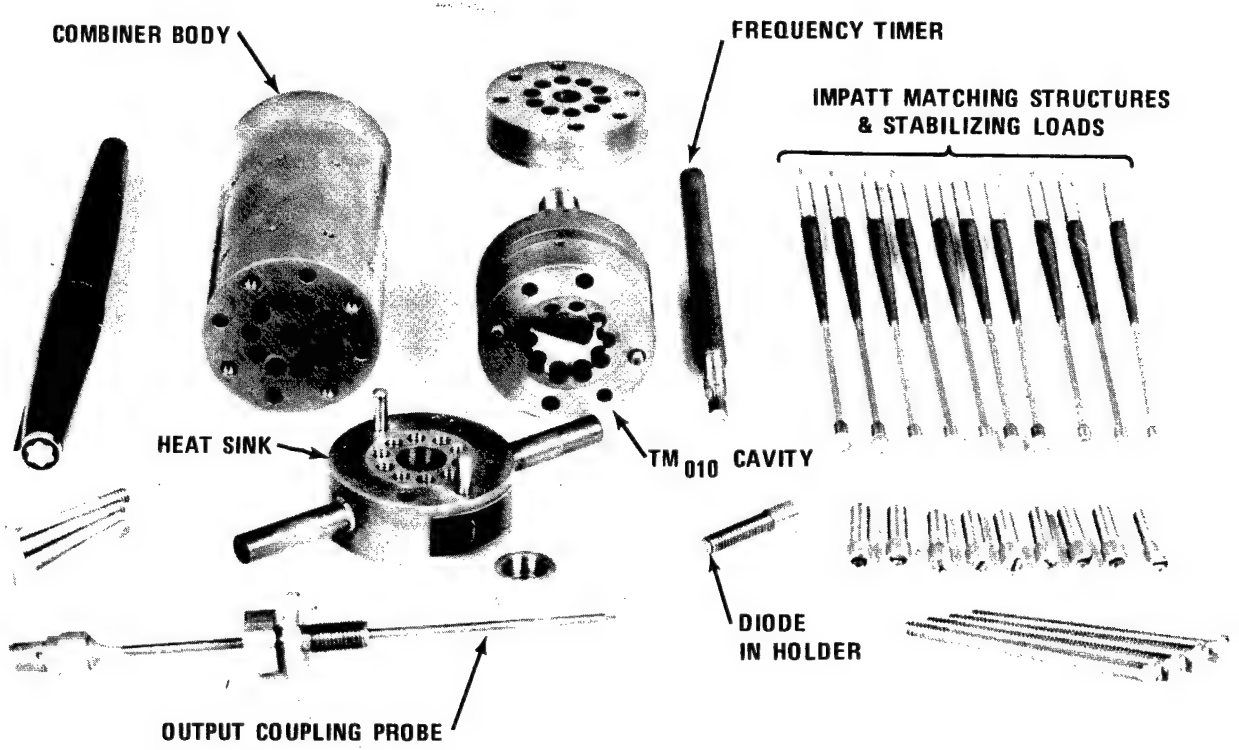

FIGURE 14. TM $_{010}$ Cavity 10-Diode Power Combiner Components.

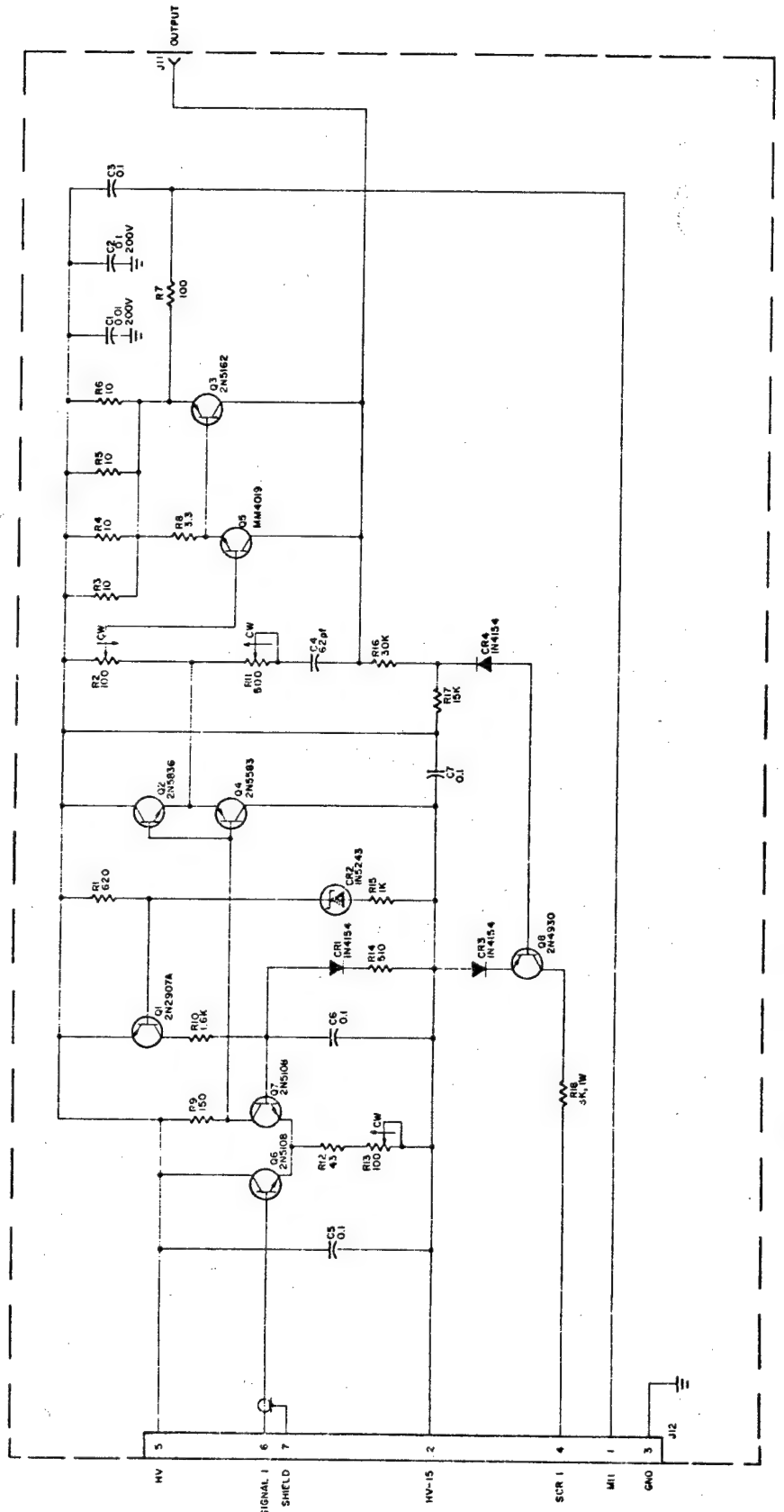

NOTES:
1. UNLESS OTHERWISE SPECIFIED:
   A. ALL RESISTANCE VALUES ARE IN OHMS, 1/4 WATT, 5%.
   B. ALL CAPACITANCE VALUES ARE IN MICROFARADS 50V, 10%.

FIGURE 15. Single Diode Impatt Modulator Schematic.

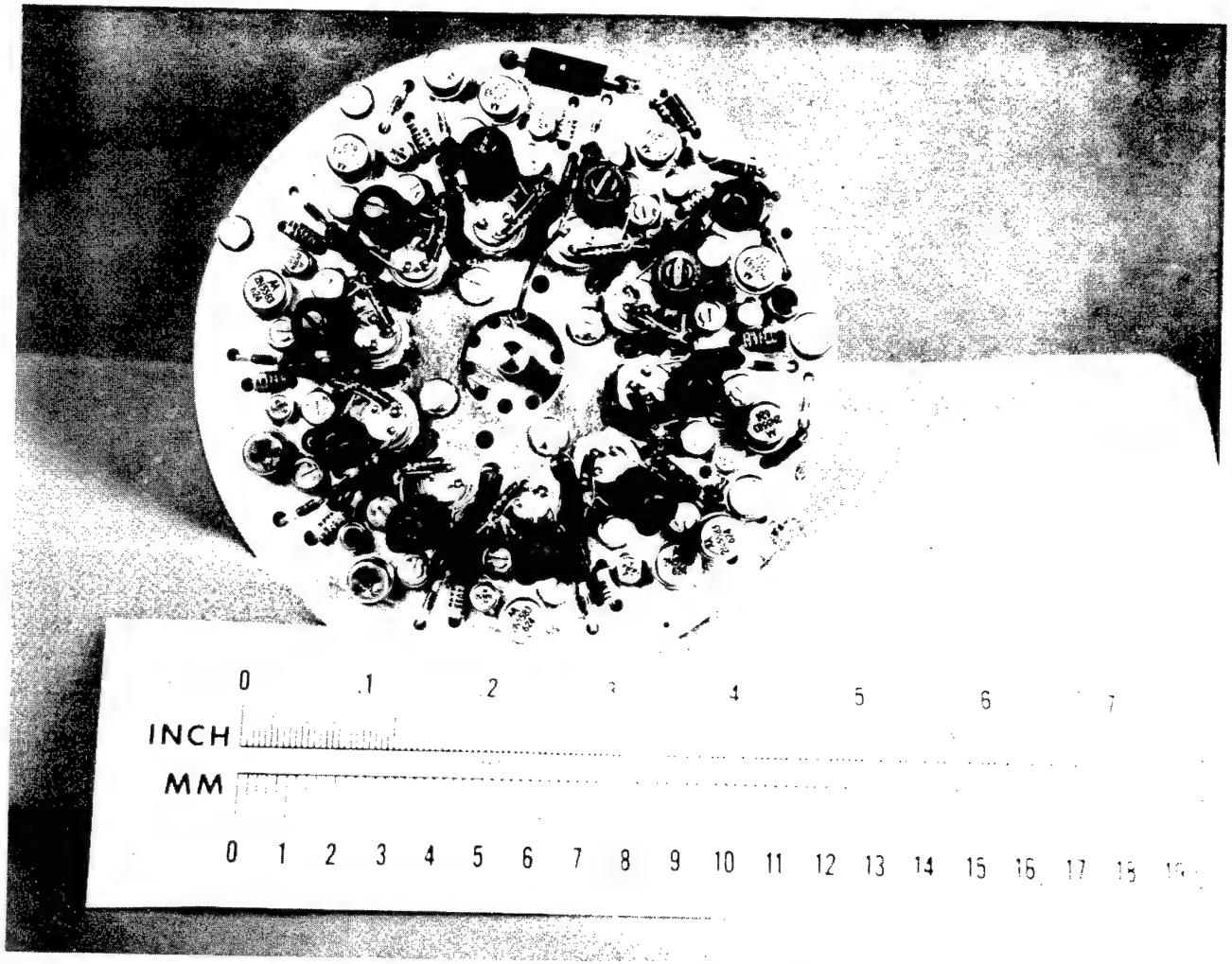

FIGURE 16 10-Diode Combiner Bias Modulator.

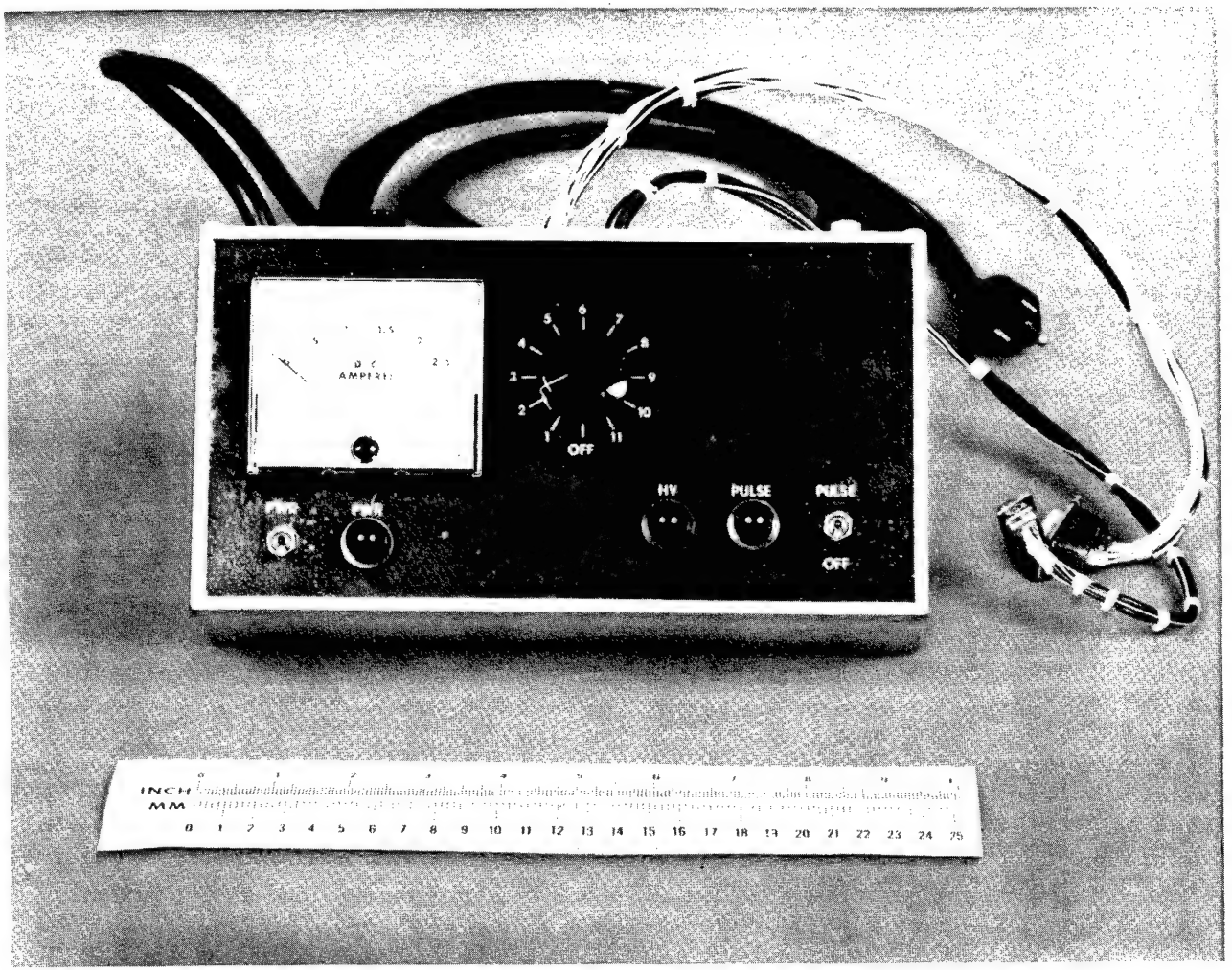

FIGURE 16A 10-Diode Combiner Bias Modulator Control and Monitor Assembly.

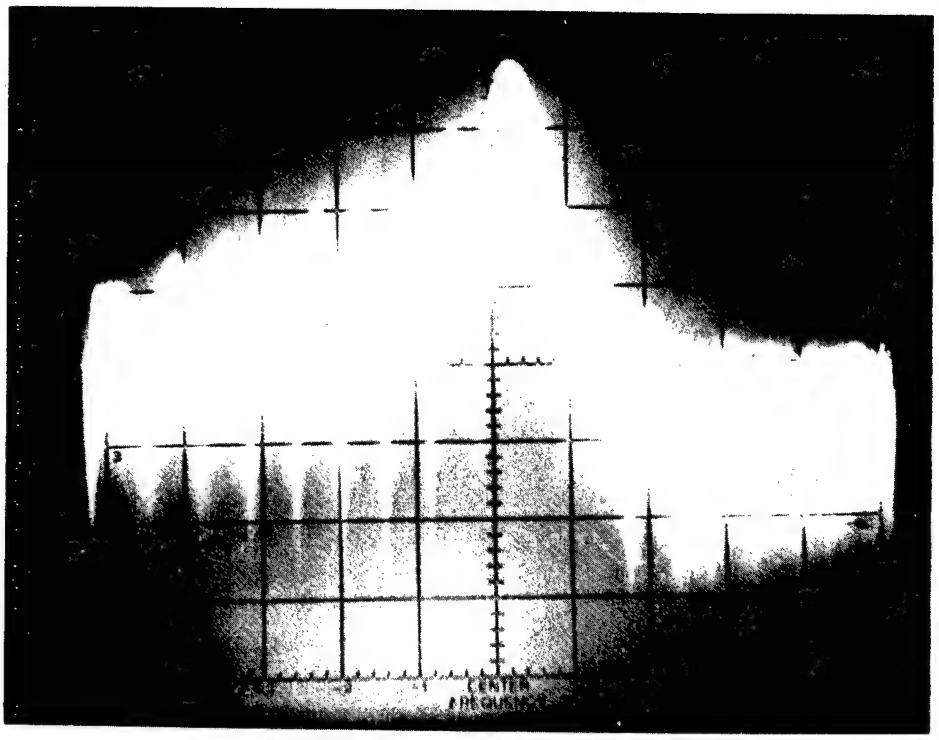

P_{OUT} = 100 WATTS PEAK

f_o ≅ 12.4 GHz

I_{BIAS} = 1.35 AMPS PEAK

SCAN WIDTH = 20 MHz/DIV

FIGURE 17 Output Power Spectrum of Free-Running TM_{010} Mode 10-Diode Power Combiner.

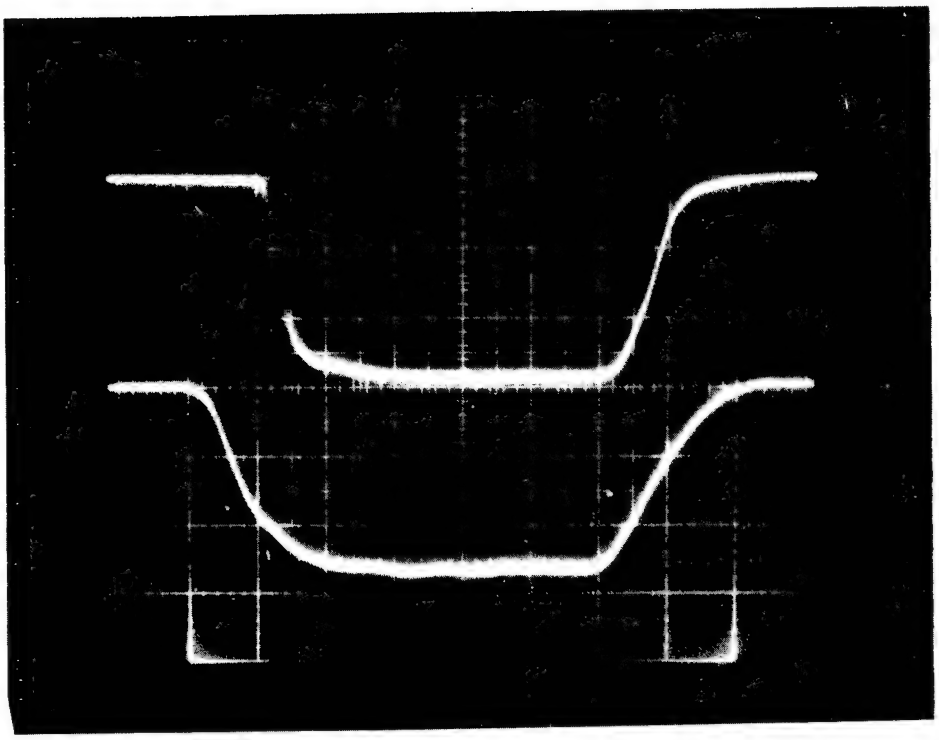

P_{OUT} = 100 WATTS PEAK

I_{BIAS} = 1.35 AMPS PEAK

VERTICAL: (TOP) 50 mV/DIV, (BOTTOM) 500 mA/DIV

HORIZONTAL: 20 NANOSEC/DIV

FIGURE 18. Detected RF Pulse (Top) and No. 1 Impatt Bias Current (Bottom) Waveforms of TM_{010} Mode 10-Diode Power Combiner.

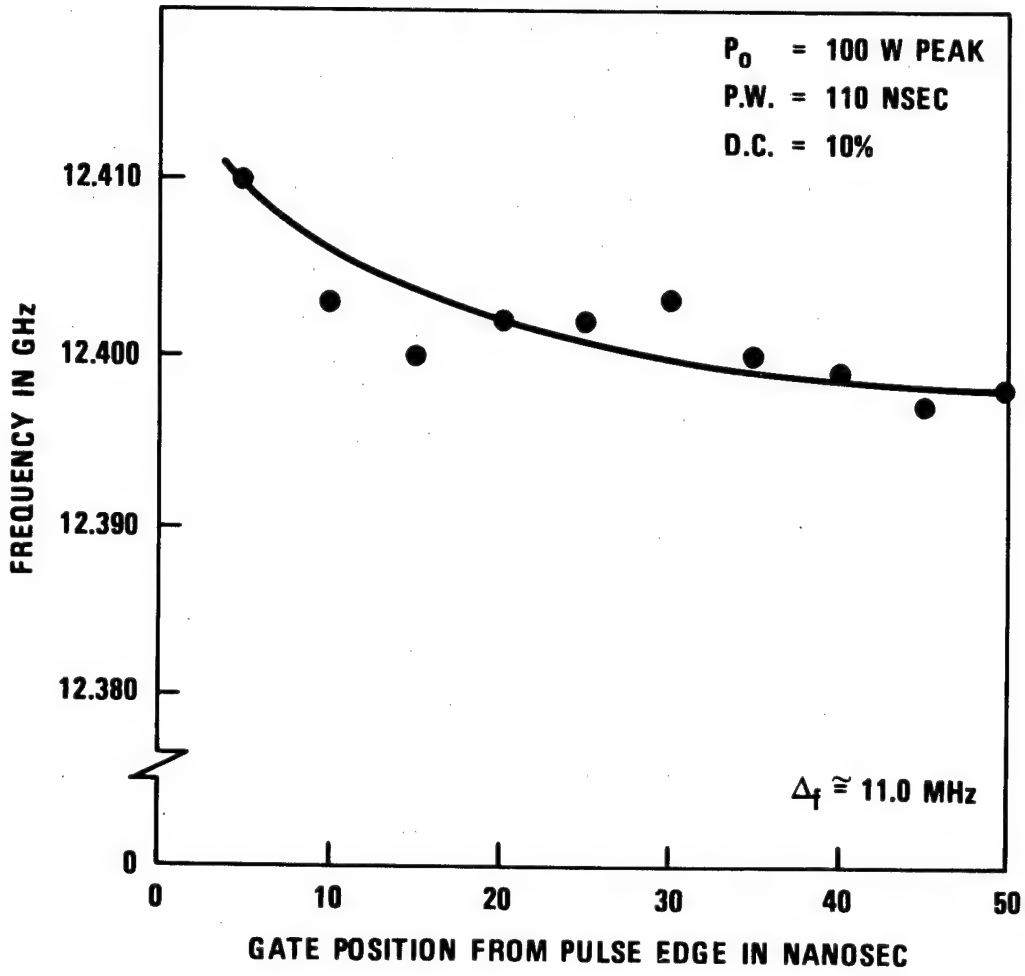

FIGURE 19. Frequency Profile of Output RF Pulse of Free-Running 10-Diode Combiner

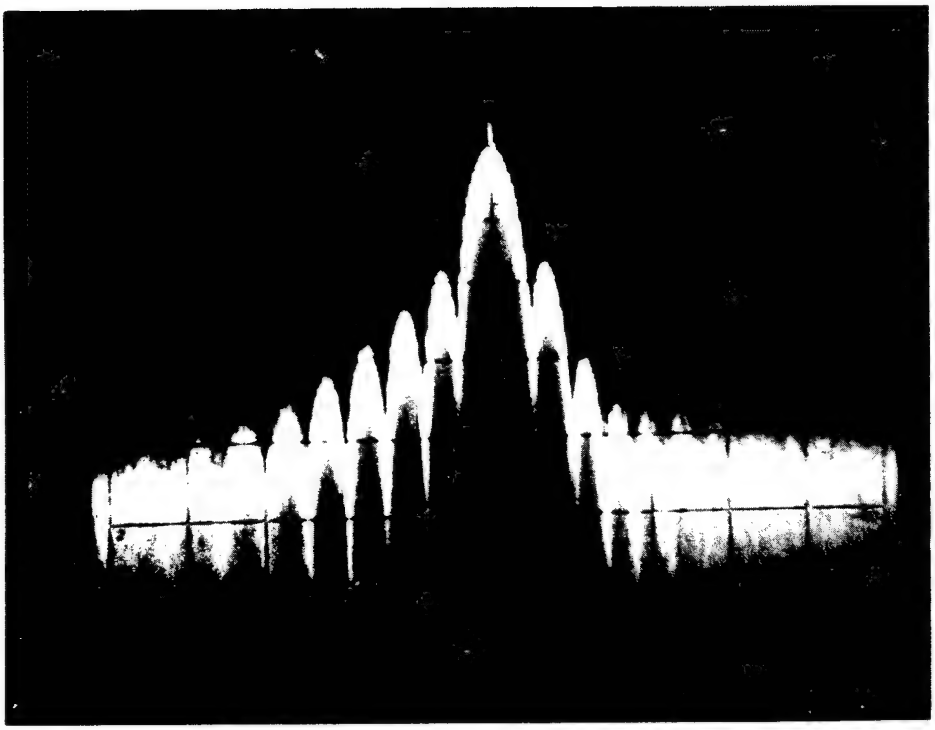

P_{OUT} = 100 WATTS PEAK

f_o = 12.3 GHz

LOCKING GAIN = 20 dB

SCAN WIDTH = 20 MHz/DIV

BANDWIDTH = 30 KHz

FIGURE 20. Output Power Spectrum of TM_{010} Mode 10-Diode Power Combiner Under Injection-Lock.

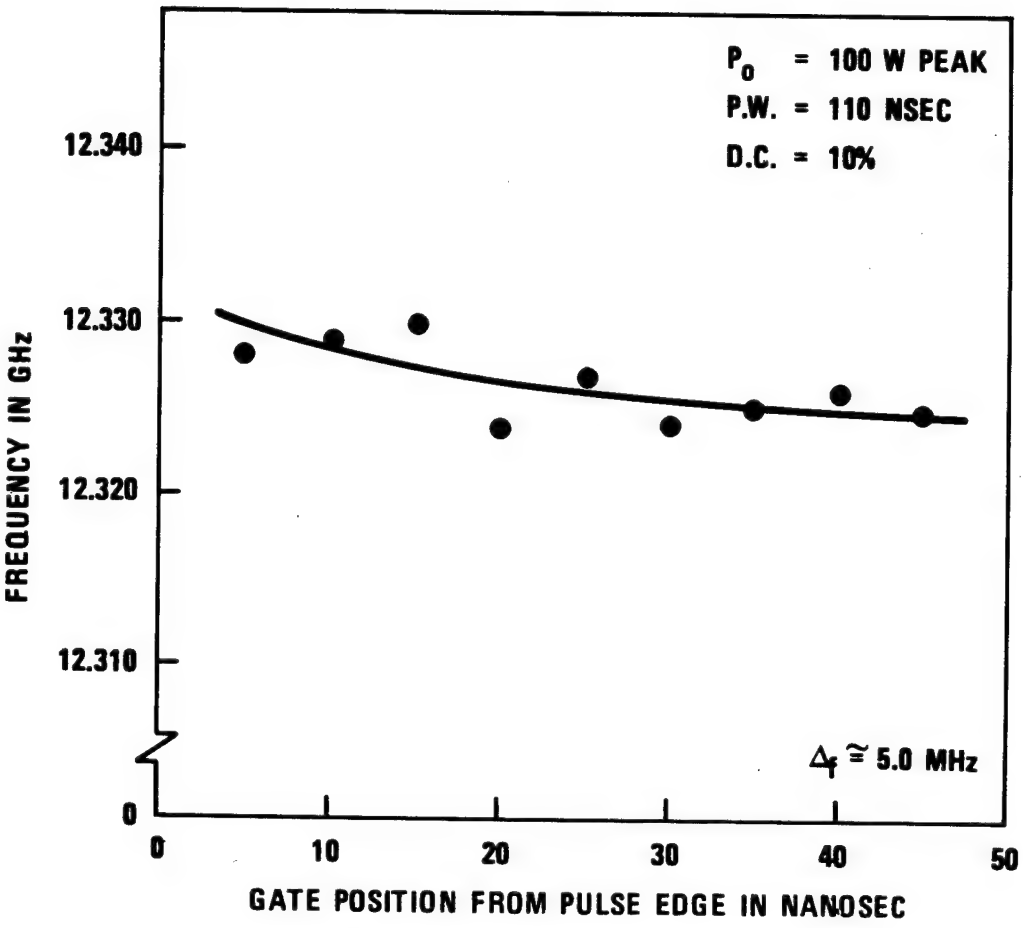

FIGURE 21. Frequency Profile of Output RF Pulse of Injection-Locked 10-Diode Combiner at 20 db Locking Gain

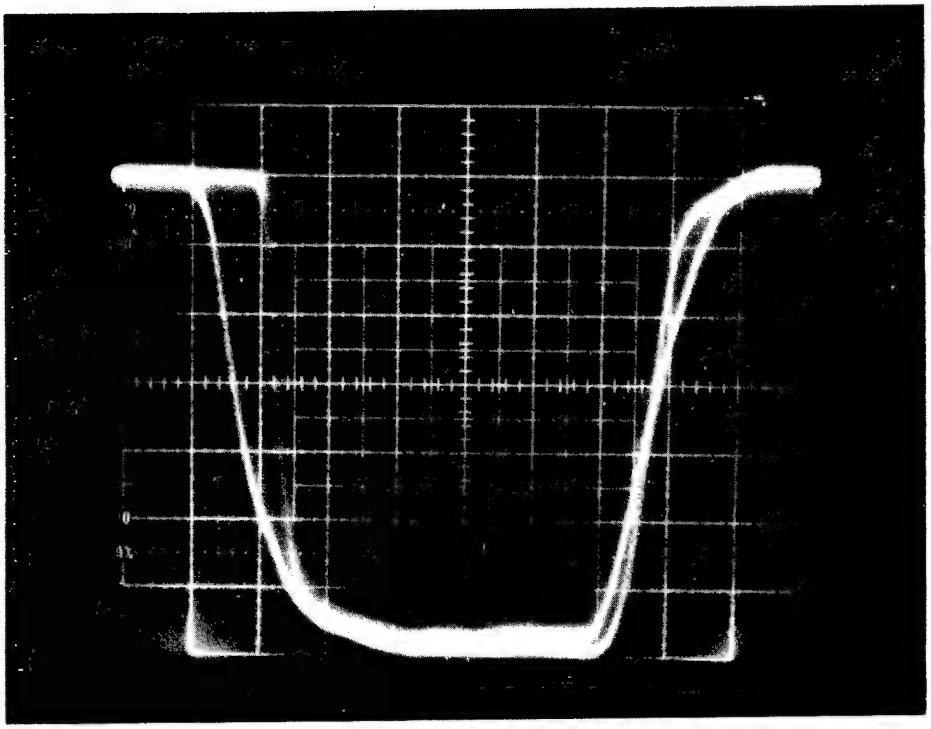

P_o = 100 WATTS PEAK

f_o = 12.3 GHz

HORIZONTAL: 20 NANOSEC/DIV

FIGURE 22. Detected RF Pulse Delay With Respect to Bias Current in Free-Running TM_{010} Mode 10-Diode Power Combiner.

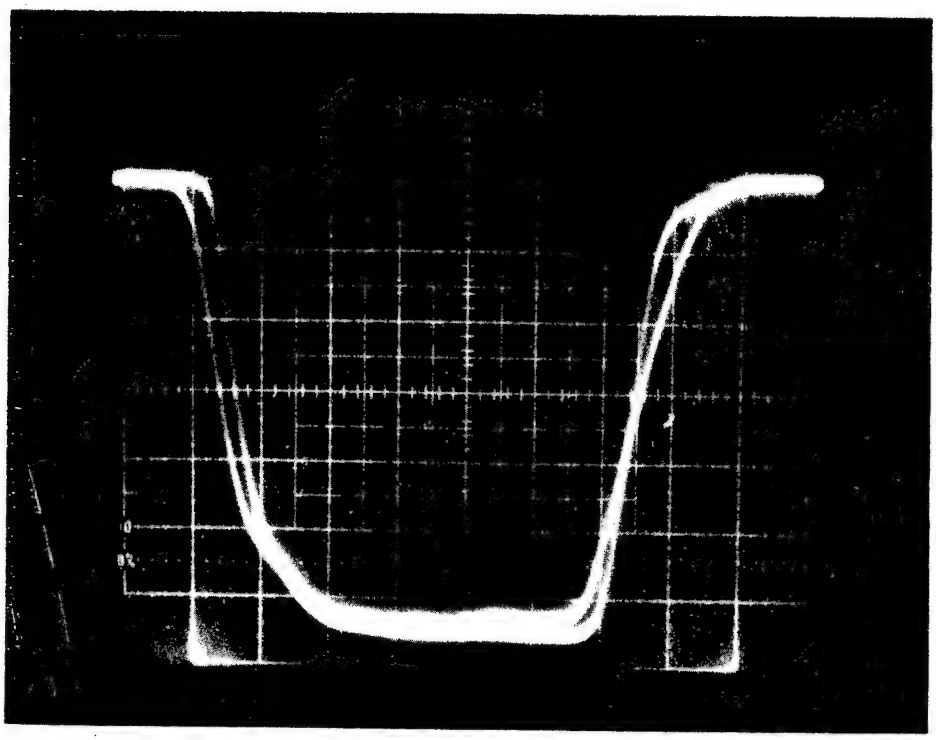

P_o = 100 WATTS PEAK

$f_o \cong$ 12.3 GHz

LOCKING GAIN = 20 dB

HORIZONTAL: 20 NANOSEC/DIV

FIGURE 23. Detected RF Pulse Delay With Respect to Bias Current Pulse in Injection-Locked TM_{010} Mode 10-Diode Power Combiner.

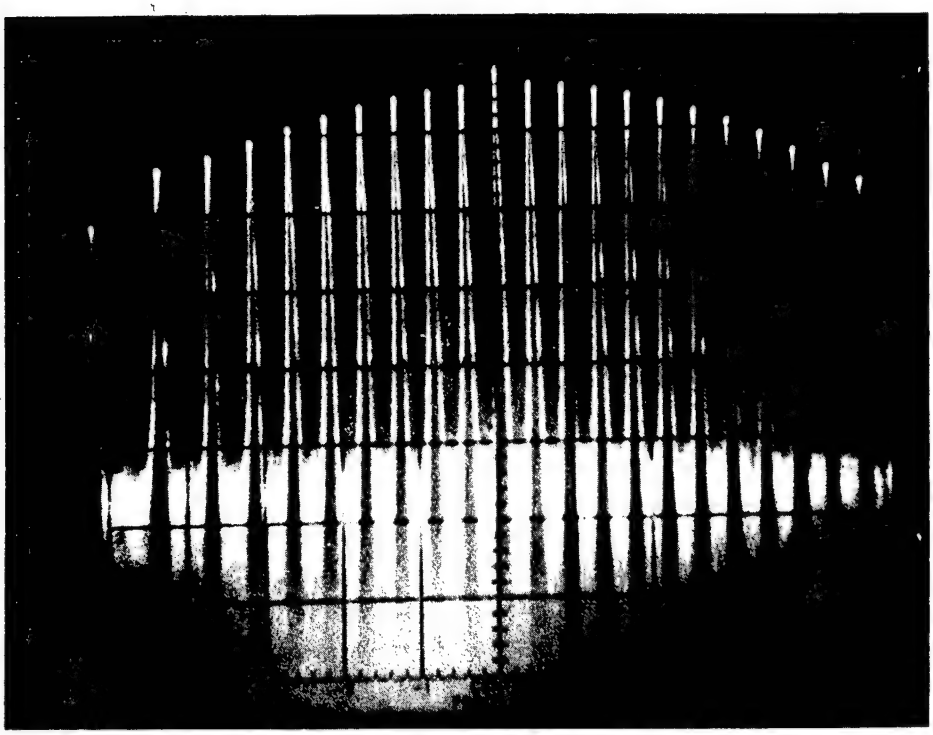

P_o = 100 WATTS PEAK

f_o = 12.3 GHz

LOCKING GAIN = 20 dB

SCAN = 2 MHz/DIV

BANDWIDTH = 30 kHz

FIGURE 24. Frequency Spectrum of Output RF Pulse of TM_{010} Mode 10-Diode Combiner Under Injection-Lock.

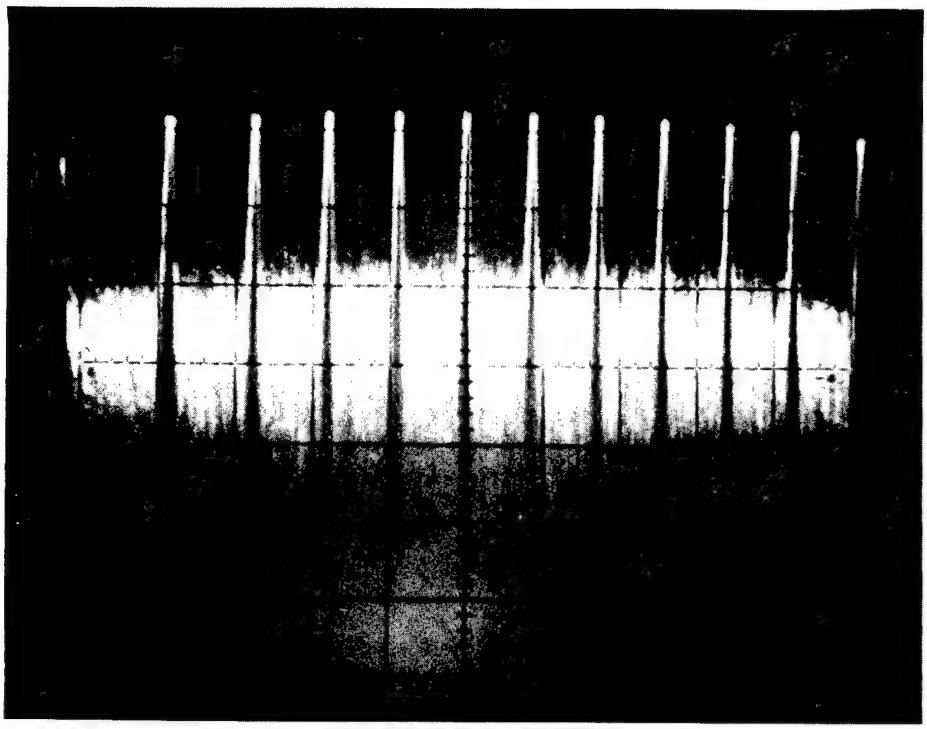

P_o = 100 WATTS PEAK
fo ≅ 12.3 GHZ
LOCKING GAIN = 54.2 db
SCAN = 2 MHZ/DIV
BANDWIDTH = 30 KHZ
LOG DISPLAY 10 db/DIV

FIGURE 25. Frequency Spectrum of Output RF Pulse of TM_{010} Mode Combiner Under Injection Lock.

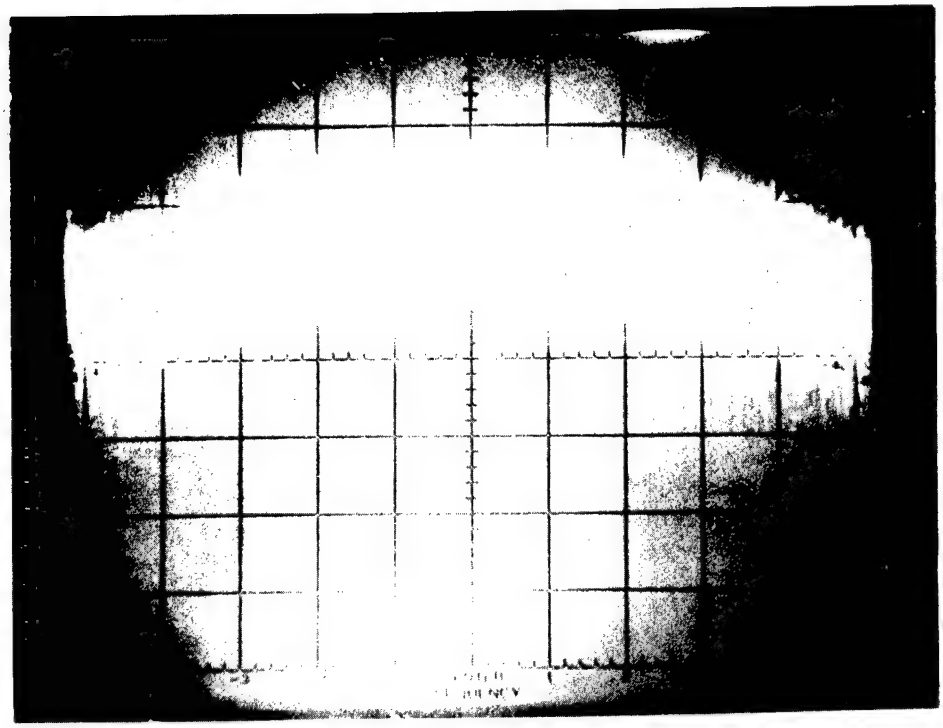

P_o = 100 WATTS PEAK
fo ≅ 12.3 GHZ
SCAN = 2 MHZ/DIV
BANDWIDTH = 30 KHZ
LOG DISPLAY 10 db/DIV

FIGURE 26. Output Power Spectrum of FREE–RUNNING TM_{010} Mode 10-Diode Combiner.

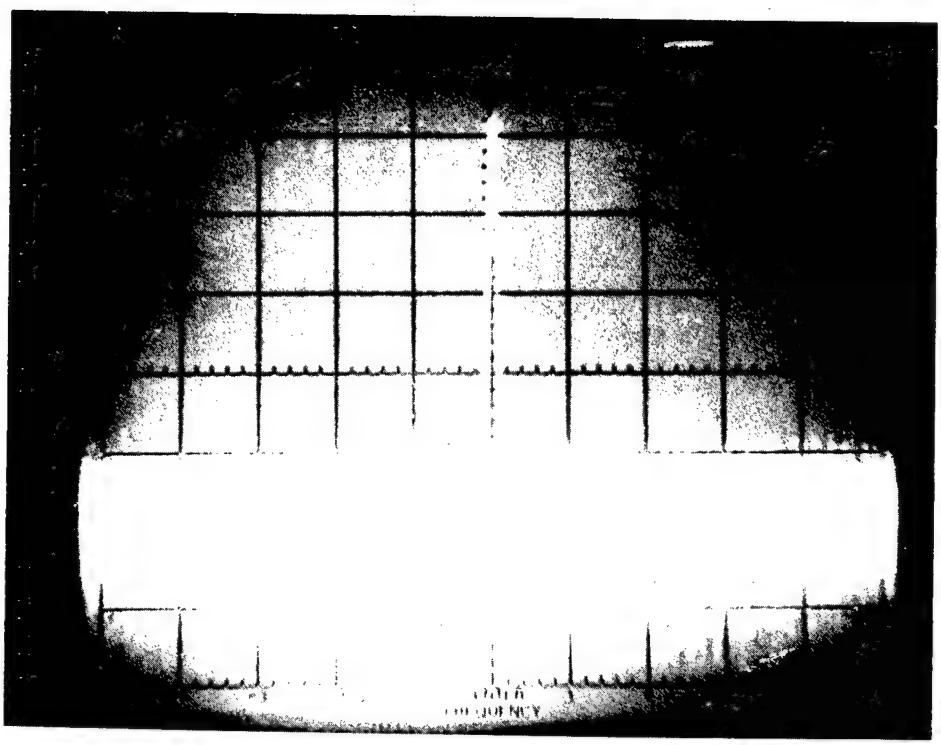

SCAN BANDWIDTH = 1 MHz/DIV

BANDWIDTH = 30 kHz

f_o = 12.3 GHz

P_{out} = 1.0 WATT CW

FIGURE 27. Frequency Spectrum of the Combiner Locking Signal.

Biographical Sketch

Marko Afendykiw was born in the Ukraine on July 22, 1928. During the German occupation of the Ukraine in WWII he was deported to Mannhartzberg Labor Camp in Austria where he worked as a logger.

In 1949 he emigrated to the United States and became a U.S. Citizen in 1956.

In 1957 he graduated from Wayne State University in Detroit, Michigan with the B.S.E.E. degree and the same year accepted a position of Electronics Engineer with the NWC (formerly NOTS), China Lake.

In 1961 and also in 1969 he was a recipient of a NWC fellowship for graduate studies. He received the M.S.E. degree and the Degree of Engineer, both in Electrical Engineering, from the University of Michigan, Ann Arbor, Michigan in 1963 and 1971 respectively.

For his Degree of Engineer dissertation he investigated the effects and transformation properties of microwave diode parasitics in solid-state circuit applications.

His professional interests include applications of statistical communications theory to passive radar detection systems, microwave transreflector antenna designs, and microwave solid-state devices and their circuit applications.

He was granted two U.S. Patents for his work in the applications of uncooperative electromagnetic energy sources to covert surveillance systems and authored several NWC technical publications.

He is a member of the Institute of Electrical and Electronics Engineers, Electron Devices and Microwave Theory and Techniques Professional groups, and ETA KAPPA NU and TAU BETA PI engineering honorary societies.

Biographical Sketch

Jon Hunt Bumgardner was born in Seattle, Washington, in 1943. He received the A.S. degree from Grays Harbor College in 1964, the B.S.E.E. degree from Washington State University in 1966, and the M.S.E.E. in Communications from the University of Southern California (by NWC fellowship) in 1973.

He worked at the Boeing Company from 1966 to 1968 as an Electronic Systems Engineer.

He was employed by the Naval Weapons Center in 1968. During the period from 1968 to 1972 he was an Electronic Circuit Design Engineer. From 1972 to the present he has been an Electronic Wideband Circuit Design Consultant. His primary professional interest is to advance the state of the art in wideband communication and measurement systems. He has designed several high speed electro optical processing circuits, communication systems, and laser range finding circuits. He was the Naval Weapons Center 1978 William B. McLean Award recipient: "For his exceptional creative ability and versatility...in the fields of Electronics, Optics, and Physics." He is the author of 4 NWC publications. He is the inventor of 9 U.S. patents with one patent pending.

Darry Kinman graduated from Fresno State College in June of 1960, receiving the B.S.E.E. degree. He was awarded the M.S.E.E. in March 1968 from the University of California, Los Angeles.

From June 1960 to the present time he has been employed by the Naval Weapons Center, China Lake, California, where he has been involved in microwave circuit and subsystem design for guided missile data links and active radar seekers.

He is a member of the Institute of Electrical and Electronics Engineers and the Microwave Theory and Technique Professional Group.

STRAPDOWN SEEKER GUIDANCE FOR AIR-TO-SURFACE TACTICAL WEAPONS

BY

CAPTAIN THOMAS R. CALLEN, USAF

Air Force Armament Laboratory
Eglin AFB, Florida

1590

Strapdown Seeker Guidance for Air-to-Surface (A/S) Tactical Weapons

Abstract

Most contemporary tactical guided weapons utilize proportional navigation (PN) as the terminal guidance law and an inertially stabilized gimballed seeker to provide guidance information. Recent advancements in seeker technology, however, include seekers which have much larger fields-of-view and tracking characteristics which do not require that the seeker centerline point in the general vicinity of the target. Thus, such seekers could be rigidly fixed to the weapon and still keep a traget within their field-of-view. These strapdown seekers could eliminate the tracking rate limits and structural limitations of the gimballed inertial systems while reducing the mechanical complexity of implementation and calibration. However, a direct measurement of inertial line-of-sight rate is not available with a strapdown seeker, so alternate guidance and filtering techniques must be developed. The specific objective of this study is to determine the best combination of guidance law structure, signal processing techniques, and achievable seeker and sensor accuracy requirements for the effective use of strapdown seekers with A/S tactical guided weapons.

This study considers state-of-the-art seeker and sensor capabilities, associated noise characteristics, and other relevant error sources. Modern statistical analyses techniques are utilized, and a 6-DOF computer simulation is employed to validate the results.

Various filtering techniques and guidance laws are examined, including direct PN, pursuit guidance, dynamic lead guidance, a combination of PN and pursuit, and a new technique, adaptive PN. This new scheme uses a dither signal to measure and correct for seeker gain errors, and overcomes stability problems associated with most of the other approaches. Its performance is shown to be comparable to PN with a gimballed seeker.

Introduction

Most contemporary tactical guided weapons utilize proportional navigation as the terminal guidance law in conjunction with an inertially stabilized gimballed seeker to provide guidance information. The proportional navigation guidance law is most often used because it can easily be implemented and provides near optimal guidance for constant velocity targets. Inertially stabilized gimballed seekers which track the target have been used in the past because of field of view (FOV) limitations, physical implementation requirements to maintain seeker lock-on, and the practical consideration that this method provides the most direct means of obtaining inertial line-of-sight rates. However, recent advances in seeker technology have resulted in seeker designs with much larger fields of view and seeker tracking characteristics which do not require that the seeker centerline point in the general vicinity of the target. Examples of such seekers include optical and radar correlators, holographic lens used with laser detectors, and phased-array antennas.

The potential advantages of such seekers are numerous and result basically from the fact that the seeker can now be rigidly attached to the weapon body. These body-fixed seekers (also referred to as strapdown seekers) have the potential of eliminating the tracking rate limits and structural limitations of inertial gimballed seekers while simultaneously reducing the mechanical complexity of implementation and calibration. The elimination of mechanical moving parts would in turn eliminate frictional cross-coupling between pitch and yaw tracking channels, accuracy degradation due to missile acceleration, and would create the potential for an increase in reliability of electronic components over mechanical ones. Finally, there are potentially significant cost savings associated with eliminating the gimbals.

Despite all these advantages, there are potential difficulties associated with integrating strapdown seekers into the overall guidance system. Most of these stem from the simple fact that a direct measurement of the inertial line-of-sight (LOS) rate is no longer available. This means that some indirect method of deriving this quantity must be established and shown to be feasible, or some other (possibly less optimal) guidance law must

be used. An indirect method of deriving inertial LOS rate is mathematically straight-forward, but full of engineering uncertainties. Most strapdown seekers only provide a direct measurement of LOS error angle relative to body coordinates. Conceptually, a simple differentiation of this signal would provide a measurement of LOS rate in body coordinates. However, such differentiation can greatly exaggerate any noise associated with the original quantity. Also, this LOS rate must then be transformed into inertial coordinates, requiring that accurate pitch, yaw, and roll rates of the weapon be available. Obtaining these measurements from rate gyros can again prove risky due to frequency-dependent phase lags resulting from the gyro inertial properties and the noise and drift phenomena inherent in all gyros. Since transformation of LOS rate from body to inertial coordinates is nothing more than a mathematically sophisticated "subtraction" of the weapon body rates from the differentiated signal, any significant noise or phase lags can severely degrade accurate guidance information - especially for relatively small inertial LOS rates.

The problems associated with the derivation of guidance laws and filtering techniques for implementation of strapdown seekers with tactical guided weapons have been studied in some detail in recent years. However, these studies have been limited in either of two ways. In many cases, the studies were purely mathematical in nature, without considering actual sensor capabilities or associated noise characteristics. Non-linearities and other critical error sources were not examined in sufficient detail to provide realistic performance data. In those few cases where hardware constraints were integrated into the mathematical study, guidance algorithms were derived for analog implementation. Recent advances in microprocessor technology have resulted in low-cost machines with adequate speed and storage capability to perform the strapdown seeker computational tasks. The Air Force recently completed a study which attempted to overcome these two shortcomings while determining the best combination of guidance law structure, signal processing techniques, and achievable seeker and sensor accuracy requirements necessary for the effective use of strapdown seekers with air-to-surface tactical guided weapon. (For the purpose of this paper, the word "sensor" refers to any device, other than seekers, whose purpose is to measure one

or more of the dynamic states of the weapon). The ultimate goal of this effort was to develop techniques which would result in the most cost effective integration of current and future strapdown seekers with state-of-the-art hardware, and to quantify the advantages and disadvantages of such systems. The following sections describe the work accomplished in this effort, and the results obtained from the study.

Math Models of Air-to-Surface Weapons

Three air-to-surface weapons were initially considered in this study to provide a wide spectrum of bandwidths, control configurations (wing and tail control), guidance modes (skid-to-turn(STT) and bank-to-turn (BTT)), and velocity characteristics (glide and powered). The weapons modelled included a tail-controlled glide bomb, a powered, wing-controlled missile, and a conceptual BTT vehicle. The models used in this study were generic in nature, and were simplified and modified to a sufficient degree to insure that the results were typical of the respective type weapons, but not significantly representative of any particular operational or developmental weapons. Co-planar 3-degree-of-freedom (DOF) transfer functions were derived for each airframe at two flight conditions; the flight conditions represented maximum and minimum dynamic pressure. Only one flight condition was considered for the BTT vehicle, as the bandwidth of the flight control system is relatively constant. These 3-DOF models included linearized aerodynamics, geometry, etc. and were used for stability analysis simulation; 6-DOF models containing nonlinearities were designed for digital simulation. A 3-DOF adjoint simulation of each seeker/airframe combination was used to assess miss distance sensitivity to random error sources. The rms miss distance due to a number of random error sources could then be determined by a single computer run; these results have been verified by numerous 6-DOF Monte-Carlo runs.

A block diagram of the flight control system for the tail-controlled glide weapon is shown in Figure 1. The sensor components include a roll attitude gyro and both a rate gyro and accelerometer for each steering channel. Tail control is accomplished via four actuators which produce fin motion. Maneuverability and angle-of-attack

are limited by the ±9 g acceleration command limit located in each channel. The unpowered vehicle's low speed contributes to its relatively low bandpass compared to the other weapons.

A simplified block diagram of the pitch channel of the autopilot for the powered, wing-controlled weapon is shown in Figure 2. The autopilot employs accelerometers, rate gyros for damping augmentation, and an hydraulic actuation system. The commanded accelerations are limited to ±15 g's. The autopilot was designed for stable operation from Mach 0.9 to Mach 3.2 and from sea level to 20,000 feet altitude. A comparison between the linearized transfer function yaw response for a typical flight condition and the 6-DOF simulation yaw response is given in Figure 3. The response in yaw rate and side-slip angle due to a small step (δ_r = 0.1 deg) of yaw wing position shows good agreement between linear analysis and simulation.

The BTT vehicle differs from the other weapons in two important respects. In the first place, the vehicle guides using proportional navigation in only one channel (i.e., pitch). The roll guidance channel rotates the body such that the total LOS rate is in the pitch plane only. Secondly, the high speeds and large wing area in the pitch plane allow the vehicle to pull high g's at relatively low angles-of-attack. Preliminary analysis of the BTT control mode demonstrated that problems outside the scope of this study were present due to the fact that steering signals exist in all three BTT missile channels (roll, pitch, and yaw). Therefore, the study of the BTT configuration was discontinued to concentrate on the more common STT weapons.

Methods of Generating LOS Rates

A large portion of the work accomplished on this program dealt with the evaluation of proportional navigation (PN) as the guidance law for tactical air-to-surface weapons utilizing strapdown seekers. The inertial LOS rate required for PN guidance is not directly measurable with strapdown seekers, so this information must be generated by some other method. Two basic methods of generating inertial LOS rate signals from

body fixed sensors were found during a literature survey. Since there are no widely accepted designations, the two methods will be referred to as "beam steering" and "additive rate compensation" for the purpose of this study. Both methods tend to be dependent upon seeker hardware, and their general forms are shown in Figure 4 for a single seeker channel.

The "beam steering" method can only be used with certain seekers such as optical area correlators and radar with phased array antenna; the "additive rate compensation" technique can be used only with seekers which have the required instantaneous FOV. The geometry of the former method is shown in Figure 5. A narrow instantaneous FOV is displaced (θ_{beam}) from the missile centerline to track the target. The steering loop centers the beam on the target by nulling the error angle, ε_{beam}, which is defined as the angle between the LOS and the beam centerline. The rate gyro information in effect removes the body motion signals from the seeker output by supplying this information to the phase shifters which steer the beam.

The "additive rate compensation" technique can be considered a special case of beam steering in which θ_{beam} is fixed. This technique combines the derivative of the seeker output with an inertial rate sensor to derive inertial LOS rate. The concept requires a wide instantaneous fixed FOV for acquisition and tracking, and this wide FOV increases the thermal or background noise. The required wide FOV can be minimized to some degree, however, by canting the beam down in pitch as opposed to the normal zero θ_{beam} configuration. A combination of the two methods is also possible; namely, moving the beam with the seeker output only and adding the gyro to the seeker output. This case would be considered if phase shifter linearity and dynamics prevent use of the full beam steering configuration.

Seeker Models and Error Sources

Once the LOS rates are accessible, mathematical models of available strapdown seekers must be developed. These models must represent state-of-the-art or near term hardware, or have development potential for actual strapdown application. The major requirement for this application is a highly linear characteristic (output voltage

as a function of centerline LOS displacement) over a relatively wide FOV. Air-to-surface weapons with reasonable launch offsets and maneuvering capability require a FOV of approximately ±15 degrees. The seekers considered for this study include semi-active laser, imaging infrared, active radar with phased-array antenna, and passive radar. In the area of inertial sensors, both rate and attitude gyros are considered. The model includes significant seeker parameters, noise characteristics, other error sources, and operational limitations, and can be used to simulate any particular seeker by proper selection of these items. This generic approach enables the sensitivities and requirements determined to be applied to seekers developed in the future.

The modelling of the seeker and sensor hardware allows one to evaluate the effect of these components on the derived LOS rate. Seekers and inertial sensors do cause errors in the computed LOS rate, and these errors in turn can produce system instability, effective navigation gain errors, and degradation of accuracy. The method of generating the inertial LOS rate also effects, to some degree, the sensitivity to each error source. The component errors to be considered fall in three broad classes: linearity or gain errors (radome, receivor/detector, phase shifter, gyro, and seeker/gyro dynamics), time-varying random errors (thermal noise, glint or apparent target motion, gyro noise), and offsets (seeker boresight errors, gyro offsets or drift). Other errors, such as cross-coupling, sampling rate, break-lock or blind range, winds, target motion, body-bending, vibrations, and launch offsets, can be shown to be of secondary importance. These component errors cause corresponding errors in the derived inertial LOS rate. Gain errors cause components of the missile body rate to appear in the derived LOS rate, which can cause stability problems and errors in the effective navigation gain. Random errors in the seeker and rate gyro cause random errors in the LOS rate with a corresponding loss of accuracy. Finally, offsets can cause anomalies in the derived LOS rate depending on their location with respect to the derivative network. Offsets in the LOS rate also result in degradation of miss distance and some increase in required maneuverability.

For example, consider the effect of seeker and gyro scale factor errors for the case of "additive rate compensation" with an attitude gyro as depicted in Figure 6. For long times-to-go, the homing loop is essentially open and the LOS angle, η_q, equals

$$\eta_q = (K_g - K_s)\ \theta.$$

Therefore, both gyro and seeker scale factors have similar effects on body attitude feedback. These scale factors are represented as gains in the block diagrams contained in this paper; however, these gains are not constant and exhibit highly nonlinear characteristics. The values of the net negative feedback gain (K_s - Kg) which cause the system to go unstable can be determined using linear analysis techniques. These critical values of net feedback gain are functions of the flight control system transfer function shown in Figure 6. With acceleration control systems, the transfer function $(\dot{\theta}/\dot{\theta}_c)$ is replaced by:

$$(\dot{\theta}/\dot{\theta}_c) \longrightarrow (N_{zc}/\dot{\theta}_c)\ (N_z/N_{zc})\ (\dot{\gamma}/N_z)\ (\dot{\theta}/\dot{\gamma})$$

These four transfer functions correspond to the guidance filter, acceleration control loop, geometry, and flight path dynamics. In the particular case of the tail-controlled glide bomb, the critical values are plotted versus the derivative network bandwidth in Figure 7. At high bandwidths, +4 percent and -3 percent variations in net scale factor cause instability. As the bandwidth is reduced, the tolerance to scale factor errors increases, but a reduction in total system response time results. The hashed line in Figure 7 represents the maximum scale factor variation allowable to achieve a system damping factor of 0.2. For a derivative network bandwidth of 5 rad/sec, +2.6% and -4.4% scale factor errors reduce the damping to 0.2; a greater desired damping would require an even smaller scale factor error tolerance. As stated earlier, a reduction in bandwidth reduces the overall system bandwidth and the time-to-go at which the homing loop goes unstable. It was found that a rapid increase in the time of homing loop instability occurs when ω_D is less than about 5.0 rad/sec. It was further determined that the general case of the effect of navigation gain variation due to scale factor errors is independent of flight control system and vehicle dynamics.

Seeker noise can also be a problem at low signal-to-noise ratios, particularly since the seeker output must be differentiated. Reducing the derivative network bandwidth minimizes these effects, but stability problems then come into play as discussed previously. Seeker boresight errors and attitude gyro offsets have no effect on the LOS rate since the d.c. gain of the derivative network is zero. However, drifts in the gyro will appear in the output of the derivative network as a LOS rate. In most cases these effects will be insignificant, however, since very small drift rates are obtainable with state-of-the-art gyros.

Simulation Results

Once the candidate airframes, seekers, and sensors were modelled, and the effects of error sources in inertial LOS rates examined, the various combinations of seekers and airframes were simulated. The linear 3-DOF adjoint simulation was used to evaluate the linearized effects of these combinations upon miss distance. Table 1 is a summary of the flight conditions for the candidate systems subjected to random noise inputs, and Table 2 presents the vehicle transfer functions used in the adjoint simulation. These transfer functions are approximations to the math model presented earlier. These approximations allow for simplification of the computer model while retaining the salient features of the math model. The root-sum square (RSS) values of miss distance for composite random noise inputs are given in Table 3. These RSS values are due solely to the random noise sources and do not include the effect of the scale factor errors mentioned previously. Notice that as the effective bandwidth of the system was increased, the vehicle was more responsive and generally was better able to handle random noise inputs. The glide weapon represents the lowest bandwidth system, while the BTT vehicle represents the highest. The results indicate that miss distance is more strongly related to vehicle bandwidth than to seeker type. The passive radar shows a smaller miss distance because the glint contribution is not present for this type seeker. Additional adjoint simulation runs were made examining the miss distance contributions from various noise sources separately as a function of vehicle and seeker types. Glint noise or laser spot jitter represents the most severe noise problem of those examined. It is difficult to reduce the effect of this error since the spot position is the only

measurement of target position available for guidance. Also, the frequency of the jitter is similar to that of the guidance information. Therefore, filtering on the basis of frequency offers little promise.

The 6-DOF nonlinear simulation was used, as previously mentioned, to verify the results of the linear analysis and adjoint simulation. The 6-DOF simulation was also the only available method by which the effects of scale factor errors and noise sources acting simultaneously could be obtained and analyzed.

Alternate Guidance Laws

The study of alternate guidance laws was made necessary by the results of the PN evaluation which indicated that a direct implementation of PN using strapdown seekers was unacceptable. A number of guidance laws suitable for use with strapdown seekers were investigated, including Dynamic Lead Guidance, Pursuit Navigation, a combination of Pursuit and Proportional Navigation, and a new technique termed Adaptive Proportional Navigation. Comparisons of these guidance laws are based on accuracy relative to PN with a gimballed seeker, sensitivity to seeker scale factor variations, field of view requirements, noise sensitivity, and mechanization requirements.

Dynamic Lead Guidance (DLG) can be considered a compromise between PN and pursuit in a number of aspects. The terminal accuracy and sensitivity to noise fall between the extremes represented by the two laws mentioned. Also, the effective navigation gain of DLG approaches that of pursuit at low homing loop frequencies, and is similar to that of PN at higher frequencies. This guidance scheme proved to be a variation of the adaptive rate compensation implementation of PN, with the navigation gain replaced by a lead network. A block diagram of this concept is shown in Figure 8. Results of the DLG evaluation indicated that this concept actually has a lower accuracy and lower tolerance to scale factor errors than PN with a strapdown seeker.

A block diagram depicting a Pursuit Navigation mechanization is shown in Figure 9. In its most basic form, pursuit guidance commands the weapon body attitude, rate, or acceleration in such a manner as to maintain a constant

strapdown seeker error angle; therefore, the missile is always pointed toward the target, thus reducing the FOV requirements. In this approach, the navigation gain is independent of seeker scale factor and gain errors. These errors affect the bandwidth of the attitude loop which can be designed with adequate frequency response and gain margin. In addition to low seeker gain error sensitivity and minimum FOV requirements, pursuit exhibits a considerable noise immunity as compared to PN or DLG. The major disadvantage of this type of guidance law is its very poor accuracy; the system is very susceptible to error sources such as boresight, wind, target motion, etc.

The combination of proportional navigation with reduced navigation gain and a parallel channel of body pointing pursuit provides a degree of compromise between the two guidance laws. The concept exhibits a greater tolerance to seeker scale factor errors than PN and a greater tolerance to boresight errors than pursuit. A block diagram of the general form of the combination is shown in Figure 10. The most significant shortcoming of this technique is the relatively poor performance in the presence of wind, target motion, and gravity compensation errors. The only situations for which this combination law performs better than PN is for large initial offsets and for large scale factor errors. The ability of the pursuit body attitude loop to zero the initial offset results in uniformly good performance for all offsets.

A new approach to the guidance law problem was also evaluated - Adaptive Proportional Navigation. This concept employs a dither generator to cause sinusoidal motion of the airframe and gain track networks for comparing the amplitude of the dither in the seeker and gyro outputs. The gain of the seeker channel is then modified to equalize the gains of the two paths. The potential instability due to net positive or negative feedback is thus eliminated. Details of the mechanization appear in the block diagram of Figure 11. The dither generator has automatic gain control (AGC) to maintain a constant dither amplitude in body motion as observed in the gyro output. This is necessary since the closed loop gain of the attitude loop at the dither frequency varies with flight condition. Holding the dither level constant is required because the gain of the adaptive loops is proportional to the dither amplitude and therefore affects the stability and speed of

response of these loops. The performance of Adaptive PN was found to be uniformly superior to the other guidance laws examined except for sensitivity to launch offsets; in this case, pursuit navigation is slightly better. A strapdown seeker mechanization utilizing Adaptive PN appears, in fact, to have performance comparable to that of PN with a gimballed seeker. Data from nominal trajectories for Adaptive PN (strapdown seeker) and PN with a gimballed seeker are given in Table 4. This comparison is for the wing-controlled, powered vehicle with an initial 2 degree yaw offset. This table depicts the similar performance of these two guidance systems.

Conclusions

Unlike the studies conducted in the past on the feasibility of implementing strapdown seekers on tactical weapons, this effort contained realistic models of seeker and sensor non-linearities and error sources, and concentrated on a digital mechanization of the guidance laws. The results of this study indicate that proportional navigation with reasonable navigation gain is sufficiently sensitive to seeker and scale factor errors to make implementation extremely difficult. Scale factor errors on the order of 1 to 2 percent reduce system damping to unacceptable levels, and errors on the order of 3 to 5 percent cause complete instability. This sensitivity is not significantly affected by vehicle configuration (wing or tail control) or guidance mode (STT or BTT). This sensitivity to scale factor errors can be reduced by resorting to other navigation laws with lower navigation gians, such as pursuit, but the loss in accuracy is generally unacceptable.

The Adaptive PN concept using a sinusoidal dither signal to measure and correct for seeker gain errors overcomes the above stability problems. Its performance has been shown to be comparable to PN with a gimballed seeker for a variety of seeker and system errors. Static scale factors of up to ± 60 percent can be tolerated without degradation of performance and error slopes of up to 0.2 degree/degree are allowable using this guidance law. The dither signal does cause moderate increases in the actuator requirements, but the loss in maximum range due to increased drag appears to be neglibible. The technique has application

to constant FOV and beam steered seekers and wing or tail control vehicles.

For some applications where high accuracy is not required, the combination of pursuit and proportional navigation offers low sensitivity to seeker errors plus a less complex mechanization than Adaptive PN. Loss of terminal accuracy due to both boresight errors and scale factor errors can be reduced to reasonable levels.

Table 5 presents a comparison between Adaptive PN, the Pursuit/PN combination, PN, Pursuit, and Dynamic Lead Guidance. The various guidance laws are ranked according to their suitability for strapdown applications with regard to accuracy, sensitivity to seeker boresight and scale factor errors, complexity, cost, and reliability. Adaptive PN is shown to be most suitable with the only disadvantages being complexity and increased actuator rate and energy requirements.

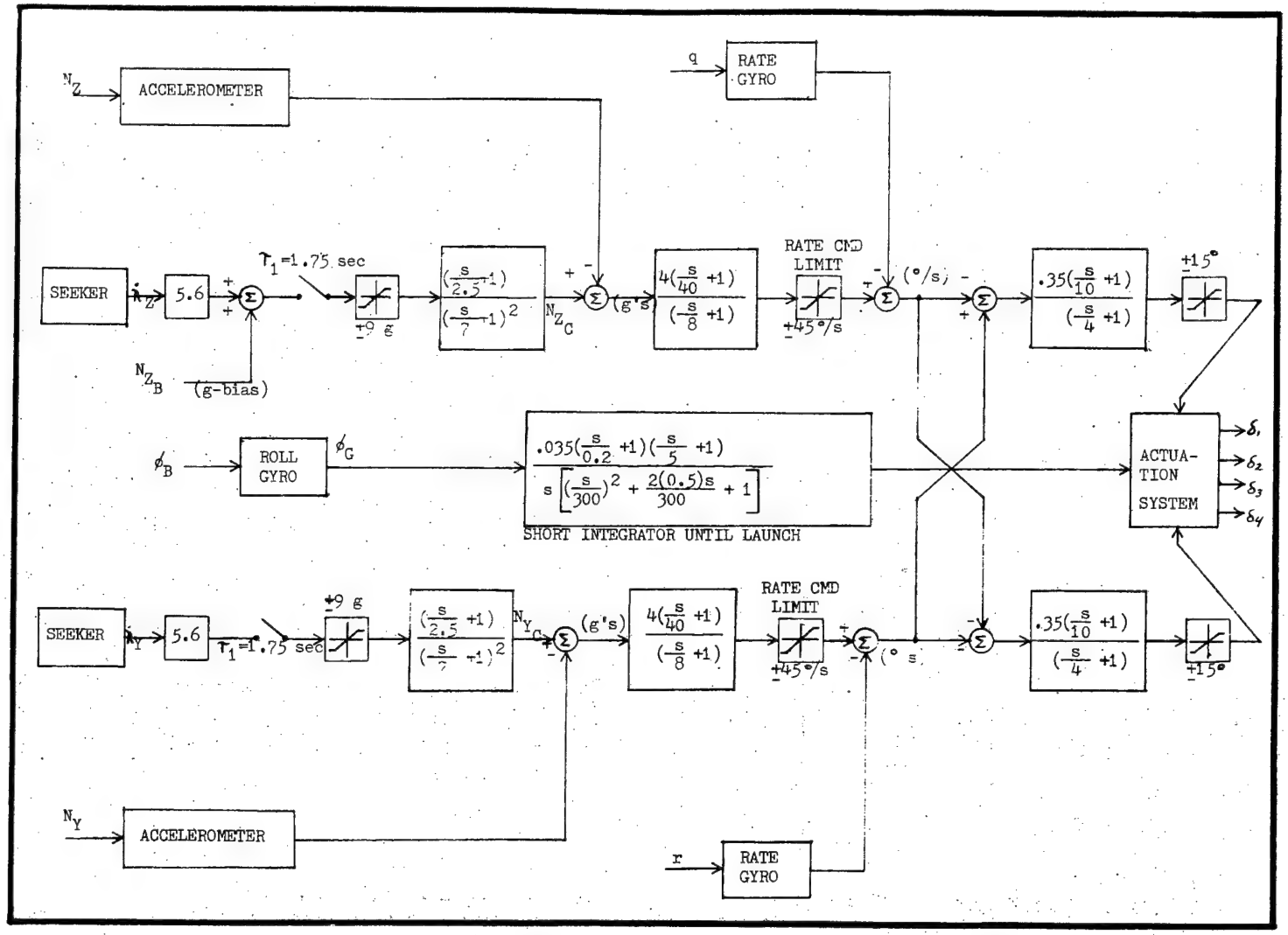

Figure 1. Flight Control System for Tail-Controlled Glide Weapon

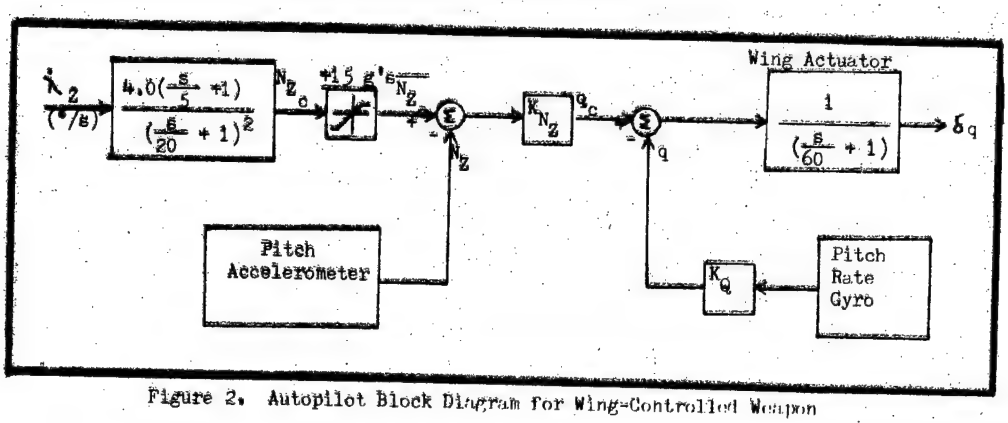

Figure 2. Autopilot Block Diagram for Wing-Controlled Weapon

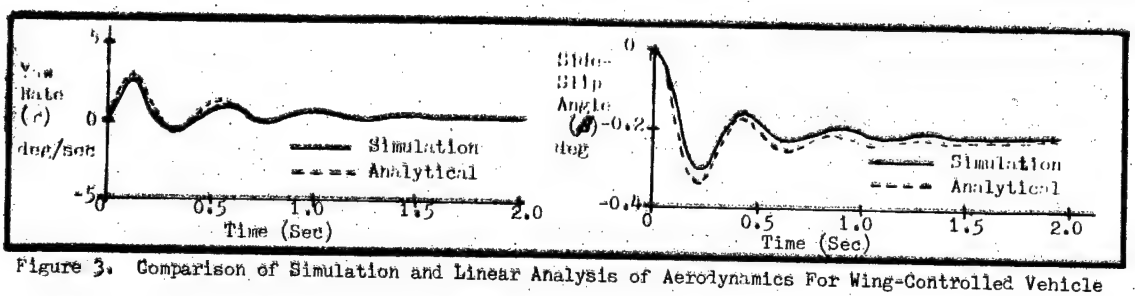

Figure 3. Comparison of Simulation and Linear Analysis of Aerodynamics For Wing-Controlled Vehicle

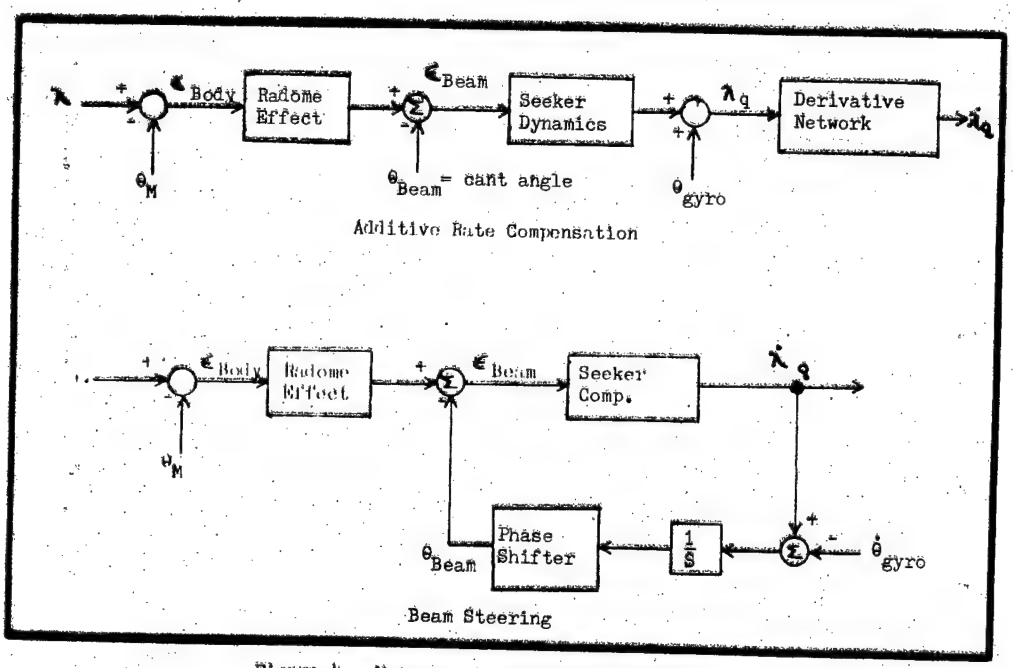

Figure 4. Methods of Generating LOS Rates

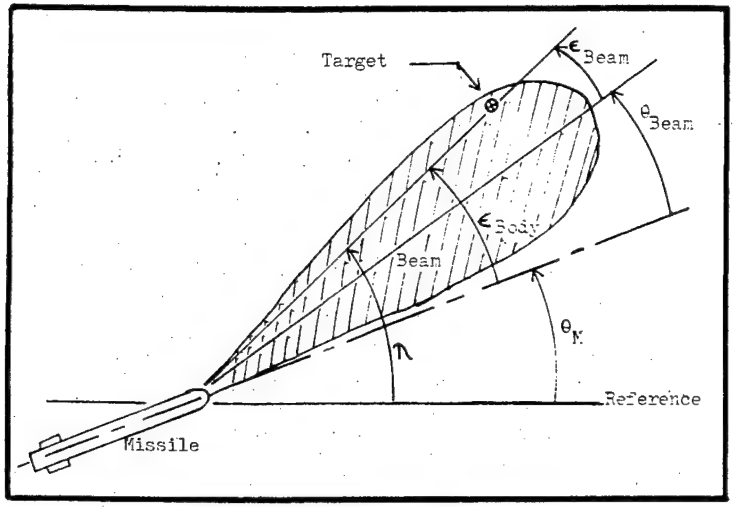

Figure 5. Geometry Definitions

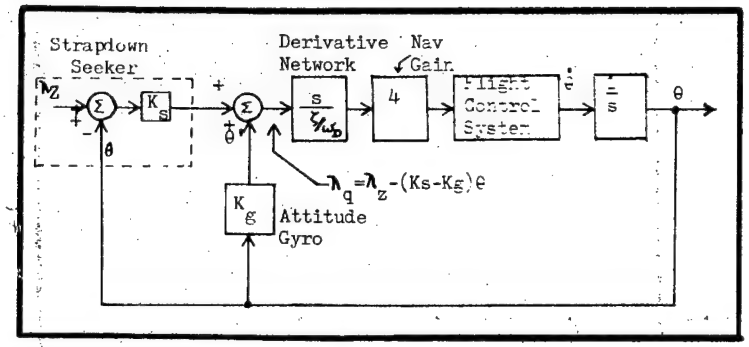

Figure 6. Additive Rate Compensation with Attitude Gyro

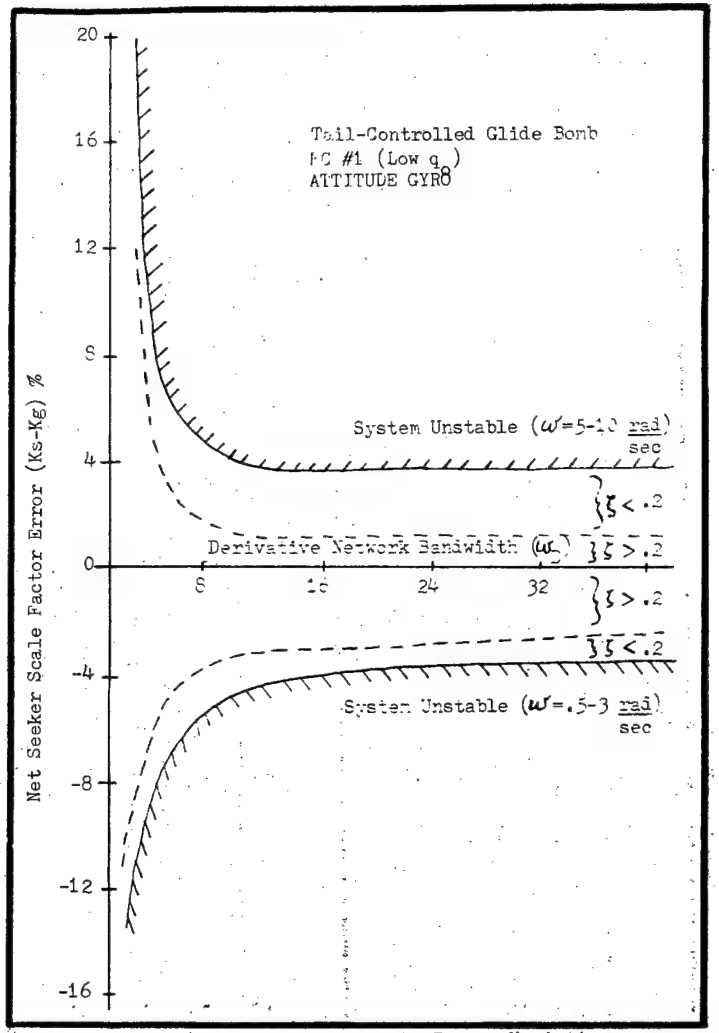

Figure 7. Sensitivity To Scale Factor Variations For Various Derivative Networks

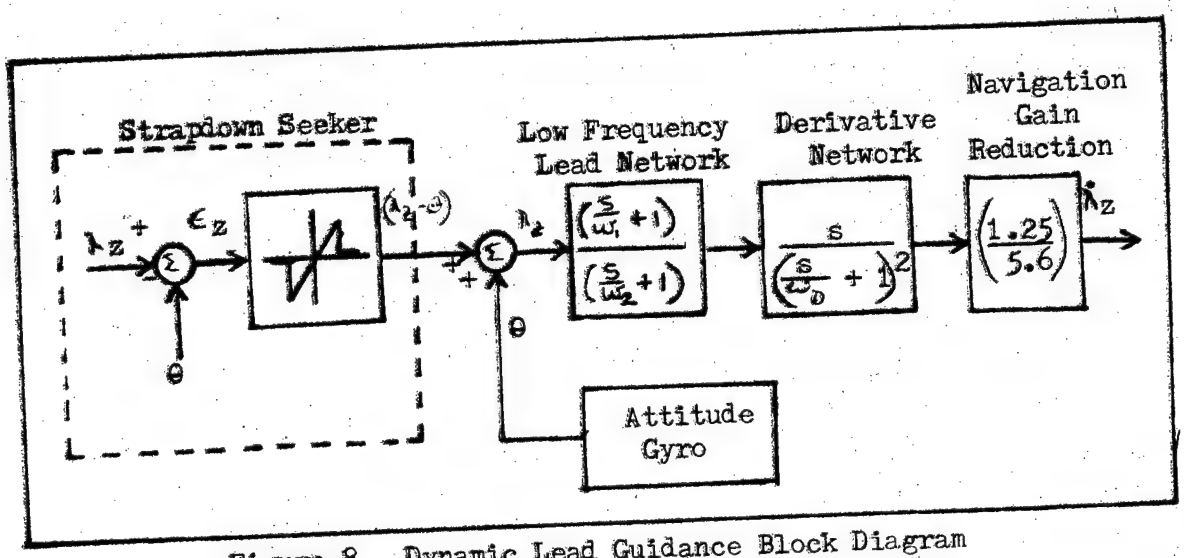

Figure 8. Dynamic Lead Guidance Block Diagram

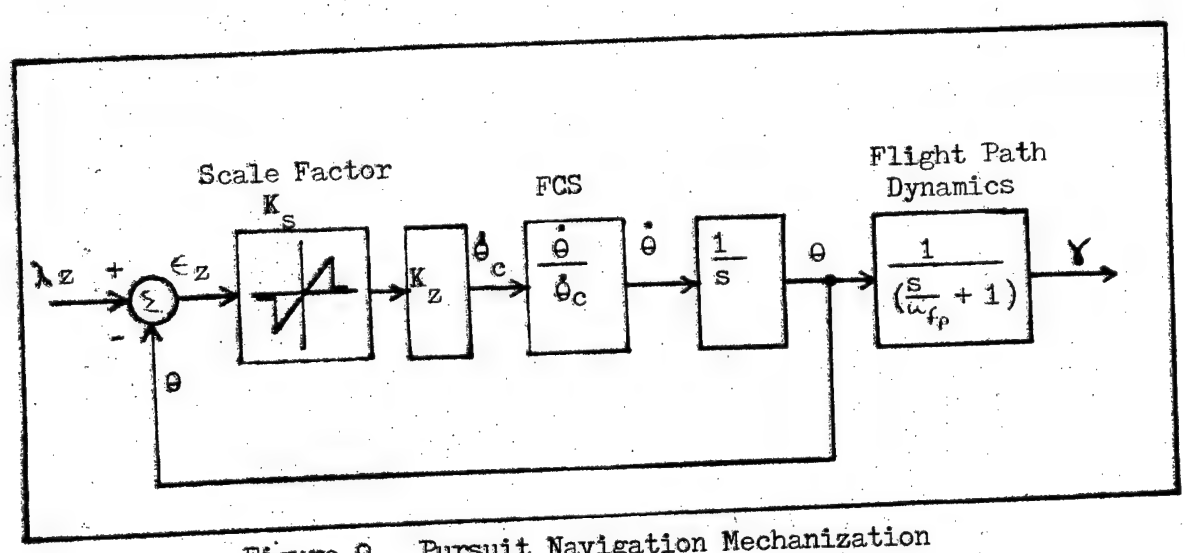

Figure 9. Pursuit Navigation Mechanization

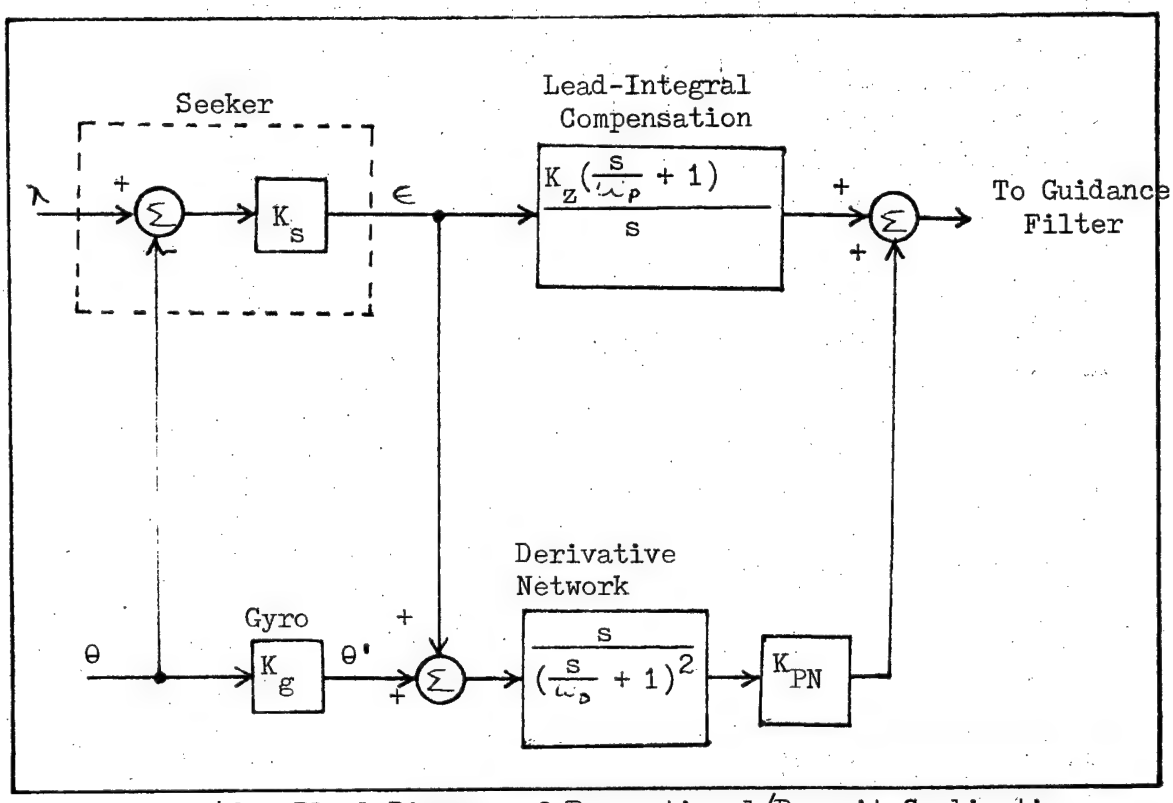

Figure 10. Block Diagram of Proportional/Pursuit Combination

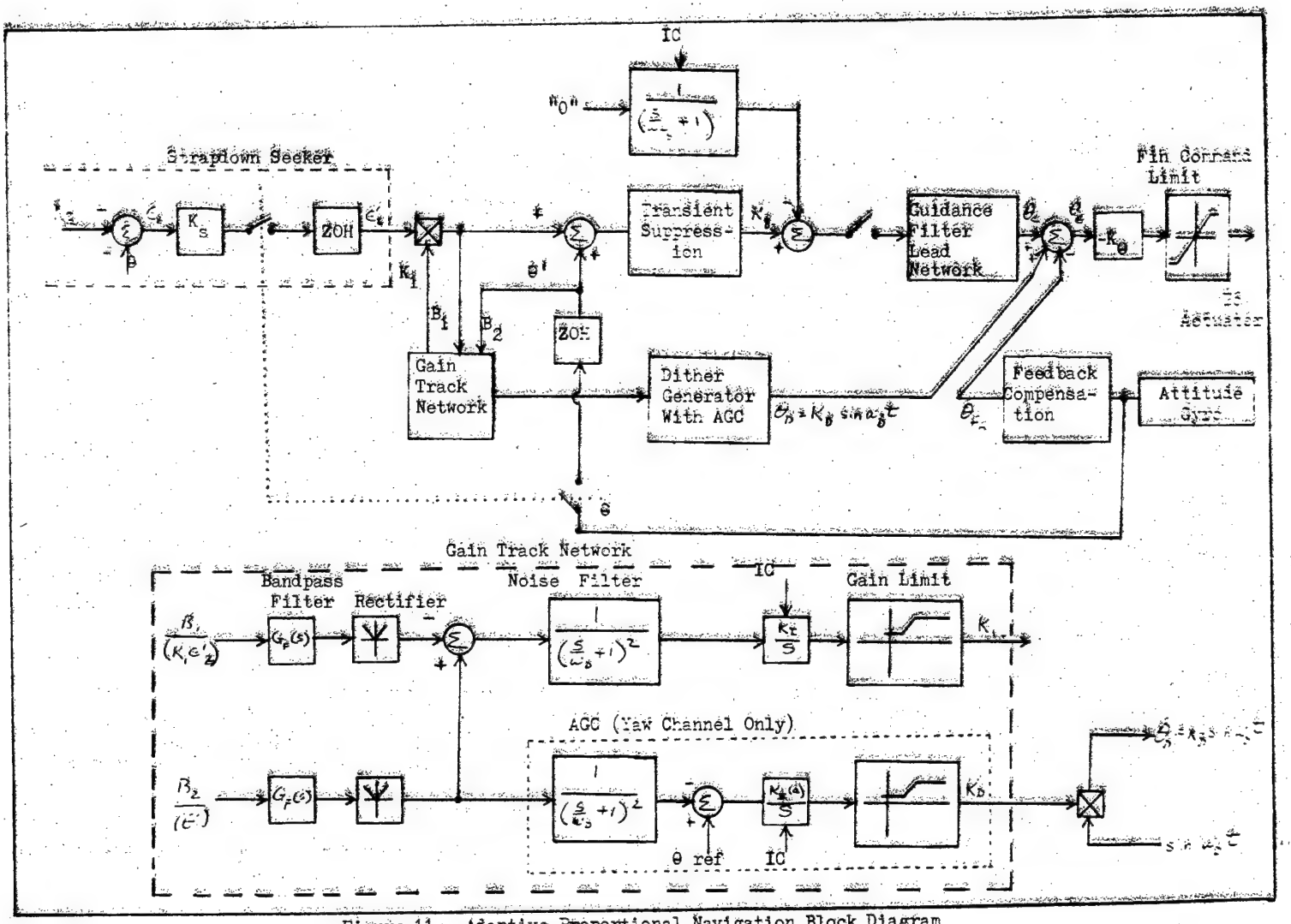

Figure 11. Adaptive Proportional Navigation Block Diagram

TABLE 1. Summary of Flight Conditions For Candidate Systems Subjected to Random Inputs

VEHICLE (*)	FLIGHT CONDITION	MACH	HEIGHT (FEET)	T (DEG)	TIME OF FLIGHT (SEC)
#1	#1	0.6	5,000	10.0	17
	#2	0.9	SEA LEVEL	2.5	10
#2	#1	0.9	20,000	10.0	11
	#2	1.3	SEA LEVEL	2.0	7
#3	#1	2.0	20,000	0.144	5

TABLE 2. Vehicle Transfer Functions Used In Adjoint Simulation

VEHICLE TRANSFER FUNCTIONS (PITCH PLANE) $\left[\frac{N_z}{N_{zc}}\right]$		
VEHICLE (*)	FLIGHT CONDITIONS	
	#1	#2
#1	$.32\frac{(200)}{(2.18)\left[\frac{.43}{8.55}\right]}$	$.44\frac{(200)}{(3.45)\left[\frac{.45}{20.66}\right]}$
#2	$\frac{.62\quad(200)}{(2.78)(35.96)(71.14)}$	$.85\frac{(200)}{(36.6)\left[\frac{.66}{9.33}\right]}$
#3	$.94\frac{(200)}{(56.96)\left[\frac{.52}{16.52}\right]}$	NONE
NOTATION: $(a) = (s/a + 1)$ $\left[\frac{\zeta}{\omega}\right] = \left(\frac{s}{\omega}\right)^2 + \frac{2\zeta}{\omega} s + 1$		

* NOTE: Vehicle #1 - Tail-Controlled Glide Bomb
Vehicle #2 - Wing-Controlled, Powered Missile
Vehicle #3 - Bank-to-Turn, Powered Weapon

1610

Table 3. Summary of RSS Miss Distance for Composite Random Noise Inputs - From Adjoint Simulation

	ADJOINT SIMULATION RSS MISS DISTANCE (FEET)				
VEHICLE (*)	#1		#2		#3
STRAPDOWN SEEKERS	FLIGHT CONDITIONS				
	#1	#2	#1	#2	#1
SEMI-ACTIVE LASER	15.55	9.95	6.21	9.38	4.97
ACTIVE RADAR	16.05	11.25	7.87	13.06	7.40
PASSIVE RADAR	9.83	5.61	3.13	3.94	1.93

* NOTE: Vehicle #1 - Tail-Controlled Glide Bomb
Vehicle #2 - Wing-Controlled, Powered Missile
Vehicle #3 - Bank-to-Turn, Powered Weapon

Table 4. Comparison Between Adaptive PN and PN with Gimballed Seeker (Yaw Trajectory Vs. Time)

Time (Sec) / System	0	1	2	3	4	5	Miss Distance (feet)
Adaptive PN #1	0.	39.00	78.46	77.70	45.27	3.04	0.17
Adaptive PN #2	0.	39.00	78.98	78.00	45.24	3.29	0.25
Gimballed PN (dither)	0.	39.00	78.62	77.49	45.10	3.30	0.16

Adaptive PN #1 (scale factor error = -10%)
Adaptive PN #2 (scale factor error = 0)

Table 5. Guidance Law Comparisons

GUIDANCE LAW	ACCURACY	TOLERANCE FOR SEEKER ERRORS (BORESIGHT/GAIN)	COST/COMPLEXITY	RELIABILITY
Proportional Nav. with Gimballed Seeker	(1) Near Optimal for Constant Velocity Target	(1) Gain Errors Only Change Seeker Bandwidth	(3) Added Cost for Gimbal Structure and Electronics	(3) Requires Mechanical Gimbal Structure
Adaptive PN	(1) Same as PN with Gimballed Seeker	(2) Large Gain Slope Errors can cause Instability	(2) Requires Added Electronics for Dither, Gain Track	(2) Requires Dithering Air Frame Increasing Actuator Reqmts.
Pursuit/PN Combination	(2) Low Accuracy for Moving Targets	(3) Moderately Sensitive to Both Errors	(1) Strapdown Seeker Potentially Lower in Cost than Gimballed Seeker	(1) Strapdown Seeker Eliminates Mechanical Structure
PN with Strapdown Seeker	(3) Low Accuracy with Seeker Gain Errors	(4) Highly Sensitive to Gain Errors Only	(1) SAA	(1) SAA
Dynamic Lead Guidance	(4) Approaches PN with Strapdown Seeker	(5) Highly Sensitive to Gain Errors Only	(1) SAA	(1) SAA
Pursuit Navigation	(5) Low Except for Offsets	(6) Highly Sensitive to Boresight Errors Only	(1) SAA	(1) SAA

(SAA = Same as Above)

Biographical Sketch

Capt Thomas R. Callen was assigned to the Air Force Armament Laboratory in January 1976. He has served in the Systems Analysis and Simulation Branch of the Guided Weapons Division since that time. His primary responsibilities include guidance and control analysis, hybrid simulation, and guided weapon system performance analysis.

Capt Callen received his Bachelor of Science Degree in General Engineering from the USAF Academy in 1971. After serving a tour of duty with the Air Training Command, Capt Callen returned to school full time in 1974 and received his Master of Science Degree in Guidance and Control from the Air Force Institute of Technology in 1975.

Capt Callen is currently serving as program manager for the Strapdown Seeker Guidance program at the Air Force Armament Laboratory.

UNCLASSIFIED

OPTIMIZING THE PERFORMANCE OF ANTENNAS MOUNTED ON COMPLEX AIRFRAMES

By

C. Long Yu, Ph.D.

Advanced Systems Division

Fuze & Sensors Department

Naval Wepaons Center
China Lake, California

Optimizing the Performance of Antennas Mounted on Complex Airframes

Abstract

The RF sensors on board such vehicles as aircraft, missiles, projectiles, and bombs frequently use antenna whose radiation patterns are strongly influenced by: antenna location on the vehicle, shape of the vehicle, antenna distance to external stores, control surfaces, openings, etc. Until recently, optimizing on-vehicle antenna performance and determining its radiation pattern was largely an empirical process. This process was slow, costly, and frequently did not result in optimized antenna performance.

The objective of this paper is to discuss the research efforts, which have been conducted at the Naval Weapons Center, in developing mathematical design analogs for predicting radiation patterns of airborne antennas in an accurate, efficient, and economical manner. The theoretical approaches employed are the Geometrical Theory of Diffraction (GTD) for objects large in terms of wavelength and the Hybrid Technique (GTD-MM Method) which combines the GTD and the Moment Method for objects a few wavelengths in size. With the aid of these analogs an optimum design of antenna systems for airborne vehicles can be achieved for specific applications.

Introduction

The RF sensors on board such vehicles as aircraft, missiles, projectiles, and bombs frequently use antennas whose radiation patterns are strongly influenced by: antenna location on the vehicle, shape of the vehicle, antenna distance to external stores, control surfaces, openings, etc. An antenna which works well in one location on a particular airframe may perform very poorly in another location depending upon the particular RF interactions between the antenna and some airframe feature. A frequent procedure followed in aircraft RF sensor development is to locate the antenna at some place on the airframe which has been selected more for aerodynamic reasons than for providing optimum antenna performance. Following this, the antenna engineer designs an antenna for free space prformance, builds a scale model and tests it on a scale model of the aircraft. When, as frequently happens, the antenna performance is degraded the designer then has the option of modifying the antenna design, changing the antenna location, if allowed, or both. In any case with this empirical procedure one has no good way of varying design parameters during the development iterations. This empirical airborne antenna design approach requires a great deal of engineering time and money and frequently does not result in optimized antenna performance. The need for an efficient and economical means of predicting the pattern performance of an antenna system in the presence of an airframe is, therefore, quite necessary.

Present practical modeling techniques provide for mathematically modeling the RF characteristics of objects by three approaches, the moment method, asymptotic solutions, and a hybrid method. Asymptotic solutions, such as the Geometrical Theory of Diffraction, are limited to bodies whose dimensions are large with respect to a wavelength. On the other hand, the moment method works well for small bodies whose dimensions are approximately a wavelength in size. Recently, a new hybrid technique (GTD-MM METHOD) which combines the Geometrical Theory of Diffraction and the moment method has been developed to analyze structures approximately 2 ~ 3 wavelengths in extent. In some cases, this technique can even be extended to larger objects of about 10 wavelengths or more. Furthermore, this technique can handle a wide variety of new problems which could not have been solved previously.

The main objective of this paper is to discuss the research efforts which have been conducted at the Naval Weapons Center and which are directed toward developing mathematical design analogs for predicting radiation patterns of airborne antennas in an accurate, efficient, and economical manner. Three versatile antenna design analogs are to be discussed in this paper. These are fuslage-mounted, wing-mounted, and hybrid technique antenna design analogs.

The hybrid technique antenna design analog uses the concept of GTD-MM method and is designed for vehicles only a few wavelength in extent. However, this analog can also be extended to treat some semi-infinite structures as the operating frequency becomes increasingly high. The fuselage-mounted and wing-mounted antenna design analogs were developed for vehicles with dimensions large in terms of wavelength. Both analogs use the principle of the Geometrical Theory of Diffraction as the theoretical basis to provide the simplicity and versatility of the ray optics approach. The wing-mounted antenna analog is intended for cases when the antenna system is mounted on a flat surface such as the wing or stabilizer surfaces. The fuselage-mounted antenna analog is intended for the situation where the antenna system is mounted on a curved surface such as the fuselage.

These three mathematical analogs have all been tested and verified by comparison with many experimental measurements. The good agreement between the calculated and measured results has demonstrated the validity, efficiency, and applicability of the analogs in predicting the radiation patterns of antenna systems on complex airframes.

The Antenna Design Analogs

A. Fuselage-mounted Antenna Design Analog

To meet the future threat and challenge of our national defense, the Navy is constantly exploring new weapon concepts and systems. One of the new weapons which is currently in development is an air breathing missile. The external configuration of a typical air breathing missile may include large air ducts adjacent to the fuze target detecting device (TDD). Preliminary tests indicate that the ducts will break up the antenna radiation pattern causing pattern nulls and high sidelobe levels. The same tests have indicated that this is true when the antenna is placed on top of the ducts as well

as between them. An optimum solution to this problem should involve selecting the best antenna location and utilizing a different, more optimum antenna system concept than currently in use. The fuselage-mounted antenna design analog is the most appropriate, useful tool available for optimizing antenna performance under these circumstances.

The fuselage-mounted antenna design analog was originally developed by Dr. Yu and his colleagues [1] at the Electro-Science Laboratory of the Ohio State University. This computer program, which used the Geometrical Theory of Diffraction as its theoretical basis, was orginally intended for use with antennas on aircraft structures with large wings. As described in Reference [1], this mathematical analog has been evaluated through extensive tests and verification and has proved to be very versatile and economical for predicting antenna performance when mounted on the fuselage of airborne vehicles. Consequently, it was used with modifications for the air breathing missile configuration to predict and analyze the pattern performance of the fuze antenna system on these missiles. With this analog the origin of the reflected and diffracted energy can be identified and determined. Hence, optimizing the fuze antenna performance is possible for almost any air breathing missile configuration.

To illustrate the capability of the mathematical analog, the radiation pattern of a quarter wavelength long monopole mounted on the fuselage of an air breathing missile and between two air ducts was calculated using a modern digital computer. The computer simulation model used in the numerical calculation was composed of a composite elliptic cylinder and a circular cylinder to simulate the missile profile and its cross section respectfully as described in Dr. Yu's work [1]. The air ducts of the missile were simulated by flat plates. Figure 1 illustrates the profile and cross-section view of a scale-modeled air breathing missile and its computer model. The calculated roll-plane radiation pattern for a centrally located monopole is presented in Figure 2. An experimental scale-model measurement (at a frequency of 5 GHz) was performed to verify the numerical results. The agreement with the calculated pattern is very favorable. The slight discrepancies displayed in the patterns in the -20^{o} to 20^{o} and 160^{o} to 200^{o} regions were due to the higher order terms such as reflected - diffracted fields which were not included in the calculation. Correction of these discrepancies is currently in progress.

It is notable that the presence of the air ducts on an air breathing missile has a strong influence on the resultant antenna patterns. It not only deteriorates the original radiation pattern of the antenna element but also creates some undesired sidelobes and nulls. The deleterious effects of the structural elements on the antenna pattern performance may lead to complete failure of some antenna systems on board airborne vehicles. Consequently, the mathematical analog presented here should be very useful in helping the antenna designers in selecting the antenna type and determining the antenna location on the airborne vehicle in achieving the optimum design of antenna systems. In addition, because the computation time for obtaining a radiation pattern takes typically 30 seconds or less on modern high speed digital computers such as the IBM 370, the analogs should provide a great aid in evaluating and designing the antenna system effeciently and economically in contrast to the lengthy scale-model measurement approach.

B. Wing-Mounted Antenna Design Analog

The wing-mounted antenna design analog [2], was developed by the Ohio State University for the Naval Weapons Center under a research contract. The object of this study was to develope a mathematical analog which can be used to optimize the design of antennas when mounted on the wing surfaces of modern high-speed aircraft. The mathematical analog is designed to be general and versatile so that it can be applied to all types of aircraft or missiles with only minor modification.The theoretical basis used in this development is also the Geometrical Theory of Diffraction.

To date the wing mounted antenna analog has not been used for an armament type application and therefore an airplane avionics type application will be discussed to demonstrate the analog performance. The application was a UHF antenna mounted on the wing of a F-4 jet aircraft. The specifications require full hemispheric coverage in the aft region of the aircraft. In order to meet the broad coverage requirement, a slot element which is vertically polarized with respect to the wing is used. The F-4 aircraft was simulated by a computer model which consisted of a finite elliptic cylinder with bent and flat plates attached. The finite elliptic cylinder represents the aircraft fuselage and the bent plates and flat plates represent the wings and stabilizers. The geometry of the F-4 aircraft and its computer model are shown in Figure 3. The

theoretical prediction of the radiation pattern for the main beam elevation plane for a slot antenna on the wing of a F-4 aircraft scale model is presented in Figure 4. An experimental measurement result is also shown in Fig. 4 for comparison purposes. The overall agreement with the calculated prediction is very favorable. However, some discrepancies do exist between the measured and calculated results. The problem is that the measurements were taken in the near field of the aircraft. As a result, one can not directly compare the measured near-field and calculated far-field patterns. Furthermore, there is also the possibility of slight inaccuracies in the measured results due to variations in the palcement of the antenna, ground reflection, etc.The comparison does show, however, the capability and applicability of predicting the radiation patterns for antennas mounted on the wing surfaces of a modern complicated aircraft.

As a result of this study, one concludes that an antenna mounted on a wing surface can interact strongly with the fuselage and wings causing large amounts of variation in the pattern. This suggests that proper antenna element design and placement of the antenna on the wings to minimize the interference problems are important considerations that must be taken into account when designing wing-mounted antenna systems. Thus, this study has shown that the mathematical analog can be very useful to the antenna engineers and system designers in anticipating the structural interference problems and optimizing the antenna performances.

C. Hybrid Technique Antenna Design Analog

Due to the critical need for mathematically modeling electrically small and medium-size missiles and aircraft this antenna design analog study was initiated at the Naval Weapons Center. This analog employs the recently developed hybrid technique called GTD-MM method as the theoretical basis. Although the basic idea of the GTD-MM method was originated by its authors [3] at the ElectroScience Laboratory of the Ohio State University, the technique was extended at NWC to treat more complicated shapes. In addition, This technique was also modified and extended to handle semi-infinite structures [4] in a more accurate, efficient and economical manner.

The Geometrical theory of Diffraction (GTD) which is basically a high frequency solution has been applied to solve numerous practical electromagnetic problems for which the structure is larger than a few wavelength. The approach has been to approximate the actual problem by a simple model which can be analyzed using GTD. The GTD solutions are, in general, accurate and efficient for models which fall within their framework. However, GTD solutions exist for relatively few geometries. This limits the theoretical models that can be utilized in practice.

The moment method (MM) is a matrix method for computing the solutions, which is based on integral equation formulations, to the electromagnetic field problems. By properly enforcing the boundary conditions on the object, the surface currents and the resulting scattered fields can be determined. This method can be applied to arbitrarily shaped objects provided that the overall size is small in terms of a wavelength. This is the basic limitation for the MM method, since for large bodies the solutions require a tremendous computer core storage and calculation time which are prohibitively expensive. Unfortunately, in actual practice it is very seldom that a UHF antenna is mounted on a vehicle as small as one wavelength. Instead, the vehicle is frequently two or three wavelengths in extent. This is too small for GTD and too large for the moment method. In order to provide a solution to this problem the recently-developed hybrid technique (the GTD-MM method) can be applied.

The hybrid technique which utilizes the advantages of both the GTD method and the MM techniques is intended to bridge the gap between the GTD solutions and the MM solutions in the frequency spectrum. In this approach one can cast the surface current density into a general GTD form in regions removed from the diffracting sections and apply current samples (MM) around the diffracting sections. Thus, an electrically large structure can be solved with very few unknowns. For example, the infinite wedge structure can be solved with as few as six unknowns [3] . In this way, the effort in solving the linear matrix on the computer can be greatly reduced and hence reduce the computation time to obtain a solution considerably. Using this approach, the solutions to problems which can not be handled by the present GTD technique or the MM method alone can be solved without difficulty.

To illustrate the applicability and capability of this analog to practical problems, the radiation patterns of a flush-mounted slot on various locations of some simple missile models have been studied. The geometries of the missile models are shown in Figure 5. Notice that these geometries represent the simplest missile profiles with no fins or stabilizers attached. Furthermore, these geometries in Figure 5 (a) and (b) can not be solved by GTD or MM alone. More precisely, it cannot be solved using MM if the structure is too large, and it cannot be solved using GTD without making certain simplifying assumptions. However, by using current samples around the end caps and known GTD current forms in the central region, one can solve for the total surface current density and the far zone field with as few as 28 unknowns for any size structure of this type. Consequently, using this new application-oriented approach, one is able to apply the Method of Moments to very large structures with only a few unknowns, which makes it a very powerful tool for high frequency application.

Figures 6 through 9 present the calculated radiation patterns for the missile models. The experimental results are also shown to verify the accuracy of the theoretical prediction. The axial slot elements used in the measurement were waveguide-fed slot radiators at frequency f = 1.48GHz and f = 2.95GHz. As one can see, the calculated results are in very good agreement with the measured results. This illustrates the capability of the GTD-MM solution in predicting the radiated pattern of antennas on finite complex structures which neither the GTD approach or the Moment Method can handle alone.

In some instances, when the antennas are operating at high microwave frequencies, the structures become so large electrically that the GTD-MM method is not sufficiently efficient. This is especially true when the antenna is located close to one end and remote from the other end of a complex structure such as missiles or bombs. For these cases, semi-infinite geometries may be used to simulate the structure. But the GTD-MM method fails to predict the fields of infinite structures accurately. Furthermore, in the case of infinite geometries, this approach requires extensive numerical integration to evaluate the coefficients and excitation of the matrix equation as well as the far field pattern. Consequently, a modified GTD-MM method, which is more accurate and economical in computation is introduced [4].

Figure 10 illustrates a two-dimensional semi-infinite structure on which an axial slot is mounted. The diffraction by a junction line between a plane and circular cylinder occurs in many practical situations, but no theoretical solution is available for the diffracted field. Although the original GTD-MM technique can be used to analyze it, the result is limited in accuracy and requires great computational effort. The key to the modified GTD-MM technique is to separate the total surface current of the infinite structure into two components, namely: the current for a perfectly conducting half plane case and the change in current due to the presence of the circular cylinder (or arbitrary cylinder). Since the half plane problem has been solved and is known rigorously, the solution derived should be very accurate and efficient.

Before one can apply this modified technique to treat airborne antenna problems, the validity of this semi-infinite structure representation of an actual finite object must be established. Figure 11 presents the radiation patterns of a slot antenna mounted on a finite structure and a semi-infinite structure. As one can see, the comparison is very favorable. This indicates that the semi-infinite structure is indeed a very good representation of finite structures whenever the antenna is operating at very high frequency such that the structure is very large in terms of the wavelength. Furthermore, the modified GTD-MM technique is more efficient, accurate and economical when used to analyze the semi-infinite structure or very large complex structure in comparison to the original GTD-MM method. Typical antenna patterns of an axial slot located 1λ away from the tip of a simulated missile model are presented in Figure 12. Again, the structure shown in Figure 12 cannot be solved either by GTD method or MM method alone. Thus, the hybrid technique can be used to solve a whole host of new problems.

Conclusions

The research effort conducted at NWC in the RF mathematical modeling area has concentrated on optimizing the pattern performance of antennas mounted on complex airborne vehicles such as aircraft, missiles, projectiles and bombs.

This is due to the fact that the scale model measurement approach of airborne antenna design requires a great deal of engineering time and money. An efficient analytical model for the prediction of the antenna system performance in the presence of complex vehicle structure is urgently needed. This solution should be able to calculate the radiation patterns of airborne antennas accurately and efficiently such that it can be used to economically determine the antenna location and optimum antenna design for a given application.

Three mathematical antenna design analogs have recently been developed. These are fuselage-mounted, wing-mounted and hybrid technique antenna design analogs. The first two analogs, which employ the Geometrical Theory of Diffraction as theoretical basis, are useful for vehicles whose dimensions are large in terms of a wavelength. The last one, which used the recently developed hybrid technique (GTD-MM Method) as analytical approach is best suitable for vehicles whose dimensions are approximately 2 to 3 wavelengths. In some cases, the technique can even be extended to large objects of about 10 wavelengths or more. As described in the main text, the GTD-MM method is intended to bridge the gap between the GTD solutions and the MM solutions in the frequency spectrum. This method can also be applied to solve a wide variety of new problems which could not be solved previously by the GTD method.

The capability and versatility of these analogs has been demonstrated through extensive applications to various aircraft and missiles. The excellent agreement between the calculated and measured antenna patterns has established the validity and credibility of these mathematical analogs in predicting the antenna (both fuselage-mounted and wing-mounted) performance in the presence of complex airborne structures. The effect of the air ducts of an air breathing missile was particularly presented to illustrate the necessity of critical and careful consideration in the selection of an antenna location in complicated modern missiles and aircraft.

These analogs have also demonstrated that it is more efficient, accurate and economical to predict and determine the antenna performance through the computer simulation than the normal practice of scale-model measurement. Thus, a tremendous amount of man-power, engineering time and money can be saved via the analytical approach. Consequently, these

mathematical analogs offer an excellent design tool for the antenna engineers and system designers in optimizing the antenna performance in meeting its specifications or requirements.

REFERENCES

1. Yu, C. L. and Burnside, W. D., and Gilreath, M.C., "Volumetric Pattern Analysis of Airborne Antennas,". IEEE Trans. Antennas and Propagation, Vol. AP-26, No. 5, September 1978, pp. 636 - 641.

2. Marhefka, R. J. and Burnside, W. D., "Pattern Optimization of Wind-Mounted Array Antennas at UHF," Report 3884-1, January 1976, The Ohio State University ElectroScience Laboratory, Department of Electrical Engineering; prepared under Contract N00163-74-C-1580 for Naval Regional Procurement Office, Long Beach, California.

3. Burnside, W. D., Yu, C. L., and Marhefka, R. J., "A Technique to Combine the Geometrical Theory of Diffraction and the Moment Method," IEEE Trans. Antennas and Propagation, Vol. AP-23, No. 4, July 1975, pp. 551-58.

4. Yu, C. L. and Burnside, W. D., "A Modified GTD-MM Technique to Analyze the Diffraction by Semi-Infinite Complex Structures," 1977 International IEEE/AP-S Symposium, 20-24 June 1977, Stanford, California.

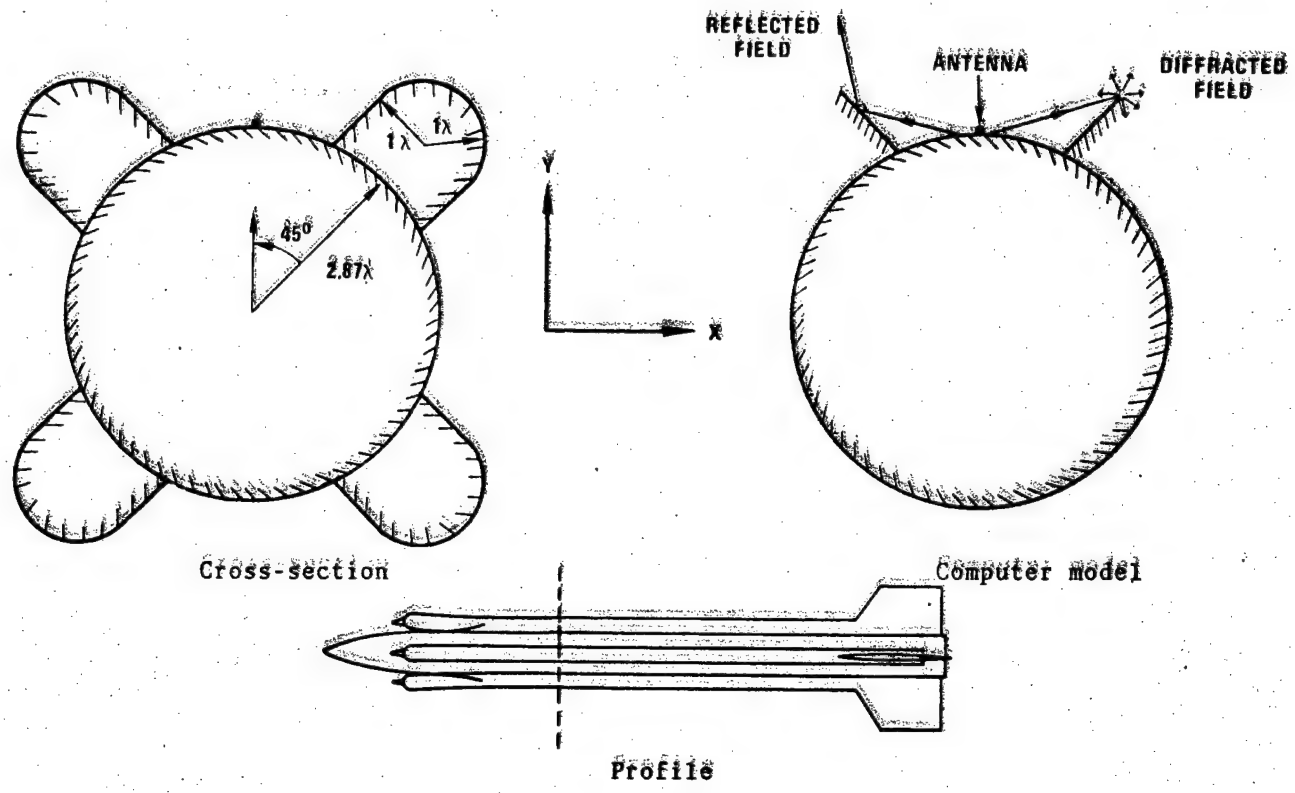

Figure 1. A Typical Air Breathing Missile (Profile and Cross Section Views) and its Equivalent Computer Model.

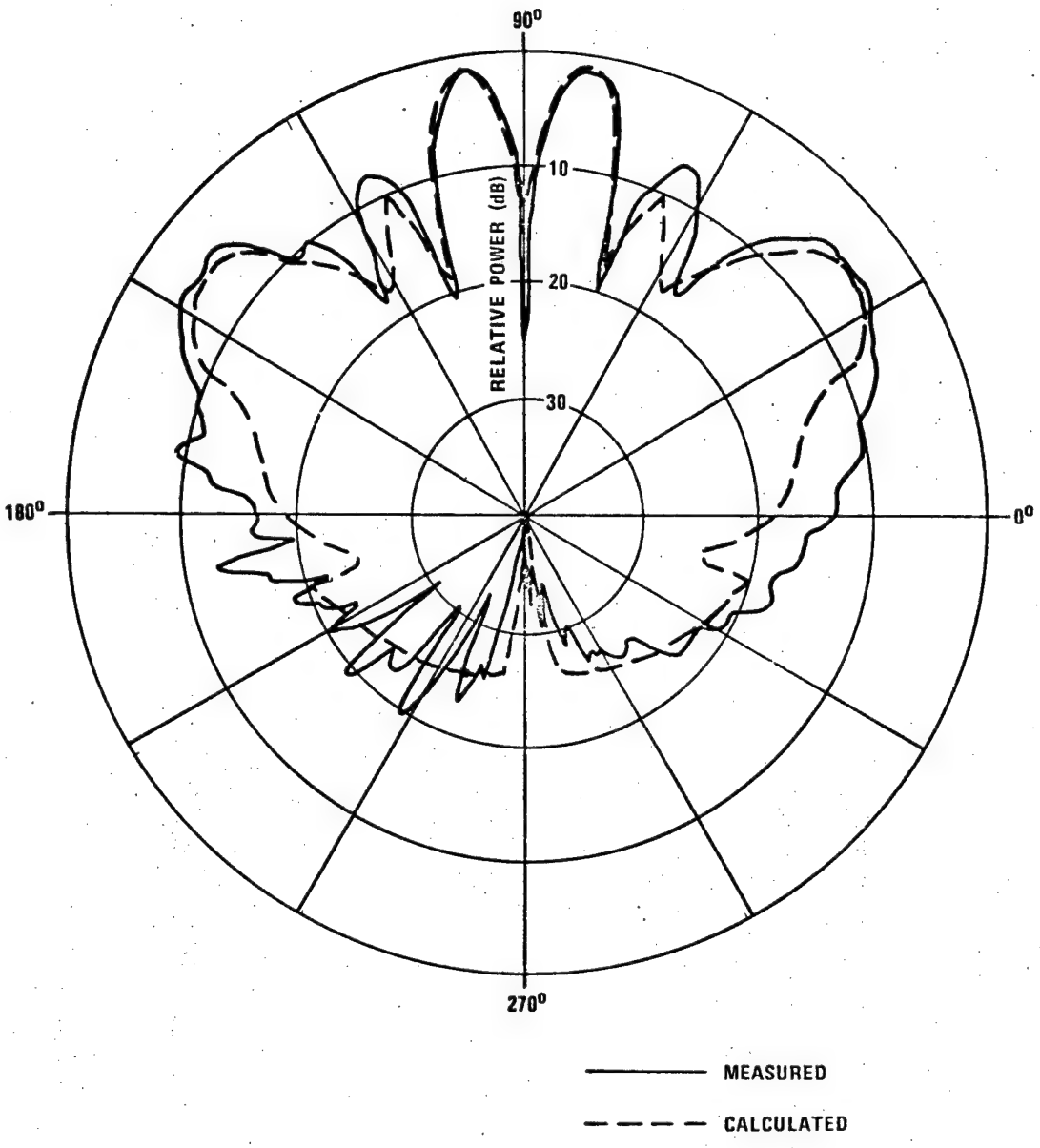

Figure 2. Roll Plane Radiation Pattern of a $\lambda/4$ Monopole Antenna Mounted on an Air Breathing Missile.

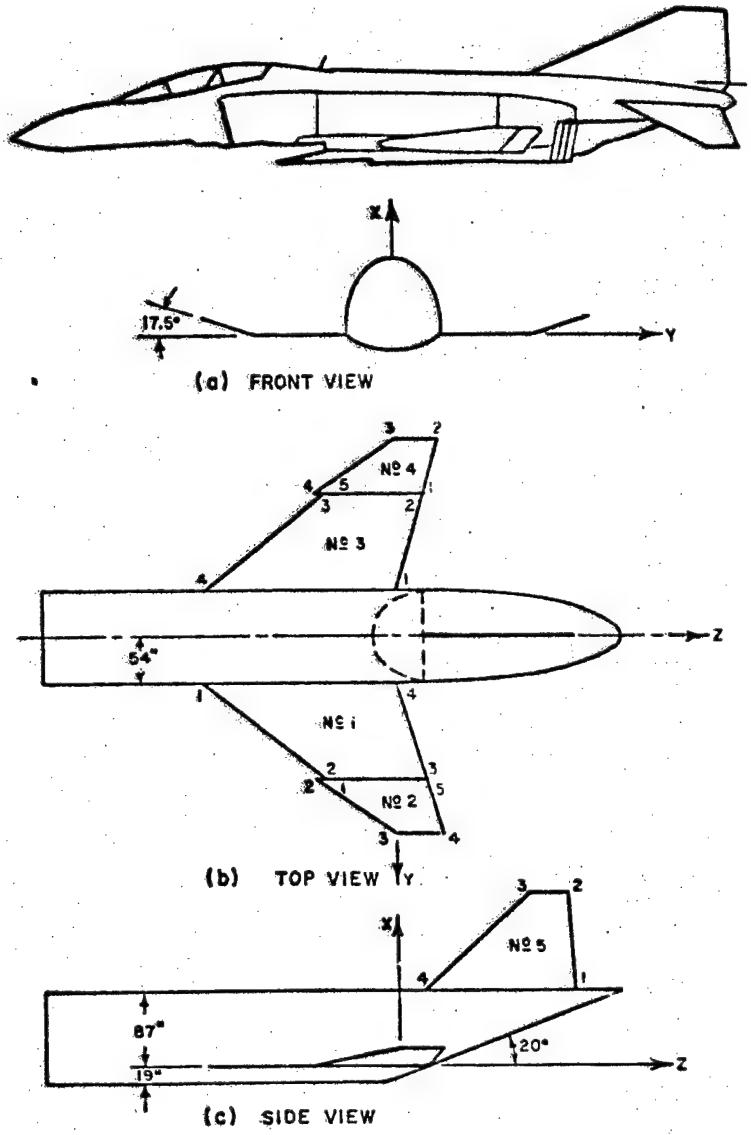

Figure 3. Illustration of the Geometry of an F-4 Aircraft and its Finite Elliptic Cylinder Model.

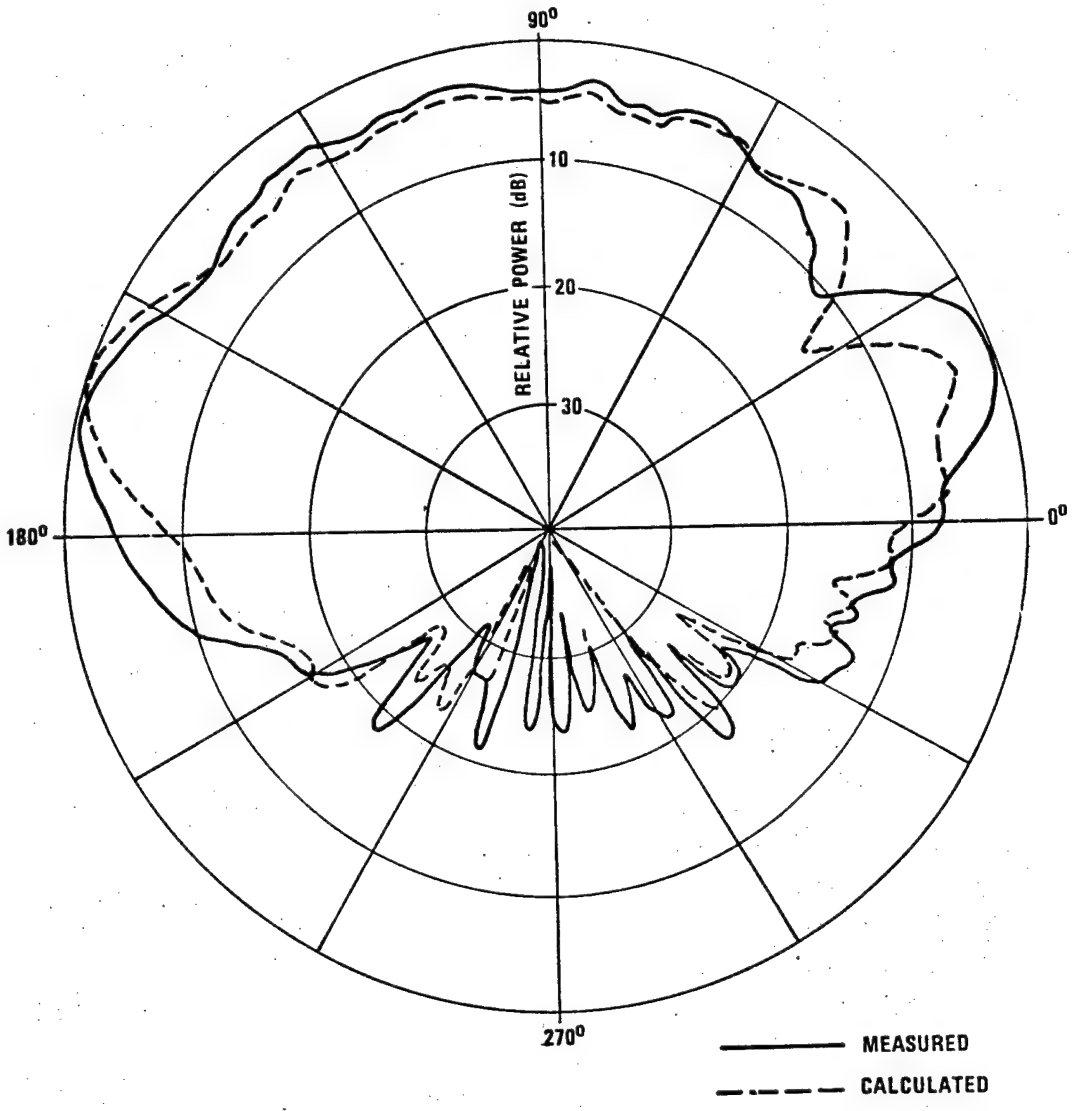

Figure 4. Comparison of NWC Measured Results on an F-4 Model with the Finite Elliptic Cylinder Model Results of Main Beam Elevation Plane Radiation Pattern.

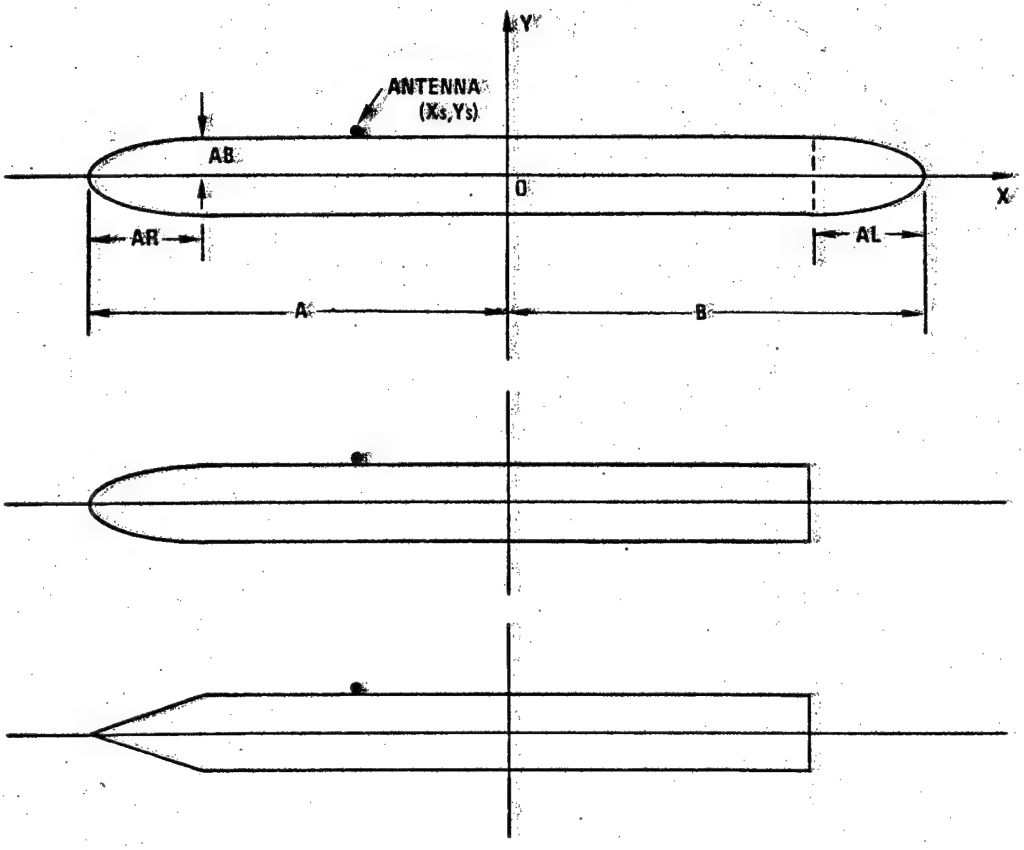

Figure 5. Some Simple Geometries Used for Missile Simulation.

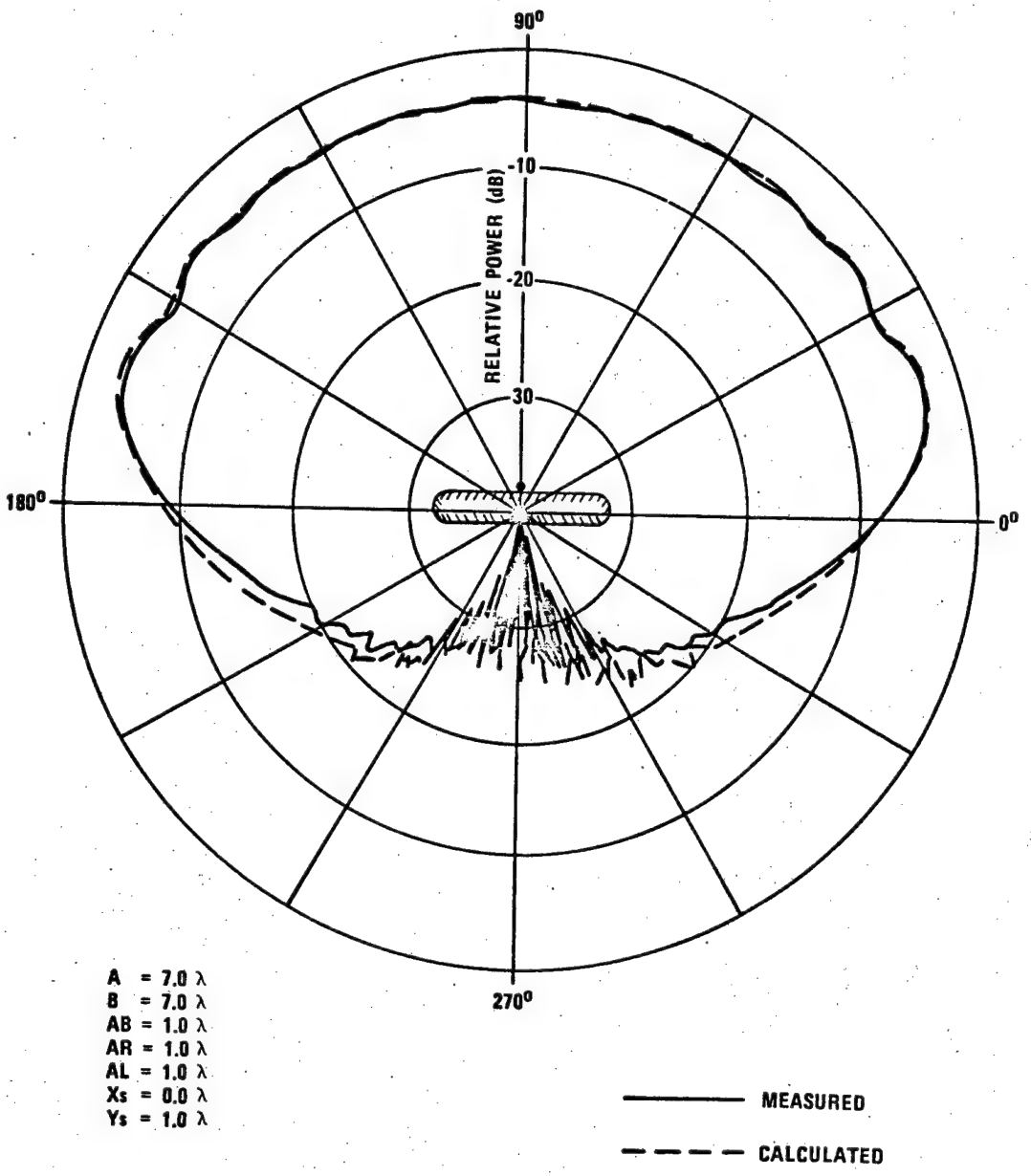

Figure 6. Elevation Pattern of an Axial Slot Mounted on a Simple Missile Model. (f = 2.95 GHz)

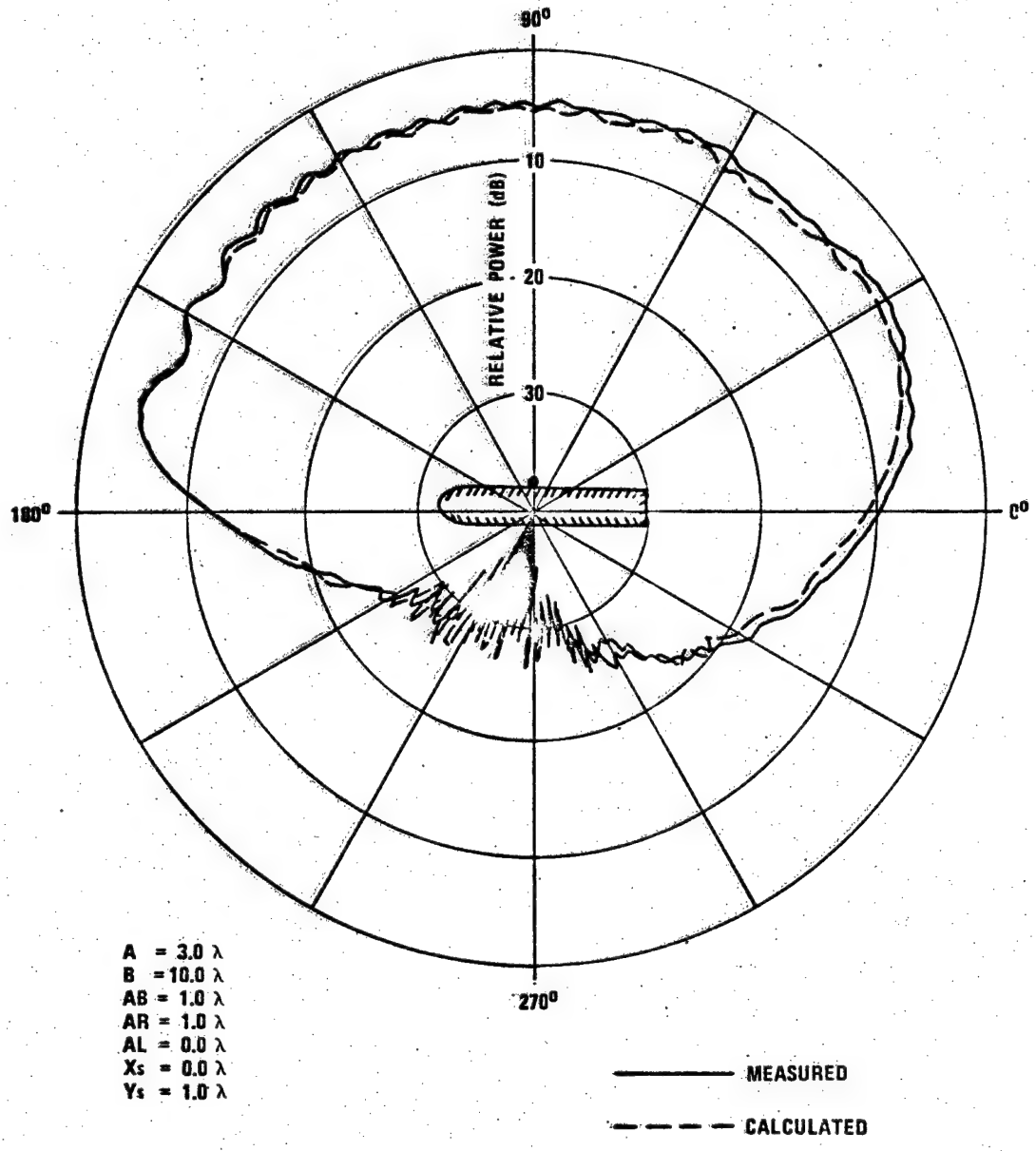

Figure 7. Elevation Pattern of an Axial Slot Mounted on a Simple Missile Model. (f = 2.95 GHz)

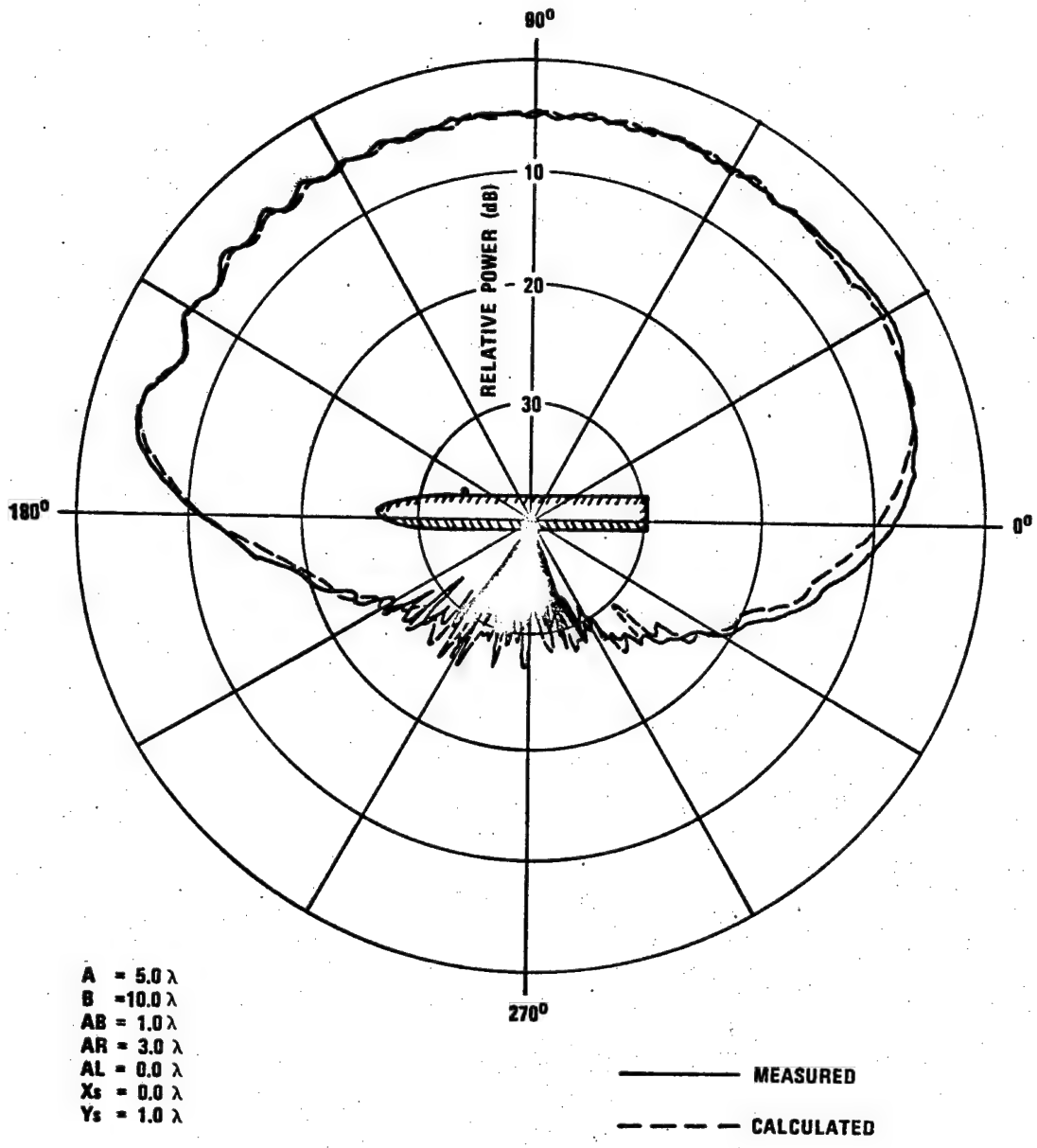

Figure 8. Elevation Pattern of an Axial Slot Mounted on a Simple Missile Model. (f = 2.95 GHz)

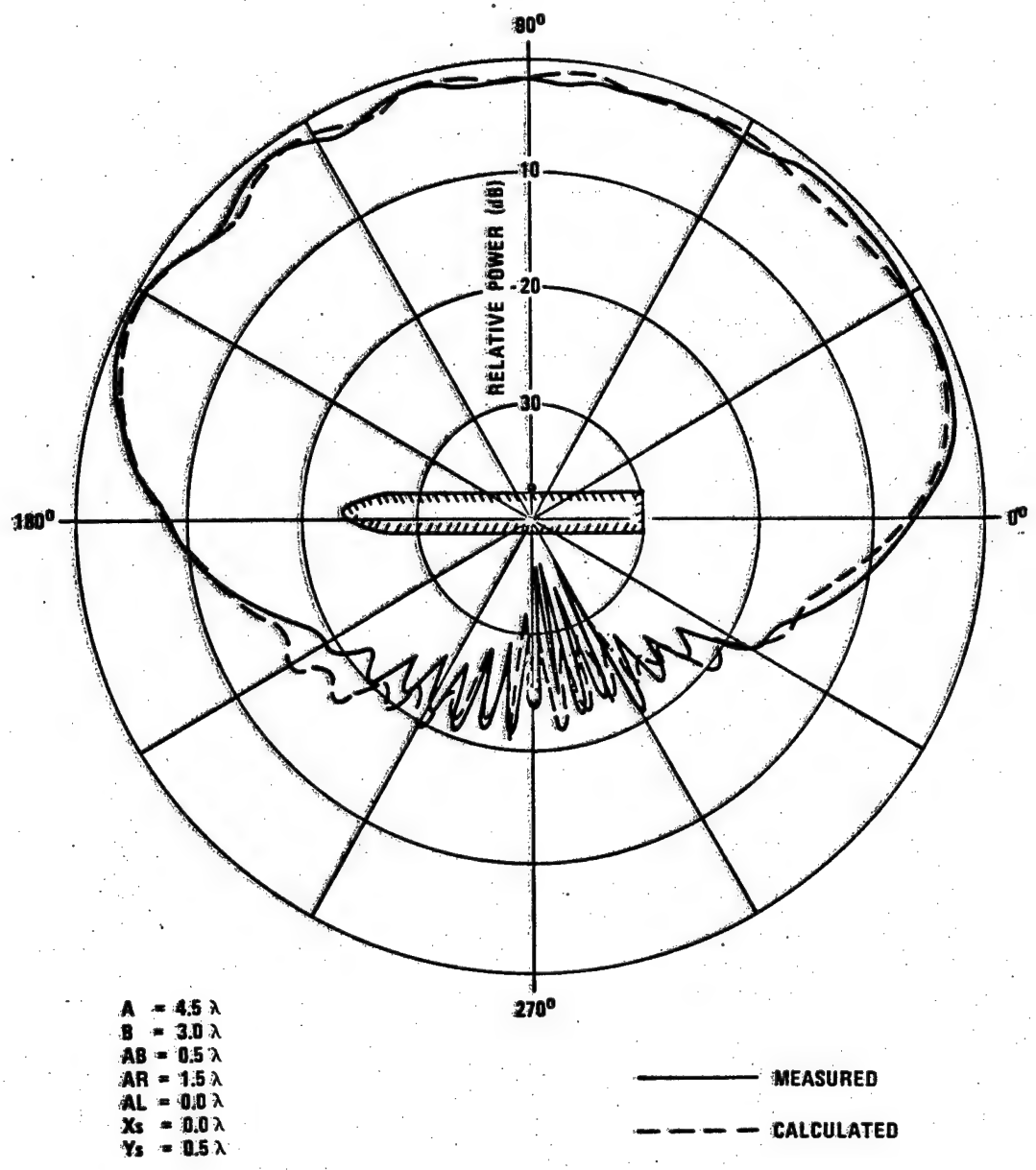

Figure 9. Elevation Pattern of an Axial Slot Mounted on a Simple Missile Model. (f = 1.48 GHz)

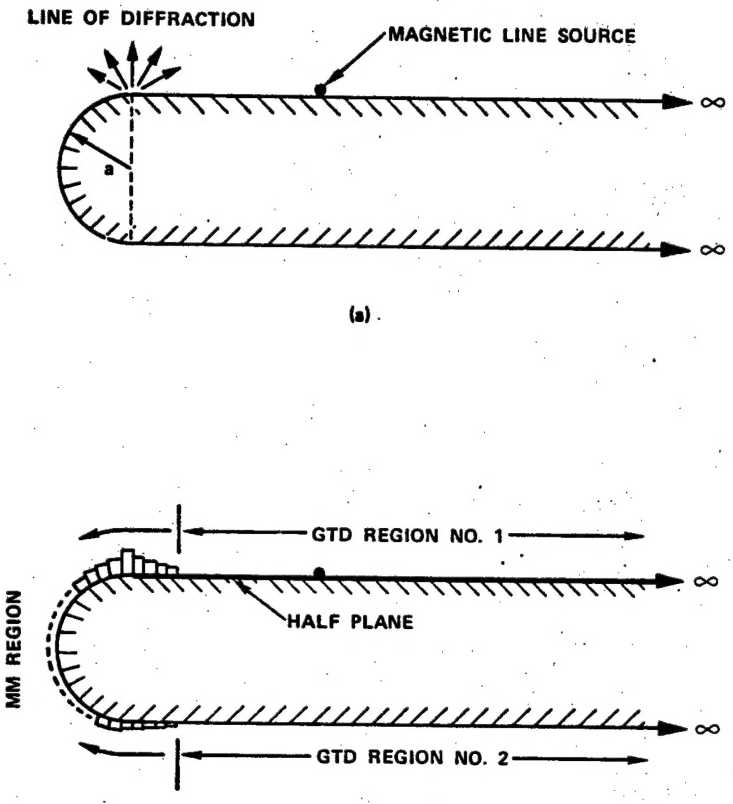

Figure 10. Diffraction at the Junction Line of a Circular Cylinder and a Thick Wedge (a) and the Distribution of Correlation Surface Current Density (b).

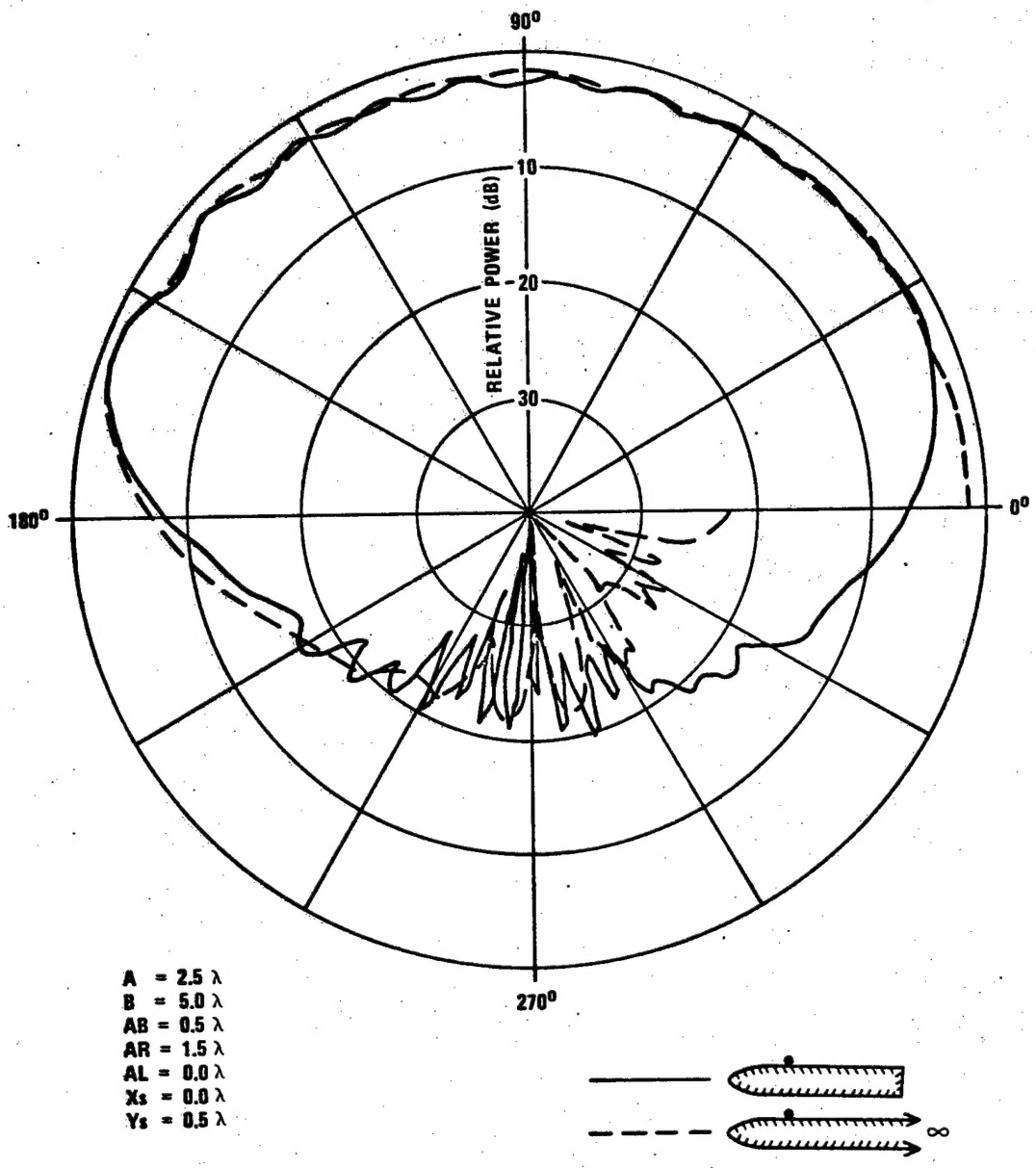

Figure 11. A Comparison of the Radiation Patterns of an Axial Slot Mounted on a Finite Structure and a Semi-Infinite Structure.

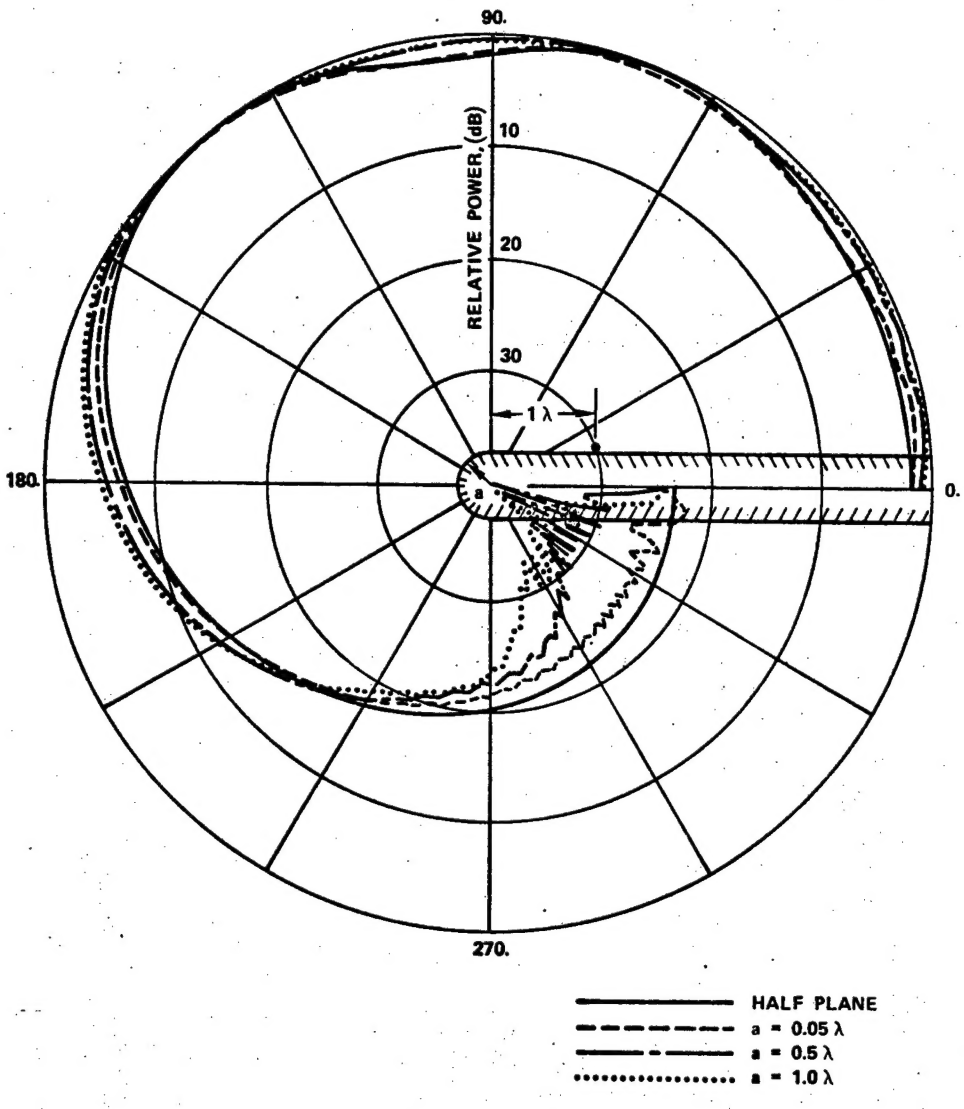

Figure 12. Radiation Patterns of an Axial Slot Mounted on a Simulated Missile Model.

Biographical Sketch

Dr. C. Long Yu was born in Taipei, Taiwan. He received the B. S. degree in Electrical Engineering from the University of Kansas, Lawrence, Kansas, in 1969, and the M. Sc. and Ph. D. degrees in Electrical Engineering from the Ohio State University, Columbus, Ohio in 1970 and 1976 respectively.

From 1969 to 1976 he was associated with the Electro-Science Laboratory, the Ohio State University, Columbus, Ohio, as a Graduate Research Assistant, a Graduate Research Associate, and later as a Research Associate. From 1976 to 1977 he was an Electronics Engineer at the Naval Weapons Center, China Lake, California, where he worked in the area of antenna designs and RF modeling techniques for airborne vehicles. From 1977 to 1978, he was a Member of the Technical Staff at the Aerospace Corporation, El Segundo, California. His work involved designing hardened antennas for the earth station as well as antenna systems on board military satellites. In May 1978, he rejoined the Naval Weapons Center.

Dr. Yu was a joint recipient of the IEEE Antennas and Propagation Society "Best Application Paper" award and the "R.W.P. King" award for 1975. He is a member of Sigma Xi, Tau Beta Pi, Eta Kappa Nu and Sigma Tau.